

Role of minor core protein V during productive  
infection with human adenovirus type 5 and  
the proteins relevance to oncogenic  
transformation processes

DISSERTATION

with the aim of achieving a doctoral degree  
at the Faculty of Mathematics, Informatics and Natural Sciences  
Department of Biology of Universität Hamburg

submitted by  
Nora Freudenberger

May 2017  
in Hamburg

Day of Disputation: 28.07.2017

Reviewer/Gutachter: Prof. Dr. Thomas Dobner  
Prof. Dr. Nicole Fischer

The English language in Nora Freudenberger's PhD thesis entitled  
**"Role of minor core protein V during productive infection with  
human adenovirus type 5 and the proteins relevance to oncogenic  
transformation processes"** reads fluently and the text is well written. I  
give my support that the English language is correctly articulated in Nora  
Freudenberger's PhD thesis.



**HelmholtzZentrum münchen**  
Deutsches Forschungszentrum für Gesundheit und Umwelt (GmbH)

Institut für Virologie  
Ingolstädter Landstr. 1 · 85764 Neuherberg

Helmholtz Zentrum München  
Deutsches Forschungszentrum für  
Gesundheit und Umwelt (GmbH)  
Ingolstädter Landstr. 1  
85764 Neuherberg  
Phone +49(0)89 3187 (0)  
Fax +49(0)89 3187 3322

info@helmholtz-muenchen.de  
www.helmholtz-muenchen.de

Aufsichtsratsvorsitzende:  
MinDir'in Bärbel Brumme-Bothe

Geschäftsführer:  
Prof. Dr. Günther Wess  
Heinrich Baßler  
Dr. Alfons Enhsen

Registergericht:  
Amtsgericht München HRB 6466  
USt-IdNr. DE 129521671

# Content

---

Zusammenfassung

Abstract

Abbreviations

1	Introduction .....	1
1.1.	Adenoviruses .....	1
1.1.1.	Classification .....	2
1.1.2.	Structure and genome organization .....	3
1.1.3.	The adenoviral life cycle .....	7
1.1.3.1.	Adsorption and entry .....	8
1.1.3.2.	The early genes E1 and E4 .....	10
1.1.3.3.	The late phase of infection .....	12
1.1.4.	The adenoviral core .....	13
1.1.4.1.	Minor core protein V .....	14
1.1.5.	Adenovirus-mediated oncogenesis .....	16
1.2.	Nuclear host domains targeted by HAdVs .....	18
1.2.1.	PML nuclear bodies .....	19
1.2.1.1.	The host SUMOylation machinery .....	21
1.2.1.2.	PML-NBs in antiviral defense .....	24
1.2.2.	Nucleoli .....	26
1.2.2.1.	Nucleophosmin and its various influences on cell homeostasis .....	29
2	Material .....	33
2.1.	Cells .....	33
2.1.1.	Bacterial strains .....	33
2.1.2.	Mammalian cell lines .....	33
2.2.	Viruses .....	34
2.3.	Nucleic acids .....	34
2.3.1.	Oligonucleotides .....	34
2.3.2.	Vector plasmids .....	36
2.3.3.	DNA templates .....	37
2.3.4.	Recombinant plasmids .....	38
2.4.	Antibodies .....	39
2.4.1.	Primary antibodies .....	39
2.4.2.	Secondary antibodies .....	41
2.4.2.1.	Antibodies for Western Blotting .....	41
2.4.2.2.	Antibodies for Immunofluorescence analysis .....	41
2.5.	Commercial systems .....	42

## CONTENT

---

2.6.	Chemicals, enzymes, reagents and equipment .....	42
2.7.	Standards and Markers .....	43
2.8.	Software and databases .....	43
3	Methods .....	46
3.1.	Bacteria.....	46
3.1.1.	Culture and Storage .....	46
3.1.2.	Chemical transformation .....	46
3.2.	Mammalian cells .....	47
3.2.1.	Maintenance and passage of cell lines.....	47
3.2.2.	Cryopreservation of cell lines.....	48
3.2.3.	Transfection of mammalian cells.....	48
3.2.3.1.	Transfection with Polyethylenimine (PEI).....	49
3.2.3.2.	Transfection with calcium phosphate (ProFection® Mammalian Transfection System) .....	49
3.2.3.3.	Transfection of linearized viral genomes with <i>Lipofectamin</i> ® 2000.....	50
3.2.3.4.	Selection of transfected human tumor cells with puromycin.....	50
3.2.4.	Harvest of mammalian cells .....	50
3.2.5.	Transformation Assay of primary baby rat kidney cells (pBRK).....	51
3.2.6.	MTT-assay.....	52
3.3.	Adenoviruses .....	52
3.3.1.	Infection of mammalian cells .....	52
3.3.2.	Propagation and storage of high-titer virus stocks.....	53
3.3.2.1.	Titration of adenovirus stocks .....	54
3.3.3.	Determination of viral progeny yields.....	55
3.4.	DNA techniques .....	55
3.4.1.	Purification of plasmid DNA from <i>E.coli</i> .....	55
3.4.2.	Purification of genomic DNA from Cultured Cells.....	56
3.4.3.	Determination of nucleic acid concentrations .....	56
3.4.4.	Polymerase chain reaction (PCR).....	56
3.4.4.1.	Site-directed mutagenesis.....	58
3.4.4.2.	Real-time PCR (RT-PCR).....	58
3.4.5.	Separation and Purification of DNA by agarose-gel electrophoresis .....	59
3.4.5.1.	Isolation of DNA from agarose gels.....	60
3.4.6.	Cloning of DNA fragments .....	60
3.4.6.1.	Enzymatic DNA restriction .....	60
3.4.6.2.	Ligation of DNA fragments .....	61
3.4.6.3.	Sanger-sequencing of DNA.....	61
3.5.	RNA techniques .....	61
3.5.1.	Isolation of total-RNA from mammalian cells .....	61
3.5.2.	Quantitative reverse transcription.....	62
3.6.	Protein techniques .....	62
3.6.1.	Preparation of total-cell lysates .....	62

## CONTENT

---

3.6.2.	Determination of protein concentrations in solution .....	63
3.6.3.	Immunoprecipitation (IP) of proteins .....	64
3.6.4.	Ni-NTA pull down of 6His-tagged proteins .....	65
3.6.5.	SDS-PAGE .....	67
3.6.6.	Western Blot analysis .....	68
3.6.7.	<i>In vitro</i> translation of proteins .....	69
3.6.8.	<i>In vitro</i> SUMOylation of proteins.....	69
3.6.9.	Immunofluorescence (IF) analysis .....	70
3.6.9.1.	Fixation of cells with methanol .....	70
3.6.9.2.	Fixation of cells with PFA.....	70
3.6.9.3.	Immunological detection.....	70
3.6.10.	Reporter gene assay.....	71
4	Results .....	72
4.1.	Subcellular distribution of HAdV-C5 pV in human cells .....	72
4.1.1.	HAdV-C5 pV N-terminally fused to a flag-tag can be expressed in human cells of tumor origin .....	72
4.1.2.	Different N-terminal tags do not influence the subcellular localization of pV in transiently transfected human cells.....	74
4.2.	Interaction of HAdV-C5 pV with PML nuclear bodies .....	77
4.2.1.	HAdV-C5 pV partially co-localizes with PML in transiently transfected HepaRG cells.....	78
4.2.2.	HAdV-C5 pV does not co-precipitate with the constitutive PML-NB components PML, Daxx and Sp100.....	79
4.2.3.	HAdV-C5 pV co-precipitates with the PML-NB associated adenoviral proteins E1B-55K and pVI ..	81
4.3.	HAdV-C5 pV is a novel target of the host SUMOylation machinery.....	84
4.3.1.	HAdV-C5 pV is post-translationally modified with SUMO proteins.....	84
4.3.1.1.	HAdV-C5 pV is modified with SUMO2 chains in transient transfection of HeLa cells .....	85
4.3.1.2.	The SUMO2 modification of pV occurs weakly during HAdV-C5 infection .....	87
4.3.1.3.	HAdV-C5 pV can be modified with SUMO1 <i>in vitro</i> .....	90
4.3.2.	<i>In silico</i> analysis reveals several SCM within HAdV-C5 pV, enabling the generation of putative pV SUMO mutants.....	91
4.3.3.	Mutation of the three SCM within HAdV-C5 pV alters the pattern of the proteins SUMO2 chain modification.....	96
4.3.4.	Mutation of the three SCM within HAdV-C5 pV alters the subcellular distribution of the viral protein .....	100
4.4.	The role of pV-SUMOylation during the course of HAdV-C5 infection.....	105
4.4.1.	Alterations in the three SCM within pV leads to reduced SUMO2-modifications of the protein during HAdV-C5 infection .....	105
4.4.2.	Viral replication is not significantly influenced by the lack of SCM within HAdV-C5 pV in H1299 cells .....	108
4.4.3.	The concentrations of different viral proteins are elevated during HAdV-C5 pV-SCM mutant infection in H1299 cells.....	109
4.4.4.	The replication cycle of the HAdV-C5 pV-SCM mutant is accelerated compared to the wildtype virus .....	

## CONTENT

---

in HepaRG cells.....	112
4.4.4.1.    Viral mRNA concentrations are elevated during HAdV-C5 pV-SCM mutant virus infection.....	114
4.4.4.2.    The lack of SCM within HAdV-C5 pV does not influence the subcellular distribution of early adenoviral proteins, whereas mutated pV shows a lower affinity to host nucleoli .....	117
4.4.4.3.    Viral DNA-replication is significantly enhanced at early time points during HAdV-C5 pV-SCM mutant virus infection .....	121
4.5.    The role of HAdV-C5 pV in oncogenic transformation processes.....	122
4.5.1.    The presence of HAdV-C5 pV represses the transformation of primary BRK cells mediated by the E1A proteins and E1B-55K of HAdV-C5 .....	123
4.5.1.1.    A cell line BRK-ABV derived by pBRK cells co-transfected with HAdV-C5 E1A, E1B-55K and pV expressing plasmids shows no sign of a classical E1-mediated transformation .....	125
4.5.2.    Inclusion of the whole HAdV-C5 E1-region cannot prevent the inhibitory effect of pV on the focus formation of pBRK cells.....	129
4.5.2.1.    Colony formation of pBRK cells is not inhibited due to SCM within HAdV-C5 pV.....	130
4.5.2.2.    The focus formation of pBRK cells induced by HAdV-C5 E1-gene products depends on the concentration of present pV .....	131
4.5.2.3.    The flag-tag fused to HAdV-C5 pV is not responsible for its inhibitory effect on pBRK cell transformation in the presence of adenoviral E1-oncogenes .....	133
4.5.3.    The number of pBRK cells positive for the HAdV-C5 proteins E1A, E1B-55K and pV remains low during the first 10 d p.t. ....	134
4.5.4.    The number of human tumor cells HEK293 and HeLa is drastically reduced after transient transfection with a flag-pV expression plasmid .....	139
5    Discussion.....	141
5.1.    The lack of consensus SUMO conjugation motifs within HAdV-C5 pV accelerates viral replication.....	141
5.1.1.    Mutational alteration of the pV primary structure could result in conformational changes within the protein, which might further influence its function and HAdV-C5 virion integrity .....	144
5.1.2.    Post-translational modification of HAdV-C5 pV might not be restricted to SUMOylation.....	147
5.2.    HAdV-C5 pV associates with nucleoli of the infected host.....	150
5.2.1.    HAdV-C5 pV might interact with PML containing structures like PML-NBs or centrosomes .....	152
5.3.    HAdV-C5 pV prevents E1-region mediated transformation of primary rat cells .....	153
5.3.1.    The inhibitory capacity of HAdV-C5 pV does not rely on the SUMOylation of the protein .....	155
5.3.2.    The co-expression of adenoviral E1-oncoproteins and pV might be lethal to mammalian cells.....	155
6    Literature .....	159
7    Publications .....	191
7.1.    Publications in scientific journals.....	191
7.2.    Presentations at scientific meetings.....	191
8    Declaration on oath/Eidesstattliche Versicherung	
9    Acknowledgements/Danksagung	

## Zusammenfassung

---

Humane Adenoviren sind nicht behüllte, ikosaedrische DNA Viren. Um replizieren zu können, müssen sie ihr lineares, doppelsträngiges Genom in den Zellkern der infizierten Wirtszelle transportieren. Der Import erfolgt durch eine Kernpore, wobei die virale DNA mit einigen ihrer schützenden Coreproteinen komplexiert bleibt. Obwohl humane Adenoviren 13 unterschiedliche Proteine in die Wirtszelle einbringen, sind deren Funktionen während der produktiven Virusinfektion weitgehend unbekannt. Das Coreprotein V (pV) beispielsweise, bindet, wie auch die übrigen Coreproteine, sequenzunabhängig an das virale Genom. Es wird angenommen, dass pV den innen liegenden Viruskern mit dem umliegenden Proteincapsid verbindet und so zur Stabilität infektiöser Adenoviruspartikel beiträgt. Protein V findet sich im Nukleoplasma infizierter Zellen und akkumuliert an deren Nukleoli. Seine Funktion in diesen Zellkompartimenten ist jedoch immer noch unbekannt.

Die Primärstruktur von pV des humanen Adenovirus Typ 5 der Spezies C (HAdV-C5) enthält eine Vielzahl von Motiven für eine kovalente Bindung von SUMO Proteinen an pV. In der vorliegenden Arbeit konnte diese post-translationale Modifikation von pV erstmals bestätigt werden. Eine Veränderung der identifizierten Konsensusmotive für die kovalente SUMO-Bindung im Protein V, die durch Punktmutationen in der kodierenden DNA herbei geführt wurde, resultierte dagegen in einer drastischen Reduktion der Protein-SUMOylierung. Um die Bedeutung der pV-SUMOylierung für den Verlauf adenoviraler Infektionen zu untersuchen, wurde eine HAdV-C5 Virusmutante generiert, in der vier mögliche Motive für die kovalente SUMO-Bindung verändert wurden (HAdV-C5 pV-SCM). Wie die Ergebnisse dieser Arbeit zeigen, beeinflussen diese Mutationen vor allem die frühe Phase der Infektion. Im Vergleich zum HAdV-C5 Wildtyp, ist die virale Genexpression während einer Infektion mit der pV-SCM Virusmutante sowohl auf transkriptioneller als auch auf translationaler Ebene beschleunigt. Gleiches gilt für die virale DNA-Replikation und die Bildung infektiöser Virusnachkommen.

Besonders auffällig ist die höhere Konzentration viraler DNA in humanen Wirtszellen bereits 1 h nach der Infektion mit der pV-SCM Virusmutante. Der Verlust distinkter SUMO-Modifikationen von pV könnte demnach schon während der Eintrittsphase für HAdV-C5 von Nutzen sein. Allerdings führte die Limitierung der pV-SUMOylierung auch zu einer verminderten Assoziation des Proteins mit den Nukleoli der Wirtszelle. Ein Verlust der SUMO-Konsensusmotive im pV scheint folglich Auswirkungen auf unterschiedliche Vorgänge

während der adenoviralen Infektion zu haben. Die SUMOylierung von viralen Proteinen durch die Wirtszelle könnte somit einen Teil der intrinsischen Virusabwehr humaner Zellen repräsentieren.

HAdV werden als Vektoren in der Gentherapie eingesetzt und sind von großem Interesse für die Entwicklung onkolytischer Viren. Für gewöhnlich verursachen HAdV milde Infektionen, die von Patienten mit einem intakten Immunsystem erfolgreich bekämpft werden können. Einige Virustypen der Spezies A und D sind jedoch in primären Nagerzellen tumorigen. Des Weiteren wurden Virusgenome von Spezies C-Typen in Lymphozyten detektiert, die humane Sarkome infiltrieren. Gerade adenovirale Vektoren zählen weltweit zu den am häufigsten eingesetzten Vektoren. Diese Vektoren rufen starke Immunantworten im Patienten hervor, welche möglicherweise durch die hohen Konzentrationen eindringender Capsidproteine ausgelöst werden. Es stellte sich deshalb die Frage, ob diese mitgeführten, adenoviralen Proteine auch Prozesse beeinflussen könnten, die eine Transformation infizierter Wirtszellen begünstigen.

Im Zuge dieser Arbeit wurde HAdV-C5 pV jedoch als potenter Inhibitor der onkogenen Transformation primärer Nierenzellen von Babyratten (pBRK) identifiziert, welche durch die E1 Onkoproteine des HAdV-C5 vermittelt wird. Ursächlich dafür könnte ein pV-induzierter Zelltod sein. Die vorliegenden Ergebnisse zeigen, dass die Anzahl an pV plus E1-exprimierenden pBRK-Zellen von Beginn an klein ist und stetig abnimmt. Die Anzahl an pBRK-Zellen, welche ausschließlich pV exprimieren, reduziert sich ebenfalls, ist jedoch zu Beginn des Experiments höher. Diese Reduktion der transfizierten Zellen scheint deshalb aus dem Zusammenspiel von HAdV-C5 pV und E1 Onkoproteinen zu resultieren. Der Effekt könnte sich außerdem auf proliferierende Zellen beschränken. Sollte pV einen Spezies C spezifischen Antagonisten der humanen Zelltransformation darstellen, könnte dies zu einer Verhinderung adenoviral induzierter Tumore im Menschen beitragen. Beschränkt sich der pV-induzierte Zelltod ferner auf proliferierende Zellen, könnte sich pV als interessantes Zielmolekül für die translationale Krebsforschung erweisen.

## Abstract

---

Human adenoviruses (HAdV) are large, non-enveloped viruses containing a linear, double-stranded DNA genome surrounded by an icosahedral capsid. To allow proper virus replication, the genome has to be transported into the host nucleus. It is imported through the nuclear pore complex and still associated with viral core proteins. However, the role of most incoming virion proteins during the early phase of infection is poorly understood. The minor core protein V (pV) is speculated to bridge the core and the surrounding protein capsid. It binds the viral genome in a sequence independent manner and localizes in the nucleus of infected cells where it accumulates at the nucleoli.

This work shows that human adenovirus type 5 (HAdV-C5) pV contains several SUMO (small ubiquitin-like modifier) conjugation motifs. Moreover, the protein is extensively modified with SUMO proteins indeed. Mutation of the consensus SUMO conjugation motifs (SCM) within pV resulted in reduced SUMOylation of the protein. To understand the role of pV-SUMOylation during productive adenovirus infection, we generated a HAdV-C5 mutant virus with four putative SCM being altered. Our data obtained from phenotypic analyses revealed that the mutation of pV-SCM is beneficial for early viral replication. The expression of several viral genes is accelerated during mutant virus infection on transcriptional as well as on translational levels. Likewise, viral DNA-replication peaks earlier during pV-SCM mutant virus infection. This faster proceeding of adenoviral infection is accompanied by a more efficient proteasomal degradation of cellular substrates, such as p53. Finally, it results in an increase of HAdV-C5 progeny. Remarkably, already 1 h after infection, more viral DNA was found in cells infected with HAdV-C5 pV-SCM, indicating a benefit of the mutant virus during entry processes. However, inactivation of pV-SCM decreases the proteins host nucleoli association as well.

Hence, the lack of SCM within pV might influence different processes during the adenoviral course of infection. SUMOylation of HAdV-C5 pV by the host SUMOylation machinery could be an important aspect of the cellular antiviral strategy to limit virus replication.

HAdV are of great interest as vectors for gene therapy and for the generation of oncolytic viruses. Usually, HAdV cause mild infections, which patients without immunodeficiency can easily control. However, some HAdV of species A and D are known to induce tumors in rodents and adenoviral genomes of species C could be found in infiltrating lymphocytes of human

sarcoma. Adenoviral vectors emerged to one of the most commonly used vectors worldwide. Most of those in clinical trials or already in clinical use are modified species C types of HAdV. These vectors, however, provoke a strong immune response in patients, which is expected to be caused by high titers of incoming viral proteins. Accordingly, we were interested in the question whether these incoming virion proteins might even cause or support transformation processes.

On the contrary, we found that pV is able to suppress the oncogenic transformation of primary baby rat kidney cells (pBRK) by the HAdV-C5 E1-region. This might be a consequence of an early cell death induced by the presence of HAdV-C5 pV. It remains to be clarified, whether this reduced cell survival requires the presence of adenoviral E1 oncoproteins or functional homologs, such as E6 and E7 of human papilloma virus (HPV). This data show that pBRK cells, which express E1 oncoproteins plus pV are rare, whereas pBRKs only expressing pV are more frequent.

If pV represents a transformation antagonist of HAdV-C types, this might explain their non-tumorigenicity. Moreover, HAdV-5 pV could be an interesting target for translational research in cancer therapy, if it specifically targets proliferating cells for cell death.

# Abbreviations

---

aa	amino acid
ab	antibody
AIDS	acquired immune deficiency syndrome
APSSP	advanced protein secondary structure prediction server
APS	ammonium persulfate
ARF	ADP ribosylation factor
ATM	ataxia telangiectasia mutated protein
ATP	adenosine triphosphate
AVP	Adenovirus protease
Bax	Bcl-2-like protein x
Bcl-2	B-cell lymphoma 2
bp	base pair
BSA	bovine serum albumin
C23	nucleolin
CAR	coxsackie/adenovirus-receptor
CDK	cyclin dependent kinase
cDNA	complementary DNA
cds	coding sequence
CMV	cytomegalovirus
CR	conserved region
CTL	cytotoxic T-lymphocytes
dapi	4', 6'-diamidine-2-phenylindole dihydrochloride
Daxx	death domain-associated protein 6
dd	double distilled
DDR	DNA damage response
DeSI	de-SUMOylating isopeptidase
DMEM	Dulbecco's modified eagle medium
DMSO	dimethyl sulfoxide
dNTP	desoxyribonucleoside-5'-triphosphat
ds	double-stranded
DTT	dithiotreitol
DUB	de-ubiquitinating enzyme
E	early

## ABBREVIATIONS

---

ECL	enhanced chemiluminescence
<i>E. coli</i>	<i>Escherichia coli</i>
EDTA	ethylenediaminetetraacetic acid
<i>et al.</i>	et alii/alia/aliae
EM	electron microscopy
FCS	fetal calf serum
ffu	fluorescence forming unit
Fig	figure
FITC	fluorescein isothiocyanate
fwd	forward
EGFP	enhanced green fluorescent protein
HA	human influenza virus hemagglutinin fragment
HAdV	human adenovirus
HEK	human embryonic kidney
HER	human embryonic retinoblasts
HIV	human immunodeficiency virus
h p.i.	hours post infection
h p.t.	hours post transfection
HRP	horseradish peroxidase
HSV-1	Herpes simplex virus type 1
IDP	internal disordered protein
IFN	interferon
Ig	immunoglobulin
IP	immunoprecipitation
ISG	interferon stimulated gene
<i>I-TASSER</i>	Iterative Threading ASSEMBly Refinement
ITR	inverted terminal repeat
<i>Jassa</i>	Joined Advanced Sumoylation Site and Sim Analyser
kb	kilo bases
L	late
LB	<i>Luria Bertani</i>
m	monoclonal, messenger (dependent on context)
MDM2	mouse double minute 2 homolog
MHC	major histocompatibility complex
MLP	major late promoter
MLTU	major late transcription unit
moi	multiplicity of infection

## ABBREVIATIONS

---

Mre11	meiotic recombination 11 homolog 1
MRN	Mre11-Rad50-Nbs1
NB	nuclear body
NEM	N-ethylmaleimide
NES	nuclear export signal
NLS	nuclear localization signal
NoLS	nucleolar localization signal
NOR	nucleoli organizer region
NPC	nuclear pore complex
NPM1/B23	nucleophosmin
nSCM	non-consensus SUMO conjugation motif
nt	nucleotide
OD	optical density
orf	open reading frame
ori	origin of replication
p/pp	polyclonal or protein/precursor protein
PBS	phosphate buffered saline
PCR	polymerase chain reaction
PEI	polyethylenimine
PFA	paraformaldehyde
PML	promyelocytic leukemia protein
Pol	polymerase
PAGE	polyacrylamide gel electrophoresis
PTM	post-translational modification
QC	quick-change
r	ribosomal
Rad	DNA repair protein
Rb	retinoblastoma protein
RBCC	RING, B-Box, coiled-coil domain
RBP	RNA-binding protein
rev	reverse
RHDV	rabbit hemorrhagic disease virus
RLU	relative luciferase unit
rpm	rounds per minute
RRM	RNA-recognition motif
RT	real time
S	sedimentation coefficient in Svedberg units

## ABBREVIATIONS

---

SAE	SUMO activating enzyme
SCM	consensus SUMO conjugation motif
SDS	sodium dodecyl sulfate
SENP	septrin specific protease
SIM	SUMO interacting motif
Sp100	speckled protein 100
SUMO	small ubiquitin-like modifier
SV40	simian virus 40
TBS	Tris-buffered saline
TEMED	N, N, N', N'-tetramethylethylenediamine
tM	thresholded Mander's coefficient
TP	terminal protein
TRIM	tripartite motif
Tris	Tris-(hydroxymethyl)-amino methane
UBF	upstream binding factor
UBL	ubiquitin-like modifier
ULP	ubiquitin-like protease
USP	ubiquitin specific protease
VA	virus-associated
VP1	virion protein 1

# 1 Introduction

---

## 1.1. Adenoviruses

Human adenoviruses (HAdVs) were first isolated from adenoid tissue in 1953 (Hillemann & Werner, 1954; Rowe *et al.*, 1953), leading to their present designation (Enders *et al.*, 1956). Adenoviruses show a great tissue tropism, whereby the primary target are terminal differentiated epithelial cells (Boyer *et al.*, 1959). This results in a broad spectrum of clinical symptoms where adenoviruses can be the causative agent of keratoconjunctivitis (Centers for Disease, 2013; Jawetz, 1959), upper and lower respiratory infections (Dingle & Langmuir, 1968; Ginsberg *et al.*, 1955), gastroenteritis (Celik *et al.*, 2015; Chhabra *et al.*, 2013) or infections of the urinary tract (cystitis) (Hofland *et al.*, 2004; Numazaki *et al.*, 1973). Usually, an adenoviral infection proceeds mildly and is self-limiting. In rare cases, however, the course of infection can be severe, leading to the development of pneumonia (Chen *et al.*, 2013; Esposito *et al.*, 2013; Lewis *et al.*, 2009), meningoencephalitis (de Ory *et al.*, 2013), myocarditis (Savón *et al.*, 2008; Shauer *et al.*, 2013; Treacy *et al.*, 2010) or hepatitis (Detrait *et al.*, 2015). Worst affected by such complications are newborns or immunocompromised patients (Berciaud *et al.*, 2012; Hierholzer, 1992; Krilov, 2005; Lion, 2014), suffering from AIDS or being a recipient of an organ transplant for example (Lenaerts *et al.*, 2008). The latter delineates a serious problem, since there is still no specific treatment available against adenoviral infections. Hence, the therapy during severe infection courses can only be symptomatic and not uncommonly results in the death of a patient (Lion *et al.*, 2003, 2010; Savón *et al.*, 2008; Treacy *et al.*, 2010). Lately, adenoviral infections have been even linked to a non-inflammatory condition, which is obesity (Esposito *et al.*, 2012; Shang *et al.*, 2014).

The majority of HAdV infections occur during childhood and there is evidence that adenoviruses can persist during young age, whereas viral titers decline while growing up. The affected tissue has not been identified yet, however, lymphocytes have emerged as candidate for adenoviral persistence (Garnett *et al.*, 2002, 2009; Rodríguez *et al.*, 2017; Roy *et al.*, 2011). A persistent adenovirus infection is not only a threat in case of immunosuppression, but might be in regard of tumor development as well. In 1962, the first human adenovirus HAdV-A12 was postulated as being oncogenic, as it was able to induce tumors in newborn hamsters (Trentin *et al.*, 1962). Moreover, DNA of adenovirus B and D types could be detected in different pediatric brain tumors (Kosulin *et al.*, 2007). Besides the adenoviral genome of

predominantly C types was found in infiltrating T-lymphocytes within different human sarcomas (Kosulin *et al.*, 2013). Nevertheless, it remains an open question, whether adenoviruses could really be the causative agents of these or other human tumors. Its solvation, however, is of great importance, since adenoviral vectors are commonly used as tools for gene delivery as well as to design oncolytic viruses (Crystal, 2014). Undoubtedly, the numerous investigations of adenovirus biology during the past half century contributed massively to the present understanding of virus-host interactions and cellular mechanisms in general. The most prominent discovery is probably the process of mRNA splicing (Bachenheimer & Darnell, 1975; Berget & Sharp, 1977; Chow *et al.*, 1977; Sharp, 1994).

### 1.1.1. Classification

To date the family of *Adenoviridae* comprises more than 100 different types. Depending on their host range the adenovirus family is divided into five genera, which are approved by the International committee on Taxonomy of Viruses (ICTV) (Harrach *et al.*, 2012). *Mastadenoviruses* are infecting mammalian hosts, thus they include human adenoviruses as well. *Aviadenoviruses* infect only avian hosts, whereas *Atadenoviruses* can infect reptiles and ruminants. *Siadenoviruses* infect exclusively amphibian hosts (Benkő & Harrach, 1998, 2003; Davison *et al.*, 2003) and *Ichtadenoviruses* comprise only one type so far, which was isolated from a sturgeon (Benkő *et al.*, 2002). The different genera are further subdivided into different species, which are 27 in case of *Mastadenoviruses* (Harrach *et al.*, 2012). These comprise the seven human adenovirus species A-G, containing at least 70 different adenovirus types (Table 1) (Gerd Liebert *et al.*, 2015; Harrach *et al.*, 2012), whereby putative new types are discovered frequently (Yoshitomi *et al.*, 2016).

Homologous recombination (HR) and mutation are important evolutionary processes driving genetic variation within HAdV genomes. The majority of new types are classified in species D. Many of them were shown to contain sequences from various other types of the same species. Hence, HAdV-D genomes seem to recombine more frequently than other human adenoviral species, whereby the recombination between hexon and fiber coding regions is remarkable (Robinson *et al.*, 2013). Types 1-51 were characterized by serotyping, depending on their hemagglutination and serum neutralization characteristics, as it was common until 2007 (Bailey & Mautner, 1994; Davison *et al.*, 2003; Wadell, 1984). The assignment to a certain species further depends on the phylogenetic distance of adenovirus types, their genome organization, nucleotide composition (GC-content), number of VA RNA genes and their oncogenicity in

rodents (Table 1) (Graham, 1984; Harrach *et al.*, 2012; Shenk, 2001). Newer adenovirus types have been mainly detected and described by genomic and bioinformatics analyses, leading to the agreement to replace the term ‘serotype’ by ‘type’ (Aoki *et al.*, 2011; Harrach *et al.*, 2012; Jones *et al.*, 2007; Lion, 2014; Liu *et al.*, 2011; Robinson *et al.*, 2011; Seto *et al.*, 2011).

### Human adenoviruses (HAdVs)

Species	A	B	C	D	E	F	G
<b>Type</b>	12, 18, 31, <i>61</i>	3, 7, 11, 14, 16, 21, 34, 35, 50, 55, 66, 68	1, 2, 5, 6, <i>57</i>	8-10, 13, 15, 17, 19, 20, 22-30, 32, 33, 36-39, 42- 49, 51, 53, 54, 56, 58- 60, 63-67, 69, 70	4	40, 41	52
<b>Oncogenicity</b>	<b>highly oncogenic</b> undifferentiated sarcomas, fibroadenomas	<b>oncogenic</b> undifferentiated sarcomas, retinoblastomas	<b>not oncogenic</b>				
				<b>highly oncogenic: 9, 10</b> mammary tumors in female rats			

**Table 1: Classification of human adenoviruses.**

Assignment of the 70 published types of HAdVs to species A-G. Types 1-51 were classified by serotyping (Davison *et al.* 2003) as well as oncogenicity, including the type of induced tumors in rodents (Shenk, 2001). HAdV types 52-70 (italic letters) are mapped according to the classification of the ICTV (international committee on taxonomy of viruses) (Harrach *et al.*, 2012). These have not been classified concerning their oncogenicity.

Most adenoviral species circulate globally, whereby their abundance can differ between countries, or geographic regions as well as it can change over time. Worldwide, the adenoviruses mostly connected with human disease are HAdV-C1, -C2, -C5, -B3, -B7, -B21, -E4 and -F41 (Lion, 2014). Especially HAdV-C types are reported to cause severe complications in immunocompromised transplant patients (Lion *et al.*, 2010).

#### 1.1.2. Structure and genome organization

HAdVs are non-enveloped, icosahedral viruses with a diameter of ~90 nm and a mass of ~150 MDa (Berk, 2007; van Oostrum & Burnett, 1985; Stewart *et al.*, 1991). Each facet of the icosahedral protein capsid (Horne *et al.*, 1959) is formed by 12 trimers of the polypeptide II, resulting in 240 hexon capsomers having a pseudo six-fold hexagonal base (Burnett *et al.*, 1985). The vertices are built from a pentamer of polypeptide III, which has been termed the

penton base. It is complexed with a trimer of polypeptide IV, the fiber protein, which is projecting from the vertices of the icosahedron (Fig. 1). Thus, the adenoviral capsid corresponds to a pseudo- $T = 25$  symmetry (San Martín, 2012).

It is further stabilized by the minor capsid proteins IIIa, VI, VIII and IX, whereby the roman numbers correspond to their order of decreasing molecular weight (Ginsberg *et al.*, 1966; Maizel *et al.*, 1968). These proteins are also termed ‘capsid cement’ or ‘capsid glue’, as they contribute to the stabilization of hexon and penton interfaces (Everitt *et al.*, 1973; Fabry *et al.*, 2005; Furcinitti *et al.*, 1989; van Oostrum & Burnett, 1985; Liu *et al.*, 2010; San Martín *et al.*, 2008; San Martín, 2012). Although not essential for adenoviral assembly, pVIII and pIX deletion mutants present lower thermostability (Colby & Shenk, 1981; Liu *et al.*, 1985). Besides, pIX is the only minor capsid protein with at least one domain exposed on the capsid surface. Hence, it is speculated to interfere with the host immune system and/or to play a role in modulating adenoviral tropism. This made it a valuable target for adenoviral vector generation, imaging and immunization (Parks, 2005; de Vrij *et al.*, 2011).

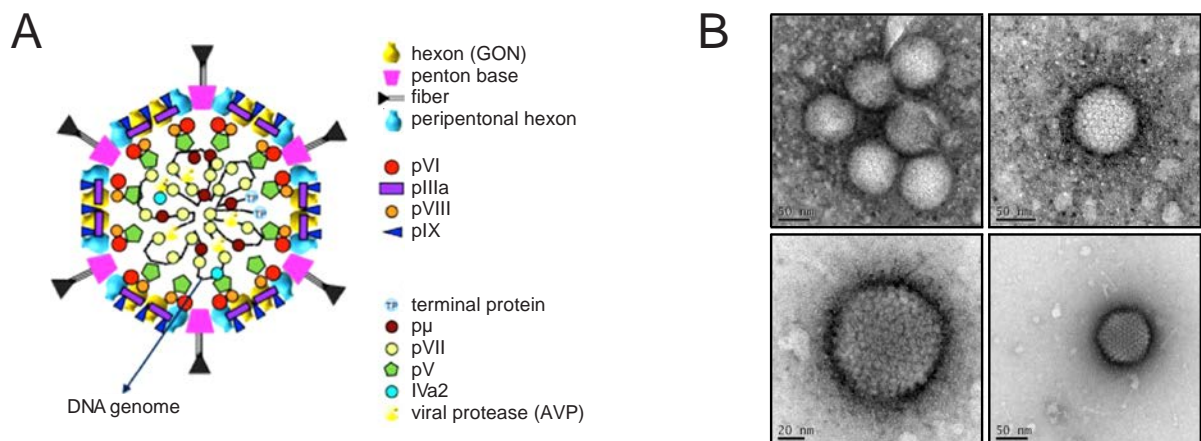


**Figure 1: Structure and organization of HAdVs.**

**A** Schematic illustration of the human adenovirus profile. The indicated locations of the proteins (depicted in different colors and with different symbols) are proximate. The corresponding protein names are listed on the *right*. The depicted protein distribution corresponds to the current model resembling the X-ray studies (adapted from Reddy & Nemerow, 2014b). **B** Electron microscope images illustrating the icosahedral structure of adenoviral particles as well as the sub-structuring into multiple capsomers (Department of Electron Microscopy, Heinrich-Pette-Institute, Leibniz Institute for Experimental Virology, Hamburg).

Based on X-ray crystallography, a differing structure is currently proposed for HAdVs. Both studies (X-ray and Cryo-electron microscopy (EM)) mainly rely on HAdV-C5 and vary the most regarding the distribution of the minor capsid proteins (Campos, 2014; Condezo *et al.*, 2015; Reddy & Nemerow, 2014a, b). In X-ray studies, pIIIa is stated to be located at the icosahedral edges on the outer surface of the viral capsid according (Reddy *et al.*, 2010), a

position exclusively assigned to pIX after Cryo-EM analysis (Liu *et al.*, 2010). In turn, the suggested pIIIa pinwheel (Liu *et al.*, 2010) underneath the vertices from Cryo-EM analysis is proposed to be five copies of a ternary complex between pVI, pVIII and minor core protein V instead (Reddy *et al.*, 2010). In this complex, pVI and pVIII are postulated to glue the peripentonal hexons, whereas pV interacts only with pVI and pVIII. (Reddy & Nemerow, 2014a). This function of pV to bridge the inner viral core, which it belongs to, with the surrounding capsid shell through interaction with pVI has been proposed already in previous work (Chatterjee *et al.*, 1985; Matthews & Russell, 1998a; Moyer & Nemerow, 2012; Saban *et al.*, 2006).

The adenoviral core contains the linear, double-stranded DNA genome with a size of 26-45 kb depending on the type and species. In case of HAdV-C5, it amounts 36 kb. This genome is assumed to be condensed in a nucleosome-like state through the association with the basic core proteins VII, V and  $\mu$  (Chatterjee *et al.*, 1985, 1986a, b, c; Corden *et al.*, 1976; Giberson *et al.*, 2011; Mirza & Weber, 1982; Pérez-Berná *et al.*, 2015; Vayda *et al.*, 1983). Additionally, the terminal protein (TP) covalently binds to the free 5'-ends of the linear viral genome (Girard *et al.*, 1977; Rekosh *et al.*, 1977). So far, no specific order or symmetry could be assigned to the adenoviral core. The 'adenosomes' seem to exist as a fluid of soft repulsive spheres without a defined DNA backbone (compare section 1.1.4) (Pérez-Berná *et al.*, 2015). Furthermore, the adenoviral core contains four to six copies of the protein IVa2, being involved in the genome encapsidation and six to eight copies of the viral cysteine protease 23 (AVP), which is necessary for the maturation of viral particles (compare section 1.1.3.3) (Benevento *et al.*, 2014; van Oostrum & Burnett, 1985).

Adenoviral genomes are characterized by an inverted terminal repeat (ITR), which is located at their 5'-ends and ranges from 36-200 bp in size, depending on the adenovirus type. The terminal 18 bp of the ITRs represent the minimal required origin of replication (*ori*), whereby four regions within the terminal 50 bp of the HAdV-C2 genome contribute to *ori* activity (Hay, 1996; Stillman *et al.*, 1982). A cis-acting packaging sequence is located next to the left ITR to direct the proper packaging of the viral genome into virions (Gräble & Hearing, 1992; Hearing *et al.*, 1987). The species within different adenovirus genera share a comparable genome organization, thus HAdVs express the same general genes, which are located at comparable positions on the viral chromosomes (Berk, 2007; Davison *et al.*, 2003). They comprise nine transcription units, the early units E1A, E1B, E2, E3 and E4, the intermediate units pIX and IVa2, as well as one major late transcription unit (MLTU) and the late transcription unit encoding the U exon protein



transcribed from E2B) by use of the same promoter E2 early (E2E) (Baker & Ziff, 1981; Chow *et al.*, 1979; Stillman *et al.*, 1982, 1981). Thus, E2 encodes the essential proteins for viral DNA-replication (Hay, 1996; de Jong *et al.*, 2003). In order to grant the need of large DBP amounts during viral DNA-replication, the E2A region has an additional E2 late (E2L) promoter, which is activated delayed (Baker & Ziff, 1981; Bhat *et al.*, 1987; Chow *et al.*, 1979). The E3 transcription unit is embedded within the MLTU. It generates at least nine mRNAs by processing of two precursor transcripts with different poly (A) sites. They are translated into seven known E3 proteins (Wold *et al.*, 1995). In case of E4, even 24 different mRNAs sharing the same 5'- and 3'-termini have been reported, although only six corresponding polypeptides could be identified so far. They are named after the open reading frames (orf) contained within E4 as E4orf1, E4orf2, E4orf3, E4orf4, E4orf6 and E4orf6/7 (Virtanen *et al.*, 1984).

### **1.1.3. The adenoviral life cycle**

As indicated by the designation of the adenoviral transcription units, the replication cycle of HAdVs is divided into an early and a late phase of infection. The early phase ranges from the adsorption of the virus at the cell surface to the expression of an early set of genes encoded by E1-E4 (compare section 1.1.2) (Berk, 2007; Green & Daesch, 1961). Depending on the cell type, this takes six to 12 h in infected tumor cell lines, whereas it is prolonged in human diploid cells. During the early phase of infection, the main goal of the virus is to create an environment with proper conditions for its replication. To achieve this, fully differentiated, resting cells have to be driven from G1 or G0 into S-phase. This is mediated predominantly by E1A and E4 gene products and is accompanied by the induction of cellular DNA synthesis, which is essentially required for viral DNA replication as well (see section 1.1.3.2). To provide the equipment for an efficient adenoviral DNA-replication, the gene products of the E2 region are expressed (compare section 1.1.2). At the same time, the virus has to protect its genome from being recognized and cleared by the host cell through various antiviral defense mechanisms, such as induction of apoptosis. This protection is mediated predominantly by E1B and E4 gene products (see section 1.1.3.2), whereas the E3 proteins antagonize the immune signaling of the infected host to prevent the recruitment of natural killer cells, macrophages or cytotoxic T lymphocytes (CTLs) (Burgert *et al.*, 1987; Ginsberg *et al.*, 1989; Windheim *et al.*, 2004). A vast number of proteins on the viral as well as on the host cell side is involved in this interplay of creating an environment for proper adenoviral replication and preventing exactly this, respectively (Berk, 2007).

With the onset of viral DNA replication the late phase is initiated, which focuses on expression of late viral genes from the MLTU. It encodes mainly structural proteins and regulatory proteins with functions assigned to the generation of factors, which are required for the proper assembly, stabilization and maturation of viral progeny. Indeed, early and late phase of infection are not clearly separated. Early genes are still expressed at low levels during the late phase, whereas proteins IVa2 and IX are expressed during an intermediate stage. In addition, the major late promoter (MLP) is active at low level early after infection. After 24-36 h, about  $10^4$  infectious particles have been produced and are released into the environment by lysis of the primary infected cell (Fig. 3). Although the replication cycle of different HAdVs was observed to be similar, it has to be kept in mind that most of the studies regarding the replication cycle of adenoviruses have been done with HAdV-C types (Berk, 2007).

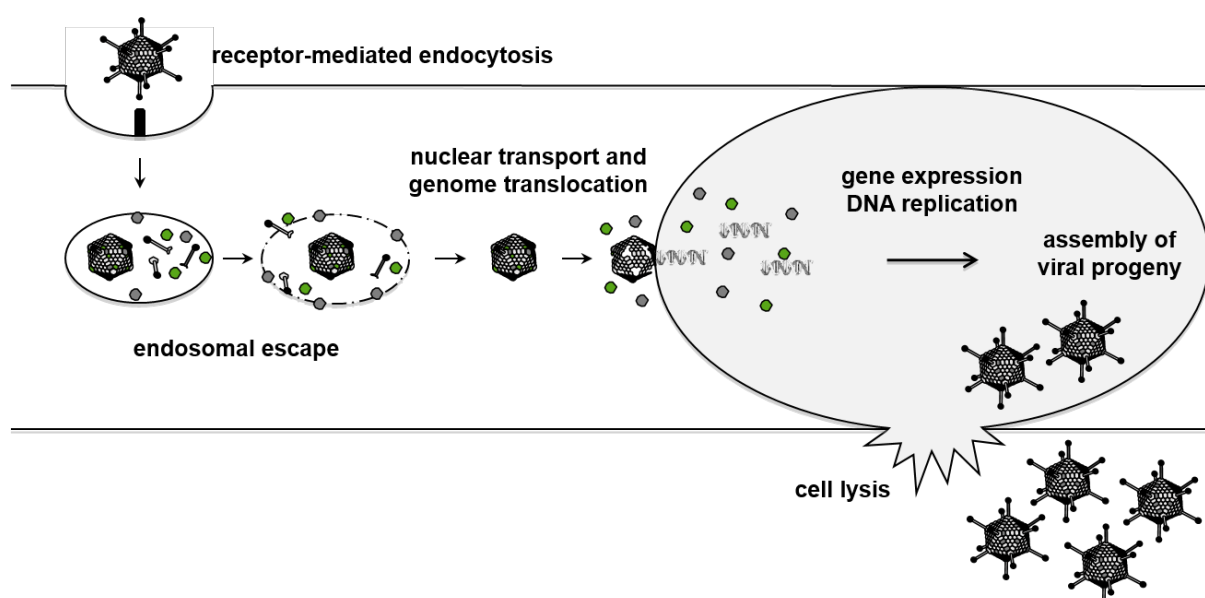


**Figure 3: Schematic illustration of the life cycle of HAdVs.**

The adenoviral life cycle starts with the receptor-mediated uptake of the virus into clathrin-coated, early endosomes. Endocytosis is accompanied by partial coating of the virions, which enables the endosomal escape through release of the membrane-lytic capsid protein VI. Upon arrival in the cytosol, adenoviral virions are transported to the nucleus via microtubules. At the nuclear pore complex, the virions finally disassemble and the viral genome is translocated into the host nucleus. Within the nucleus, the transcription of early viral genes is initiated, followed by replication of the viral genome, the expression of late and structural proteins and finally the assembly of viral progeny. After production of around  $10^4$  new infectious particles, the infected host cell is lysed to release them.

### 1.1.3.1. Adsorption and entry

The primary receptor for most HAdVs is CAR (Coxsackie/Adenovirus-receptor), which is a component of epithelial tight junctions and abundantly expressed in various human tissues (Bergelson *et al.*, 1997; Lonberg-Holm & Philipson, 1969; Roelvink *et al.*, 1998; Walters *et al.*,

2002). HAdVs bind the CAR receptor through the C-terminal knob domain of the projecting fiber protein. This first interaction is followed by an interaction between a flexible loop, the RGD-motif, on the penton base and  $\alpha_v$ -integrins on the cell surface (Stewart *et al.*, 1997; Wickham *et al.*, 1993). Thereby HAdVs provoke a signaling cascade, which promotes the viral uptake into clathrin-coated, early endosomes (Greber *et al.*, 1993; Li *et al.*, 1998a, b; Wang *et al.*, 1998a). The endocytosed viral particles are fiberless (Martin-Fernandez *et al.*, 2004) and it was shown that the controlled uncoating of HAdVs is already initiated at the cell surface by mechanical forces, which are caused by the interplay between CAR drifting motion and binding of the virus to immobile integrins (Burckhardt *et al.*, 2011).

To escape the cellular immune response, HAdVs need to depart from the endosomes quickly. The mechanism proposed starts with further dismantling of the vertex region of the virus, whereby capsid protein VI (pVI) is released, apart from pentons, pIIIa and likely, the peripentonal hexons, pIX and pVIII (Greber *et al.*, 1993; Nguyen *et al.*, 2010; Smith *et al.*, 2010; Wiethoff *et al.*, 2005; Wiethoff & Nemerow, 2015). This process is accompanied by a drop in pH inside the endosome, which was assumed essential for the rupture of the endosome. However, pVI has the capacity to induce positive curvature in lipid bilayers through its N-terminal amphipathic helix region, which leads to their fragmentation (Maier *et al.*, 2010; Maier & Wiethoff, 2010; Martinez *et al.*, 2015; Moyer *et al.*, 2011). This ability is likely to enable the rupture of the endosomal membrane, which is to date assumed to be independent of a drop in pH (Suomalainen *et al.*, 2013).

Upon arrival in the cytosol, the partially uncoated virions associate with dynein motor proteins and are transported along microtubules to the microtubule organizing center (MTOC) in proximity to the nucleus (Bremner *et al.*, 2009; Dales & Chardonnet, 1973; Greber & Way, 2006; LeoPold *et al.*, 2000; Suomalainen *et al.*, 1999; Wodrich *et al.*, 2010). The interaction of virion proteins, especially hexon, with components of the nuclear pore complex (NPC) likely facilitates the final disassembly of the viral particles and the translocation of the viral genome into the nucleus of the infected host cell (Dales & Chardonnet, 1973; Greber *et al.*, 1997; Strunze *et al.*, 2005; Trotman *et al.*, 2001). To date, it is very certain that the viral DNA remains associated with the major core protein VII during this process. However, the role of p $\mu$  is completely unknown and minor core protein V seems more likely to enter the nucleus independently (Chatterjee *et al.*, 1986b, c; Hindley *et al.*, 2007a; Le *et al.*, 2006; Matthews & Russell, 1998a; Trotman *et al.*, 2001; Wodrich *et al.*, 2006).

### 1.1.3.2. The early genes E1 and E4

After the viral genome has reached the host cell nucleus, E1A is the first transcription unit expressed (compare section 1.1.2) (Nevins *et al.*, 1979). E1A-13S and E1A-12S are expressed early during infection, whereas the smaller isoforms 9S and 10S are increasing not until late phases of infection during which the levels of 13S and 12S decline (Radko *et al.*, 2015; Stephens & Harlow, 1987). The large E1A isoform (E1A-13S) is the main trans-activator of other viral genes (Dery *et al.*, 1987; Montell *et al.*, 1982; Winberg & Shenk, 1984). This function is mediated by its conserved region (CR) 3 that is missing in the E1A-12S protein. Since it is not able to bind DNA (Ferguson *et al.*, 1985), E1A-13S binds to numerous cellular transcription factors and DNA-binding activators instead, acting upstream of viral promoter and enhancer elements through the C-terminal end of CR3 (Berk *et al.*, 1979; Frisch & Mymryk, 2002; Lillie & Green, 1989; Liu & Green, 1994; Nevins, 1981; Pelka *et al.*, 2008; Wang & Berk, 2002). Yet, little is known about its influence on cellular transcription.

E1A-12S predominantly activates the transcription of the adenoviral E2 region (Bagchi *et al.*, 1990). This function is supported by another adenoviral early protein, which is E4orf6/7. This protein interacts with transcription factors of the E2F family, induces their dimerization and thereby increases their affinity for the inverted E2F binding site within the E2 early promoter (Douglas & Nevins, 1994; Marton *et al.*, 1990; Neill *et al.*, 1990; Neill & Nevins, 1991; Obert *et al.*, 1994). Generally, however, E1A-12S is considered as a transcriptional repressor. This function involves the N-terminal region, as well as the other conserved regions within the major E1A isoforms CR1, CR2 and CR4 (Kimelman *et al.*, 1985; van Ormondt *et al.*, 1980). E1A-12S has been shown to modulate about 10000 cellular promoters during adenoviral infection (Ferrari *et al.*, 2014). It causes a global redistribution of transcription factors and epigenetic markers on chromatin (Ferrari *et al.*, 2008, 2012). One example is the well-studied binding of E1A-12S to the family of retinoblastoma (Rb) proteins (Shenk, 2001), which suppress the activity of E2F family transcription factors by binding to their activation domains. E1A competes with this binding through an LxCxE-motif within CR2 in cooperation with the N-terminal ~10 aa of CR1 (Lee *et al.*, 1998; Liu & Marmorstein, 2007). This leads to the release of E2F and subsequently to the activation of E2F responsive genes (Bagchi *et al.*, 1990, 1991; Bandara & La Thangue, 1991; Ghosh & Harter, 2003). These comprise genes required for the S-phase entry, such as cyclin dependent kinase 2 (CDK2), cyclin A/E or c-myc (Blais & Dynlacht, 2004). This is a nice example how HAdVs elegantly activate all genes required for viral DNA-replication by mediating the activity of the same transcription factors.

To prevent the induction of apoptosis by the host cell, due to abnormal stimulation of cell growth, HAdVs additionally express the E1B as well as the E4 gene products. Among others, the tumor suppressor protein p53 is stabilized in response to E1A actions to mediate the induction of apoptosis (Querido *et al.*, 1997a). This is antagonized by adenoviruses in different ways. On the one hand the protein E1B-55K associates with another early viral protein E4orf6 and different cellular proteins to form an E3 ubiquitin ligase complex, which targets different cellular factors for proteasomal degradation (Querido *et al.*, 2001b). Among them are the mentioned p53 as well as Mre11 (meiotic recombination 11 homolog 1) and Rad50 (DNA repair protein Rad50). Both proteins are components of the MRN complex being involved in the sensing of DNA damage (Blanchette *et al.*, 2004; Carson *et al.*, 2003; Liu *et al.*, 2005; Querido *et al.*, 1997b; Steegenga *et al.*, 1998; Stracker *et al.*, 2002; Thomas *et al.*, 2016). Moreover, E1B-55K inhibits the transcriptional activation of p53 dependent genes through binding to the N-terminal activation domain of p53 (Teodoro & Branton, 1997; Yew & Berk, 1992). E4orf6 supports this function by interacting with p53 itself (Dobner *et al.*, 1996) as well as through inactivation of another protein of the p53 family, which is p73 (Higashino *et al.*, 1998; Steegenga *et al.*, 1999). This protein can partially compensate for the lack of p53 by activating transcription through p53 binding sites. Another gene product of the E1B-region is E1B-19K. This protein interferes with the induction of apoptosis through its binding to the proapoptotic Bcl-2 (B-cell lymphoma 2) family members Bak (Bcl-2 homologous antagonist/killer) and Bax (Bcl-2-like protein x). Being a Bcl-2 homologue, E1B-19K thereby prevents the co-oligomerization of these proteins, which would lead to the formation of pores in the outer mitochondrial membrane and a release of cytochrome c as well as other apoptotic proteins. The consequence would be an activation of caspases 3 and 9 and a subsequent apoptosis (Cory *et al.*, 2003; Cuconati *et al.*, 2002; Cuconati & White, 2002; White *et al.*, 1992).

A further important regulator of the adenoviral early phase is the E4orf3 protein. It redistributes PML nuclear bodies (PML-NBs) into ‘track-like’ structures to counteract their function as sites for post-translational modification (PTM) of proteins and for the assembly of protein complexes involved in the cellular DNA damage response (DDR) and apoptosis (compare section 1.2.1). Upon track formation, MRN accumulates in those PML structures (Evans & Hearing, 2005; Stracker *et al.*, 2002) and is subsequently translocated to cytoplasmic aggresomes where the degradation of its components is proposed to be facilitated (Liu *et al.*, 2005). In addition, it was recently shown that E4orf3 collaborates with E1B-55K. Together, these proteins can prevent a localized MRN-ATM response at the viral genome, which is proposed to be independent of the global DDR triggered by the formation of viral replication centers (Shah & O’Shea, 2015).

### 1.1.3.3. The late phase of infection

Accumulating E2 proteins TP, Pol and DBP initiate adenoviral DNA-replication (Challberg et al., 1982; Cleat & Hay, 1989; Lichy et al., 1982; Liu et al., 2003; Temperley & Hay, 1992), which is accompanied by a drastic increase of MLP activity and the following expression of the MLTU (Shaw & Ziff, 1980). Although E1A already contributes to an activation of the MLP (Parks & Shenk, 1997; Shaw & Ziff, 1980), it is assumed that its main activation requires a cis-acting change in the viral chromosome (Thomas & Mathews, 1980). Such a change would be initiated with the onset of viral DNA-replication and enhanced by virus-encoded transcription factors like the intermediate polypeptide IVa2 (Pardo-Mateos & Young, 2004; Tribouley et al., 1994). The tripartite leader on late transcripts contributes to a stimulation of viral late mRNA translocation to the cytoplasm (Huang & Flint, 1998) where they are preferentially translated (Cuesta et al., 2001). HAdVs benefit from an alternative form of translation called ‘ribosome shunting’, which is facilitated by the 5’-tripartite leader sequence of late mRNAs. As a consequence, they are unaffected by the inhibition of the cellular translation initiation factor eIF4F for cap-dependent translation (Huang & Schneider, 1991; Yueh & Schneider, 1996, 2000).

The mechanism of adenoviral capsid assembly is still not completely solved. The multimerization of hexon as well as penton monomers (compare section 1.1.2) seems to occur already in the cytoplasm, whereas the assembly of viral particles is conducted in the host nucleus (Hong *et al.*, 2005; Horwitz *et al.*, 1969). One mechanism proposed is related to the encapsidation of large bacteriophage (Koonin, 1993). It assumes the assembly of empty capsids first, followed by the encapsidation of the viral genome to result in pre-mature ‘young virions’ and finally their maturation. The encapsidation of the adenoviral genome requires a coordinated interplay between the late proteins IVa2, L1-52/55K, L4-22K, L4-33K and IIIa as well as the packaging sequence  $\psi$  of the viral DNA (Christensen *et al.*, 2008; Crosby & Barry, 2014; Guimet & Hearing, 2013; Ma & Hearing, 2011; Ostapchuk *et al.*, 2011; Ostapchuk & Hearing, 2008; Perez-Romero *et al.*, 2005; Wu *et al.*, 2012, 2013; Zhang *et al.*, 2001; Zhang & Arcos, 2005; Zhang & Imperiale, 2000, 2003). However, infectious particles only emerge, if the contained precursor proteins of IIIa, VI, VII, VIII,  $\mu$  and TP are processed by cleavage of the adenoviral protease (AVP) (Anderson *et al.*, 1973; Ishibashi & Maizel, 1974; Mangel & Initiative, 2014; Ruzindana-umunyana *et al.*, 2002). Until today, it is not clear, whether empty particles are truly intermediates of viral assembly or rather defective products. They are very stable and particle assembly does not occur either, if one of the factors involved in genome

encapsidation is defective or missing, although this process is supposed to follow capsid assembly (Gustin & Imperiale, 1998; Hasson *et al.*, 1989, 1992; Khittoo & Weber, 1977; Zhang & Imperiale, 2003).

#### **1.1.4. The adenoviral core**

In contrast to the icosahedral protein capsid of HAdVs, the nucleoprotein core has no distinct order or symmetry. Consequently, there is only little structural information existing about the adenoviral core. It contains three highly basic proteins, which bind the viral genome in a sequence unspecific manner, the major core protein VII (pVII), the minor core protein V (pV) and the small peptide  $\mu$  ( $p\mu$ , pX) (Chatterjee *et al.*, 1985, 1986a). All of them are encoded by distinct mRNAs of the L2 family (Alestrom *et al.*, 1984; Sato & Hosokawa, 1984). With 500-800 copies per virion, pVII is the most abundant core protein (Benevento *et al.*, 2014; van Oostrum & Burnett, 1985). It is tightly bound to the adenoviral DNA and assumed to organize the genome into a nucleosome-like structure with 180-200 subunits, also referred to as ‘adenosomes’. Protein V has been proposed to occupy the inter-adenosome spacing (Corden *et al.*, 1976; Mirza & Weber, 1982; Sung *et al.*, 1983; Vayda *et al.*, 1983). Later studies revealed that also  $p\mu$  contributes to this condensation of adenoviral DNA (Pérez-berná *et al.*, 2009), which had been proposed already (Anderson *et al.*, 1989; Keller *et al.*, 2002).

The basic viral core proteins share remarkable similarities with cellular histones, which are classified as DNA-benders, -wrappers or -bridgers (Luijsterburg *et al.*, 2008). Protein VII shares an N-terminal sequence homology with histone 3 (H3) (Lee *et al.*, 2003). Thus, in the context of HAdVs, it reflects the role of a DNA-wrapper the most. Protein  $\mu$  on the other hand, would comply with a DNA-bridger. Recent cryo-electron tomography studies described the adenovirus core as hard spheres, representing the condensing proteins, immersed in a ‘soup’ of DNA, which mediates an effective soft repulsive interaction, but has no defined backbone. (compare section 1.1.2) (Pérez-Berná *et al.*, 2015).

The core proteins VII and  $\mu$  are synthesized as precursor proteins, which have to be cleaved by the AVP during the last step of particle assembly to produce mature, infectious particles (compare section 1.1.3.3) (Anderson *et al.*, 1973, 1989; Sung *et al.*, 1983). It could be shown that immature cores are more rigid than the mature ones. Consequently, maturation of HAdVs leads to a pressurization of the viral particle, which is assumed to facilitate the stepwise disassembly of the virions following infection (Ortega-Esteban *et al.*, 2015).

### 1.1.4.1. Minor core protein V

Minor core protein V is specific for *Mastadenoviruses*. It has a length of 368 amino acids with a calculated molecular weight of 41 kDa (Davison *et al.*, 2003). Protein V is present in ~157 copies per virion and speculated to bridge the viral core with the surrounding capsid through its interaction with pVI (compare section 1.1.2). Moreover, early cross-linking studies indicated that pV exists in complex with pVII, p $\mu$  and both proteins together, whereas pVII and p $\mu$  could not be detected in complexes without pV (Chatterjee *et al.*, 1985; Everitt *et al.*, 1975). It was further shown that pV is able to dimerize in solution (Pérez-Vargas *et al.*, 2014). Based on these findings, a model was proposed for the stoichiometric adenosome organization in which the viral DNA wraps around six molecules of pVII, which are interspaced by one molecule of pV. The position of p $\mu$  in this condensed DNA structure remains elusive, though (Chatterjee *et al.*, 1985; Sung *et al.*, 1983). Complexes between pV and DNA have been shown to be very stable. They tolerate even temperatures of 95 °C, which is mediated predominantly by the N-terminal two-thirds of pV. Due to its ability to facilitate interactions between the other core proteins and the viral genome, it is speculated to have functions similar to those of cellular histone 1 (H1) (Pérez-Vargas *et al.*, 2014). H1 seals each nucleosome to form tightly condensed structures, but is the first histone to be displaced from the chromatin (Harvey & Downs, 2004). The latter could reflect the finding of pV being less tightly associated with viral DNA than pVII (Brown *et al.*, 1975; Nermut, 1979; Prage *et al.*, 1970; Vayda *et al.*, 1983).

So far, no functional domains could be identified within the primary sequence of HAdV-C5 pV. However, it contains several regions, which target the protein to the nucleus (NLS) as well as to the nucleolus (NoLS) of infected host cells (Fig. 4). The N-terminal motif (aa 23-78) and the C-terminal motif (aa 315-337) target the protein to the nucleoli as well as to the nucleoplasm independently of each other. The central NLS on the other hand can only mediate a localization of pV in the nucleoplasm (Matthews, 2001).

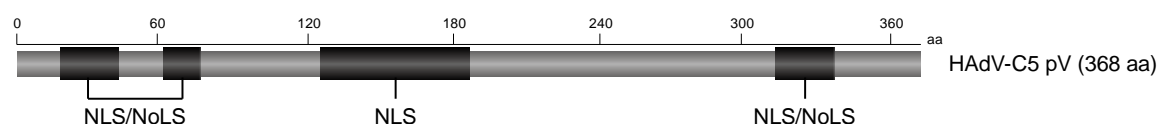


**Figure 4: Regions within HAdV-C5 pV targeting the protein to the host nucleus and/or nucleolus.**

Schematic illustration of the regions within the primary sequence of HAdV-C5 pV, which target the protein to the host nucleus and/or nucleolus according to Matthews, 2001. The protein is depicted with its N-terminus on the *left* and its C-terminus on the *right*. NLS means nuclear localization signal, NoLS means nucleolar localization signal.

Indeed, newly synthesized pV is found exclusively in the nucleus during HAdV-C5 infection where it co-localizes with nucleoli as well, but spares adenoviral replication centers (Matthews, 2001; Matthews & Russell, 1998a; Puntener *et al.*, 2011). Protein V was found to induce the relocalization of two major nucleolar proteins nucleolin (C23) and nucleophosmin (B23/NPM1) to the cytoplasm during transfection experiments. During productive HAdV infection, however, only C23 translocated to the cytoplasm, whereas B23 accumulates in the nucleoplasm. In any case, the rRNA synthesis remains uninfluenced by the presence of pV (Matthews, 2001). Two publications in 2012 revealed that a knockdown of B23.1 is accompanied by a defect in viral progeny production, although adenoviral DNA and late proteins are synthesized normally. B23.1 was reducing the association of adenoviral core proteins and cellular histones with the viral chromatin. Consequently, B23.1 was proposed as a chaperone involved in the regulation of viral chromatin formation and subsequent adenovirus assembly (Samad *et al.*, 2007, 2012). Likewise, the lack of pV in a HAdV-C5 rescue mutant (AdV-dV/TSB; Uga *et al.*, 2007) interferes with adenoviral progeny production, independent of the multiplicity of infection (moi). Interestingly, the restriction is only determining in primary endothelial cells, whereas the pV deletion mutant is replicating well in different tumor cell lines. Since B23.1 is often overexpressed in tumor cells and abundant in the nucleoplasm as well (compare section 1.2.2.1), these results indicate that nucleoplasmic B23.1 is required for adenoviral replication (Hindley *et al.*, 2007b; Ugai *et al.*, 2012). Except for the rescue mutant AdV-dV/TSB, which contains three mutations within the coding sequence (cds) of ppv, the deletion of protein V results in a replication deficient adenovirus as well, indicating that not only the right balance between NPM1 and pV is crucial for viral progeny production (Ugai *et al.*, 2007).

Several studies investigated the behavior of incoming protein V within the first hours of an adenovirus infection. Predominantly performed with high moi, they agree on a rapid transport of pV to the host nucleus where it partially associates immediately with nucleoli (Hindley *et al.*, 2007a; Matthews & Russell, 1998a; Ugai *et al.*, 2010, 2012). The results of one study are opposing though. Puntener and co-workers claim that pV is not entering the nucleus early after infection. It is proposed to dissociate in two sequential steps. The first portion of protein V is released from the viral particle when it is released from an endosome to the cytoplasm. This process is assumed associated with the disassembly of the capsid vertices. The second portion of pV is released during final capsid uncoating at the NPC and could not be observed inside the nucleus afterwards (compare sections 1.1.2 and 1.1.3.1). Consequently, the viral genome translocation is proposed to follow in complex with core protein VII, but not with pV (Puntener

*et al.*, 2011). Regarding the latter hypothesis, Hindley and co-workers come to a similar conclusion. On the contrary, they can detect pV in the nucleus at early time points after adenovirus infection and conclude that pV is able to enter the nucleus independent of the viral DNA/pVII-complex (Hindley *et al.*, 2007a).

### **1.1.5. Adenovirus-mediated oncogenesis**

All human adenoviruses investigated so far can transform rodent cells to a malignant state. However, only few of these types are also able to induce tumors in animals *in vivo* (see Table 1) (Berk, 2007; Graham *et al.*, 1984; Graham, 1984; Shenk, 2001; Wold & Horwitz, 2007). In general, the adenovirus E1A and E1B regions of the viral genome are sufficient for the oncogenic phenotype and are retained within the transformed rodent cells where they continuously express the E1 gene products. One exception is HAdV-D9, which induces estrogen dependent mammary tumors in female rats dependent on the protein E4orf1 (Ankerst & Jonsson, 1989; Javier & Shenk, 1996; Javier, 1994). In all remaining cases E1A proteins lay the foundation for oncogenic transformation with its function to stimulate gene expression, which is required for a cell cycle progression to the S-phase (Howe & Bayley, 1992; Zamanian & La Thangue, 1992; Zerler *et al.*, 1987). Usually, such a forced S-phase entry would be accompanied by the induction of apoptosis through the activation of p53 and other proapoptotic pathways (Rao *et al.*, 1992). However, this outcome is counteracted by the adenoviral E1B proteins (compare section 1.1.3.2). Interestingly, the deletion of CR4 within E1A prevents the transformation of primary rodent cells by E1A and E1B genes (Subramanian *et al.*, 1991). E1A binds to the cellular co-repressor protein CtBP (C-terminal binding protein) through a high affinity motif PXDLS within CR4. This interaction could inhibit CtBP activity in order to promote the activity of cellular repressors on transcription, thus facilitate the conditions required for oncogenic transformation (Zhao *et al.*, 2006, 2007).

Moreover, the E4 proteins E4orf3 and E4orf6 were shown to be capable of substituting E1B functions independently, as they can cooperate with E1A to transform primary rodent cells as well (Moore *et al.*, 1996; Nevels *et al.*, 1997, 1999a). In addition, they can enhance the oncogenic potential of the E1 region (Nevels *et al.*, 1999b, 2000). Since E1B-55K forms an E3 ubiquitin ligase complex with E4orf6 and different cellular proteins, which marks the tumor suppressor p53 and different MRN components for proteasomal degradation (compare section 1.1.3.2), this shows causality. Comparably, E4orf3 mediates the rearrangement of PML-NBs, thus interfering with the DDR as well (compare section 1.2.1). Remarkably, the adenoviral

DNA does not integrate into the host genome in most of the primary rodent cells, which have been transformed by cooperation of E1A proteins with E4orf3 or E4orf6. This phenotype was assigned to a 'hit-and-run' mechanism where the viral oncogenes are only required as causative agents (Nevels *et al.*, 2001). The following cell transformation is only a consequence, maybe due to a high mutation rate within the cells or a genomic instability resulting from the interference with the host DDR (Stracker *et al.*, 2002).

In spite the high transformation efficacy of primary rodent cells, provoked by the adenoviral E1 oncogenes, only very few examples of primary human cells could be successfully transformed by HAdV-A12 or HAdV-C5 DNA fragments. They comprise human embryonic kidney (HEK293) cells (Graham *et al.* 1977; Whittaker *et al.* 1984), human embryonic lung (HEL) cells (van den Heuvel *et al.* 1992), human embryonic retinoblasts (HERs) (Byrd *et al.* 1982; Gallimore *et al.* 1986; Fallaux *et al.* 1996, 1998), amniocytes (Schiedner *et al.* 2000). Very recently, human mesenchymal stroma cells (HMSCs) (Speiseder *et al.*, 2017) could be added. However, only HERs and amniocytes can be transformed reproducibly in culture. The most obvious reason why primary rodent cells can be easily transformed by any HAdV in cell culture, whereas human cells cannot, seems to be the lacking permissivity of the viruses in a rodent host. In addition, murine cells express telomerase and it could be shown that the small T antigen of the simian virus 40 (SV40) in cooperation with an activated human ras (Hras) protein and the catalytic domain of telomerase was able to transform human fibroblasts. Without the telomerase, however, this phenotype could not be achieved (Hahn *et al.*, 2002; Weinberg *et al.*, 1999a, b).

The tumorigenicity of HAdVs in rodents seems to depend largely on the thymus dependent CTL response. CTLs recognize foreign antigens presented on the cell surface by MHC (major histocompatibility complex) class I molecules, which is encoded by the human leukocyte antigen (HLA) system in humans. In case of non-oncogenic adenoviruses like species C types, E1A peptides themselves seem to provoke the CTL response, leading to the lysis of the transformed cells (Bellgrau *et al.*, 1988). E1A of the highly tumorigenic HAdV-A12, however, is able to repress the expression of MHC class I antigen already on transcriptional level, which inhibits the CTL response (Bernards *et al.*, 1983; Schrier *et al.*, 1983; Tanaka *et al.*, 1985). The main reason for this difference in tumorigenicity seems to be a 20 amino acid sequence between CR2 and CR3 within HAdV-A12 E1A, which is missing in HAdV-C5 E1A (Williams *et al.*, 2004). Of course, the CTL response is not the only determinant of tumorigenicity *in vivo*. Besides so far unknown contributors, the susceptibility of transformed cells to natural killer

(NK) cells was found to play an important role, which is mediated by the E1A gene as well (Cook *et al.*, 1987; Sawada *et al.*, 1985). Despite the discovery of certain adenoviral genomes within different human tumors (Kosulin *et al.*, 2007, 2013), no clear correlation of an infection with any HAdV and the following development of human tumors could be found so far. Hence, human adenoviruses have not been classified as human tumor viruses.

## 1.2. Nuclear host domains targeted by HAdVs

The nucleus is a highly ordered organelle, which itself contains different membrane-less sub-compartments often referred to as nuclear bodies. They consist of specific proteins and often RNAs that mediate their structural integrity (Nunes & Moretti, 2016). It is widely assumed that nuclear bodies are needed to concentrate proteins in a defined area to increase reaction efficiencies and facilitate their regulation (Lam & Trinkle-Mulcahy, 2015; Misteli, 2001). A possible underlying mechanism of compartmentalization could be weak binding interactions between intrinsically disordered low-complexity sequences (LCSs), which are typical for RNA- and DNA-binding proteins. The interaction of LCSs in various cytoplasmic RNA-binding proteins can promote phase transitions from liquid to hydrogel droplets (Han *et al.*, 2012; Kato *et al.*, 2012). Nuclear bodies are raising increasingly awareness as organizers of many cellular functions, including gene expression, DNA repair or RNA biogenesis as well as protein modification, apoptosis and cell cycle control. In this regard, it is no surprise that their organization is often manipulated during viral infections or during the development of cancers. Table 2 gives an overview of identified nuclear bodies in humans and their main correlated functions (Nunes & Moretti, 2016; Russo & Russo, 2017).

<b>Nuclear body</b>	<b>Scaffold proteins</b>	<b>Size [<math>\mu\text{m}</math>]</b>	<b>Assigned functions</b>
cajal bodies	Coilin	0.1-2	biogenesis, maturation and recycling of small RNAs
clastosome	19S, 20S proteasome	0.1-1.2	sites of proteasomes, ubiquitin-conjugates and substrates of the proteasome
gems nuclear body	SMN	0.1-2	pre-mRNA splicing
histone body	NPAT, FLASH	0.2-1.2	histone gene synthesis

nuclear speckles	SRF2, SRF1, Malat1	0.8-1.8	storage and recycling of splicing factors
nuclear stress body	HSF1, HAP	0.3-3	regulation of transcription and splicing under stress
nucleolus	RNA Pol I machinery	0.5-8	ribosome biogenesis, stress sensor
paraspeckle	PSP1, P54NRB, PSF	0.5	mRNA regulation, RNA editing
perinucleolar compartment	PTB, CUGBP	0.2-1	post-transcriptional regulation of a subset of Pol III RNAs
PML nuclear bodies	PML	0.1-1	regulation of genome stability, DNA repair, transcriptional regulation, viral defense, senescence/apoptosis, stem cell renewal

**Table 2: Major nuclear sub-compartments.**

Assignment of the major nuclear sub-compartments to important biological functions within the human cell. No guarantee can be given for the completeness of contents (adapted from Nunes & Moretti, 2016).

### 1.2.1. PML nuclear bodies

PML nuclear bodies (PML-NBs), which are also termed Nuclear domain-10 (ND-10) or PML oncogenic domains (PODs) (Hodges *et al.*, 1998) are nuclear, spherical multi-protein complexes, located in the inter-chromosomal space where they are tightly bound to the nuclear matrix (Bernardi & Pandolfi, 2007; Plehn-Dujowich *et al.*, 2000). The latter describes the nuclear scaffold, which is resistant to nucleases as well as high salt extraction and assumed to support the nuclear organization and compartmentalization (Razin *et al.*, 2014; Stuurman *et al.*, 1990). The number of PML-NBs varies from 5-30 per nucleus. It depends on the cell type, its differentiation stage, the cell cycle phase and further on external conditions like stress and nutrition (Ascoli & Maul, 1991; Bernardi & Pandolfi, 2007; Dellaire *et al.*, 2006a, b; Dyck *et al.*, 1994; Koken *et al.*, 1994; Lallemand-Breitenbach & de Thé, 2010; Maul *et al.*, 1995; Salomoni & Pandolfi, 2002; Weis *et al.*, 1994). PML-NBs range from 0.1-1  $\mu\text{m}$  in size (compare Table 2) whereby a sphere of proteins surrounds an empty space, which might contain micro granular material, such as ribonucleoproteins (Lallemand-Breitenbach & de Thé, 2010), but no nucleic acids. DNA and RNA can be found at the periphery of the protein sphere where

PML-NBs make contact with chromatin fibers (Boisvert *et al.*, 2000; Dellaire & Bazett-Jones, 2004).

The major scaffolding protein of PML-NBs is the promyelocytic leukemia protein (PML) (Ishov *et al.*, 1999). After its identification in acute promyelocytic leukemia (APL) (Borrow *et al.*, 1992; Chen & Chen, 1992; Koken *et al.*, 1994; Nervi *et al.*, 1992; Pandolfi *et al.*, 1992; de Thé *et al.*, 1991; Weis *et al.*, 1994), it was found to be deregulated in various cancer types and consequently classified as a tumor suppressor (Salomoni & Pandolfi, 2002). The protein is expressed as seven different isoforms (PML I-VII) through alternative splicing, whereby PML I is the longest and most abundant isoform. All PML isoforms coincide in their N-terminal homo-multimerization domain, also termed RBCC or TRIM (tripartite motif) domain, which allows the formation of high order multi-protein complexes and can be found in many SUMO or ubiquitin E3 ligases (Meroni & Diez-Roux, 2005; Reymond *et al.*, 2001). It comprises a RING finger domain (R), two cysteine/histidine-rich B-Box domains (B) and an  $\alpha$ -helical coiled-coil domain (CC). The PML isoforms differ only in the length of their C-terminal region with PML VII being the shortest one identified to date (Fagioli *et al.*, 1992; Jensen *et al.*, 2001). The existence of unique isoforms presumes exclusive functions of the different PML proteins and might hint to the formation and maintenance of functionally different PML-NBs as well (Brand *et al.*, 2010; Condemine *et al.*, 2006; Nisole *et al.*, 2013; Weidtkamp-Peters *et al.*, 2008).

There are different models explaining how the formation of PML-NBs might work mechanistically. It has been widely accepted that the 3D-structure of PML-NBs emerges because of a post-translational modification of the PML protein with the small ubiquitin-like modifier (SUMO). Since PML further contains a SUMO interacting motif (SIM), it can interact non-covalently with SUMO-modified proteins as well (see section 1.2.1.1), thus enabling itself to form a 3D-PML network (Duprez *et al.*, 1999; Lallemand-Breitenbach *et al.*, 2001; Shen *et al.*, 2006a; Zhong *et al.*, 2000a). This model was underlined by the finding that PML II and PML V form nuclear bodies independently of their N-terminal RBCC domain (Geng *et al.*, 2012), which was proposed to be essential for the formation of multiprotein complexes (Jensen *et al.*, 2001; Shen *et al.*, 2006b). However, PML VI, which is not equipped with a SIM motif, as well as PML III mutants, lacking their SUMO conjugation sites are still capable of forming polymeric structures (Lallemand-Breitenbach *et al.*, 2001; Shen *et al.*, 2006a). Therefore, the second model proceeds from the oxidation of PML by reactive oxygen species (ROS), facilitating the formation of disulfide bonds between cysteine residues of PML proteins and thereby the growth of an empty, spherical PML-framework. Only the further expansion of

PML-NBs is believed to rely on SUMO-SIM interactions in a way that partner proteins, which are SUMOylated or contain a SIM motif, are recruited to the existing PML-framework, which is extensively SUMOylated after its formation (Umut *et al.*, 2014). PML is also known to be phosphorylated and acetylated, which might further contribute to partner recruitment and subsequent protein-protein interactions at the PML-NBs (Cheng & Kao, 2012; Sahin *et al.*, 2015; Schmitz & Grishina, 2012).

This competence to expand their structure dependent on different post-translational modifications (PTMs) makes PML-NBs heterogeneous and highly dynamic. It has been estimated that more than 160 proteins functionally interact with PML (van Damme *et al.*, 2010), whereas 120 proteins have been identified to physically interact with PML (Guan & Kao, 2015). These interactions can be either transient or constitutive, as for the cellular chromatin-remodeling factor Daxx (death domain associated protein) and the transcriptional effector Sp100 (speckled protein 100 kDa). As a consequence, PML-NBs are associated with the regulation of a vast number of cellular pathways such as the DDR, tumor suppression, anti-viral and anti-bacterial responses, inflammatory responses, metabolism, ageing, unfolded protein responses, transcriptional regulation or senescence/apoptosis (Bernardi & Pandolfi, 2014; Dellaire & Bazett-Jones, 2004; Guan & Kao, 2015; Sahin *et al.*, 2014a; Umut *et al.*, 2014).

### **1.2.1.1. The host SUMOylation machinery**

Many of the processes associated with PML-NBs are linked to a PTM of involved proteins, termed SUMO. SUMO is a short term for small ubiquitin-like modifier, since it shares around 18 % of sequence similarity with ubiquitin and is covalently bound to its target proteins in a mechanistically comparable manner. The SUMO protein family comprises five isoforms to date, although SUMO1-3 constitute the main members. They are often referred to as SUMO1 and SUMO2/3, since the latter share 95 % sequence identity, whereas they match only ~45 % of the SUMO1 sequence (Hay, 2005; Saitoh & Hinchey, 2000; Wang & Dasso, 2009). In case of SUMO4 it is not assured, whether it can be conjugated to target proteins *in vivo* and its expression seems to be restricted to kidneys, lymph nodes and spleen (Bohren *et al.*, 2004; Owerbach *et al.*, 2005). SUMO5 has not been confirmed on protein level yet (Liang *et al.*, 2016). In contrast to SUMO1, SUMO2/3 proteins are able to form polymeric chains, as they contain a conserved acceptor lysine residue within their sequence (Tatham *et al.*, 2001). Nevertheless, SUMO1 can be detected in mixed SUMO chains, leading to the assumption that it functions as a chain terminator (Matic *et al.*, 2007). Later on, an inverted SUMO conjugation motif was found within the sequence of SUMO1, which might contribute to the formation of

SUMO chains as well, although with lower efficiency than SUMO 2/3 (Blomster *et al.*, 2010; Galisson *et al.*, 2011; Matic *et al.*, 2010).

The attachment of SUMO proteins to their targets occurs in a three-step enzymatic cascade, which is reversible (Fig. 5). All isoforms are expressed as precursor proteins, which need to be processed by sentrin specific proteases (SENPs) to liberate a di-glycine motif at the C-terminus of SUMO (Hay, 2007; Mukhopadhyay & Dasso, 2007). Through this motif, mature SUMO proteins can interact with the catalytic domain of the activating enzyme E1, leading to the formation of a thioester bond with consumption of ATP (Desterro *et al.*, 1999; Hay, 2005; Johnson *et al.*, 1997; Lois & Lima, 2005). E1 is a heterodimer, consisting of the subunits SAE1 and SAE2, whereby the latter contains the catalytically active cysteine. E1 enables the transfer of SUMO proteins to the conjugating enzyme E2, termed Ubc9, through formation of another thioester bond (Desterro *et al.*, 1997; Okuma *et al.*, 1999). Ubc9 is able to recognize the SUMO conjugation site within target proteins and enables the required E3 SUMO ligase to mediate the formation of an isopeptidyl bond between the C-terminal di-glycine residues of SUMO and an  $\epsilon$ -amino group of a target lysine residue (Rodriguez *et al.*, 2001).

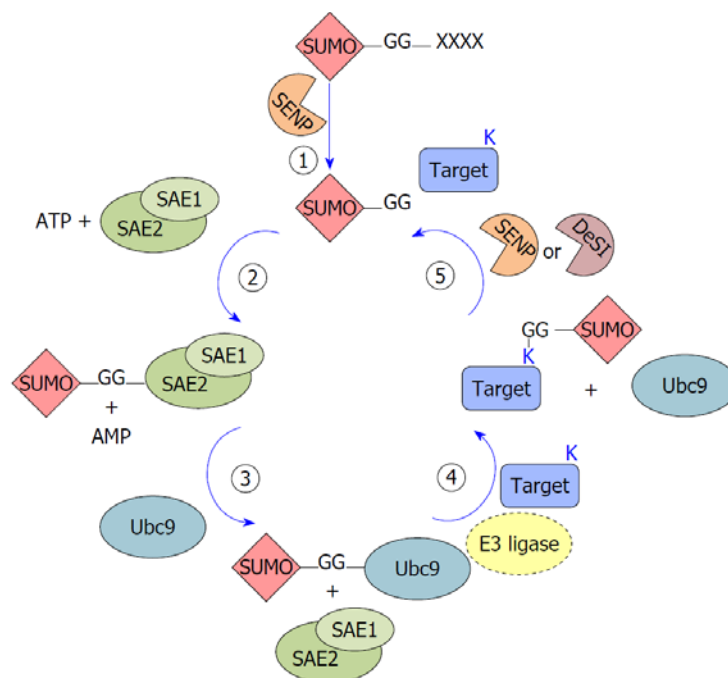


**Figure 5: Schematic illustration of the reversible SUMO conjugation cascade.**

① SUMO protein precursors are processed by SUMO specific proteases (SENPs). ② The mature SUMO is activated by adenylation at the C-terminal diglycine motif (-GG) through the SUMO activating enzyme E1 (SAE1/SAE2). ③ Subsequently, it is transferred to a cysteine residue of the conjugating enzyme E2 (Ubc9) by forming a thioester bond again. ④ This step is followed by the final transfer of the SUMO protein to its target with support of a suitable E3 SUMO ligase under formation of an isopeptide bond between the diglycine motif and a target lysine residue (K). ⑤ SUMO is cleaved off the target protein by SENPs or deSUMOylating-isopeptidases (DeSIs). (adopted from Mattoscio *et al.*, 2013).

The transfer of SUMO from Ubc9 to the target does not absolutely require the presence of an E3 ligase (Bernier-Villamor *et al.*, 2002; Seeler & Dejean, 2003). However, it stabilizes the transition state and thereby reduces the activation energy needed for an efficient transfer. This way, the presence of E3 kinetically facilitates the SUMO conjugation. In contrast to the unique enzymes E1 and E2, several unrelated proteins have been attributed E3 SUMO ligase activity (van Damme *et al.*, 2010; Melchior *et al.*, 2003).

Analogous to the processing of premature SUMO proteins, SENPs are capable to revert the SUMO-conjugation, thus releasing the target protein. To date there are six SENP isoforms known, SENP1-3 and SENP5-7 (Gong & Yeh, 2006; Mukhopadhyay & Dasso, 2007). They differ in their subcellular localization and their affinity to different SUMO proteins, regarding either their maturation or their de-conjugation from substrates. All SENPs localize to the nucleus or to nucleus-associated structures. SENP2, for instance, is localized at the nuclear pore where it de-conjugates both SUMO1 and 2/3 (Hang & Dasso, 2002; Texari & Stutz, 2015). In contrast, SENP3 and SENP5 are located to the nucleolus (Yun *et al.*, 2008) where SENP3 and SENP5 target SUMO2/3 modifications (Di Bacco *et al.*, 2006; Gong & Yeh, 2006).

The SUMOylation of target proteins can influence their functions in various ways. It can facilitate or inhibit the interaction with other proteins and it can alter their conformation, stability or their subcellular localization (Hendriks & Vertegaal, 2016). As already mentioned in the previous section, SIM motifs are contributing to these processes, as they facilitate non-covalent interactions with SUMO-proteins (Hecker *et al.*, 2006; Keusekotten *et al.*, 2014; Song *et al.*, 2004). Enzymes, which are part of the SUMOylation machinery contain SIMs themselves (Matic *et al.*, 2007). Hence, they and other SIM-containing proteins (Lin *et al.*, 2006; Sung *et al.*, 2011; Umut *et al.*, 2014) might be captured by cellular structures like PML-NBs that are enriched with SUMO proteins and in turn promote the SUMOylation of surrounding target proteins (Gonzalez-Prieto *et al.*, 2015; Sahin Umut *et al.*, 2014). This regulation of SUMO modifications due to spatial proximity could contribute to mediating the specificity of the SUMO system, since the involvement of only few enzymes can hardly account for it. Moreover, it could be involved in the cross-regulation of other PTMs.

In a recent analysis of 22 different human proteomic studies, approximately 86 % of the top 1000 identified SUMO target proteins were annotated as nuclear. They are usually enriched at the chromatin (Hendriks *et al.*, 2014, 2015; Nathan *et al.*, 2003; Shii & Eisenman, 2003) as well as within nuclear bodies, in particular at PML-NBs (van Damme *et al.*, 2010; Sahin *et al.*, 2015). However, only ~44% of the top 2,500 identified sites of SUMOylation correspond to the

classical consensus motif  $\psi$ KxE, with  $\psi$  representing a hydrophobic amino acid and x any amino acid residue (Rodriguez *et al.*, 2001; Sampson *et al.*, 2001). Under conditions of different cellular stresses this number even dropped to ~23 %, indicating that target SUMOylation becomes less stringent in response to stress induction. A general response to cellular stress seems to be an upregulation of cell cycle- and DDR-factor-SUMOylation, whereas nucleosome components or transport factors are less SUMOylated. A clustering of SUMOylated proteins in regard of their functions revealed a major involvement in pre-mRNA splicing as well as ribosome biogenesis. Interestingly, SUMO proteins are believed to regulate the rate of ribosome biogenesis in yeast and a similar dependence is imaginable in humans too (compare section 1.2.2.1; Yun *et al.*, 2008). Further functional clusters are correlated with chromatin remodeling, the DDR, transcriptional regulation (also of viruses), DNA-replication, SUMO-ligase activity, nuclear body organization, pathways involved in the development of cancer and to a lesser extent cell cycle regulation (Hendriks & Vertegaal, 2016).

#### **1.2.1.2. PML-NBs in antiviral defense**

Interferons (IFNs), which are cytokines that are secreted by the cell as a response to pathogen infiltration, promote the PML gene transcription (Stadler *et al.*, 1995). Consequently, the PML concentration as well as the size and number of PML-NBs increases within virus infected cells. The same holds true for the expression of SUMO (Sahin *et al.*, 2014b) and different PML-NB associated factors, such as Sp100 (Grötzinger *et al.*, 1996; Guldner *et al.*, 1992). In Turn, PML emerges as a positive regulator of IFN-signaling, as it promotes the expression of IFN- $\beta$  and is required for an efficient transcription of interferon induced genes (ISGs) (Kim & Ahn, 2015). In this regard, PML II seems to be of particular importance. The protein associates with different transcription factors of the type I and type II IFN signaling pathways, such as interferon regulatory factor 3 (IRF3) and signal transducer and activator of transcription 1 (STAT1) (Chen *et al.*, 2015). Besides, there are indications that PML affects the production of proinflammatory cytokines as well, indicating a broad role of PML in innate immune signaling (Lunardi *et al.*, 2011). Consequently, various human viruses, among them DNA as well as RNA viruses, have evolved distinct mechanisms to antagonize the intrinsic defense of PML-NBs (Fig. 6). Nevertheless, the replication of many DNA viruses occurs in close proximity to the PML-NBs within the nucleus. This points towards a more complex relation between virus and PML-NB where the virus might take advantage of some components of the PML-NBs while antagonizing others (Everett, 2001; Everett & Chelbi-Alix, 2007; Scherer & Stamminger, 2016; Tavalai *et al.*, 2008, 2011).

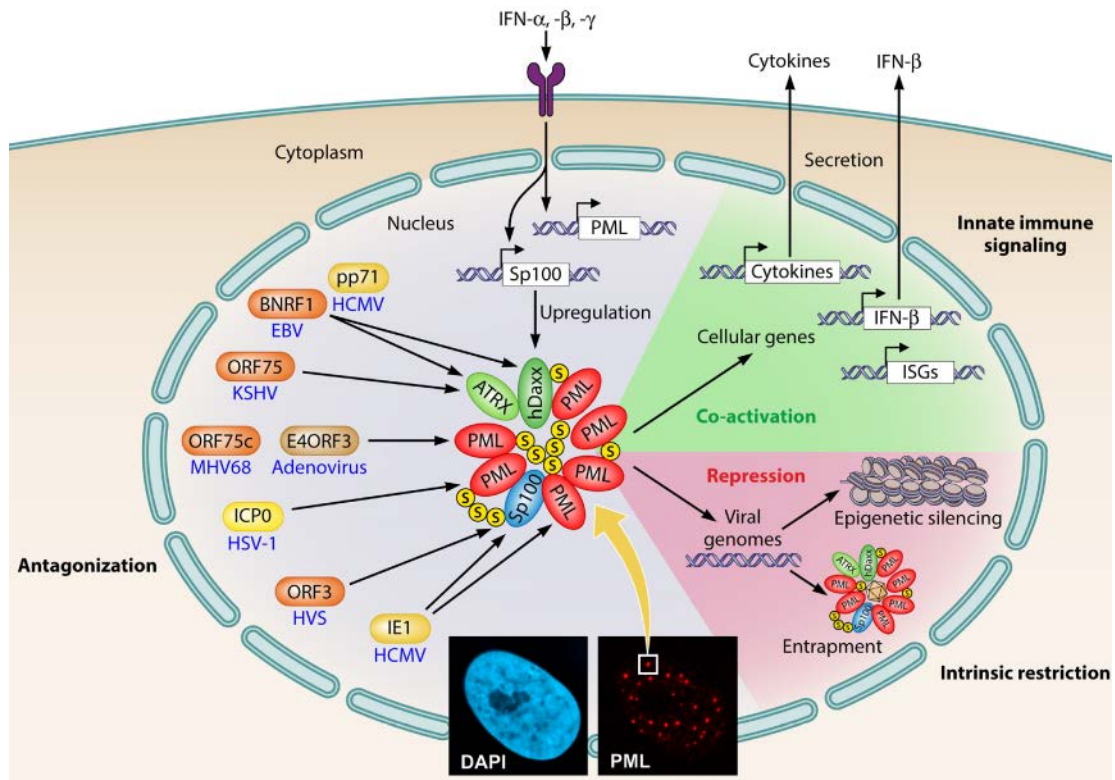


**Figure 6: Schematic illustration of the interplay between different DNA viruses and PML-NBs and their role in innate immune signaling.**

PML-NBs counteract viral replication by epigenetic silencing, entrapment of produced viral particles or needed components. Moreover, they are able to stimulate the transcription of genes, which are part of innate immune signaling, such as IFN- $\beta$ , ISGs or certain cytokines. In turn, type I IFNs stimulate the expression of PML, SUMO and several partner proteins of the PML-NBs like Sp100. As a response, many viruses, especially herpesviruses as well as HAdVs developed strategies to counteract these antiviral properties of PML-NBs in different ways. Either they target specific PML-NB components for degradation or relocalization (affected components are indicated by arrows for each virus) or they disrupt the whole PML-NB structure. The immunofluorescence image of primary human fibroblast cells stained for PML and chromatin (DAPI) illustrates the morphology of PML-NBs. EBV (Epstein-Barr virus), KSHV (Kaposi sarcoma-associated herpesvirus), MHV68 (murine gamma herpesvirus 68), HCMV (human cytomegalovirus), HSV-1 (herpes simplex virus type 1), HVS (herpesvirus saimiri), IFN (interferon), ISG (interferon-stimulated gene), S (SUMO/small ubiquitin-like modifier) (adopted from Scherer & Stamminger, 2016).

In case of HAdV-C5, different viral proteins are known to interact with the PML-NBs. In the early phase of infection, E4orf3 oligomerizes to a linear and branched network within the nuclear volume and thereby reorganizes PML-NBs into track-like structures, through interaction with PML (Carvalho *et al.*, 1995; Hoppe *et al.*, 2006; Ou *et al.*, 2012; Vink *et al.*, 2015). Besides, E1A-13S was found to interact with PML II, which enhances the transactivating capacity of E1A-13S towards adenoviral genes (Berscheminski *et al.*, 2013; Carvalho *et al.*, 1995). In addition, the PML-NB constitutive proteins Daxx and Sp100 are targeted by HAdV-C5. To benefit from the activating capabilities of Sp100A and simultaneously limit repression by Sp100B, -C and -HMG, the virus induces the relocalization of Sp100B, -C and -HMG from PML-NBs to viral replication centers, whereas Sp100A is kept at the PML tracks

(Berscheminski *et al.*, 2014). Furthermore, Daxx, which represents a cellular transcriptional repressor, is subjected to proteasomal degradation by the early adenoviral protein E1B-55K (Schreiner *et al.*, 2010) to name only some of the adenoviral proteins involved.

### 1.2.2. Nucleoli

The nucleolus is a membrane-less, nuclear organelle, which forms around clusters of ribosomal DNA (rDNA) genes, located near the tips of five chromosomes, also referred to as the nucleolar organizer region (NOR) (Lam *et al.*, 2005; Raška *et al.*, 2006; Scheer & Hock, 1999). Nucleoli are primarily known as the site of ribosome biogenesis (Fig. 7). This complex process starts with the transcription of rDNA, which requires the presence of upstream binding factor (UBF), the promoter selectivity factor (SL1) and the RNA polymerase I (Pol I) complex at the rDNA promoter region. Nucleolar transcription generates the 47S precursor rRNA, which is post-transcriptionally modified and processed into 18S, 5.8S and 28S rRNAs. Moreover, nuclear transcribed 5S rRNA accumulates within the nucleoli as well as ribosomal proteins to allow the proper assembly and following nuclear export of the mature ribosome subunits 40S and 60S (Drygin *et al.*, 2010; Fatica & Tollervey, 2002; Grummt, 2013; Grummt & Längst, 2013; Grummt & Pikaard, 2003). This process further requires the presence of numerous non-ribosomal proteins and small nucleolar RNAs (snoRNA) (Fatica & Tollervey, 2002), making ribosome biogenesis the most demanding procedure in terms of energetic and metabolic costs (Russo & Russo, 2017).

Nucleoli are fluctuating compartments, whose size depends on the cell type and the rate of protein synthesis. With the onset of mitosis, the nucleoli disassemble and rDNA transcription is repressed. Only certain factors, like UBF remain associated with the NORs to maintain their competency (Russell, Jackie, Zomerdijk, 2006). When CDK1/cyclin B activity decreases at mitotic exit the nucleoli reassemble again, accompanied by the resumption of rDNA transcription (Hernandez-Verdun, 2011). The interphase nucleolus comprises three different compartments. The fibrillary center (FC) contains factors, which are important for the initiation of nucleolar transcription, whereas the surrounding dense fibrillary compartment (DFC) is harboring early pre-RNA processing factors. Both compartments are embedded in a granular compartment (GC), being the site of later rRNA processing and ribosome subunit assembly (Raška *et al.*, 2006). Nucleoli are not as dense as believed for long. The viscosity of nucleoli is ATP dependent and shows a liquid droplet-like behavior, meaning that nucleoli can freely diffuse and fuse with each other (Brangwynne *et al.*, 2011; Handwerger *et al.*, 2005; Marko,

2012). This might also explain their capability to accommodate assembly of the icosahedral adeno-associated virus capsid AAV2, while other nucleolar functions continue normally (Sonntag *et al.*, 2010).

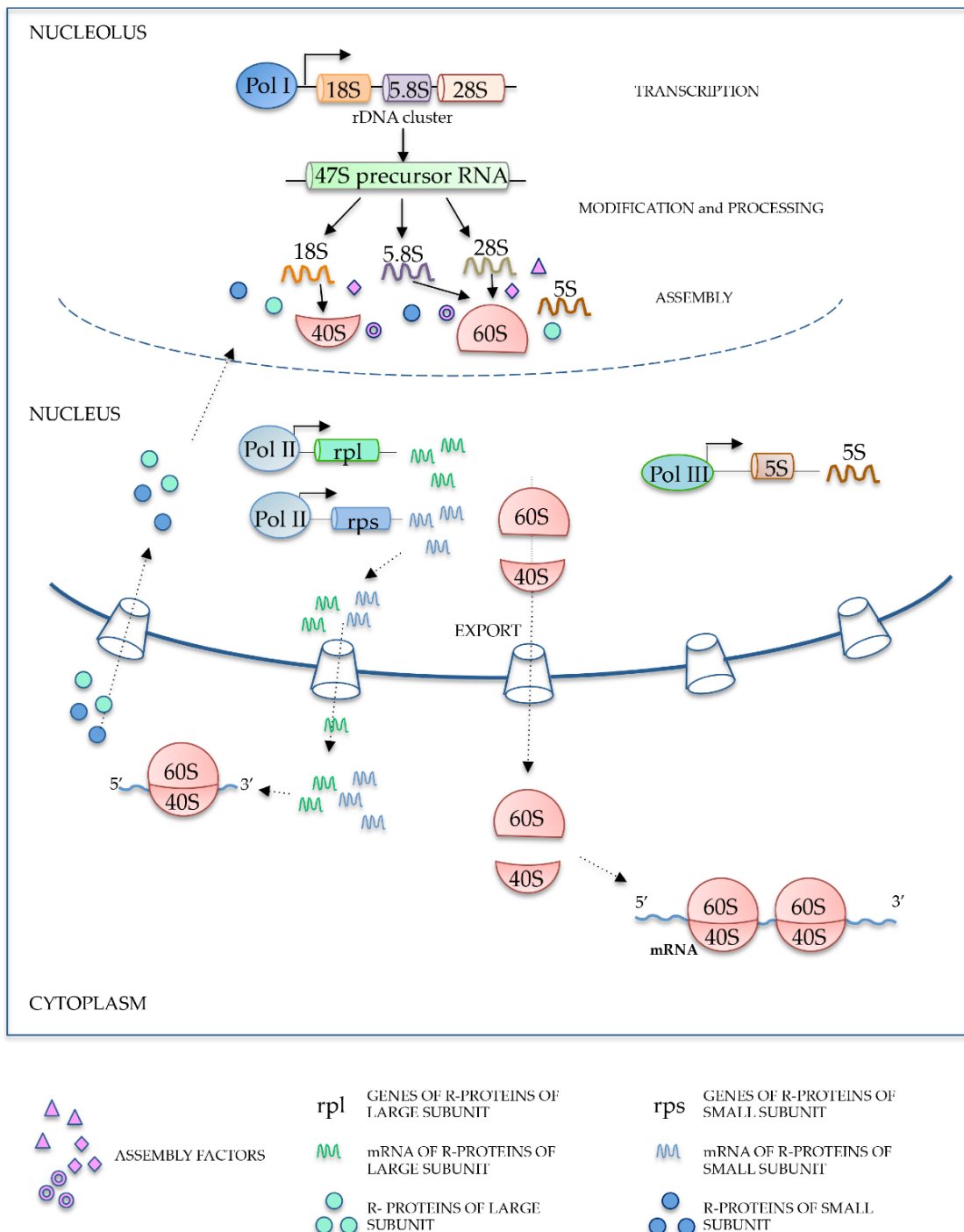


**Figure 7: Schematic illustration of ribosome biogenesis.**

rDNA means ribosomal DNA, Pol means polymerase, r-protein means ribosomal protein, mRNA means messenger RNA, 40S represents the small subunit of the ribosome, whereas 60S represents its large subunit and S means sedimentation coefficient in Svedberg units (adopted from Russo & Russo, 2017).

To date, more than 4500 proteins have been identified as part of the nucleolar proteome (Ahmad *et al.*, 2009), most of which being not mainly involved in ribosome biogenesis. Instead, they have been uncovered to be involved in many different cellular processes, such as cell cycle progression and apoptosis, cell proliferation and differentiation, DNA damage repair, genome organization, ageing, stress sensing, protein folding and degradation or mRNA-export (Olson *et al.*, 2000; Pederson & Tsai, 2009; Warner & McIntosh, 2009; Woods *et al.*, 2015). Hence, nucleoli contribute to the cellular surveillance system with the aim of maintaining cell homeostasis. Conditions, provoking nucleolar stress, such as UV radiation, hypoxia, oncogenes, or an imbalance of rRNA and ribosomal proteins, activate signaling pathways, which can be dependent or independent of p53. Moreover, this signaling can be induced by ribosomal proteins exhibiting extra-ribosomal functions or by non-ribosomal proteins, involved in alternative nucleolar stress-signaling and is leading to cell cycle arrest or apoptosis (Andersen *et al.*, 2005; Boisvert *et al.*, 2007; Boulon *et al.*, 2010; Castro *et al.*, 2008; Cuccurese *et al.*, 2005; Pestov *et al.*, 2001; Zhang & Lu, 2009). A failure of this activation can result in the development of pathologies, such as neurodegenerative disorders like Parkinson's disease (Parlato & Liss, 2014) or even cancer (Tsai & Pederson, 2014). The expression of many ribosomal proteins is upregulated in solid tumors and leukemia cells (Chaudhuri *et al.*, 2007; Wang *et al.*, 2006). Likewise, non-ribosomal, nucleolar proteins like NPM1 are often overexpressed in tumor cells.

Upon cellular stress, many proteins have been found to be sequestered into or released from the nucleolus (Boulon *et al.*, 2010; Emmott & Hiscox, 2009). This temporary trapping efficiently regulates the availability of their functions. As a consequence, a spatially separated nucleolar detention center forms, whereas ribosome biogenesis halts (Jacob *et al.*, 2013). HAdVs are known to influence the nucleoli of infected cells as well. The productive infection with HAdVs was shown to affect the nuclear export of cellular rRNAs 18S and 28S. In the late phase of infection, nucleolar rRNA synthesis, processing and nuclear exit of 18S rRNA were disturbed, whereas the levels of newly synthesized 28S rRNA entering the cytoplasm were reduced rapidly (Castiglia & Flint, 1983). Moreover, alterations of the nucleolar structure have been observed (Puvion-Dutilleul & Christensen, 1993; Walton *et al.*, 1989), as well as the sequestration of several adenoviral proteins, such as IVa2, V, VII and  $\mu$ , to the nucleoli during the course of infection with HAdVs (Lee *et al.*, 2004, 2003; Lutz *et al.*, 1996; Matthews & Russell, 1998a). A common import signal of ribosomal proteins is their very basic character (Russo *et al.*, 1997), a feature holding true for those adenoviral proteins too (compare section 1.1.4). The functional correlation, however, remains enigmatic.

Certain nucleolar proteins, such as NPM1 and UBF, were found to be relocalized upon adenoviral infection and assumed to influence viral replication, since they were located in close proximity to adenoviral replication centers (Hindley *et al.*, 2007b; Lawrence *et al.*, 2006). A complete analysis of the nucleolar proteome was performed late in adenovirus infection to get a better impression on the influenced processes. However, the results are incomplete. In total, only few nucleolar proteins were identified to be altered in amount, localization or both. This could also reflect a general nucleolar stress caused by the presence of an infectious agent. In addition, no viral protein could be identified within isolated nucleoli, contradicting previous findings (Lam *et al.*, 2010).

#### **1.2.2.1. Nucleophosmin and its various influences on cell homeostasis**

Nucleophosmin (NPM1, B23, No38 or Numatrin) is an abundant nucleolar phosphoprotein in proliferating cells, which shuttles between the nucleolus, nucleoplasm and cytoplasm (Borer *et al.*, 1989; Negi & Olson, 2006), whereas its predominant location are the nucleoli. It seems to be involved in numerous cellular processes, such as ribosome biogenesis (Murano *et al.*, 2008; Savkur & Olson, 1998; Yu *et al.*, 2006), mRNA processing, chromatin remodeling, embryogenesis (Grisendi *et al.*, 2005), control of cell cycle progression, centrosome duplication and maintaining genomic stability through its functioning in different DNA repair pathways and its role in regulating apoptosis (Lindström, 2011).

Nucleophosmin exists in at least two isoforms NPM1.1 (B23.1) and NPM1.3 (B23.2). NPM1.3 lacks the 35 C-terminal amino acids of NPM1.1 and is sparsely expressed in human cells where it is located in the cytoplasm and in the nucleoplasm (Wang *et al.*, 1993). NPM1 belongs to the nucleophosmin/nucleoplasmin family of histone chaperones and is proposed to function as a kind of ‘storage platform’ for histones (Akey & Luger, 2003; Eirin-Lopez *et al.*, 2006). It exists in an equilibrium of monomers and a homo-pentameric, donut-shaped complex. The oligomerization is mediated by the highly conserved, N-terminal core domain (Box *et al.*, 2016; Hingorani *et al.*, 2000). The central acidic region is involved in the binding to histones through its negatively charged residues, presumably mimicking DNA or RNA (Gadad *et al.*, 2011; Okuwaki, 2008; Okuwaki *et al.*, 2001). The C-terminus is specific for NPM1 and consists of a basic amino acid cluster, followed by aromatic residues, which constitute an atypical NoLS. The positively charged C-terminus allows the binding of NPM1 to nucleic acids (Dumbar *et al.*, 1989; Wang *et al.*, 1994) and is further implicated in ATP-binding (Chang *et al.*, 1998; Choi *et al.*, 2008), histone transfer and ribonuclease activity (Hingorani *et al.*, 2000). Apart from these functions, NPM1 was found to bind small basic proteins, which can be also viral as the

HIV-1 Rev and Tat proteins (Fankhauser *et al.*, 1991) or HAdV pV (compare section 1.1.4.1). The huge variety of NPM1 functions is regulated at least in part by post-translational modifications of the protein. The most extensively studied one is phosphorylation at different sites of NPM1 (Koike *et al.*, 2010; Okuda *et al.*, 2000; Peter *et al.*, 1990; Szebeni *et al.*, 2003), regulating for example the dynamic changes in localization and function during the progression through mitosis (Negi & Olson, 2006; Zatsepina *et al.*, 1999). Moreover, NPM1 can be acetylated, which contributes to a disruption of nucleosomes and therefore transcriptional activation. NPM1 was further shown to be SUMOylated, which is promoted by the ARF tumor suppressor protein (den Besten *et al.*, 2006; Kuo *et al.*, 2008; Neo *et al.*, 2015; Tago *et al.*, 2005). The SUMOylation of NPM1 is proposed to regulate its subcellular localization and mediate its functions to promote cell proliferation and survival (Liu *et al.*, 2007). Thereby K263 seems to be crucial for the nucleolar localization of the protein, a residue additionally assessed essential for ATP-binding (Choi *et al.*, 2008). This SUMO modification can be reversed by SENP3 (Haindl *et al.*, 2008; Nishida & Yamada, 2008), which is located with SENP5 at nucleoli (compare section 1.2.1.1) where both proteins interact with NPM1. The tight regulation of the SUMO machinery within the nucleoli seems to be crucial for proper ribosome biogenesis, since the knockdown of either the nucleolar SENPs or NPM1 causes severe defects in this process (Yun *et al.*, 2008). Related to the SUMOylation of NPM1 is its ubiquitination (Enomoto *et al.*, 2006; Itahana *et al.*, 2003). The de-ubiquitination of NPM1 in turn, is mediated through the nucleolar ubiquitin specific protease USP36, leading to a stabilization of NPM1 and improve of its nucleolar functions (Endo *et al.*, 2009).

The translocation of NPM1 is one of the most typical hallmarks of nucleolar stress (Yao *et al.*, 2010), which is currently defined as ‘alterations in the nucleolar structure and function that can be induced by various abnormal conditions’ (Holmberg Olausson *et al.*, 2012). Recently, it could be demonstrated that nucleolar oxidation is a general response to various cellular stresses. Upon these redox changes within the nucleolus, NPM1 is modified by S-glutathionyl at cysteine 275, resulting in the translocation of NPM1. The S-glutathionylation of Cys<sup>275</sup> might sterically hinder the interaction of NPM1 and nucleolar nucleic acids and thereby trigger a relocalization of the protein. Only nucleoplasmic NPM1 can bind to MDM2 (Colombo *et al.*, 2002; Kurki *et al.*, 2004), which prevents the ubiquitination of p53 and its subsequent proteasomal degradation, leading to the induction of apoptosis. This nucleoplasmic localization of NPM1 seems to be a prerequisite of p53 accumulation under conditions of nucleolar stress, as the binding of the tumor suppressor p14<sup>ARF</sup> or other ribosomal proteins to MDM2 was shown to be

insufficient, if NPM1 remains nucleolar. (Yang *et al.*, 2016).

The ARF-NPM1-MDM2-p53 axis is linked to various physiological and pathological pathways (Chen *et al.*, 2010). Like NPM1, nucleoplasmic p14<sup>ARF</sup> binds to MDM2, thus preventing p53 from degradation and facilitating its stabilization (Ryan *et al.*, 2001; Zhang *et al.*, 1998). After the stabilization of nuclear p53, an activation of p53-responsive genes would be expected, which can be actually observed (Dhar & St. Clair, 2009). Several of these genes encode mitochondrial proapoptotic proteins such as Bax (Miyashita & Reed, 1995) or Noxa (Phorbol-12-myristate-13-acetate-induced protein 1) (Oda *et al.*, 2000), which are both members of the Bcl-2 family. Hence, an induction of apoptosis would be expected subsequently (Benchimol, 2001; Ryan *et al.*, 2001). If NPM1 is highly concentrated in the nucleoplasm, however, an induction of apoptosis is not observed (Nozawa *et al.*, 1996; Subong *et al.*, 1999). It could be shown that NPM1 enhances p53 level in the nucleus, but reduces them in the mitochondria (Dhar & St. Clair, 2009). In turn, a lack of NPM1 in embryonic fibroblasts containing functional p53, resulted in rapid apoptosis of the cells, whereas p53 double knock-out cells survived (Colombo *et al.*, 2002). It is assumed that the lack of mitochondrial p53 prevents the induction of apoptosis, as the protein precedes changes in the mitochondrial membrane potential, cytochrome c release and caspase-activation (compare section 1.1.3.2) (Erster *et al.*, 2004; Marchenko *et al.*, 2000). Hence, NPM1 might act as an upstream regulator of p53-dependent apoptosis.

These findings conclusively substantiate the observation that the levels of NPM1 expression are associated with cell survival. The upregulation of NPM1 is primarily associated with cell proliferation (Itahana *et al.*, 2003) accompanied by a suppression of apoptosis. This might also explain, why NPM1 levels are elevated in various cancer types (Grisendi *et al.*, 2006; Lim & Wang, 2006; Nozawa *et al.*, 1996; Subong *et al.*, 1999).

Another important finding in regard of cancer development is the identification of NPM1 as a key mediator of genomic stability. It has been known for years to associate with unduplicated centrosomes and is able to dissociate only after its phosphorylation at Thr<sup>199</sup> by CDK2/cyclin E (Okuda *et al.*, 2000; Tokuyama *et al.*, 2001). The centrosome is the main microtubule-organizing center (MTOC) in mammalian cells, directing the formation of bipolar mitotic spindles to assure an accurate distribution of chromosomes during cell division. The core of the centrosomes is constituted by the centrioles (Firat-Karalar & Stearns, 2014). The release of NPM1 from the centrosome is essential to initiate centriole duplication during late G1 to S-phase transition and allows for the proper subsequent formation of the spindle apparatus

(Tokuyama *et al.*, 2001). During mitosis, NPM1 re-associates with the centrosomes at the mitotic spindle poles (Zatsepina *et al.*, 1999), which might depend on the phosphorylation of different residues due to CDK1/cyclin B (Tokuyama *et al.*, 2001). Consequently, the depletion of NPM1 or the mutation of Thr<sup>199</sup> within the protein inhibits a centrosome duplication, which can result in mitotic arrest due to spindle checkpoint activation and p53 induction, formation of unaligned chromosomes or micronuclei. (Amin *et al.*, 2008a, b; Wang *et al.*, 2005). Interestingly, the lack of another nucleolar protein C23, which is also known to function as a histone chaperone, has comparable consequences (Ugrinova *et al.*, 2007). The understanding of this dual role of B23 and C23, however, remains elusive.

A lately emerging correlation concerns the cross-talk between the nucleolus and the DNA damage response (Antoniali *et al.*, 2014; Ogawa & Baserga, 2017). Also in this relation, NPM1 seems to play various roles. Following DNA double-strand breaks or the induction of DNA-repair, phosphorylated NPM1 is recruited from the nucleolus to the site of damage at the chromatin (Lee *et al.*, 2005; Lin *et al.*, 2010). These sites are marked by K63-linked ubiquitin conjugates in dependence of the E3 ubiquitin ligases RNF8 and RNF168. Comparable to the findings during centrosome duplication, the depletion of NPM1 or the mutation of Thr<sup>199</sup> within the protein leads to a persistence of Rad51 foci, indicating that DNA-repair cannot be completed. In addition, more DNA lesions are detectable in such cells (Koike *et al.*, 2010). Moreover, NPM1 was recently identified as one key factor in translesion synthesis (TLS), which can replicate DNA across bulky lesions (Ziv *et al.*, 2014) and it facilitates nucleotide excision repair (NER) (Dijk *et al.*, 2014; Wu & Yung, 2002), as well as the base excision repair pathway (BER) (Poletto *et al.*, 2014; Vascotto *et al.*, 2009, 2014).

## 2 Material

---

### 2.1. Cells

#### 2.1.1. Bacterial strains

---

Strain	Genotype
DH5 $\alpha$	<i>supE44</i> , $\Delta$ <i>lacU169</i> , (80d <i>lacZ</i> $\Delta$ M15), <i>hsdR17</i> , <i>recA1</i> , <i>endA1</i> , <i>gyrA96</i> , <i>thi-1</i> , <i>relA1</i> (Hanahan & Meselson, 1983)
XL2 blue	<i>recA1</i> , <i>endA1</i> , <i>gyrA96</i> , <i>thi-1</i> , <i>hsdR17</i> , <i>supE44</i> , <i>relA1</i> , <i>lac</i> , [F' <i>proAB</i> , <i>lacI</i> <sup>q</sup> $\Delta$ ZM15, <i>Tn10</i> (Tet <sup>r</sup> ), <i>Amy</i> , <i>Cam</i> <sup>r</sup> ] (Agilent Technologies)

---

#### 2.1.2. Mammalian cell lines

---

Cell line	Genotype
H1299	human lung carcinoma cell line, p53 negative (Mitsudomi <i>et al.</i> , 1992)
HepaRG	human hepatic progenitor cell line expressing stem cell properties, able to undergo complete hepatocyte differentiation, derived from hepatoma (Gripon <i>et al.</i> , 2002)
HEK 293	established HAdV-C5-transformed, human embryonic kidney cell line stably expressing the adenoviral E1A and E1B oncoproteins (Graham <i>et al.</i> , 1977)
A549	human lung carcinoma cell line expressing wild-type p53 (Giard <i>et al.</i> , 1973)
HeLa	human cervix carcinoma cell line, p16 negative (Ehrmann & Gey, 1953; Gey, 1958)
6His-SUMO1 HeLa	HeLa cells stably expressing N-terminally His <sub>6</sub> -tagged SUMO1 under puromycin selection (2 $\mu$ g/ml) (Girdwood <i>et al.</i> , 2003; Tatham <i>et al.</i> , 2009)
6His-SUMO2 HeLa	HeLa cells stably expressing N-terminally His <sub>6</sub> -tagged SUMO2 under puromycin selection (2 $\mu$ g/ml) (Tatham <i>et al.</i> , 2009; Vertegaal <i>et al.</i> , 2004)
pBRK	primary baby rat kidney cells, freshly isolated and propagated from 3-5 day old CD-rats (Sprague Dawley; Charles River)
AB120	baby rat kidney cells stably expressing E1A proteins and E1B-55K, derived from pBRK transfected with pE1A (3 $\mu$ g) and pE1B-55K (3 $\mu$ g), polyclonal,

resistance: G418 (Endter *et al.*, 2001)

<b>BRK-AB</b>	baby rat kidney cells stably expressing E1A proteins and E1B-55K, derived from pBRK transfected with pE1A (2 µg), pcDNA3-E1B-55K (2 µg) and pCMX3b-flag (2 µg), polyclonal
<b>BRK-ABV</b>	baby rat kidney cells, derived from pBRK transfected with pE1A (2 µg), pcDNA3-E1B-55K (2 µg) and flag-pV (2 µg), polyclonal

## 2.2. Viruses

Adenovirus	Characteristics	Source
<b>H5pg4100</b>	wt HAdV-C5 containing an 1863 bp deletion (nt 28602-30465) in the E3 region (Kindsmüller <i>et al.</i> , 2007)	group database
<b>H5pm4242</b>	HAdV-C5 containing 4 point mutations A→G in the pV-cds (nt 16564, 16612, 16615 and 17029) leading to an K→R substitution in the HAdV-C5 protein V	this work

## 2.3. Nucleic acids

### 2.3.1. Oligonucleotides

The following oligonucleotides were used for sequencing, PCR, RT-PCR and site-directed mutagenesis (QC-PCR). All oligonucleotides were ordered from Metabion and numbered according to the internal group *Filemaker Pro* database.

#	Name	Sequence	Purpose
635	<b>pcDNA3 fwd</b>	5'-ATG TCG TAA CAA CTC CGC-3'	sequencing
636	<b>pcDNA3 rev</b>	5'-GGC ACC TTC CAG GGT CAA G-3'	sequencing
366	<b>cmv</b>	5'-CCC ACT GCT TAC TGG C-3'	sequencing
675	<b>cmv-3'</b>	5'-CCA ATT ATG TCA CAC CA-3'	sequencing
2361	<b>BamHI-pV fwd</b>	5'-ACA GGA TCC TCC AAG CGC AAA ATC AAA GAA GAG ATG C-3'	PCR amplification

MATERIAL

2362	<b>EcoRI-pV rev</b>	5'-ACA GAA TTC TTA AAC GAT GCT GGG GTG GTA GCG-3'	PCR amplification
1371	<b>18S rRNA fwd</b>	5'-CGG CTA CCA CAT CCA AGG AA-3'	RT-PCR
1372	<b>18S rRNA rev</b>	5'-GCT GGA ATT ACC GCG GCT-3'	RT-PCR
1686	<b>E1A RT fwd</b>	5'-GTG CCC CAT TAA ACC AGT TG-3'	RT-PCR
1687	<b>E1A RT rev</b>	5'-GGC GTT TAC AGC TCA AGT CC-3'	RT-PCR
1441	<b>Hexon-qPCR-fw</b>	5'-CGC TGG ACA TGA CTT TTG AG-3'	RT-PCR
1442	<b>Hexon-qPCR-rev</b>	5'-GAA CGG TGT GCG CAG GTA-3'	RT-PCR
1767	<b>E4orf6-qPCR-rev</b>	5'-CCC TCA TAA ACA CGC TGG AC-3'	RT-PCR
1768	<b>E4orf6-qPCR-fwd</b>	5'-GCT GGT TTA GGA TGG TGG TG-3'	RT-PCR
1571	<b>DBP-qPCR-fw</b>	5'-GAA ATT ACG GTG ATG AAC CCG-3'	RT-PCR
1572	<b>DBP-qPCR-rev</b>	5'-CAG CCT CCA TGC CCT TCT CC-3'	RT-PCR
3395	<b>pV RT fwd</b>	5'-CCC GAA AGC TAA AGC GGG TC-3'	RT-PCR
3396	<b>pV RT rev</b>	5'-CGT AAA GAC TAC GGT GGT GC-3'	RT-PCR
1569	<b>E1B RT fwd</b>	5'-GAG GGT AAC TCC AGG GTG CG-3'	RT-PCR
1570	<b>E1B RT rev</b>	5'-TTT CAC TAG CAT GAA GCA ACC ACA-3'	RT-PCR
2775	<b><math>\beta</math>2-microglobulin fwd</b>	5'-TGA GTA TGC CTG CCG TGT GA-3'	RT-PCR
2776	<b><math>\beta</math>2-microglobulin rev</b>	5'-CCA TGT GAC TTT GTC ACA GCC CAA GAT AGT T-3'	RT-PCR
2746	<b>Ad5-pV K7R fwd</b>	5'-CCA AGC GCA AAA TCA GAG AAG AGA TGC TCC-3'	QC-PCR
2747	<b>Ad5-pV K162R fwd</b>	5'-CCA AGC GCA AAA TCA GAG AAG AGA TGC TCC-3'	QC-PCR
2748	<b>Ad5-pV K23/24R fwd</b>	5'-CTA TGG CCC CCC GAG GAG GGA AGA GCA GGA TTA C-3'	QC-PCR

2749	<b>Ad5-pV K7R rev</b>	5'-GGA GCA TCT CTT CTC TGA TTT TGC GCT TGG-3'	QC-PCR
2750	<b>Ad5-pV K162R rev</b>	5'-CAC CAG ACT CGC GCC TTA GGC CGC GCT TTT-3'	QC-PCR
2751	<b>Ad5-pV K23/24 rev</b>	5'-GTA ATC CTG CTC TTC CCT CCT CGG GGG GCC ATA G-3'	QC-PCR
2958	<b>ATG pV fwd</b>	5'-ACA GGA TCC ATG TCC AAG CGC AAA ATC AAA GAA GAG-3'	PCR amplification
64	<b>E1B bp2043 fwd</b>	5'-CGC GGG ATC CAT GGA GCG AAG AAA CCC ATC TGA GC-3'	PCR amplification
110	<b>E1B bp 361-389 rev</b>	5'-CGG TGT CTG GTC ATT AAG CTA AAA-3'	PCR amplification
330	<b>E1A bp 626 fwd</b>	5'-CCG AAG AAA TGG CCG CCA GTC TTT TGG ACC AGC-3'	PCR amplification
332	<b>E1A 13S bp1073 rev</b>	5'-GCC ACA GGT CCT CAT ATA GCA AAG CG-3'	PCR amplification
811	<b>Abra. seq fwd 17120 bp</b>	5'-GCG ACT GGA AGA TGT CTT GG-3'	PCR amplification
3397	<b>vDNA pV rev</b>	5'-CTT AAA CGA TGC TGG GGT GG	PCR amplification

### 2.3.2. Vector plasmids

The following vector plasmids were used for sub-cloning or as transfection controls. They are numbered according to the internal group *Filemaker Pro* database.

#	Name	Purpose	Reference
136	<b>pcDNA3</b>	expression vector for mammalian cells, CMV promoter	Invitrogen
152	<b>pCMX3b-flag</b>	expression vector for mammalian cells, CMV promoter, N-terminal flag-tag	group database
196	<b>pcDNA3-Flu</b>	expression vector for mammalian cells, CMV promoter, N-terminal HA-tag	group database

77	<b>pGL3 basic</b>	<i>Firefly</i> -Luciferase-Assay	Promega
180	<b>pRL-TK</b>	<i>Renilla</i> -Luciferase-Assay	Promega
96	<b>pBabePuro</b>	retroviral expression vector for mammalian cells, SV40 promoter, puromycin resistance (Morgenstern & Land, 1990)	group database
146	<b>pEGFP-C1</b>	green Fluorescent Protein mut1 expressing vector for mammalian cells, CMV promoter, C-terminal protein fusion possible (GeneBank Accession #U55763)	Clontech

### 2.3.3. DNA templates

The following DNA templates were used in PCR for product amplification. They are numbered according to the internal group *Filemaker Pro* database.

#	Name	Description	Reference
2622	<b>Ad5pPG-S5 PVI K131R</b>	recombinant bacmid-DNA of HAdV-C5 containing a single nt exchange in the L3 pVI-cds	group database
2738	<b>flag-pV</b>	N-terminal flag-tag fused to HAdV-C5 protein V	this work
2963	<b>flag-pVK7R</b>	N-terminal flag-tag fused to HAdV-C5 protein V, single nt exchange in the pV-cds (nt 20)	this work
2964	<b>flag-pVK23/24R</b>	N-terminal flag-tag fused to HAdV-C5 protein V, two nt exchanges in the pV-cds (nt 68 and 71)	this work
2968	<b>flag-pVK23/24/162R</b>	N-terminal flag-tag fused to HAdV-C5 protein V, three nt exchanges in the pV-cds (nt 68, 71 and 485)	this work
1547	<b>pPentonBox (pL3)</b>	HAdV-C5 nt 13280-21460	group database
	<b>pPentonBox-pVK7R</b>	HAdV-C5 nt 13280-21460 containing a single nt exchange in the pV-cds (nt 16564)	this work
	<b>pPentonBox-pVK7/23/24R</b>	HAdV-C5 nt 13280-21460 containing three nt exchanges in the pV-cds (nt 16564, 16612 and 16615)	this work

### 2.3.4. Recombinant plasmids

The following recombinant plasmids were used or generated during this work. They are numbered according to the internal group *Filemaker Pro* database.

#	Name	Vector	Insert	Source
608	<b>pXC15</b>	pXC15	E1-region of HAdV-C5 (nt 1-5790)	group database
737	<b>pE1A</b>	pML	HAdV-C5 E1A	group database
1319	<b>pcDNA3-E1B-55K</b>	pcDNA3	HAdV-C5 E1B-55K	group database
1154	<b>Ad5pPG-S2 (Noah)</b>	pPG-S2	HAdV-C5 wild-type	group database
1547	<b>pPentonBox (pL3)</b>	pPG-S5	HAdV-C5 nt 13280- 21460	group database
2420	<b>pGL3-Basic Prom E1A</b>	pGL3-basic	E1A promoter	group database
2421	<b>pGL3-Basic Prom E1B</b>	pGL3-basic	E1B promoter	group database
2422	<b>pGL3-Basic Prom pIX</b>	pGL3-basic	pIX promoter	group database
2423	<b>pGL3-Basic Prom E2E</b>	pGL3-basic	E2 <i>early</i> promoter	group database
2428	<b>pGL3-Basic Prom E2L</b>	pGL3-basic	E2 <i>late</i> promoter	group database
2425	<b>pGL3-Basic Prom E3</b>	pGL3-basic	E3 promoter	group database
2424	<b>pGL3-Basic Prom MLP</b>	pGL3-basic	major late promoter	group database
2635	<b>HA-spacer-pV</b>	pcDNA3-Flu	HAdV-C5 pV	group database
2738	<b>flag-pV</b>	pCMX3b-flag	HAdV-C5 pV	this work
2969	<b>flag-pV4xKR</b>	pCMX3b-flag	HAdV-C5 pV	this work
2970	<b>pcDNA3-pV</b>	pcDNA3	HAdV-C5 pV	this work
2963	<b>flag-pVK7R</b>	pCMX3b-flag	HAdV-C5 pV	this work
2964	<b>flag-pVK23/24R</b>	pCMX3b-flag	HAdV-C5 pV	this work
2965	<b>flag-pVK162R</b>	pCMX3b-flag	HAdV-C5 pV	this work
2966	<b>flag-pVK7/23/24R</b>	pCMX3b-flag	HAdV-C5 pV	this work
2968	<b>flag-pVK23/24/162R</b>	pCMX3b-flag	HAdV-C5 pV	this work
2967	<b>flag-pVK7/162R</b>	pCMX3b-flag	HAdV-C5 pV	this work

## 2.4. Antibodies

### 2.4.1. Primary antibodies

Name	Properties	Dilution	Source
<b>M73</b>	monoclonal mouse ab against HAdV-C5 E1A proteins 12S and 13S (Harlow <i>et al.</i> , 1985, 1986)	WB 1:10 IF 1:10	group database
<b>AC-15</b>	monoclonal mouse ab (IgG1) against $\beta$ -actin	WB 1:5000	Sigma Aldrich, A-5441
<b>4E8</b>	monoclonal rat ab against the central region (aa 94-110) of HAdV-C5 E1B-55K (Kindsmüller <i>et al.</i> , 2009)	WB 1:10 IF 1:10	group database
<b>3F10</b>	monoclonal rat ab against the HA-epitope	WB 1:10 IF 1:10	Roche, 2013819
<b>M2</b>	monoclonal mouse ab against the flag-epitope	WB 1:2000 IF 1:400	Sigma Aldrich, F3165
<b>6F7</b>	monoclonal rat ab (IgG1) against the flag-epitope	WB 1:10	group database
<b>DO-1</b>	monoclonal mouse ab (IgG2a) against the N-terminal aa 11-25 of human p53 (Vojtesek <i>et al.</i> , 1992)	WB 1:1000	Santa Cruz, sc-126
<b><math>\alpha</math>-PML</b>	polyclonal rabbit ab against human PML isoforms (aa 375-425)	WB 1:1000 IF 1:300 IP 1 $\mu$ l	Novus <i>Biologicals</i> , NB100-59787
<b>B6-8</b>	monoclonal mouse ab against HAdV-C5 E2A protein (Reich <i>et al.</i> , 1983)	WB 1:10 IF 1:10	group database
<b><math>\alpha</math>-pV</b>	polyclonal rabbit ab against HAdV-C5 pV (Matthews & Russell, 1998b)	WB 1:5000 IF 1:10000 IP 0.2 $\mu$ l	kindly provided by Dr. Matthews/ University of Birmingham, GB
<b>FC-61991</b>	monoclonal mouse ab (IgG1) against the C-terminus of human NPM/B23	WB 1:1000 IF 1:100	Invitrogen, 32-5200

MATERIAL

<b>Ab-1</b>	polyclonal rabbit ab against human as well as rat Daxx	WB 1:2000 IP 1 $\mu$ l	Upstate/Millipore, 0747
<b>GH3</b>	polyclonal rabbit ab against human SP100 isoforms	WB 1:5000 IP 1 $\mu$ l	kindly provided by H. Will/ former HPI
<b><math>\alpha</math>-pVI</b>	polyclonal rabbit ab against HAdV-C5 pVI (Wodrich <i>et al.</i> , 2010)	WB 1:1000	kindly provided by H. Wodrich/ University de Bordeaux, Fr
<b>2A6</b>	monoclonal mouse ab against N-terminus of HAdV-C5 E1B-55K (Sarnow <i>et al.</i> , 1982)	WB 1:10 IF 1:10 IP 100 $\mu$ l	group database
<b>E1B-19K</b>	polyclonal rabbit ab against HAdV-C5 E1B-19K (Lomonosova <i>et al.</i> , 2005)	WB 1:5000	group database
<b><math>\alpha</math>-pIX</b>	polyclonal rabbit ab against HAdV-C5 pIX (Lutz <i>et al.</i> , 1997)	WB 1:2000	kindly provided by M. Rosa-Calatrava/ Institut de Génétique et de Biologie Moléculaire et Cellulaire, Strasbourg, Fr
<b>6B10</b>	monoclonal rat ab (IgG2a) against N-terminus (255 aa) of HAdV-C5 L4-100K (Kzhyshkowska <i>et al.</i> , 2004)	WB 1:20	group database
<b>L133</b>	polyclonal rabbit serum against HAdV-C5 capsid proteins (Kinds Müller <i>et al.</i> , 2007)	WB 1:5000	group database
<b><math>\alpha</math>-Mre11</b>	polyclonal rabbit ab against human Mre11	WB 1:5000	Abcam/Novus, pNB 100-142
<b>RSA3</b>	monoclonal mouse ab against N-terminus of HAdV-C5 E4orf6 and E4orf6/7 (Marton <i>et al.</i> , 1990)	WB 1:10	group database
<b><math>\alpha</math>-6His</b>	monoclonal mouse ab (IgG2a) against 6xHis-tag	WB 1:5000	Clontech, 631212

## 2.4.2. Secondary antibodies

### 2.4.2.1. Antibodies for Western Blotting

Product	Properties	Source
<b>HRP-<math>\alpha</math>-mouse</b>	polyclonal horseradish peroxidase (HRP) conjugated antibody against mouse IgG (H+L, F(ab') <sub>2</sub> fragment), host: goat, affinity purified, dilution: 1:10000 in PBST	Jackson, 115 -036-003
<b>HRP-<math>\alpha</math>-rat</b>	polyclonal horseradish peroxidase (HRP) conjugated antibody against rat IgG (H+L, F(ab') <sub>2</sub> fragment), host: goat, affinity purified, dilution: 1:10000 in PBST	Jackson, 112 -036-003
<b>HRP-<math>\alpha</math>-rabbit</b>	polyclonal horseradish peroxidase (HRP) conjugated antibody against rat IgG (H+L, F(ab') <sub>2</sub> fragment), host: goat, affinity purified, dilution: 1:10000 in PBST.	Jackson, 111 -036-003

### 2.4.2.2. Antibodies for Immunofluorescence analysis

Product	Properties	Source
<b>FITC-<math>\alpha</math>-rabbit</b>	polyclonal Fluorescein isothiocyanate (FITC) conjugated antibody against rabbit IgG (H+L, F(ab') <sub>2</sub> fragment), host: donkey, affinity purified, dilution: 1:200 in PBS	Jackson, 711-096-152
<b>Texas Red-<math>\alpha</math>-mouse</b>	polyclonal <i>Texas red</i> (TR) conjugated antibody against mouse IgG (H+L, F(ab') <sub>2</sub> fragment), host: donkey, affinity purified, dilution: 1:200 in PBS	Jackson, 715-076-151
<b>Alexa Flour<sup>TM</sup> 488-<math>\alpha</math>-mouse</b>	polyclonal Alexa <sup>TM</sup> 488 conjugated antibody against mouse IgG (H+L, F(ab') <sub>2</sub> fragment), host: goat, affinity purified, dilution: 1:200 in PBS	Invitrogen, A-11001
<b>Alexa Flour<sup>TM</sup> 488-<math>\alpha</math>-rabbit</b>	polyclonal Alexa <sup>TM</sup> 488 conjugated antibody against rabbit IgG (H+L, F(ab') <sub>2</sub> fragment), host: goat, affinity purified dilution: 1:200 in PBS	Invitrogen, A-11008
<b>Cy3-<math>\alpha</math>-rabbit</b>	polyclonal Cyanine (Cy <sup>TM</sup> 3) conjugated antibody against rabbit IgG (H+L), host: donkey, affinity purified, dilution: 1:200 in PBS	Jackson, 711 -165-152
<b>Cy3-<math>\alpha</math>-mouse</b>	polyclonal Cyanine (Cy <sup>TM</sup> 3) conjugated antibody against	Jackson,

	mouse IgG (H+L), host: donkey, affinity purified, dilution: 1:200 in PBS	715-165-150
<b>Cy3-<math>\alpha</math>-rat</b>	polyclonal Cyanine (Cy <sup>TM</sup> 3) conjugated antibody against rat IgG (H+L, F(ab') <sub>2</sub> fragment), host donkey, affinity purified, dilution: 1.200 in PBS	Jackson, 712-166-153
<b>Cy5-<math>\alpha</math>-rat</b>	polyclonal Cyanine (Cy <sup>TM</sup> 5) conjugated antibody against rat IgG (H+L), host donkey, affinity purified, dilution: 1.200 in PBS	Jackson, 712-175-150

## 2.5. Commercial systems

<b>Product</b>	<b>Source</b>
<i>Dual-Luciferase<sup>®</sup> Assay System</i>	Promega
<i>Plasmid Purification Mini, Midi und Maxi Kit</i>	Qiagen
<i>Protein Assay</i>	BioRad
<i>SuperSignal<sup>®</sup> West Pico Chemiluminescent Substrate</i>	Pierce
<i>Reverse transcription System</i>	Promega
<i>Lipofectamin<sup>®</sup> 2000</i>	Invitrogen
<i>ProFection<sup>®</sup> Mammalian Transfection System</i>	Promega
<i>QIAamp DNA Mini Kit</i>	Qiagen
<i>TNT<sup>®</sup> Coupled Wheat Germ Extract System</i>	Promega
<i>SUMOLink<sup>TM</sup> SUMO-1 Kit</i>	Active Motif

## 2.6. Chemicals, enzymes, reagents and equipment

If not stated differently in the text, chemicals, enzymes and reagents used in this study were obtained from Agilent, Applichem, Biomol, Invitrogen, Merck, New England Biolabs (NEB), Promega, Qiagen, Roche, Sigma Aldrich, Stratagene and ThermoFisher Scientific. Cell culture materials, general plastic material as well as equipment were supplied by BioRad, Biozym, Brand, Engelbrecht, Eppendorf GmbH, Falcon, Gibco BRL, Greiner, Hartenstein, Hellma, Nunc, Pan, Sarstedt, Protean, Schleicher & Schuell, VWR and Whatman.

## 2.7. Standards and Markers

Product	Source
1 kb and 100 bp <i>DNA ladder</i>	NEB
<i>Page Ruler<sup>TM</sup> Prestained Protein Ladder</i>	Pierce

## 2.8. Software and databases

Software	Purpose	Source
<i>Acrobat X Pro</i>	PDF data processing	Adobe
<i>CLC Main Workbench 7.0</i>	sequence data processing	CLC bio
<i>Mendeley Desktop 1.16.1</i>	reference management	Mendeley Ltd.
<i>Filemaker Pro 11</i>	database management	FileMaker, Inc.
<i>Illustrator CS2 und CS6</i>	layout processing	Adobe
<i>Photoshop CS2 und CS6</i>	image processing	Adobe
<i>PubMed</i>	literature database, open sequence analysis, <a href="http://www.ncbi.nlm.gov/PubMed/">http://www.ncbi.nlm.gov/PubMed/</a>	open software (provided by NCBI)
<i>Word 2013</i>	text processing	Microsoft
<i>Prism 5 und 7</i>	data graphing, statistical analysis	GraphPad
<i>NIS-Elements Viewer 4.20</i>	imaging Software	Nikon
<i>NIS-Elements</i>	image capturing of confocal images	Nikon
<i>LASAF Lite</i>	image processing	Leica
<i>Leica Application Suite</i>	image capturing of fluorescence images	Leica
<i>Rotor-Gene Q 2.3.1</i>	RT-PCR data processing	Qiagen
<i>Gen5</i>	absorbance, fluorescence or luminescence measurement with <i>Synergy5 plate reader</i>	BioTek
<i>EPSON Scan</i>	scanning of raw data	Epson
<i>Excel</i>	tabular data processing	Microsoft

<i>Gene tools</i>	image capturing of agarose gels and transformation assays	GBox-Systems (Syngene)
<i>SUMOPlot<sup>TM</sup></i>	prediction of protein SUMOylation, <a href="http://www.abgent.com/sumoplot">http://www.abgent.com/sumoplot</a>	Abgent
<i>GPS-SUMO</i>	prediction of protein SUMOylation, <a href="http://sumosp.biocuckoo.org/online.php">http://sumosp.biocuckoo.org/online.php</a>	Ren <i>et al.</i> , 2009; Zhao <i>et al.</i> , 2014
<i>Jassa</i>	prediction of protein SUMOylation, <a href="http://www.jassa.fr/">http://www.jassa.fr/</a>	Beauchair <i>et al.</i> , 2015
<i>I-TASSER</i>	prediction of protein structure elements, <a href="http://zhanglab.ccmb.med.umich.edu/I-TASSER">http://zhanglab.ccmb.med.umich.edu/I-TASSER</a>	Roy <i>et al.</i> , 2010; Yang <i>et al.</i> , 2015; Yang & Zhang, 2015; Zhang, 2008
<i>APSSP2</i>	prediction of protein secondary structure, <a href="http://www.imtech.res.in/raghava/apssp2/">http://www.imtech.res.in/raghava/apssp2/</a>	Raghava, 2002
<i>PSIPRED V3.3</i>	prediction of protein structure, <a href="http://globin.bio.warwick.ac.uk/psipred">http://globin.bio.warwick.ac.uk/psipred</a>	McGuffin <i>et al.</i> , 2000
<i>iUbiq-Lys</i>	prediction of protein ubiquitination, <a href="http://www.jci-bioinfo.cn/iUbiq-Lys">http://www.jci-bioinfo.cn/iUbiq-Lys</a>	Qiu <i>et al.</i> , 2015
<i>UbiProber</i>	prediction of protein ubiquitination, <a href="http://bioinfo.ncu.edu.cn/UbiProber.aspx">http://bioinfo.ncu.edu.cn/UbiProber.aspx</a>	Xiang Chen <i>et al.</i> , 2013
<i>iMethyl-PseAAC</i>	prediction of protein methylation, <a href="http://www.jci-bioinfo.cn/iMethyl-PseAAC">http://www.jci-bioinfo.cn/iMethyl-PseAAC</a>	Wang <i>et al.</i> , 2011
<i>BPB-PPMS</i>	prediction of protein methylation, <a href="http://www.bioinfo.bio.cuhk.edu.hk/bpbppms/">http://www.bioinfo.bio.cuhk.edu.hk/bpbppms/</a>	Shao <i>et al.</i> , 2009
<i>ASEB</i>	prediction of protein acetylation, <a href="http://bioinfo.bjmu.edu.cn/huac/">http://bioinfo.bjmu.edu.cn/huac/</a>	Li <i>et al.</i> , 2012, 2014; Wang <i>et al.</i> , 2012
<i>BRABSB-PHKA</i>	prediction of protein acetylation, <a href="http://www.bioinfo.bio.cuhk.edu.hk/bpbphka/">http://www.bioinfo.bio.cuhk.edu.hk/bpbphka/</a>	Shao <i>et al.</i> , 2012
<i>NetPhos 2.0</i>	prediction of protein phosphorylation, <a href="http://www.cbs.dtu.dk/services/NetPhos/np.html">http://www.cbs.dtu.dk/services/NetPhos/np.html</a>	Blom <i>et al.</i> , 1999

---

<i>Scanprosite</i>	motif scan for functional sites within proteins, <a href="http://prosite.expasy.org/scanprosite/">http://prosite.expasy.org/scanprosite/</a>	ExPASy, Bioinformatics resource portal (Swiss Institute of Bioinformatics)
<i>The ELM resource</i>	motif scan for functional sites within proteins, <a href="http://elm.eu.org/">http://elm.eu.org/</a>	Dinkel <i>et al.</i> , 2016
<i>Fiji</i> , plugin: <i>Colocalization Threshold</i>	co-localization analysis of pixel intensities in two fluorescent channels	on GitHub, modified from MBF ImageJ
<i>blastp</i>	prediction of RNA-recognition motifs within proteins; <a href="https://blast.ncbi.nlm.nih.gov/Blast.cgi?PROGRAM=blastp&amp;PAGE_TYPE=BlastSearch&amp;LINK_LOC=blasthome">https://blast.ncbi.nlm.nih.gov/ Blast.cgi?PROGRAM=blastp&amp;PAGE_TYPE= BlastSearch&amp;LINK_LOC=blasthome</a>	open software (provided by NCBI)

---

## 3 Methods

---

### 3.1. Bacteria

#### 3.1.1. Culture and Storage

Liquid cultures of bacteria (*E. coli*) were grown in sterile LB-media containing the appropriate antibiotic (100 µg/ml ampicillin; 50 µg/ml kanamycin) at 30-37 °C and 200 rpm in an *Inova 4000 Incubator* (New Brunswick) for 16-24 h. The starter cultures were single bacteria colonies derived from solid LB-media plates (self-made), containing 15 g/l agar and the appropriate antibiotics (100 µg/ml ampicillin; 50 µg/ml kanamycin).

Plated bacteria from glycerol culture or plated transformed bacteria were incubated at 30-37 °C in appropriate incubators (Heraeus) for 16-20 h. Such solid plate cultures can be stored at 4°C for several weeks, if sealed with *Parafilm* (Pechiney Plastic Packaging).

Glycerol stocks from single colony bacteria were generated from 5 ml of the corresponding liquid culture prior to reaching confluency. Contained bacteria were centrifuged at 4°C and 4000 rpm for 5 min (*Megafuge 1.0*; Heraeus). Subsequently, they were resuspended in 1 ml LB-media, containing sterile glycerol (1:1, v/v) and transferred to *CryoTubes<sup>TM</sup>* (Sarstedt) for long-time storage at -80 °C.

<b>LB Media</b>	10 g/l	trypton
	5 g/l	yeast extract
	5 g/l	NaCl
		→ autoclave
<b>antibiotic solution</b>	50 mg/ml	ampicillin
	10 mg/ml	kanamycin
		→ filter sterile and store at -20 °C

#### 3.1.2. Chemical transformation

Chemical competent bacteria strains *E.coli DH5α* (self-made) or *XL2 blue* (Stratagene) were thawed on ice. 100 µl of thawed bacteria were transferred into a pre-cooled polypropylene

reaction tube (15 ml; Falcon) containing 1  $\mu$ l  $\beta$ -mercaptoethanol (1.22 M) and 10  $\mu$ g of desired plasmid-DNA, mixed gently (pipet up and down) and incubated on ice for 30 min. A heat shock at 42°C ensued for 30 s, followed by a re-cooling of the bacteria on ice for 2 min. Subsequently, 1 ml LB-media was added and the bacteria were incubated at 37°C and 200 rpm in an *Inova 4000 Incubator* (New Brunswick) for 45-60 min. Finally, different volumes (usually 100-200  $\mu$ l) were plated on solid LB-media plates (see section 3.1.1). If the growth of bacteria colonies was expected to be weak, the total volume (1 ml) was centrifuged at 4°C and 4000 rpm for 2 min (*Megafuge 1.0*; Heraeus) and sedimented bacteria were resuspended in 150  $\mu$ l fresh LB-media, prior to plating.

XL2 blue bacteria were only used for the transformation of bacmid DNA.

## **3.2. Mammalian cells**

### **3.2.1. Maintenance and passage of cell lines**

All tissue culture techniques were performed in special flow hoods under sterile conditions. This work is based on adherent cells, which are growing in monolayers on polystyrene cell culture dishes (Sarstedt/Eppendorf GmbH). They were cultivated in *Dulbecco's Modified Eagles Medium* containing 0.11 g/l sodium pyruvate (DMEM; Sigma-Aldrich) (Dulbecco & Freeman, 1959), 1 % of a penicillin/streptomycin solution (1000 U/ml penicillin & 10 mg/ml streptomycin in 0.9 % NaCl; Pan), 5% FCS (v/v) in case of H1299, HEK 293, A549 or HeLa cells and 10% FCS (v/v, Pan) in case of HepaRG, pBRK, AB120, BRK-A or BRK-ABV cells. If cell lines were compared in an experiment, they were cultured under the same serum conditions. In case of HepaRG cells, the culture medium was additionally mixed with 5  $\mu$ g/ml bovine insulin (Sigma-Aldrich) and 0,5  $\mu$ M hydrocortisone (Sigma-Aldrich) (Gripon *et al.*, 2002). All cells were cultivated at 37°C in a CO<sub>2</sub>-incubator (Heraeus), which is generating a 5 % CO<sub>2</sub>-atmosphere.

During cell passage, existing medium was removed from sub confluent cells whereupon they were washed with PBS once. The cells were detached from cell culture dishes with appropriate amounts of trypsin/EDTA (Pan) for 5-15 min (depending on the cell type) at 37 °C. Afterwards, trypsin was inactivated by adding culture medium (1:1, v/v). Detached cells were transferred to appropriate reaction tubes (15 ml/50 ml; Sarstedt) and centrifuged at 2000 rpm for 3 min (*Multifuge 3S-R*; Heraeus). After discarding the supernatant, pelleted cells were resuspended in an appropriate volume of culture medium to dilute them (1:5 up to 1:20) for further propagation.

Cells destined for experimental approaches were counted with a hemocytometer (*Neubauer cell counter*; Carl Roth) prior to seeding. Therefore, a small volume of cell-suspension was mixed with a solution of trypan blue (1:1, v/v) and pipetted onto the cell counter. Leaky and dead cells take up this dye. This way, they can be excluded from the wanted number of viable cells in a light microscope (Leica DMIL). The number of cells per ml is given by the following formula:

$$\frac{\text{cells}}{\text{ml}} = \text{counted cells} \times 2 (\text{dilution factor}) \times 10^4$$

<b>PBS</b>	140 mM	NaCl
	3 mM	KCl
	5 mM	Na <sub>2</sub> HPO <sub>4</sub>
	1.5 mM	KH <sub>2</sub> PO <sub>4</sub> in H <sub>2</sub> O
		→ autoclave
<b>trypan blue-solution</b>	0.15 % (w/v)	trypan blue
	0.85 % (w/v)	NaCl in H <sub>2</sub> O
		→ autoclave

### 3.2.2. Cryopreservation of cell lines

For long-time storage, sub confluent cells were trypsinized and sedimented as described in section 3.2.1. Instead of resuspending them in fresh culture medium, they were taken up in an appropriate amount of FCS supplemented with 10 % DMSO (v/v). From this suspension, aliquots of 1 ml were transferred into 1.5 ml *CryoTubes<sup>TM</sup>* (Sarstedt) and gradually cooled down to -80 °C with help of a *Mr. Frosty* (Zefa Laborservice).

To re-cultivate frozen cells, they were thawed at 37 °C in a water bath (GFL, Gesellschaft für Labortechnik), mixed with the appropriate, pre-warmed culture medium (1:1, v/v) and centrifuged with 2000 rpm for 3 min (*Multifuge 3S-R*; Heraeus). The sedimented cells were resuspended in a suitable volume of pre-warmed culture medium and seeded on culture dishes of appropriate size prior to incubation at standard conditions (see section 3.2.1).

### 3.2.3. Transfection of mammalian cells

The transfection of mammalian cells was performed 16-24 h after seeding an appropriate number of cells into culture dishes of a certain scale in a way that they reach a confluency of 60-80 % at the time of transfection.

diameter [mm]	16	22	35	60	100
culture dish	24-well	12-well	6-well		
cell number seeded [ $\times 10^5$ ]	1	1.5	2-4	20	40

### 3.2.3.1. Transfection with Polyethylenimine (PEI)

PEI (Polysciences) is a cationic polymer of 25 kDa, which complexes DNA through interactions with its anionic phosphate backbone and thereby reverts its surface charge. This way the PEI/DNA-complex can be endocytosed by mammalian cells. PEI was solved in dd water (1 mg/ml) and adjusted to pH 7.2 through adding 0.1 N HCl. The solution was filtered sterile (pore size 0.45  $\mu\text{m}$ ; VWR) and stored at  $-80^\circ\text{C}$  up to six months.

Plasmid-DNA to be transfected was diluted with 600  $\mu\text{l}$  of pre-warmed DMEM without nutrients or antibiotics. Afterwards, pre-warmed PEI-solution was added 1:10 (DNA:PEI, v/v). The mixture was vortexed gently, centrifuged shortly to avoid the loss of random amounts through the lids and incubated at room temperature for 10-20 min. During this time, the culture medium of cells to be transfected was changed to pre-warmed DMEM without additives and to half of the previous volume, before the DNA/PEI-mixture was added dropwise. All culture plates were swirled gently to distribute the transfection mixture and incubated at  $37^\circ\text{C}$  with 5 %  $\text{CO}_2$  for 4-6 h. After incubation time, the medium was changed to the appropriate culture medium again to propagate the transfected cells further.

The PEI-transfection is the standard method of transfection in this work, if not indicated other.

### 3.2.3.2. Transfection with calcium phosphate (ProFection<sup>®</sup> Mammalian Transfection System)

All transfection reagents (sterile, deionized water, HBS (2x) and  $\text{CaCl}_2$  (2M)) have to be warmed to room temperature. Plasmid-DNA to be transfected was diluted with sterile, deionized water to 180  $\mu\text{l}$ /437.5  $\mu\text{l}$  (6-well/100 mm cell culture dish), mixed and centrifuged shortly. Equal amounts of two times concentrated (2x) HBS were pipetted into the bottom of a 15 ml conical tube (Sarstedt), before  $\text{CaCl}_2$  (20  $\mu\text{l}$ /62.5  $\mu\text{l}$ ; 2M) was added to the diluted DNA. The prepared DNA solution was added dropwise to HBS, while blowing air through it with a Pasteur pipette to generate equal DNA precipitates of calcium phosphate. The mixture was incubated 30-60 min at room temperature, while the culture medium of cells to be transfected was replaced by fresh, pre-warmed culture medium (half of the initial volume). After incubation

time, the DNA-precipitates were vortexed gently and added dropwise to the cells. All culture plates were swirled carefully to distribute the transfection mixture and incubated at 37°C with 5 % CO<sub>2</sub> for 24-48 h, before changing the culture medium to initial volumes again (2 ml/10 ml). This procedure has been modified from the actual manufacturer's protocol, the *ProFection*<sup>®</sup> *Mammalian Transfection System* (Promega).

### **3.2.3.3. Transfection of linearized viral genomes with *Lipofectamin*<sup>®</sup> 2000**

8 µg of HAdV-C5 genomes in 20 µl *PacI*-reaction mix were adjusted to 500 µl with DMEM in a 1.5 ml reaction tube (Sarstedt). In a second tube of this size, 20 µl *Lipofectamin*<sup>®</sup> 2000 were adjusted to 500 µl with DMEM as well. Both solutions were unified, mixed gently, centrifuged shortly and finally incubated at room temperature for 20 min in the dark. The culture medium of H1299 cells to be transfected (seeded on 60 mm dishes) was removed; the cells were washed with DMEM once and supplied with 600 µl DMEM each. After incubation time, the *Lipofectamin*<sup>®</sup> 2000/DNA mixture was added dropwise to the cells. All culture plates were swirled carefully to distribute the transfection mixture and incubated at 37°C with 5 % CO<sub>2</sub> for 6 h, whereby the plates were swirled hourly. Subsequently, the medium was changed to culture medium again (4 ml) to propagate the transfected cells further.

### **3.2.3.4. Selection of transfected human tumor cells with puromycin**

In section 4.5.4, HEK293 and HeLa cells were co-transfected with a vector plasmid (#96), which contains a puromycin selection marker. This enables the selection of transfected cells with puromycin, since the plasmids of interest do not express a resistance gene. In order to eliminate untransfected cells, the culture medium was replaced by fresh culture medium supplemented with puromycin (final concentration 1.5 µg/ml). Two days p.t. the culture medium was renewed again three days p.t. containing puromycin (final concentration 1 µg/ml). This concentration was kept until the end of the experiment (10 d p.t.) where the medium was removed and the remaining cell colonies were fixed and stained with an aqueous solution containing 25 % MeOH (methanol) and 1 % crystal violet. This way, grown cell foci can be visualized and preserved.

### **3.2.4. Harvest of mammalian cells**

Adherent mammalian cells designated for protein techniques or virus preparations were detached carefully with a cell scraper and collected with their culture medium in conical-bottom

tubes (15 ml/50 ml; Sarstedt). The cells were sedimented with 2000 rpm for 3 min (*Multifuge 3S-R*; Heraeus). The supernatant was discarded; the cells were washed with 5 ml PBS once and stored at -20 °C as pellets for following protein techniques or resuspended in a suitable amount of DMEM for viral preparations.

Adherent mammalian cells designated for nucleic acid isolation were trypsinized as described in section 3.2.1 to avoid cell damage. They were sedimented with 2000 rpm for 3 min (*Multifuge 3S-R*; Heraeus), the supernatant was discarded and the cells were washed once with appropriate amounts of PBS. For following RNA isolation, the cell pellets of 100 mm cell culture plates ( $4 \times 10^6$  seeded cells) were resuspended in 600  $\mu$ l *TRIzol*<sup>®</sup> (ThermoFisher) and stored at -80°C to prevent RNA degradation. If DNA isolation followed, pelleted cells of 60 mm cell culture dishes were stored at -20 °C.

### **3.2.5. Transformation Assay of primary baby rat kidney cells (pBRK)**

Primary BRK cells were seeded (section 3.2.1) into 6-well dishes ( $5 \times 10^5$  cells /well) 24-48 h prior to transfection. The first experiments were performed with the standard transfection reagent PEI (section 3.2.3.1), however, with the transfection medium containing 5 % FCS. Moreover, the cells were washed once with PBS at the end of incubation time, before they were supplied with culture medium again. To improve the assay efficiency the procedure was changed to a transfection with calcium phosphate (section 3.2.3.2) during this work, starting in section 4.5.2. 2 d p.t. the transfected pBRK cells were thinned out by transferring them from 6-well dishes to 100 mm cell culture plates. Therefore, each well was washed with PBS once before 600  $\mu$ l trypsin were added to each well. The cells were incubated at 37 °C until all cells detached from the culture dish and the cells of each well were directly transferred to a 100 mm cell culture plate containing 10 ml of warm culture medium. To avoid any loss of cells each well was washed once with culture medium again, which was added to the 100 mm plate as well.

These pBRK cells were propagated 4-8 weeks, while the culture medium was renewed weekly. After visible cell colony formation and before the colonies grow too dense, the culture medium was removed and the cells were fixed and stained at once with an aqueous solution containing 25 % MeOH and 1 % crystal violet. This way grown cell foci can be visualized and preserved or statistical analysis.

Importantly, handling of pBRK cells requires the pre-warming of all reagents in use.

### 3.2.6. MTT-assay

Dimethylthiazolyldiphenyltetrazolium bromide (MTT, Carl Roth) is cleaved by mitochondrial dehydrogenases leading to a blue/purple staining of the cells. Hence, only viable cells are able to convert MTT with MTT concentrations being proportional to the amount of living cells. For reliable results, cells should be in their logarithmic phase of growth ( $< 10^6$  cells /cm<sup>2</sup>) at the time of seeding.

The MTT-Assay was used in this work to compare the growth of differently transformed cell lines AB120, H1299, BRK-AB and BRK-ABV (section 4.5.1.1). As they are growing quickly, only 400 cells/well were seeded on 12-well cell culture dishes to allow their monitoring for 10 days. The MTT-turnover was measured 1 day after seeding to define the baseline of seeded cells as well as 3, 6 and 10 d after seeding. The MTT working solution for the whole experiment was derived by dilution of an MTT stock solution (1:50, v/v) with PBS to yield a final concentration of 5 mg/ml MTT. It has to be kept in the dark at 4 °C and can be used for 2 weeks. At each time point to measure, 100 µl MTT working solution were added per well, which contains 1 ml culture medium, thus 10 % (v/v) and the cells were incubated for 2 h at 37 °C and 5 % CO<sub>2</sub>. Afterwards, the medium was removed and MTT was extracted from the cells by 200 µl/well N-propyl alcohol (0.1 N in HCl). 100 µl/well of this solution were transferred into single wells of a 96-well plate (flat bottom; Sarstedt) and its absorbance at 540 nm was measured with a *Synergy5 plate reader* (BioTek) using the *Gen5* software. According to the law of *Lambert-Beer*, the absorbance of a colored solution is proportional to the substance, which is solved in a colorless solvent, if it does not exceed 1 or amounts less than 0.1 (Beer, 1852; Mills *et al.*, 2010).

<b>MTT stock solution</b>	1 g 10 ml	MTT PBS → -20 °C for up to 6 month, protect from light
---------------------------	--------------	---

## 3.3. Adenoviruses

### 3.3.1. Infection of mammalian cells

Cells were seeded prior to adenoviral infection as indicated in sections 3.2.1 and 3.2.3. The

culture medium was removed and replaced by half the volume of DMEM without supplements. Adenovirus dilutions with the required multiplicity of infection (moi) were prepared in 1 ml DMEM per dish according to the following formula:

$$V_{virus\ stock\ solution} [\mu l] = \frac{moi [ffu] \times seeded\ cell\ number}{virus\ titer [ffu/\mu l]}; ffu = fluorescence\ forming\ units$$

All cell culture dishes were incubated 90 min with Adenoviruses at 37 °C with 5 % CO<sub>2</sub>. Afterwards, the infectious medium was removed and the cells were supplied with the appropriate culture medium again to propagate them until the experimentally required time post infection (p.i.).

### 3.3.2. Propagation and storage of high-titer virus stocks

Propagation of high-titer adenovirus stocks was performed in H1299 cells. Those cells were infected at 60-80 % confluency in 150 mm cell culture dishes with moi 20 as described in section 3.3.1. The cells were collected 3-5 days p.i. as described in section 3.2.4 and resuspended in 1ml DMEM without supplements per 150 mm culture plate. HAdV used in this work contain deletions within their E3-region, which hampers their release. Therefore, the release of viral particles is forced by repeated freeze and thaw cycles between liquid nitrogen and a 37°C water bath (GFL, Gesellschaft für Labortechnik). Afterwards, cell-suspensions were centrifuged with 4500 rpm for 15 min (*Multifuge 3S-R*; Heraeus) to pellet the cell debris. The supernatant containing HAdV was supplemented with 10 % sterile glycerol (v/v) and preserved at -80 °C. At 4°C, viral titers remain constant for several weeks.

A similar procedure followed the *Lipofectamin*<sup>®</sup> 2000 transfection in section 3.2.3.3. The 60 mm cell culture dishes were harvested 5 d p.i., although without washing. To avoid any loss of newly built infectious particles the freeze and thaw cycles were performed directly in the harvested culture medium, followed by the centrifugation of cell debris. Since, the titer of these initial HAdV productions is unknown, but assumed to be small, two 150 mm cell culture dishes with 60-80 % confluent H1299 cells were reinfected each with 2 ml of the obtained supernatant to produce high-titer virus stocks as described above. The first charge was stored in the group database at -80 °C, while further virus productions were used in experiments. To confirm the integrity of the virus in the first high-titer stock solution, genomic DNA of infected H1299 cells (150 mm cell culture dish) was isolated (section 3.4.2) and the introduced mutations were confirmed by Sanger-sequencing.

### 3.3.2.1. Titration of adenovirus stocks

Titration of the obtained virus solutions was done by determining the fluorescence forming units (ffu) of re-infected H1299 cells. Therefore, 6-well cell culture dishes were equipped with  $4 \times 10^5$  H1299 cells/well as described in section 3.2.1 and infected with 1ml of decreasing dilutions of the virus stock solution ranging from  $10^{-5}$  to  $10^{-3}$  as described in section 3.3.1. 24 h p.i. the cells were washed with 1 ml sterile PBS/well and subsequently fixed with 1 ml ice-cold MeOH/well for 10 min at  $-20^\circ\text{C}$ . After incubation, the alcohol was removed and the cells were air-dried prior to their immunostaining. At this stage, the 6-wells can be stored at  $-20^\circ\text{C}$ .

To reduce unspecific binding of the antibodies, each well was treated with 1ml TBS-BG for 1 h (blocking). Afterwards, the fixed cells in each well were treated with 1ml of primary antibody solution (B6-8 in TBS-BG, 1:10, v/v) for 2 h at  $4^\circ\text{C}$ . This antibody binds to the E2A coded protein DBP (Reich *et al.*, 1983), which induces the formation of viral replication centers in the nuclei of infected cells. Hence, these cells become fluorescent upon treatment with a secondary antibody linked to a fluorophore. Therefore, the cells were washed three times with TBS-BG (5 min each) after incubation with the primary antibody to be treated with Alexa<sup>TM</sup> 488 in TBS-BG (1:1000, v/v) for additional 2 h at  $4^\circ\text{C}$  and exclusion of light. The cells were washed with 1 ml TBS-BG three times again (5 min each). Finally, each well was overlaid with 1 ml of TBS-BG to be analyzed with a fluorescence microscope (Leica DMIL). This way, the 6-wells can be stored approximately 48 h at  $4^\circ\text{C}$  with exclusion of light.

To analyze viral titers properly, the cells have to be distributed evenly in each well, since fluorescent cells are counted in different visual fields in each well to be averaged afterwards. The resulting HAdV titer [ffu/ $\mu\text{l}$ ] can be calculated considering the dilution and the factor corresponding to the objective, which has been used for counting.

<b>TBS-BG</b>	20 mM	Tris/HCl (pH 7.6)
	137 mM	NaCl
	3 mM	KCl
	1.5 mM	MgCl <sub>2</sub>
	0.05 % (v/v)	Tween20
	0.05 % (w/v)	NaN <sub>3</sub>
	5 % (w/v)	glycine
	5 % (w/v)	BSA

### 3.3.3. Determination of viral progeny yields

Adenoviral progeny in certain cell lines was determined by infecting 6-well culture dishes (Sarstedt) containing  $4 \times 10^5$  cells/well at a confluency of 60-80 % with moi 20 (section 3.3.1). The infected wells were harvested at different time points (section 3.2.4), usually 24 h, 48 h and 72 h p.i., resuspended in appropriate amounts of DMEM and stored at  $-20\text{ }^{\circ}\text{C}$  until samples were complete. After release of HAdVs through repeated freeze and thaw cycles, dilutions ranging from  $10^{-2}$  to  $10^{-4}$  were prepared from the remaining solution and H1299 cells were reinfected to determine the viral titers as described in section 3.3.2. Considering, the amount of initially seeded cells, the average amount of viral progeny per cell could be defined [ffu/cell].

## 3.4. DNA techniques

### 3.4.1. Purification of plasmid DNA from *E.coli*

For large scale production of plasmid-DNA a pre-culture containing a single bacteria colony was incubated at  $37\text{ }^{\circ}\text{C}$  in 1 ml LB medium for 4-6 h or in 5 ml at  $30\text{ }^{\circ}\text{C}$  overnight (*Inova 4000 Incubator*, New Brunswick). Following this, the pre-culture was diluted with 50 ml/500 ml LB-medium, supplemented with the appropriate antibiotics and further incubated at  $30\text{ }^{\circ}\text{C}$ - $37\text{ }^{\circ}\text{C}$  and 200 rpm for 16-24 h. The bacteria were sedimented with 6000 rpm for 10 min at  $10\text{ }^{\circ}\text{C}$ . After discarding the supernatant, contained plasmid DNA was isolated according to the manufacturer's protocol by use of a *Midi/Maxi Kit* (Qiagen). The resulting DNA was rehydrated in an appropriate amount of Tris/HCl (10 mM, pH 8) yielding a final concentration of 1  $\mu\text{g/ml}$  (w/v).

For analytical purposes, 800  $\mu\text{l}$  of a liquid bacteria culture were processed to isolate contained plasmid DNA according to a modified protocol of Sambrook and Russell (Sambrook *et al.*, 1989). The bacteria were sedimented with 13000 rpm for 1 min (*Zentrifuge 5417 R*, Eppendorf GmbH), the supernatant was discarded and the pelleted bacteria were resuspended in 300  $\mu\text{l}$  P1 (buffer 1; Qiagen). Afterwards, the suspension was alkalized with P2 (buffer 2; Qiagen) for 5 min and finally neutralized with 300  $\mu\text{l}$  of P3 (buffer 3; Qiagen). The resulting cell debris was sedimented with 13000 rpm for 10 min (*Zentrifuge 5417 R*, Eppendorf GmbH) and 750  $\mu\text{l}$  of the supernatant were transferred into a 1.5 ml reaction tube (Sarstedt) containing 600  $\mu\text{l}$  *iPrOH* to precipitate the DNA. This precipitation was performed for 15 min with 13000 rpm at room temperature. After discarding the supernatant, the DNA pellet was washed with EtOH (75 %, v/v) once and air-dried.

For following Sanger-sequencing (section 3.4.6.3), the DNA was solved in Tris/HCl (10 mM, pH 8) yielding a final concentration of 1 µg/ml (w/v). For analysis of fragmentation patterns by restriction enzymes (section 3.4.6.1), the DNA was directly solved in the required reaction mix.

### 3.4.2. Purification of genomic DNA from Cultured Cells

Collected cell pellets (section 3.2.4) were resuspended each in 200 µl of PBS and supplemented with 20 µl of proteinase K (Sigma-Aldrich). All further steps have been performed according to the *QIAamp DNA Mini and Blood Mini Handbook* (Qiagen). Purified genomic DNA was dissolved 5 min in 200 µl of nucleic acid free-water (Promega) per sample and stored at -20 °C.

To determine the remaining DNA in BRK-AB and BRK-ABV cells (section 4.5.1.1) 5 µg of total-proteins from total-cell lysates were digested with 10 µl proteinase K (2 mg/ml; Peqlab). The reaction mix was adjusted to 90 µl with nucleic acid-free water containing 0.5 µl Tween20 and incubated for 1 h at 55 °C in a Thermomixer (*Thermomixer comfort*, Eppendorf GmbH). To inactivate proteinase K, the reaction was exposed to 95 °C for 10 min, before being rapidly cooled down to 4 °C. 12.5 µl of this reaction were subjected to PCR with a *Taq* polymerase and primer pairs specific for the DNA fragment of interest. In each case, the originally transfected plasmid DNA was included as a positive control (25 ng). All reactions were adjusted to 50 µl sample volume as described in section 3.4.4 and run under conditions described in the same section.

### 3.4.3. Determination of nucleic acid concentrations

The concentration of nucleic acids was determined with a *NanoDrop1000* spectrophotometer (Peqlab) at a wavelength of 260 nm. An extinction (OD) of 1 corresponds to 50 µg DNA per ml and 40 µg RNA per ml, respectively. Their purity was assessed by the ratio  $OD_{260}/OD_{280}$  where values of 1.8 refer to high purity DNA and values > 2.0 denote RNA of high purity.

### 3.4.4. Polymerase chain reaction (PCR)

The polymerase chain reaction (PCR) serves as a tool to amplify DNA *in vitro* (Saiki *et al.*, 1988). A 50 µl reaction in thin-walled, 0.2 ml reaction tubes (Biozym) requires 25 ng of the template DNA to be amplified, 125 ng of a suitable forward primer, 125 ng of a suitable reverse primer, 1 µl dNTPs (10 mM; NEB), 5 µl of the polymerase working buffer (10x) and 1 µl of a thermally stable DNA-polymerase. In this work, the polymerases *Pfu-Ultra2* (5 U/µl;

Stratagene) and *Taq* (5 U/μl; ThermoFisher Scientific) have been used and the reaction was performed in *FlexCyclers* (Analytic Jena).

**Reaction conditions:**

<b>HAdV-C5 E1A in BRK-AB/ABV (section 4.5.1.1)</b> primer: #330, #332 Pol: <i>Taq</i>		
initial DNA denaturation	95 °C	2 min
DNA denaturation	95 °C	30 s
primer annealing/elongation	72 °C	3 min
structural corrections	72 °C	10 min
storage	4 °C	∞
cycles	35	

<b>HAdV-C5 pV in BRK-AB/ABV (section 4.5.1.1)</b> primer: #811, #3397 Pol: <i>Taq</i>		
initial DNA denaturation	95 °C	2 min
DNA denaturation	95 °C	30 s
primer annealing	58 °C	1 min
elongation	72 °C	2 min
structural corrections	72 °C	10 min
storage	4 °C	∞
cycles	35	

<b>HAdV-C5 pV (section 4.1.1)</b> primer: #2361, #2362 template: #2622 Pol: <i>Pfu-Ultra2</i>		
initial DNA denaturation	95 °C	2 min
DNA denaturation	95 °C	1 min
primer annealing	60 °C	40 s
elongation	72 °C	40 s
structural corrections	68 °C	5 min
storage	4 °C	∞
cycles	27	

<b>HAdV-C5 E1B in BRK-AB/ABV (section 4.5.1.1)</b> primer: #64, #110 Pol: <i>Taq</i>		
initial DNA denaturation	95 °C	2 min
DNA denaturation	95 °C	30 s
primer annealing	60 °C	1 min
elongation	72 °C	2 min
structural corrections	72 °C	10 min
storage	4 °C	∞
cycles	35	

DNA denaturation, primer annealing and DNA chain elongation were performed in repeated cycles. To determine the PCR efficiency, 5 μl of the reaction-mix were subjected to analytical agarose-gel electrophoresis (section 3.4.5). PCR-derived DNA, which should be used for cloning of specific DNA, was purified by preparative agarose-gel electrophoresis (section 3.4.5.1).

### 3.4.4.1. Site-directed mutagenesis

Site-directed point mutations were introduced into plasmid DNA with a quick-change PCR (QC-PCR). The sample scale is described in section 3.4.4, *Pfu-Ultra2* was used as polymerase and the primers contained the nucleotide exchange to be introduced. DNA denaturation, primer annealing and DNA chain elongation were performed in repeated cycles. The PCR efficiency was controlled by subjecting 5 µl of the reaction-mix to analytical agarose-gel electrophoresis (section 3.4.5). The remaining 45 µl were incubated with 2 µl *DpnI* (NEB) for 2 h at 37 °C in a Thermomixer (*Thermomixer comfort*, Eppendorf GmbH) to digest the template DNA. Subsequently, 10 µl of the PCR-reaction were transformed into chemical competent *DH5α* bacteria (section 3.1.2). After amplification, purification and preparation of a glycerol stock (sections 3.1.1 and 3.4.1), the mutated DNA was analyzed by Sanger-sequencing (section 3.4.6.3) and stored in the group database at -20 °C or at 4°C for further usage.

#### Reaction conditions:

<b>flag-pVK7R, K23/24R, K7/23/24R, 4xKR HAdV-C5 pVK7R, K7/23/24R</b>		
primer: #2746, #2749 #2748, #2751		
template: #2738, #2963, #2968 (section 4.3.2) #1547, pPentonBox-pVK7R (section 4.5)		
initial DNA denaturation	98 °C	2 min
DNA denaturation	95 °C	1 min
primer annealing	60 °C	1 min
elongation	68 °C	8 min
structural corrections	66 °C	10 min
cycles	17	

<b>flag-pVK162R, K23/24/162R HAdV-C5 pV4xKR</b>		
primer: #2747, #2750		
template: #2738, #2964 (section 4.3.2) pPentonBox-pVK7/23/24R (section 4.5)		
initial DNA denaturation	98 °C	2 min
DNA denaturation	95 °C	1 min
primer annealing	55 °C	1 min
elongation	68 °C	8 min
structural corrections	66 °C	10 min
cycles	19	

### 3.4.4.2. Real-time PCR (RT-PCR)

RT-PCR was used to compare the DNA content (section 4.4.4.3) or cDNA content (section 4.4.4.1) of distinct samples relative to each other. Therefore, purified samples (sections 3.4.2 and 3.5.1) were diluted 1:100 with nucleic acid-free water (Promega). 4.5 µl of these dilutions were mixed with 5 µl *SensiMix Plus SYBR* (Quantace) and 0.5 µl of appropriate primers (5 µM Primer-Mix). All primers used amplify a short fragment of 100-200 bp within a DNA coding sequence. The reaction was performed in a *0.1 ml Strip Tube* (LTF Labortechnik) in a *Rotor-Gene 6000* (Corbett Life Sciences) machine. Each sample was measured in technical duplicates to determine the average threshold cycle (CT). Levels of viral mRNA, represented by their

cDNA, were calculated relative to cellular 18S rRNA/cDNA (section 4.4.4.1), whereas genomic viral DNA was calculated relative to the cellular one-copy gene  $\beta$ 2-microglobuline (section 4.4.4.3). Recording of the melting curves as well as agarose-gel electrophoreses of the RT-PCR products ensured the purity of samples/products.

#### Reaction conditions:

primer: #1371, #1372 #1686, #1687 #1767, #1768 #1571, #1572 #3395, #3396 #1569, #1570		
initial DNA denaturation	95 °C	10 min
DNA denaturation	95 °C	30 s
primer annealing	62 °C	30 s
elongation	72 °C	30 s
cycles	40	

primer: #1441, #1442 #2775, #2776		
initial DNA denaturation	95 °C	10 min
DNA denaturation	95 °C	30 s
primer annealing	60 °C	30 s
elongation	72 °C	30 s
cycles	40	

#### 3.4.5. Separation and Purification of DNA by agarose-gel electrophoresis

An appropriate amount of agarose (*Seakem<sup>®</sup> LE agarose*; Biozym) was suspended in TBE buffer and supplemented with 50 ng/ml ethidium bromide. This suspension was boiled in a microwave (Moulinex) for 5 min to yield a homogenous solution, which can be poured into a gel chamber of suitable size (*PerfectBlue<sup>TM</sup> Gel System*; VWR Peqlab), if it has been cooled down to 40-50 °C. Typical densities of routine agarose gels range from 0.66-0.8 % (w/v). DNA samples to be separated were supplemented with 20 % (v/v) loading buffer (6x) prior to their application. 1kb- and 100 bp-DNA ladders (NEB) were used as references and the separation of DNA-fragments was performed with 5-10 V/cm gel length in TBE.

To protect the DNA in preparative agarose gels from UV-induced damage, they were supplemented with 1 mM guanosine (Gründemann & Schömig, 1996) and the bands of interest were isolated in long-wave UV light (365 nm) with minimal required intensities. Analytical agarose gels were documented with a *G-Box system* UV-Transilluminator (Syngene) at a wavelength of 312 nm by use of the *Gene tools* software (Syngene).

<b>5x TBE</b>	450 mM	Tris/HCl, pH 8
	450 mM	B(OH) <sub>3</sub>
	10 mM	EDTA
		→ pH 7.8 (glacial acetic acid)

---

---

<b>6x loading buffer</b>	0.25 % (w/v)	bromophenol blue
	0.25 % (w/v)	xylene cyanol
	50 % (v/v)	glycerol
	2 % (v/v)	50x TAE (Tris acetate)

### 3.4.5.1. Isolation of DNA from agarose gels

Elution of DNA from isolated agarose gel pieces (section 3.4.5.1) into the surrounding aqueous phase was forced through centrifugation (20000 rpm, 90 min, 10 °C; *RC 5B Plus*; Sorvall). This aqueous phase was transferred into a 1.5 ml reaction tube (Sarstedt) and supplemented with 10 % (v/v) NaOAc (3M) and 90 % (v/v) *i*PrOH. Subsequently, the DNA was precipitated by centrifugation (13000 rpm, 15 min, Zentrifuge 5417; Eppendorf GmbH), washed with EtOH (75 %, v/v), air-dried and rehydrated in 35 µl-45 µl Tris/HCl (10 mM, pH 8). The quality of derived DNA was controlled through an analytical agarose gel by application of 5 µl DNA in Tris/HCl, which also allowed for the estimation of its concentration. The latter was done by comparison of the DNA signal intensities with those of known concentrations belonging to the size references (section 3.4.5).

### 3.4.6. Cloning of DNA fragments

#### 3.4.6.1. Enzymatic DNA restriction

Restriction endonucleases (NEB) were utilized to cut DNA designated for cloning into specific fragments, which can be ligated afterwards with fragments of the same interface. Therefore, 10-20 µg of DNA were incubated with an appropriate single-cutter enzyme (50 U) in its corresponding buffer (provided by the manufacturer NEB) for 2-16 hours at 37 °C in a Thermomixer (*Thermomixer comfort*, Eppendorf GmbH). If necessary, multiple enzymatic restriction reactions were carried out sequentially, intermitted by isopropanol precipitation of the DNA. To obtain the required fragments, the DNA was separated by preparative agarose-gel electrophoresis and isolated from suitable gel parts by centrifugation (sections 3.4.5-3.4.5.1). Finally, the DNA integrity was controlled by subjecting 5 µl of DNA in Tris/HCl (10 mM, pH 8) to agarose-gel electrophoreses, which also allows for the assessment of sample concentration to be used in following ligation steps (section 3.4.6.2).

Restriction enzymes were also used for analytical purposes to validate the integrity of DNA-products through their fragmentation pattern after cloning. Therefore, 0.5-10 µg DNA were incubated for 90 min to 3 h at 37 °C with the appropriate restriction enzyme (3-10 U) in a

---

Thermomixer (*Thermomixer comfort*, Eppendorf GmbH) and subjected to agarose-gel electrophoreses (section 3.4.5.1) in the following.

### 3.4.6.2. Ligation of DNA fragments

Usually, 25-50 ng backbone-DNA (vector or viral) were supplemented with a 10-15-fold excess of the DNA-fragment to be inserted to yield in a final sample volume of 10  $\mu$ l. This DNA-mixture was adjusted to 20  $\mu$ l with a ligation buffer (2x; Roche) and 5 U of T4-DNA-Ligase (Roche). The reaction was performed at least for 4 h at varying temperatures (15-22 °C) and if possible over night at 13 °C in a Thermomixer (*Thermomixer comfort*, Eppendorf GmbH). Prior to transformation into bacteria (section 3.1.2), the reaction was heated to 37 °C for 15 min.

### 3.4.6.3. Sanger-sequencing of DNA

In order to sequence purified DNA 1.2  $\mu$ g of DNA in Tris/HCl (10 mM, pH 8) were supplemented with 30 pmol of an appropriate sequencing primer and adjusted to 15  $\mu$ l with Tris/HCl (10 mM, pH 8). *Seqlab* (Göttingen) performed the sequencing.

## 3.5. RNA techniques

### 3.5.1. Isolation of total-RNA from mammalian cells

To avoid contamination with foreign nucleic acids or RNases, the working space as well as the whole equipment has been cleaned thoroughly with water and *RNase AWAY*<sup>®</sup> (Carl Roth). The cell samples in *TRIzol*<sup>®</sup> (ThermoFisher) (section 3.2.4) were thawed and acclimatized 5 min to room temperature, before 60  $\mu$ l 1-bromo-3-chloropropane (substitute for chloroform to reduce DNA contamination and toxicity) were added to each sample. All samples were shaken for 15 s, incubated for 10 min at room temperature and centrifuged with 12000 g for 15 min at 4 °C (*Zentrifuge 5417 R*, Eppendorf GmbH). The aqueous phase was transferred into a fresh reaction tube (1.5 ml; Sarstedt) on ice and 500  $\mu$ l of isopropanol were added to each sample. All samples were mixed thoroughly prior to their centrifugation (12000 g, 10 min, 4 °C; *Zentrifuge 5417 R*, Eppendorf GmbH) to precipitate contained nucleic acids. Each pellet was washed with 1 ml ethanol (75 %, v/v) by vortexing and centrifuged additional 5 min with 7500 g at 4 °C (*Zentrifuge 5417 R*, Eppendorf GmbH). The pellets were air-dried for 5-10 min and resuspended carefully in 80  $\mu$ l, consisting of 70  $\mu$ l RDD-buffer and 10  $\mu$ l of RNase-free DNase I (Qiagen; DNase I is sensitive to physical denaturation) to digest traces of remaining DNA.

The solution was incubated at room temperature for 30 min and heated to 75 °C for 5 min in a Thermomixer (*Thermomixer comfort*, Eppendorf GmbH) to inactivate the DNase I. RNase-free LiCl solution (Applied Biosystems) was added to each sample (final concentration 2.5 M) to precipitate the RNA for 30 min at -20 °C. It was pelleted afterwards with 16000 g for 20 min at 4 °C (*Zentrifuge 5417 R*, Eppendorf GmbH) and washed once with ice-cold ethanol (75 %, v/v). Each RNA pellet was air-dried for 5-10 min and resuspended in 50 µl of nucleic acid-free water (Promega), its solvation was accelerated through incubation at 58 °C for 10 min in a Thermomixer (*Thermomixer comfort*, Eppendorf GmbH).

### **3.5.2. Quantitative reverse transcription**

In order to transcribe purified RNA into complementary DNA (cDNA) 1 µg of purified RNA (sections 3.5.1 and 3.4.3) were adjusted to 7 µl with nucleic acid-free water (Promega) and incubated at 70 °C for 10 min in a Thermomixer (*Thermomixer comfort*, Eppendorf GmbH). The samples were cooled on ice and mixed each with 13 µl of reverse transcription-mix according to the protocol of the used *Reverse Transcription System* (Promega). The reaction was primed with oligo (dT) primers to select for mRNAs and was incubated 15 min at 42 °C, inactivated at 95 °C for 5 min and finally cooled down on ice. Transcribed cDNAs were stored at -20 °C.

All samples were additionally prepared without the reverse transcriptase to determine the level of background-DNA contamination during RT-PCR (section 3.4.4.2). No sample showed DNA concentrations higher than random background.

## **3.6. Protein techniques**

### **3.6.1. Preparation of total-cell lysates**

Handling of protein solutions requires temperatures < 4 °C to minimize the activity of proteases. Consequently, pelleted cells were lysed on ice for 30 min in appropriate amounts of ice-cold RIPA lysis buffer. The protease inhibitors PMSF (phenylmethylsulfonyl fluoride, 0.2 mM), aprotinin (5 mg/ml), leupeptin (10 mg/ml) and pepstatin A (1 mg/ml) were added freshly to the buffer prior to lysis of the cells, which were transferred to pre-cooled 1.5 ml reaction tubes (Sarstedt) with the buffer. During lysis, the cell suspensions were vortexed every 10 min. In the following, each sample was sonicated for 30 s at 4°C (40 pulses, output 0.6, 0.8 impulses/s;

*Branson Sonifier 450*). To discard unsolved cell debris, the samples were centrifuged with 11000 rpm for 3 min at 4°C (*Zentrifuge 5417 R*, Eppendorf GmbH) and the supernatant was transferred to fresh 1.5 ml reaction tubes (Sarstedt) on ice. Contained protein concentrations were determined photometrically (section 3.6.2).

All samples destined for SDS-PAGE (section 3.6.5) were adjusted to same protein concentrations and volumes by adding pre-cooled water. Subsequently, the samples were denatured by adding the required volume of 5x SDS sample buffer and 3 min of boiling at 95°C in a Thermomixer (*Thermomixer comfort*, Eppendorf GmbH) afterwards. All total-cell lysates were stored at -20 °C.

<b>RIPA lysis buffer</b>	50 mM	Tris/HCl (pH 8)
	150 mM	NaCl
	5 mM	EDTA
	1 % (v/v)	Nonidet P-40
	0.1 % (w/v)	SDS
	0.5 % (v/v)	sodium desoxycholate
<b>SDS sample buffer (5x)</b>	100 mM	Tris/HCl (pH 6.8)
	200 mM	DTT
	10 % (w/v)	SDS
	0.2 % (w/v)	bromophenol blue

### 3.6.2. Determination of protein concentrations in solution

The protein concentration in aqueous phases was determined with the *Protein Assay* (BioRad) and the photometer *SmartSpec™ plus* (BioRad). This assay relies on the Bradford-protein quantification (Bradford, 1976), which makes use of hydrophobic interactions between *Coomassie BB* and proteins in solution. The dye reaches its maximal absorbance at 470 nm; however, in complex with proteins, this maximum shifts to 595 nm. Hence, the absorbance of an aqueous solution at 595 nm is proportional to its protein concentration, if the absorbance is < 1 (Lambert-Beer's law; Beer, 1852).

1 µl of each sample was adjusted to 800 µl with double-distilled (dd) water in a polystyrene cuvette and supplemented with 200 µl of the chromophore (*Bradford Reagent*; BioRad) to measure the sample absorbance against a blank sample (800 µl H<sub>2</sub>O+200 µl *Bradford Reagent*). Protein concentrations were determined by interpolation from a freshly recorded standard curve of BSA (bovine serum albumin; NEB; concentrations: 1, 2, 4, 8 and 16 µg).

### 3.6.3. Immunoprecipitation (IP) of proteins

Immunoprecipitation (IP) of proteins was performed from total-cell lysates in RIPA lysis buffer (sections 3.6.1-3.6.2). For IP experiments, the cysteine protease inhibitors IAA (iodoacetamide, 25 mM) and NEM (N-ethylmaleimide, 25 mM) were added to the lysis buffer. 500-1000  $\mu$ g total-protein, but equal amounts were used per IP. To reduce unspecific protein binding to the protein A sepharose-matrix (Sigma-Aldrich), the samples were pre-cleared with pansorbin (50  $\mu$ l/IP; Calbiochem), which was washed twice with 1 ml RIPA lysis buffer before usage. Intermediate sedimentation was done by centrifugation with 6000 rpm for 3 min at 4 °C (*Zentrifuge 5417 R*, Eppendorf GmbH). Pansorbin contains heat-killed, formalin-fixed *Staphylococcus aureus* cells that bear a high cell-surface density of protein A, which in turn has a high affinity for the F<sub>c</sub> domain (fragment crystallizable region) of IgG.

This way specific IgG are coupled to the protein A sepharose as well. 3 mg lyophilized protein A sepharose were used per IP. The sepharose was rehydrated in 1 ml RIPA lysis buffer (20-30 min, 4 °C) through rotation in an overhead shaker (GFL, Gesellschaft für Labortechnik). Before usage, it was washed twice with ice-cold RIPA lysis buffer, while it was centrifuged with 600 g for 3 min at 4 °C (*Zentrifuge 5417 R*, Eppendorf GmbH). Antibody concentrations to be bound to the sepharose are indicated in section 2.4.1.

Pre-clearing of protein lysates as well as antibody coupling to protein A sepharose were performed at 4°C for 1 h by rotating the samples in a total volume of 1 ml (adjusted with RIPA lysis buffer) in an overhead shaker (GFL, Gesellschaft für Labortechnik). To eliminate remaining uncoupled antibodies, the sepharose was washed three times with 1 ml RIPA lysis buffer with intermediate centrifugation steps of 600 g for 3 min at 4 °C (*Zentrifuge 5417 R*, Eppendorf GmbH). Subsequently, it was resuspended in a suitable amount of RIPA lysis buffer and distributed equally to pre-cooled 1.5 ml reaction tubes (Sarstedt). Pansorbin was sedimented with 6000 rpm for 3 min at 4°C (*Zentrifuge 5417 R*, Eppendorf GmbH) and the pre-cleared protein lysates were transferred to the reaction tubes containing antibody-bound sepharose. A second rotation step for 2 h at 4 °C followed, during which the target protein of the sepharose-bound antibody was precipitated with all bound interaction partners. It has to be kept in mind that RIPA lysis buffer has a high stringency, which might eliminate weak protein-protein interactions.

Protein A sepharose was sedimented with 600 g for 3 min at 4 °C (*Zentrifuge 5417 R*, Eppendorf GmbH), the protein lysate was aspirated and the samples were washed three times each with 1 ml RIPA lysis buffer. Finally, the sepharose samples were mixed with 10  $\mu$ l 2x SDS sample

buffer (Sambrook *et al.*, 1989), boiled 5 min at 95 °C in a Thermomixer (*Thermomixer comfort*, Eppendorf GmbH) to elute all bound proteins and stored at -20 °C for further analysis (sections 3.6.5-3.6.6).

<b>SDS sample buffer (2x)</b>	100 mM	Tris/HCl (pH 6.8)
	200 mM	DTT
	4 % (w/v)	SDS
	0.2 % (w/v)	bromophenol blue
	20 % (v/v)	glycerol

#### 3.6.4. Ni-NTA pull down of 6His-tagged proteins

Transiently transfected (section 3.2.3.1) HeLa, 6His-SUMO1 HeLa or 6His-SUMO2 HeLa cells were harvested 48 h p.t. To ensure sufficient amounts of 6His-SUMOylated proteins, two 100 mm cell culture dishes were prepared per sample. All cells were detached carefully with a cell scraper and collected with their culture medium in 15 ml conical-bottom tubes (Sarstedt), whereby same samples were combined. The cells were sedimented with 2000 rpm for 3 min (*Multifuge 3S-R*; Heraeus), the supernatant was discarded and the cells were resuspended in 5 ml PBS. 1 ml of cell suspension were transferred into a 1.5 ml reaction tube (Sarstedt) to determine steady state protein levels later on as described in sections 3.6.1-3.6.2. Therefore, the collected cells were pelleted with 2000 rpm for 3 min (*Zentrifuge 5417 R*, Eppendorf GmbH), the supernatant was aspirated and the cell pellets were stored at -20 °C. The remaining 4 ml of cells were sedimented again to be immediately resuspended in a guanidinium hydrochloride (GuHCl) lysis buffer. To avoid rapid changes of intracellular SUMOylation events during the stress causing cell harvest, the whole procedure should not take longer than 20 min.

Lysed cells in GuHCl lysis buffer can be stored at -80 °C. Otherwise, they were immediately sonicated for 30 s each (40 pulses, output 0.6, 0.8 impulses/s; *Branson Sonifier 450*). Afterwards, each sample was supplemented with 25 µl Ni-NTA agarose, which had been washed three times with 1 ml GuHCl lysis buffer before. Intermediate sedimentation of the agarose was performed with 900 g for 3 min (*Zentrifuge 5417 R*, Eppendorf GmbH). The samples were incubated over night at 4 °C in an overhead shaker (GFL, Gesellschaft für Labortechnik). After incubation time, the samples were centrifuged with 4000 rpm for 10 min at 4 °C (*Megafuge 1.0*; Heraeus). The viscous supernatant was aspirated carefully, whereas the sedimented agarose was transferred with 500 µl GuHCl lysis buffer to 1.5 ml reaction tubes (Sarstedt). The agarose was sedimented again with 900 g for 3 min (*Zentrifuge 5417 R*,

Eppendorf GmbH), before each sample was washed once with 1 ml wash buffer 1 (pH 8). Two further washing steps followed with a more stringent wash buffer 2 (pH 6.3). After aspirating the final wash buffer, bound 6His-SUMO conjugates were eluted from the Ni-NTA agarose with 30  $\mu$ l/sample of Nickel resin elution buffer. Finally, all samples were boiled at 95 °C for 5 min in a Thermomixer (*Thermomixer comfort*, Eppendorf GmbH). They can be stored at -20 °C until further analysis (sections 3.6.5-3.6.6).

All buffers used in this protocol should be prepared freshly. After lysis of the cells in GuHCl, all steps can be done at room temperature. The protocol is adapted from Tatham *et al.*, 2009.

<b>GuHCl lysis buffer</b>	6 M	GuHCl
	100 mM	94,7 % Na <sub>2</sub> HPO <sub>4</sub> 5,3 % NaH <sub>2</sub> PO <sub>4</sub>
	10 mM	Tris/HCl (pH 8)
	20 mM	imidazole
	5 mM	$\beta$ -mercaptoethanol
	1 $\mu$ g/ml	leupeptin
	1 $\mu$ g/ml	pepstatin
<b>wash buffer 1 (pH 8)</b>	8 M	urea
	100 mM	94,7 % Na <sub>2</sub> HPO <sub>4</sub> 5,3 % NaH <sub>2</sub> PO <sub>4</sub>
	10 mM	Tris/HCl (pH 8)
	20 mM	imidazole
	5 mM	$\beta$ -mercaptoethanol
	1 $\mu$ g/ml	leupeptin
	1 $\mu$ g/ml	pepstatin
<b>wash buffer 2 (pH 6.3)</b>	8 M	urea
	100 mM	22.5 % Na <sub>2</sub> HPO <sub>4</sub> 77.5 % NaH <sub>2</sub> PO <sub>4</sub>
	10 mM	Tris/HCl (pH 6.3)
	20 mM	imidazole
	5 mM	$\beta$ -mercaptoethanol
	1 $\mu$ g/ml	leupeptin
	1 $\mu$ g/ml	pepstatin
<b>Ni resin elution buffer</b>	200 mM	imidazole
	5 % (w/v)	SDS
	150 mM	Tris/HCl (pH 6.7)
	30 % (v/v)	glycerol
	720 mM	$\beta$ -mercaptoethanol
	0.01 %	bromophenol blue → store at -20 °C

### 3.6.5. SDS-PAGE

Denatured protein samples in Ni resin elution buffer, 2x or 5x SDS sample buffer (Sambrook *et al.*, 1989) were separated through SDS-polyacrylamide-gel electrophoresis (PAGE). SDS (sodium dodecylsulfate) is used to mask the local protein charges, which makes their electrophoretic mobility only dependent on their size/molecular weight. The efficiency of protein separation is further increased by discontinuous buffer conditions (Laemmli, 1970). All proteins were concentrated in a 5 % stacking gel of lower pH (6.8) before they entered the separating gel (pH 8.8). The separating gel density is dependent on the proteins of interest size and ranges from 10-12 % in this work. The gels were prepared with a 30 % acrylamide stock solution (37.5:1 *Rotiphorese Gel 30*, Carl Roth) and diluted as listed below (Harlow & Lane, 1988). All needed equipment was set up according to the manufacturer's instructions (*Multigel SDS-PAGE* system; Biometra) and the *Page Ruler™ Plus Prestained Protein Ladder* (10-200 kDa; Pierce) was used as reference of protein sizes. SDS-PAGE was run in TGS buffer with 10 mA/ gel until the samples reached the separating gel. Afterwards the current was increased to 15 mA/gel.

<b>30 % acrylamide stock solution</b>	29 % (w/v)	acrylamide
	1 % (w/v)	N, N'-methylenebisacrylamide
<b>5 % stacking gel</b>	17 % (v/v)	acrylamide solution (30 %)
	120 mM	Tris/HCl (pH 6.8)
	0.1 % (w/v)	SDS
	0.1 % (w/v)	APS
	0.1 % (v/v)	TEMED
<b>10 % separating gel</b>	0.01 %	bromophenol blue
	34 % (v/v)	acrylamide solution (30 %)
	250 mM	Tris/HCl (pH 8.8)
	0.1 % (w/v)	SDS
	0.1 % (w/v)	APS
	0.04 %	TEMED
<b>12 % separating gel</b>	40 % (v/v)	acrylamide solution (30 %)
	250 mM	Tris/HCl (pH 8.8)
	0.1 % (w/v)	SDS
	0.1 % (w/v)	APS
	0.04 %	TEMED
<b>TGS buffer</b>	25 mM	Tris
	200 mM	glycine
	0.1 % (w/v)	SDS

### 3.6.6. Western Blot analysis

Separated proteins from SDS-PAGE (section 3.6.5) were transferred to a nitrocellulose membrane ( $\varnothing$  0.45  $\mu\text{m}$ ; Whatman) per gel to immobilize them for an immunoluminescent detection. Polyacrylamide gels, membranes, blotting papers (Whatman) of appropriate size and two blotting pads (provided by the manufacturer) were soaked in *Towbin* buffer and stacked into a blotting frame (also provided) as follows: Blotting pad, 2 blotting papers, gel, membrane, 2 blotting papers, blotting pad. The stacks were rolled carefully to remove air-bubbles before the frame was closed tightly. The protein transfer was performed in a *Trans-Blot*<sup>®</sup> *Electrophoretic Transfer Cell* (BioRad) in *Towbin* buffer ('full wet' mode) with 400 mA for 90 min.

After completion of the protein transfer, all membranes were incubated with non-fat milk (5 % (w/v; Frema) in PBS) at 4 °C over night on an orbital shaker (GFL). This 'blocking'-step is supposed to saturate sites of unspecific antibody binding on the nitrocellulose. Prior to their treatment with primary antibodies, the membranes were washed with PBST buffer (3x for 10 min each). All required primary antibodies were diluted in PBST buffer as indicated in section 2.4.1. and protein-containing membranes were incubated 3-5 h with the required antibody at 4°C on an orbital shaker (GFL). Subsequently, the membranes were washed again with PBST buffer (3x for 10 min each) to incubate them for 2 h at 4 °C with a suitable secondary antibody (section 2.4.2.1) supplemented with 3 % non-fat dry milk (w/v; Frema). All secondary antibodies used in Western Blot analysis are conjugated to horseradish peroxidase (HRP). HRP catalyzes the *luminol* oxidation, which produces chemiluminescence when the oxidized substrate relaxes from triplet to singlet excitation state.

This capacity of HRP is used for protein detection in the *SuperSignal*<sup>®</sup> *West Pico Chemiluminescent* system (Pierce). Therefore, all membranes were washed after their incubation with secondary antibodies (PBST buffer, 3x, 10 min each) to be incubated with the *SuperSignal*<sup>®</sup> *West Pico Chemiluminescent Substrate* and its co-substrate  $\text{H}_2\text{O}_2$  (1:1, v/v; 2 ml per membrane) for 5 min. Nitrocellulose membranes were covered with transparent films and the chemiluminescence of stained proteins was detected on *medical X-ray films* (CEA RP *new*) in the dark. The time of exposition ranged from 10 s to 4 h. All X-ray films were developed using a *GBX Developer* (Kodak) according to the manufacturer's instructions.

Figures containing Western Blot analysis in this work were prepared by scanning of developed X-ray films and subsequent processing of all data to be visualized with *Photoshop CS2/CS6* and *Illustrator CS2/CS6* (Adobe).

<b>Towbin buffer</b>	25 mM	Tris/HCl (pH 8.3)
	200 mM	glycine
	0.05 %	SDS
	20 % (v/v)	methanol
<b>PBST</b>	0.1 % (v/v)	Tween20 in PBS

### 3.6.7. *In vitro* translation of proteins

To transcribe/translate proteins from plasmid DNA *in vitro*, the *TNT<sup>®</sup>Coupled Wheat Germ Extract Systems* (Promega) has been used according to the manufacturer's protocol; although in a total volume of 25  $\mu$ l (all reactants were halved). 1  $\mu$ g of plasmid DNA (#2635 and #2738) were used per reaction, which had been incubated with required reactants in a Thermomixer (90 min, 30 °C; *Thermomixer comfort*, Eppendorf GmbH) without shaking and without radioactive labelling. Instead, a mixture of amino acid mix-methionine and amino acid mix-leucine (1:1, v/v) was used.

To control the quality of protein translation 2  $\mu$ l of each sample were diluted with 10  $\mu$ l of ice-cold water and 10  $\mu$ l SDS sample buffer (2x), boiled at 95 °C for 5 min in a Thermomixer (*Thermomixer comfort*, Eppendorf GmbH) and subjected to SDS-PAGE (section 3.6.5) and following Western Blot analysis (section 3.6.6).

### 3.6.8. *In vitro* SUMOylation of proteins

A modification of proteins with SUMO1 proteins *in vitro* was achieved with the *SUMOlink<sup>TM</sup> SUMO-1 Kit* (Active Motif). All reactions were performed according to the manufacturer's instructions. Only the scale was halved and all enzymes were diluted 1:5 (v/v). All proteins of interest were obtained by *in vitro* translation (section 3.6.7) and adjusted to comparable amounts with sterile water. A mutated SUMO1 protein, which cannot be conjugated to target proteins anymore, serves as a negative control (provided by the kit). All reactions were incubated for 3 h at 30°C in a Thermomixer (*Thermomixer comfort*, Eppendorf GmbH) with gentle shaking. Reactions were stopped by adding 10  $\mu$ l of SDS sample buffer (2x) to each sample, which were denatured afterwards through boiling for 3 min at 95 °C in a second Thermomixer (*Thermomixer comfort*, Eppendorf GmbH). To analyze the occurrence of protein modification the samples were subjected further to SDS-PAGE (section 3.6.5) and Western-Blot analysis (section 3.6.6).

### **3.6.9. Immunofluorescence (IF) analysis**

$2 \times 10^5$  adherent, eukaryotic cells were seeded on sterile glass coverslips positioned in 6-well cell culture dishes. 24 hours later the cells were treated as experimentally required and at the time point of interest, all treated cells were fixed either with methanol or with paraformaldehyde (PFA, 4 % (v/v) in PBS).

#### **3.6.9.1. Fixation of cells with methanol**

To fix eukaryotic cells in 6-well cell culture dishes with methanol, the culture medium was aspirated and each well was washed with 1 ml sterile PBS. Subsequently, the wells were overlaid with 1 ml ice-cold methanol each and incubated for 10 min at  $-20\text{ }^{\circ}\text{C}$ . Afterwards, the methanol was aspirated and the cells were air-dried for 5 min. This way they can be stored at  $-20\text{ }^{\circ}\text{C}$ .

#### **3.6.9.2. Fixation of cells with PFA**

To fix eukaryotic cells in 6-well cell culture dishes with PFA, the culture medium was aspirated and each well was washed with 1 ml sterile PBS. Subsequently, the wells were overlaid with 0.5 ml PFA each and incubated for 20 min at room temperature. After fixation, the cells were washed with 1 ml PBS/well (3x, 5 min each). This way they can be stored at  $4\text{ }^{\circ}\text{C}$  for approximately 16 h. Ideally, they were immediately prepared for immunological staining.

#### **3.6.9.3. Immunological detection**

To inactivate terminal aldehyde groups of PFA, each well was supplemented with three drops of glycine (1 M, pH 8.5) for 5 min. Three washing steps with 1 ml PBS/well for 5 min each followed. Afterwards, the cells had to be permeabilized with 0.5 % (v/v) Triton X-100 in PBS for 10 min, before they were washed again with 1 ml PBS/well three times. To prevent unspecific antibody binding, potential sites for this were saturated through incubation with 1 ml TBS-BG/well for 10 min. In case of cells fixed with methanol, the protocol was started with this step. Since primary antibodies used for immunostaining were diluted in PBS as indicated in section 2.4.1, all wells were washed again with 1 ml PBS (3x, 5 min each). Incubation with required primary antibodies was performed in a moisty chamber for 30 min by laying each coverslip in a single drop of  $20\text{ }\mu\text{l}$  antibody solution. After incubation time all coverslips were transferred back to the original 6-well dishes to be washed three times with 1 ml PBS (5 min each). Subsequently, this procedure was repeated for the incubation with appropriate secondary

antibodies diluted in PBS (section 2.4.2.2). Only the incubation time was reduced to 20 min. Finally, each coverslip was treated for 5 min with 20  $\mu$ l dapi in PBS (1:1000, v/v; Sigma-Aldrich), rinsed with dd water and mounted on a clean object slide with 7  $\mu$ l of the mounting medium *glow* (EnerGene). This fixation of the coverslips was completed over night at 4 °C, which is also the required temperature for storage of the samples.

IF analysis was performed with a DM6000 Leica fluorescence microscope or a confocal fluorescence microscope (Nikon) and the corresponding software *NIS-Elements Viewer 4.20*, *NIS-Elements* (Nikon) and *LASAF Lite, Leica Application Suite* (Leica), respectively. Further image processing was done with *Fiji*, *Photoshop CS2/CS6* and *Illustrator CS2/CS6*.

### 3.6.10. Reporter gene assay

In order to compare the activities of different adenoviral promoters in the presence of specific proteins, the *Dual-Luciferase<sup>®</sup> Reporter Assay System* (Promega) was used modified from the manufacturer's protocol. Plasmid DNA, which is expressing the *firefly* luciferase (*Photinus pyralis*) under the control of different HAdV-C5 promoters, was already established in the laboratory (#77, #2420-#2425, #2428). In a dual-luciferase assay, the *firefly* luciferase expression can be quantified through its emission of chemiluminescence in the presence of a suitable substrate. This emission in turn is normalized to the light emission of a *renilla* luciferase (#180) within the same sample, which is added to the experiment as an internal transfection control. Consequently, the conditions in each sample are reflected by the relative luciferase activity RLU (*firefly* activity/*renilla* activity). Moreover, all samples were subjected to a background subtraction, determined with empty controls.

Dual-Luciferase Assays were performed in technical triplicates with  $1.5 \times 10^5$  H1299 cells/well in 12-well cell culture dishes (Sarstedt). The cells were transfected with 1.5  $\mu$ g plasmid DNA (section 3.2.3.1) expressing either a firefly luciferase dependent on an adenoviral promoter, a *renilla* luciferase or a protein of interest (0.5  $\mu$ g each). 24 h p.t. the turnover was measured. Therefore, the culture medium was aspirated and the cells were washed with 0.5 ml PBS/well to be incubated with 100  $\mu$ l *passive lysis buffer* per well for 10 min with vigorous shaking on an orbital shaker (GFL). 10  $\mu$ l of total-cell lysate from one well were mixed with 20  $\mu$ l of the *firefly luciferase substrate* to measure the firefly emission immediately for 10 s in a *Lumat LB 9507 luminometer* (Berthold Technologies). The reaction was stopped by adding 20  $\mu$ l of the second substrate *stop and glow*, which is converted by the *renilla* luciferase whose emission is measured again for 10 s.

## 4 Results

---

### 4.1. Subcellular distribution of HAdV-C5 pV in human cells

Different from early adenoviral proteins, such as E1A or E1B-55K, the structural proteins have not been intensively studied. Among them is the minor core protein V, a structural component of mature virions and a DNA binding protein (Chatterjee *et al.*, 1985; Mirza & Weber, 1982; Nermut, 1979; Vayda *et al.*, 1983). As an incoming virion protein, pV is present in the infected host-cell already in the initial phase of infection. As such, it could have a yet unknown regulatory influence on the establishment of conditions favorable to the onset of viral replication. Furthermore, it is a late phase protein, which might not only be packed into newly infectious particles, but could also be part of the regulation of virion assembly (compare section 1.1.4.1) (Samad *et al.*, 2012; Ugai *et al.*, 2007, 2012). The knowledge of both, the immediate early phase of adenoviral infections and the last steps comprising virion assembly, viral DNA encapsidation, virion maturation and the escape of viral progeny are still fragmentary. Hence, functional studies of adenoviral structural proteins like pV might contribute to a profound understanding of these complex processes.

#### 4.1.1. HAdV-C5 pV N-terminally fused to a flag-tag can be expressed in human cells of tumor origin

To be able to discriminate between the functions of protein V during HAdV-C5 infection and its own influence on host cell processes, the generation of HAdV-C5 pV encoded plasmids was essential. Next to an already existing plasmid expressing N-terminally HA-tagged pV (Freudenberger, 2012), a further plasmid should be generated, which expresses pV fused to a flag-tag at its N-terminus. In contrast to the HA-tag, which is a human influenza virus hemagglutinin fragment (HA1, aa 75-110: YPYDVPDYA, Field *et al.*, 1988), the flag-tag is an artificial polypeptide. It is highly hydrophilic and therefore unlikely to denature or inactivate proteins to which it is attached. Its primary sequence is DYKDDDDK with a weight of 1.012 kDa (Hopp *et al.*, 1988). The use of different tags simplifies the detection of HAdV-C5 pV in further experiments and allows the recognition of differences specific for this protein.

The cloning strategy to generate the N-terminally flag-tagged expression plasmid is shown in Figure 8.

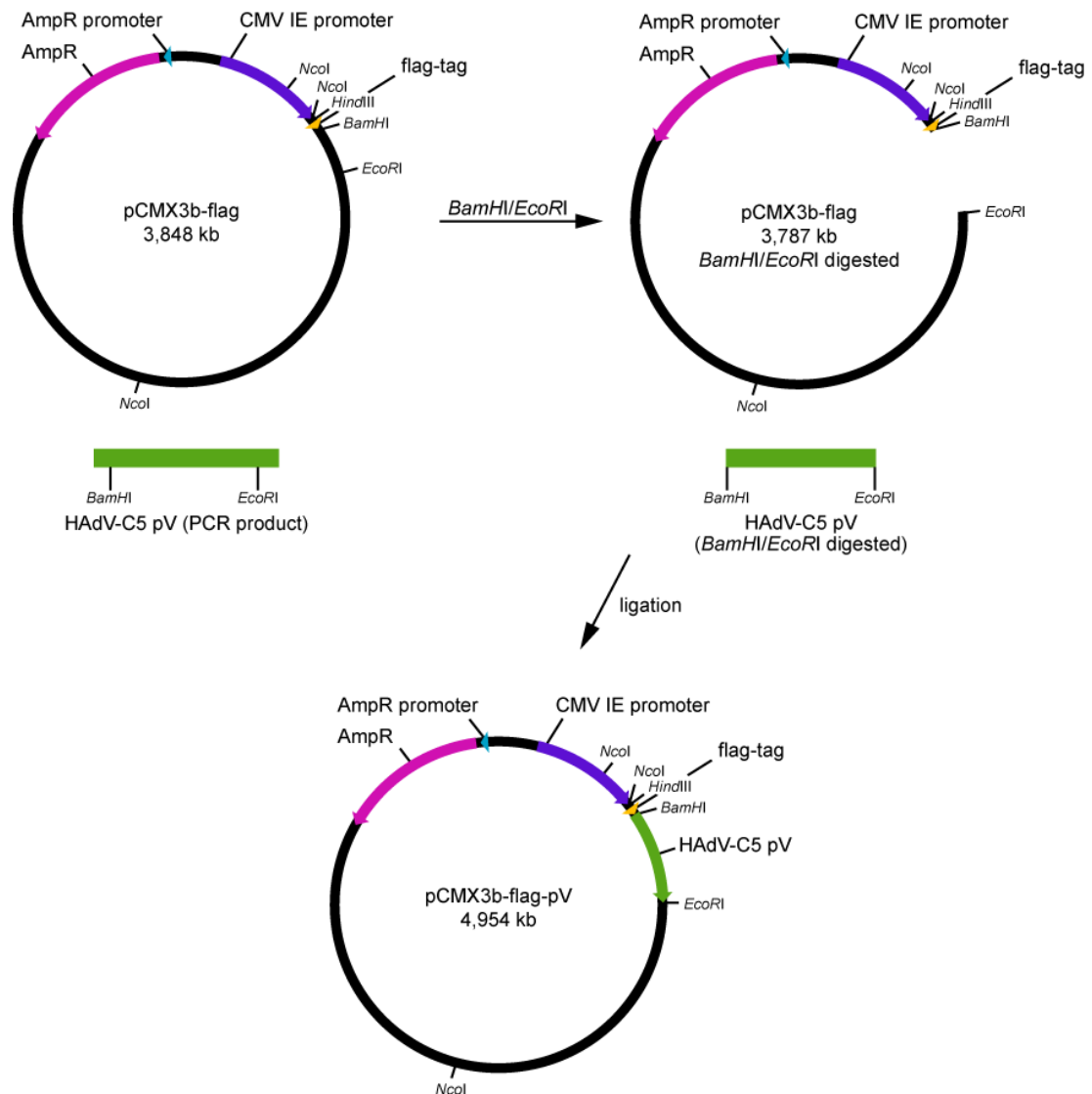


**Figure 8: Cloning strategy of an N-terminally flag-tagged HAAdV-C5 pV expression plasmid.**

HAAdV-C5 pV was amplified by PCR with the oligonucleotide primers #2361/2362 introducing a *Bam*HI restriction site at the 5'-end and an *Eco*RI restriction site at the 3'-end of the coding sequence. HAAdV-C5 genome bacmid-DNA (#2622) was used as template. The vector plasmid pCMX3b-flag (#152) and the PCR product were digested with the restriction enzymes *Bam*HI and *Eco*RI, followed by a directed ligation of the pV-cds into the open vector plasmid pCMX3b-flag.

The required restriction sites *Bam*HI and *Eco*RI were introduced at the termini of the HAAdV-C5 pV coding sequence by PCR (5'-end: *Bam*HI, 3'-end: *Eco*RI). After digesting both, the vector plasmid pCMX3b-flag and the pV-PCR product, with *Bam*HI and *Eco*RI restriction enzymes, the pV-coding sequence could be ligated into the vector in a directed manner. This leads to a new plasmid expressing N-terminally flag-tagged HAAdV-C5 pV (flag-pV) in eukaryotic cells. The product sequence was confirmed by Sanger-sequencing.

To confirm that the generated flag-pV expression plasmid actually allows the synthesis of a flag-tagged protein V in human cells, it was transiently transfected in three different cell lines

of tumor origin, H1299, HepaRG and A549. HepaRG cells are derived from a hepatocellular carcinoma, but they share remarkable similarities with hepatocyte primary cultures. During proliferation, they show an epithelial phenotype and do not express several characteristics of hepatocyte traits. If confluence is reached and the cells are treated additionally with DMSO, however, they differentiate into hepatocyte-like cells. HepaRG cells have only few major chromosomal rearrangements and are pseudodiploid (Gripon *et al.*, 2002). With these characteristics, HepaRG cells represent a great surrogate for primary hepatocytes (Aninat *et al.*, 2006; Guillouzo *et al.*, 2007). They are used in this work, in their undifferentiated state, as a 'pseudo-primary' cell line in comparison to fully transformed epithelial cells, such as H1299. Figure 9 shows that pV, N-terminally tagged with the flag-epitope, is expressed in all three cell lines investigated. It can be detected, as a single band, at a molecular weight between 35 kDa and 55 kDa. The calculated molecular weight of HAdV-C5 pV is 42 kDa (Davison *et al.*, 2003).

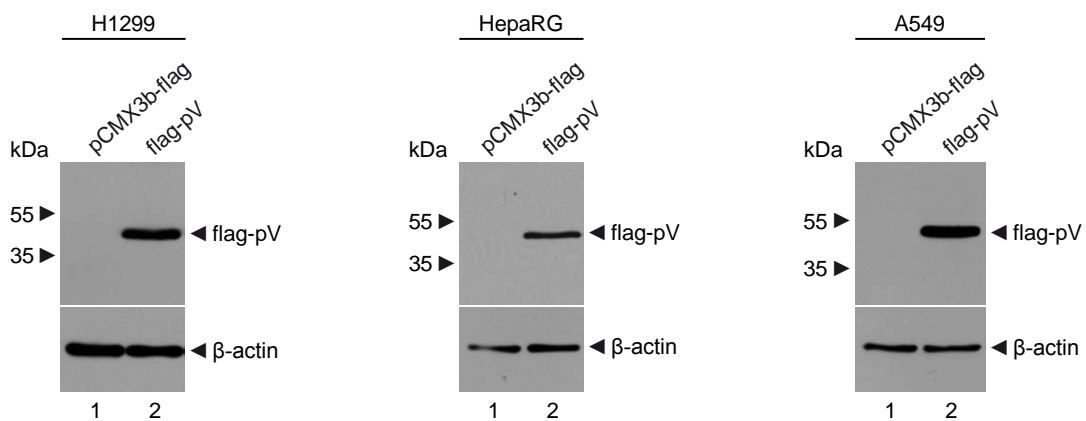


**Figure 9: Expression profile of HAdV-C5 pV in H1299, HepaRG and A549 cells.**

All cells were transfected with 10  $\mu$ g of a flag-pV expression plasmid (#2738) or its empty vector control pCMX3b-flag (#152) and harvested 48 h p.t. Total-cell lysates were resolved by 12% SDS-PAGE and visualized by immunoblotting (400 mA, 90 min, nitrocellulose  $\varnothing = 0.45 \mu$ m). Input levels of flag-pV (100  $\mu$ g) were detected by using mab M2 ( $\alpha$ -flag) and input levels of  $\beta$ -actin (25  $\mu$ g) were detected by using mab AC-15 ( $\alpha$ - $\beta$ -actin). Molecular weights in kDa are indicated on the *left*, while corresponding proteins are labeled on the *right*.

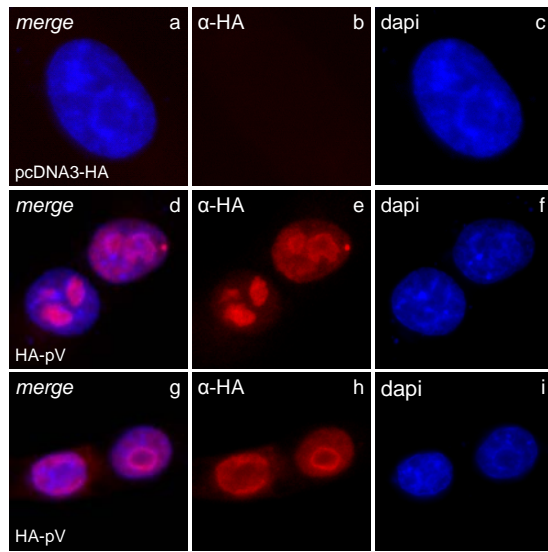
#### 4.1.2. Different N-terminal tags do not influence the subcellular localization of pV in transiently transfected human cells

In previous reports, pV was shown to localize in the nuclei of infected cells where it can be found as accumulations at the nucleoli as well as diffusely spread throughout the nucleoplasm (Matthews & Russell, 1998, Matthews 2001). To validate the localization pattern of the newly generated flag-pV, HepaRG cells were transfected with the flag-pV expression plasmid and prepared for immunofluorescence analysis (Fig. 10). The results are shown in Figure 10B

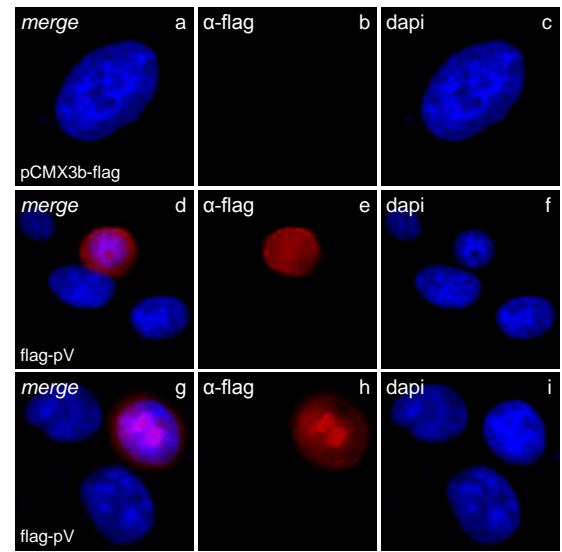
(panels e and h) in comparison to independent experiments where HepaRG cells were either transfected with an already existing HA-pV expression plasmid (Fig. 10A, panels e and h) or infected with HAdV-C5 wt virus (H5pg4100; Fig. 10C, panels e and h and 10D, panels e and h). Figures 10A-D convincingly reveal that all three pV variants are localized in the nuclei of HepaRG cells. Although cells were fixed and stained differently in Figures 10A and B, we observe a very similar pV localization in both transfection experiments. In 64 % of captured cells, transfected with the HA-pV expression plasmid (n = 59), accumulations of pV were found in the nucleus, which appear from completely filled (Fig. 10A, panel e) to ring-like structures (Fig. 10A, panel h). 36 % of the captured cells do not show these accumulations. In these cells, HA-pV is diffusely distributed over the nucleoplasm with an increasing density of signal to the periphery of the nucleus (Fig. 10A, panel h). In case of HepaRG cells transfected with the flag-pV expression plasmid, 89 % of the captured ones (n = 64) show the same kind of accumulations (Fig. 10B, panel h). In this experiment however, the percentage of captured cells showing an additional pV portion in the nucleoplasm is only 68 % compared to 100 % of the HA-pV positive cells. Surprisingly, in 77% of the captured, flag-pV positive HepaRG cells the fluorescence signal exceeds the nucleus.

A comparison of the differently transfected cells with HepaRG cells, which were infected with HAdV-C5, reveals similar accumulations of pV in the nucleus (Fig. 10C, panels e and h and Fig. 10D, panels e and h). As before, they occur filled and unfilled and can be found in 90 % of captured, pV positive cells (n = 40). All these cells also have a pV portion in the nucleoplasm and lack a cytoplasmic signal. These cells, as well as the cells in Figure 10A, were fixed with PFA, in contrast to the experiment shown in Figure 10B where cells have been fixed with methanol. Hence, the methanol-fixation might have damaged the cells in a way that nucleoplasmic flag-pV was partially washed out and therefore could be additionally detected in the cytoplasm. A double staining of pV and nucleophosmin (B23), which is a cellular marker of nucleoli (Spector *et al.*, 1984), revealed a co-localization of the pV-accumulations in HAdV-C5 infected HepaRG cells and B23 (Fig. 10D, panels d and g). The analysis of pixel intensities within nucleolar regions and their direct surrounding (Fig. 10D, *right* panels) by use of the *Fiji* plugin *Colocalization Threshold* resulted in a linear correlation of the red and green channel pixels with the gradient reflecting the ratio of their intensities. The plugin uses an auto threshold determination by use of the Costes method (Costes *et al.*, 2004) and the proportion of signal in one channel that co-localizes with the signal in the other channel is reflected by the thresholded Mander's correlation coefficients (tM) (Manders *et al.*, 1993). The tM ranges from 0 to 1 where 0 means no co-localization and 1 means perfect co-localization of signal intensities.

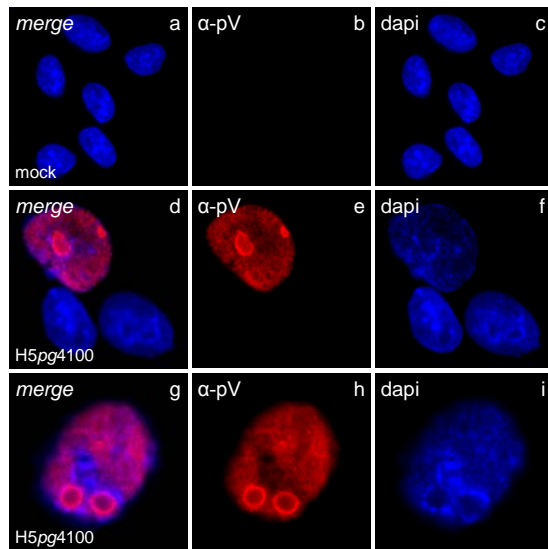
A



B



C



D

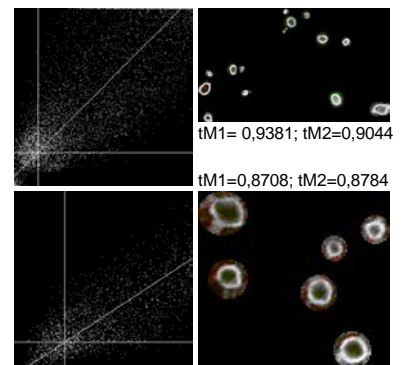
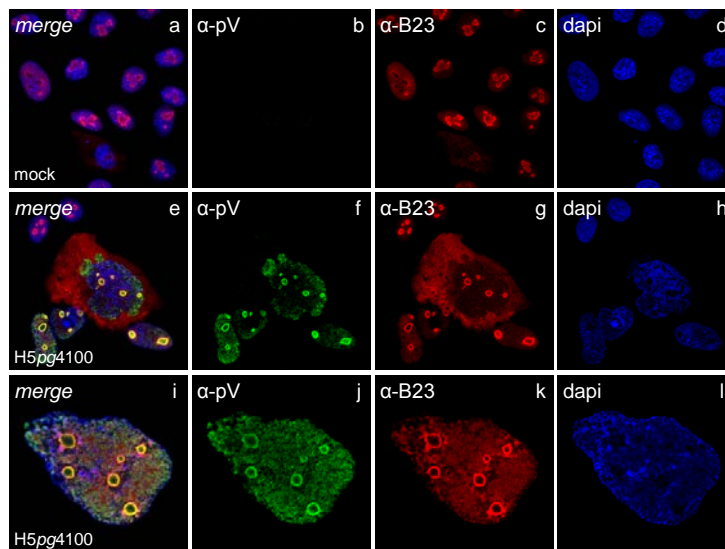


**Figure 10: Intracellular localization of HAdV-C5 flag-pV compared to HA-pV or pV in HepaRG cells.**

HepaRG cells were transfected with 2  $\mu$ g of **A** an HA-pV expression plasmid (#2635) or its empty vector control pcDNA3-HA (#196) and **B** a flag-expression plasmid (#2738) or its empty vector control pCMX3b-flag (#152) and fixed with **A** 4% PFA or **B** MeOH 48 h p.t. **C-D** HepaRG cells were infected with HAdV-C5 wt virus (H5pg4100, moi 20) and fixed with 4% PFA 24 h p.i. Mock means uninfected control. To visualize pV the cells were treated either with **A** mab 3F10 ( $\alpha$ -HA), **B** mab M2 ( $\alpha$ -flag) or **C-D** pab  $\alpha$ -pV. B23 was visualized with mab FC-61991 ( $\alpha$ -B23). Primary antibodies were detected with Alexa488- (green) or Cy3- (red) conjugated secondary antibodies and nuclei were stained with dapi (blue). **A-D** *merge* indicates the overlay of single images of each row. Images were captured with **A-C** a Leica fluorescence wide field microscope or **D** a Nikon confocal fluorescence microscope. **D** The co-localization of HAdV-C5 pV and B23 at host nucleoli is depicted on the *right* by 2D-histograms, which are correlating the pixel intensities of two channels, on the one side and the corresponding channel overlay of the analyzed regions of interest (ROI) on the other side, tM means thresholded Mander's split coefficient where the number indicates the channel, 1 corresponds to the red channel (B23) and 2 corresponds to the green channel (pV).

The tM values in Figure 10D average the signal correlation in all nucleolar regions of one image. It amounts to tM = 0.94 for panels e-h and to tM = 0.87 for panels i-l. Accordingly, the published association of HAdV-C5 pV with host nucleoli could be confirmed in HepaRG cells.

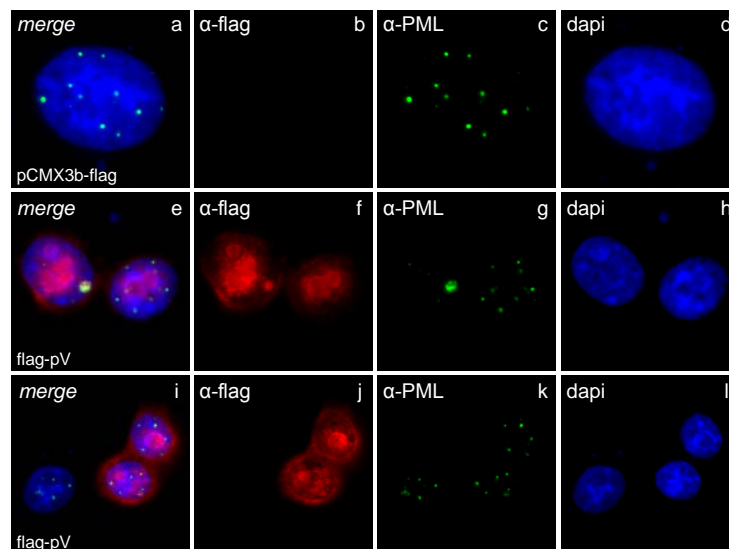
#### 4.2. Interaction of HAdV-C5 pV with PML nuclear bodies

Figure 10 demonstrates a strong nuclear localization of HAdV-C5 pV. Next to the huge accumulations of pV, identified as nucleoli of the host cell, it was also found in smaller nuclear dots in several cells (Fig. 10A, panel e and Fig. 10D, panel e). These accumulations remind of other known nuclear domains, the PML nuclear bodies (PML-NBs). The variety of cellular pathways where the PML-NBs are involved is enormous. They comprise DNA damage and repair (Bischof *et al.*, 2001; Carbone *et al.*, 2002; Dellaire & Bazett-Jones, 2004), apoptosis (Bernardi *et al.*, 2008; Hofmann & Will, 2003; Wang *et al.*, 1998b; Zhu *et al.*, 2004), senescence (Bischof *et al.*, 2002; Ferbeyre *et al.*, 2000; Pearson *et al.*, 2000), transcription (Li *et al.*, 2000; Zhong *et al.*, 2000b), carcinogenesis (Salomoni & Pandolfi, 2002) and epigenetic regulation (Torok *et al.*, 2009) among others (compare section 1.2.1). In addition, different viruses interact with the PML-NBs. For a long time, they have been proposed to be part of an intracellular antiviral defense, since different viruses like HSV-1, HCMV or HAdVs disrupt or reorganize these sub nuclear structures (Everett, 2001; Everett & Chelbi-Alix, 2007; Tavalai & Stamminger, 2008). In case of HAdV-C5, different viral proteins are known to interact with the PML-NBs. On the one hand, they disrupt the integrity of the PML-NBs to disturb specific antiviral functions. On the other hand, they target certain components of PML-NBs to take advantage of their functions for adenoviral replication (compare section 1.2.1.2). These findings hint to an important and complex role of PML-NB components in viral infections and raise the question, whether there might be more adenoviral proteins involved or orchestrated.

#### 4.2.1. HAdV-C5 pV partially co-localizes with PML in transiently transfected HepaRG cells

To elucidate, whether the incoming virion protein HAdV-C5 pV has the potential to interact with the PML-NBs, HepaRG cells were transfected with the flag-pV expression plasmid and prepared for immunofluorescence analysis. As in Figure 10, pV accumulates in the nucleus of transiently transfected cells, next to a weak nucleoplasmic portion and a sphere of pV, which exceeds the nucleus (Fig. 11, panels e-f and i-j). PML appears in an expected, speckled distribution throughout the nucleus, marking the PML-NBs (Fig. 11, panels a,c,i and k). In 15 % of flag-positive cells ( $n > 50$ ), single PML-dots are enlarged and less NBs are observed. In these cells, the enlarged PML-signal always overlaps with a similar shaped, nuclear portion of pV (Fig. 11, panels e-g). According to the *Fiji* plugin *Colocalization Threshold*, the corresponding Mander's correlation coefficients are  $tM1 = 0.87$  (red) and  $tM2 = 0.92$  (green), indicating that both signals actually co-localize.

Hence, there might be different pV-aggregates in the host nucleus, partially able to interact with PML and thereby even inducing their reorganization to huger bulks.

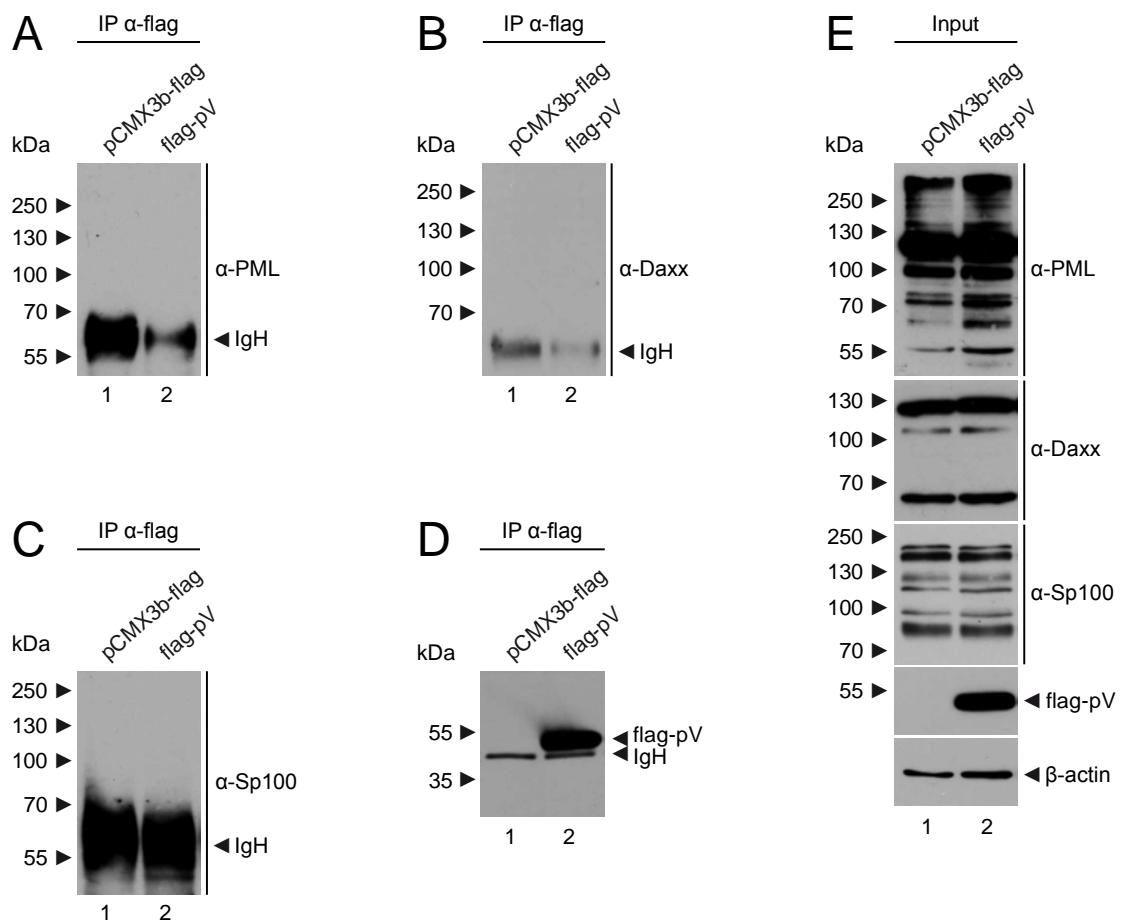


**Figure 11: Flag-pV partially co-localizes with enlarged PML-NBs in transiently transfected HepaRG cells.** HepaRG cells were transfected with 2  $\mu$ g of a flag-expression plasmid (#2738) or its empty vector control pCMX3b-flag (#152) and fixed with MeOH 48 h p.t. The cells were double stained with mab M2 ( $\alpha$ -flag) and pab  $\alpha$ -PML. Primary antibodies were detected with FITC- (green) or Texas red-conjugated secondary antibodies and nuclei were stained with dapi (blue). *Merge* indicates the overlay of single images in each row. Images were captured with a Leica fluorescence wide field microscope.

#### 4.2.2. HAdV-C5 pV does not co-precipitate with the constitutive PML-NB components PML, Daxx and Sp100

In order to investigate the interaction of HAdV-C5 pV with the host PML-NB structures further, co-immunoprecipitation assays were performed in H1299 cells (Fig. 12). The cells were transiently transfected with the flag-pV expression plasmid and harvested 48 h p.t. for lysis and protein preparation. H1299 cells were chosen for this experiment, since they were shown to support flag-pV protein expression (Fig. 9) and the transfection efficiency is higher than for ‘pseudo-primary’ HepaRG cells. The precipitation with an  $\alpha$ -flag specific antibody, however, did not lead to detectable amounts of any isoform of the constitutive PML-NB proteins PML, Daxx or Sp100 (Fig. 12A-C, lane 2 in comparison to 12E). Flag-pV itself was precipitated in high amounts, though (Fig. 12D, lane 2).

The reverse experiment yielded in similar results. Immunoprecipitation with an  $\alpha$ -PML specific antibody gave no signal for flag-pV (Fig. 12F, lane 2). Although immunoprecipitation with an  $\alpha$ -Daxx specific antibody revealed a faint signal of flag-pV (Fig 12G, lane 2), there was no convincing co-precipitation of both proteins in repeated experiments.



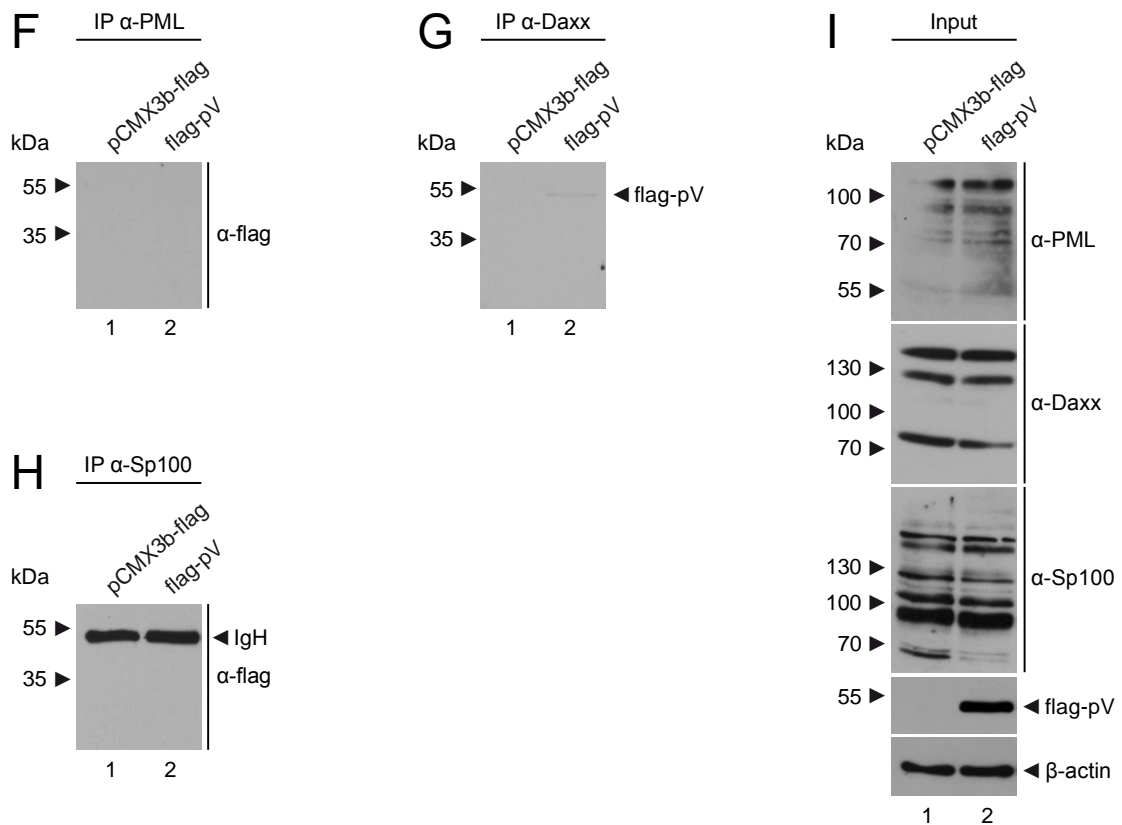


**Figure 12: HAdV-C5 pV does not co-precipitate with the PML-NB components PML, Daxx and Sp100.**

H1299 cells were transfected with 10  $\mu$ g of a flag-pV expression plasmid (#2738) or its empty vector control pCMX3b-flag (#152) and harvested 48 h p.t. Immunoprecipitation (IP) was performed by usage of **A-D** mab M2 ( $\alpha$ -flag), **F** pab  $\alpha$ -PML, **G** pab  $\alpha$ -Daxx or **H** pab GH3 ( $\alpha$ -Sp100), resolved with total-cell lysates as input control **E,I** by 10% SDS-PAGE and visualized by immunoblotting (400 mA, 90 min, nitrocellulose  $\phi = 0.45 \mu$ m). Co-precipitated and input proteins were detected by using mab M2 ( $\alpha$ -flag, 50  $\mu$ g input), pab  $\alpha$ -PML (50  $\mu$ g), pab  $\alpha$ -Daxx (100  $\mu$ g input), pab GH3 ( $\alpha$ -Sp100, 100  $\mu$ g input) and AC-15 ( $\alpha$ - $\beta$ -actin, 25  $\mu$ g input). Molecular weights in kDa are indicated on the *left*, while corresponding proteins are labeled on the *right*. IgH means heavy chain of the antibody used for immunoprecipitation.

In case of precipitation with an  $\alpha$ -Sp100 specific antibody, there is no possibility of a definite statement, since the potential signal of flag-pV is competing with the size of the heavy chain of the  $\alpha$ -Sp100 specific antibody (Fig. 12H).

Taken together, there is no sufficient evidence from this data pointing towards an interaction of HAdV-C5 pV with one of the major PML-NB components PML, Daxx and Sp100 in H1299 cells. Despite these findings, an interaction with temporary factors of the PML-NBs is still a possibility, since the composition of the nuclear bodies is dynamic. So far, at least 166 interaction partners of the PML-NBs are described in literature, of which approximately one-half plays a role in transcriptional regulation (compare section 1.2.1). Another well represented functional group of PML-NBs interaction partners comprise proteins involved in virus-host interactions (van Damme *et al.*, 2010), thus containing lots of potential interaction partners.

### 4.2.3. HAdV-C5 pV co-precipitates with the PML-NB associated adenoviral proteins E1B-55K and pVI

To date, there are different adenoviral proteins known to interact with the PML-NBs. Besides the already mentioned proteins E1A and E4orf3 (compare section 1.2.1.2), another early protein, E1B-55K, partially localizes to PML-NBs and binds the PML-isoforms IV and V (Leppard & Everett, 1999; Wimmer *et al.*, 2010). Additionally, the E2A protein, an essential factor for adenoviral DNA-replication, targets the PML-NBs where its oligomerization is required to selectively recruit the PML-NB components Sp100 and USP7 (Komatsu *et al.*, 2015). Besides those regulatory proteins, two structural proteins, pVI and pIX, are known to associate with the PML-NBs. Protein IX is speculated to act as a late PML-neutralizer, which drives both nucleoplasmic and track-associated PML into clear amorphous inclusions. It is thought to thereby prevent the reassembly of PML-NBs late in infection, ensuring optimal viral proliferation (Rosa-Calatrava *et al.*, 2003). Protein VI, on the other hand, interacts with the cellular factor Daxx to relocate it from its active sites at the PML-NBs and the viral chromatin. Thereby it reverts the transcriptional repressive functions of the Daxx protein (Schreiner *et al.*, 2012). Furthermore, pVI was shown to bind pV. This interaction is thought to bridge the adenoviral core with the surrounding capsid in mature virions (compare sections 1.1.2 and 1.1.4.1), making pVI a good candidate to mediate an interaction between pV and the PML-NBs.

To reveal yet unknown interactions between HAdV-C5 pV and PML-NB associated adenoviral proteins, additional co-immunoprecipitation assays were performed in infected H1299 cells (Fig. 13). As expected from previous publications (Chatterjee *et al.*, 1985; Matthews & Russell, 1994, 1995, 1998a), pVI could be co-precipitated with pV after usage of an  $\alpha$ -pV specific antibody (Fig. 13D, lane 2), serving as a positive control of the experimental conditions. In spite of some background detection, the pVI-characteristic double band at approximately 25 kDa is clearly detectable. The capsid protein IX as well as the early proteins E1A and E2A was not detectable after precipitation of pV (Fig. 13A,C and E). Interestingly however, E1B-55K was co-precipitated with pV (Fig. 13B, lane 2), indicating an interaction of both proteins.

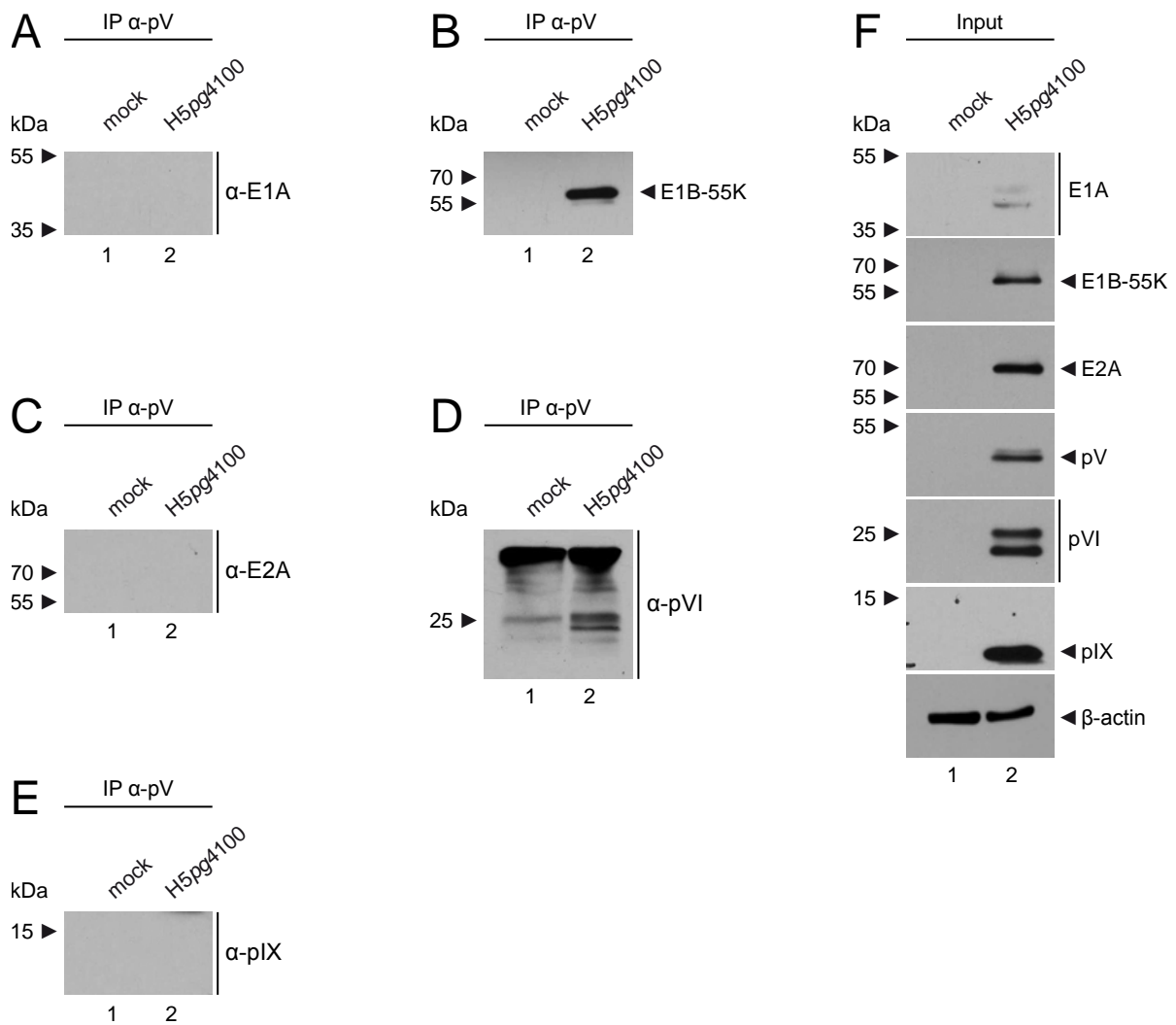


**Figure 13: Protein V co-precipitates with E1B-55K and pVI from HAdV-C5 infected H1299 cell lysates.** H1299 cells were infected with HAdV-C5 (H5pg4100, moi 20) and harvested 24 h p.i. Immunoprecipitation (IP) A-E was performed by usage of pab  $\alpha$ -pV, resolved with total-cell lysates as input control F by 10-12% SDS-PAGE and visualized by immunoblotting (400 mA, 90 min, nitrocellulose  $\phi = 0.45 \mu\text{m}$ ). Co-precipitated and input proteins were detected by using pab  $\alpha$ -pV (25  $\mu\text{g}$  input), mab M73 ( $\alpha$ -E1A, 100  $\mu\text{g}$  input), mab 2A6 ( $\alpha$ -E1B-55K, 25  $\mu\text{g}$  input), mab B6-8 ( $\alpha$ -E2A, 25  $\mu\text{g}$  input), pab  $\alpha$ -pVI (25  $\mu\text{g}$  input), pab  $\alpha$ -pIX (100 $\mu\text{g}$  input) and mab AC-15 ( $\alpha$ - $\beta$ -actin, 25  $\mu\text{g}$  input). Molecular weights in kDa are indicated on the *left*, while corresponding proteins are labeled on the *right*. Mock means uninfected control.

As there was no sample containing the viral proteins separately, the possibility remained that E1B-55K binds unspecific to the  $\alpha$ -pV-coupled sepharose A beads. Consequently, the immunoprecipitation experiment was repeated in H1299 cells, transiently transfected with a flag-pV expressing plasmid, an E1B-55K expressing plasmid or both plasmids together (Fig. 14). Unfortunately, it was not possible to separate the precipitated proteins from the heavy chains of the different antibodies used for immunoprecipitation (Fig. 14A-B). In case of 2A6, an  $\alpha$ -E1B-55K specific antibody (species mouse), the heavy chain signal was attempted to be minimized by use of primary antibodies against pV derived from other species, such as the polyclonal rabbit ab  $\alpha$ -pV or the monoclonal rat ab 6F7 ( $\alpha$ -flag). In repeated experiments,

however, the signal corresponding to the 2A6 heavy chain still interfered with flag-pV, which is occurring at a similar size after protein separation with SDS-PAGE (Fig. 14A and C).

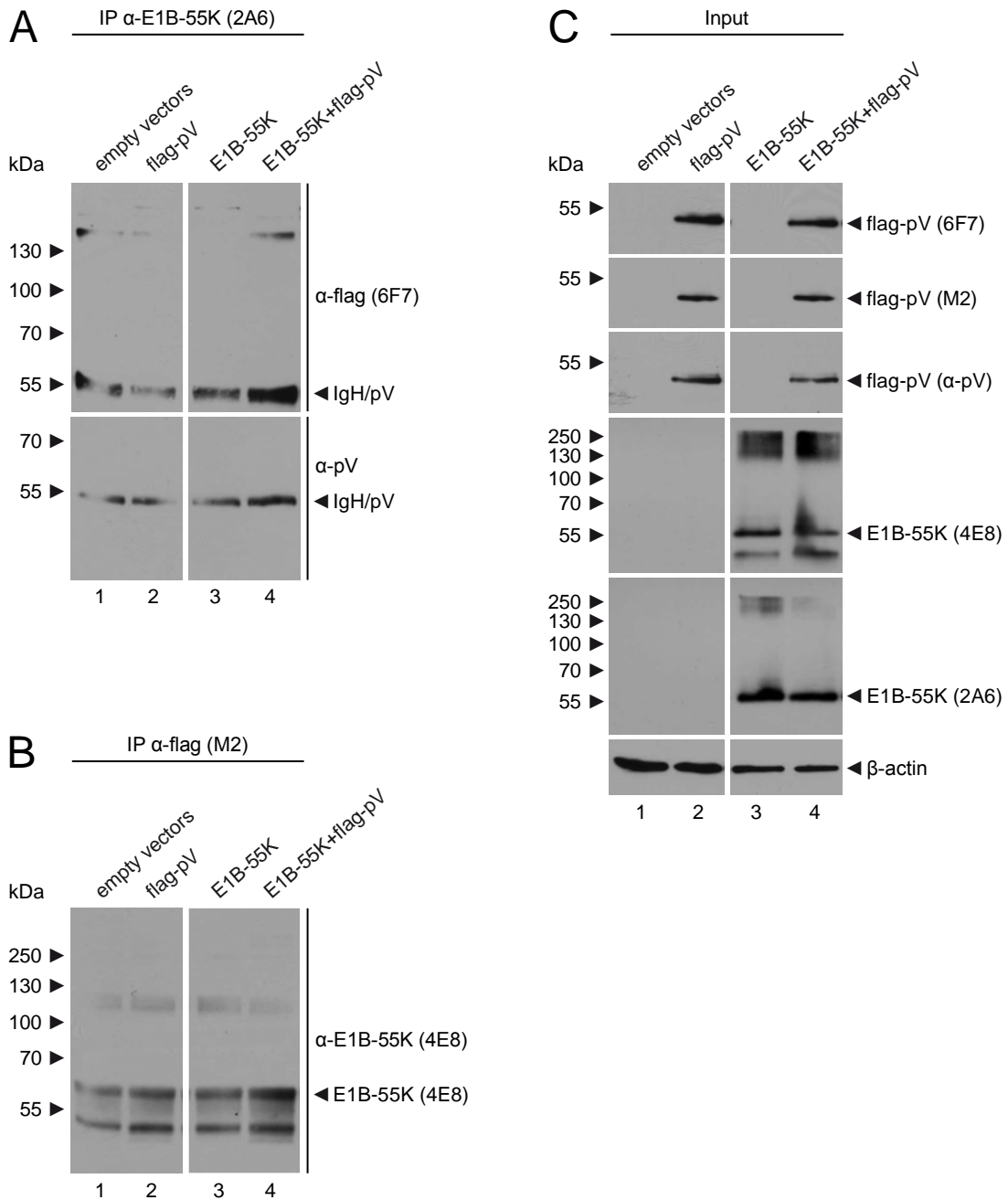


**Figure 14: Co-precipitation of HAdV-C5 pV and E1B-55K is not definite in transiently transfected H1299 cells.**

H1299 cells were transfected with 5  $\mu$ g of a flag-pV expression plasmid (#2738), 5  $\mu$ g of an E1B-55K expressing plasmid (#1319) or both plasmids together. All DNA-amounts were adjusted with corresponding empty vector plasmids. The cells were harvested 48 h p.t. and immunoprecipitation was performed by usage of **A** mab 2A6 ( $\alpha$  E1B-55K) or **B** mab M2 ( $\alpha$ -flag), resolved with total-cell lysates as input control **C** by 10% SDS-PAGE and visualized by immunoblotting (400 mA, 90 min, nitrocellulose  $\phi = 0.45 \mu$ m). Co-precipitated and input proteins were detected by using mab M2 ( $\alpha$ -flag, 30  $\mu$ g input), mab 6F7 ( $\alpha$ -flag, 50  $\mu$ g input), pab  $\alpha$ -pV (50  $\mu$ g input), mab 2A6 ( $\alpha$ -E1B-55K, 30  $\mu$ g input), mab 4E8 ( $\alpha$ -E1B-55K, 30  $\mu$ g input) and AC-15 ( $\alpha$ - $\beta$ -actin, 30  $\mu$ g input). Molecular weights in kDa are indicated on the *left*, while corresponding proteins are labeled on the *right*. IgH means heavy chain of the antibody used for immunoprecipitation.

Nevertheless, there is a stronger signal detectable, if E1B-55K and flag-pV are present together (Fig. 14A-B, lane 4). The same holds true for the reverse experiment where a monoclonal mouse  $\alpha$ -flag ab was used for immunoprecipitation and E1B-55K was visualized with 4E8, a monoclonal rat  $\alpha$ -E1B-55K antibody, instead of 2A6 (Fig. 14B). This results in two dominant bands of which the upper one corresponds to E1B-55K (compare 2A6-staining in Fig. 14C, lanes 3-4). As it could be found for HAdV-C5 pV in the presence of E1B-55K before, the E1B-55K signal slightly increases in the presence of flag-pV (Fig. 14B, lane 4).

In all immunoprecipitation experiments with transiently transfected H1299 cells, no specific signal appeared exclusively, if both viral proteins are present. Hence, an interaction of HAdV-C5 pV and E1B-55K neither can be stated absolutely certain nor can it be ruled out.

### **4.3. HAdV-C5 pV is a novel target of the host SUMOylation machinery**

#### **4.3.1. HAdV-C5 pV is post-translationally modified with SUMO proteins**

SUMOylation has been discussed as essential for maintaining the 3D-structure of PML-NBs for years. It has been proposed that SUMO-SIM-interactions recruit further SUMOylated proteins, such as the constitutive PML-NB factors Sp100 and Daxx to build higher order structures (Everett *et al.*, 1999; Hattersley *et al.*, 2011; Lallemand-Breitenbach *et al.*, 2001; Lang *et al.*, 2010; Shen *et al.*, 2006a; Sternsdorf *et al.*, 1997, 1999; Zhong *et al.*, 2000a). Furthermore, the PML-NBs have been discussed as nuclear sites to mediate post-translational modifications of partner proteins, especially the SUMO modification (compare section 1.2.1.). All enzymes involved in SUMOylation and some of the enzymes mediating the deSUMOylation of proteins are present at the PML-NBs and PML itself has been proposed to have an E3 SUMO-ligase activity (van Damme *et al.*, 2010; Dellaire & Bazett-Jones, 2004; Shen *et al.*, 2006a).

In co-immunoprecipitation assays with HAdV-C5 pV and constitutive components of the PML-NBs PML, such as Daxx and Sp100, no convincing interaction could be detected (Fig. 12), although pV was found to partially co-localize with PML-NBs (Fig. 11). However, longer exposure times of immunoblots from total-cell-lysates, which contain exogenously expressed pV, revealed different slower migrating bands of HAdV-C5 pV (Fig. 15), if cysteine protease inhibitors had been used during lysis of the cells. This could indicate post translational modifications of the protein, since also SUMO-specific (SENP, DeSI) (Nayak & Müller, 2014) and ubiquitin-specific proteases (DUBs) (Turcu *et al.*, 2009) are affected by these inhibitors.

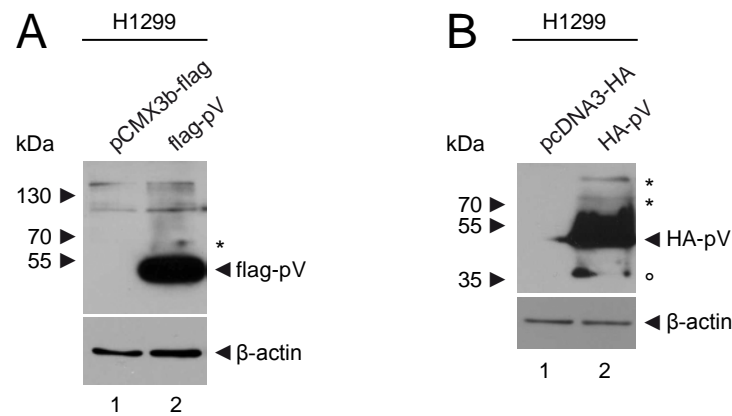
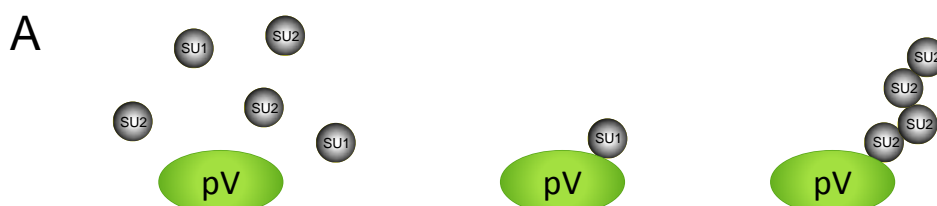


**Figure 15: HAAdV-C5 pV transfected H1299 cells reveal additional protein signals during immunoblotting.** H1299 cells were transfected with **A** 10  $\mu\text{g}$  of a flag-pV expression plasmid (#2738) or its empty vector control pCMX3b-flag (#152) and **B** 10  $\mu\text{g}$  of a HA-pV expression plasmid (#2635) or its empty vector control pCDNA3-HA (#196) and harvested 48 h p.t. Total-cell lysates were resolved by **A** 10% and **B** 12% SDS-PAGE and visualized by immunoblotting (400 mA, 90 min, **A** nitrocellulose  $\phi = 0.45 \mu\text{m}$ , **B** PVDF  $\phi = 0,2 \mu\text{m}$ ). Input levels of flag-pV (50  $\mu\text{g}$ ) and HA-pV (100  $\mu\text{g}$ ) were detected by using mab M2 ( $\alpha$ -flag) and mab 3F10 ( $\alpha$ -HA), input levels of  $\beta$ -actin (25  $\mu\text{g}$ ) were detected by using mab AC-15 ( $\alpha$ - $\beta$ -actin). Molecular weights in kDa are indicated on the *left*, while corresponding proteins are labeled on the *right*.

Flag-pV shows an additional band between 55 and 70 kDa (Fig. 15A, lane 2 \*), which would match the size of a conjugated SUMO protein ( $\sim 12$  kDa). Furthermore, a smear towards higher molecular weights was detected, which is typical for the formation of SUMO or ubiquitin chains. Similarly, HA-pV shows discrete slower migrating bands, matching the size of poly SUMOylation (Fig. 15B, lane 2 \*). Even a faster migrating portion was found at approximately 35 kDa (Fig. 15B, lane 2  $\circ$ ), which could indicate a yet unknown, C-terminally shortened isoform of HAAdV-C5 pV. On the other hand, it could be a sign of beginning protein degradation as well.

#### 4.3.1.1. HAAdV-C5 pV is modified with SUMO2 chains in transient transfection of HeLa cells

To elucidate whether HAAdV-C5 pV can be really modified with SUMO proteins, a flag-pV expressing plasmid was transiently transfected into HeLa cells, which are stably expressing 6His-tagged SUMO1 or 6His-tagged SUMO2. A following Ni-NTA purification of these cells leads to different possible outcomes (Fig. 16A).

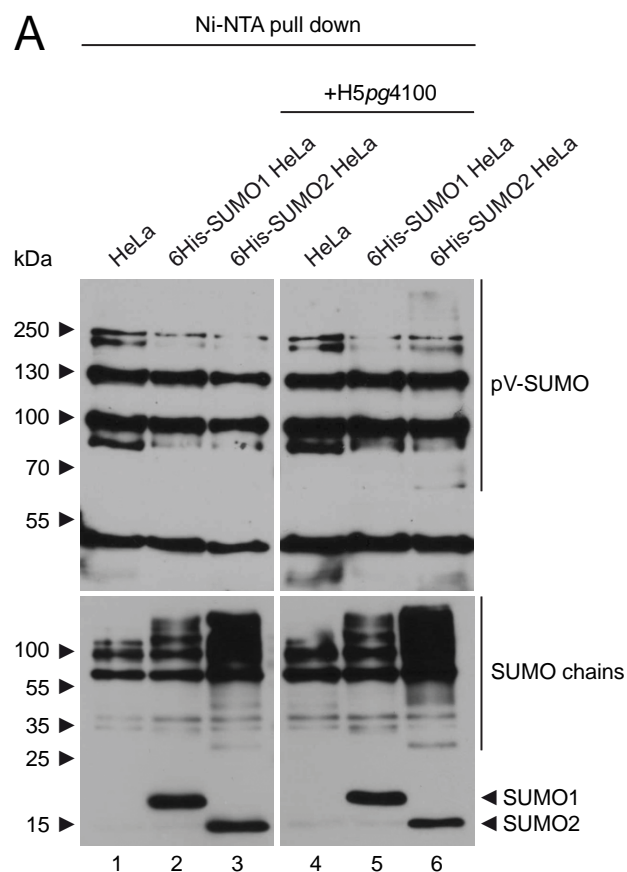




(upper right panel, lane 6). Additionally, the protein itself, migrating at a size of approximately 50 kDa, is pulled down, indicating an unspecific interaction of flag-pV with the Ni-NTA matrix, since flag-pV is not fused to a His-tag (Fig. 16B, upper right panel, lanes 4 and 6). Interestingly, there is no signal detectable in 6His-SUMO1 HeLa cells (Fig. 16B, upper right panel, lane 5), although pV is even pulled down from the total-cell lysate of parental HeLa cells (Fig. 16B, upper left panel, lane 4). This occurs, most likely, due to the low expression level of pV in the 6His-SUMO1 HeLa cells. Protein V concentrations are higher in 6His-SUMO2 cells, whereas the most pV is expressed in parental HeLa cells (Fig. 16B, lower right panels, lanes 4-6). Hence, a modification of pV with SUMO1 cannot be ruled out.

#### 4.3.1.2. The SUMO2 modification of pV occurs weakly during HAdV-C5 infection

A similar picture was observed during the course of HAdV-C5 infection, illustrated in Figure 17. Despite the strong background of the freshly prepared  $\alpha$ -pV antibody, a faint ladder of protein signals could be detected in 6His-SUMO2 HeLa cells, infected with HAdV-C5 (Fig. 17A, upper right panel, lane 6). This result indicates a modification of pV with SUMO2 during HAdV-C5 infection as well. In comparison to the transient transfection experiment (Fig. 16), the pV-SUMO signal is weak, though.



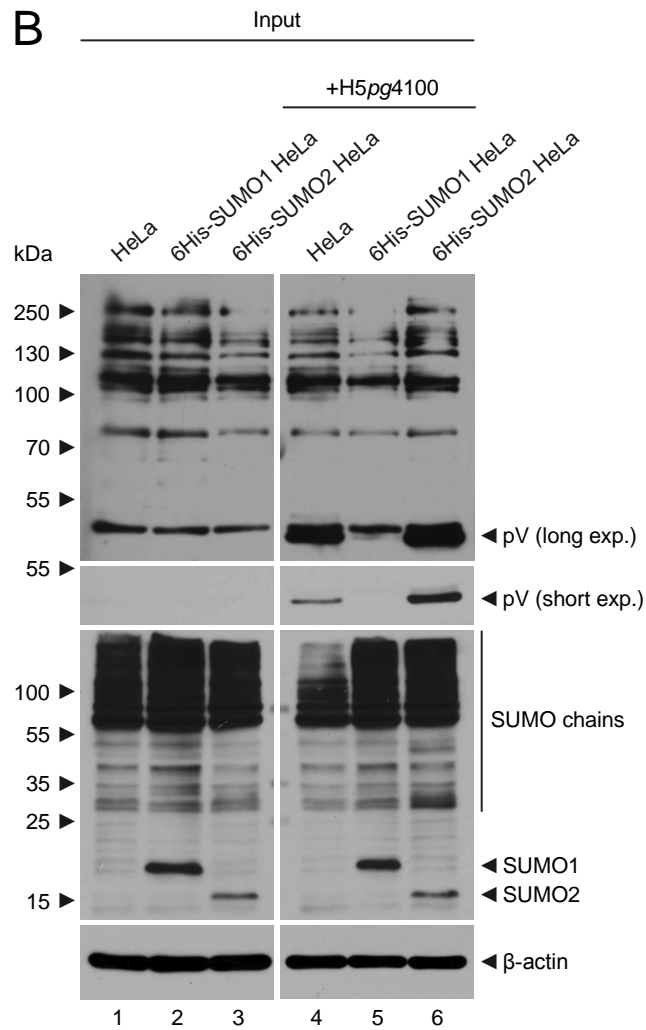


**Figure 17: Modification of pV with SUMO2 is weak during HAdV-C5 infection in HeLa cells.**

HeLa cells and HeLa cells stably expressing 6His-SUMO1 or 6His-SUMO2 were infected with HAdV-C5 (H5pg4100, moi 20), harvested 24 h p.i. and subjected to a guanidinium chloride buffer. **A** 6His-SUMO conjugates were purified by usage of a Ni-NTA-matrix, resolved with **B** total-cell lysates as input control by 10-12 % SDS-PAGE and visualized by immunoblotting (400 mA, 90 min, nitrocellulose  $\varnothing = 0.45 \mu\text{m}$ ). Ni-NTA purified and input proteins were detected by using pab  $\alpha$ -pV (25  $\mu\text{g}$  input), mab  $\alpha$ -6His (50  $\mu\text{g}$  input) and AC-15 ( $\alpha$ - $\beta$ -actin, 25  $\mu\text{g}$  input). Molecular weights in kDa are indicated on the *left*, while corresponding proteins are labeled on the *right*, exp. means exposure.

A SUMO1 modification of pV was not visible again (Fig. 17A, upper right panel, lane 5), which might be the cause of low pV levels in 6His-SUMO1 HeLa cells, even during adenoviral infection (Fig. 17B, middle right panel, lane 5). As a consequence, this cell line has not been used in further experiments of this study.

To examine whether the SUMOylation of pV might be repressed in the presence of other adenoviral factors, the previous experiment was repeated in superinfected cells, transiently expressing flag-pV.

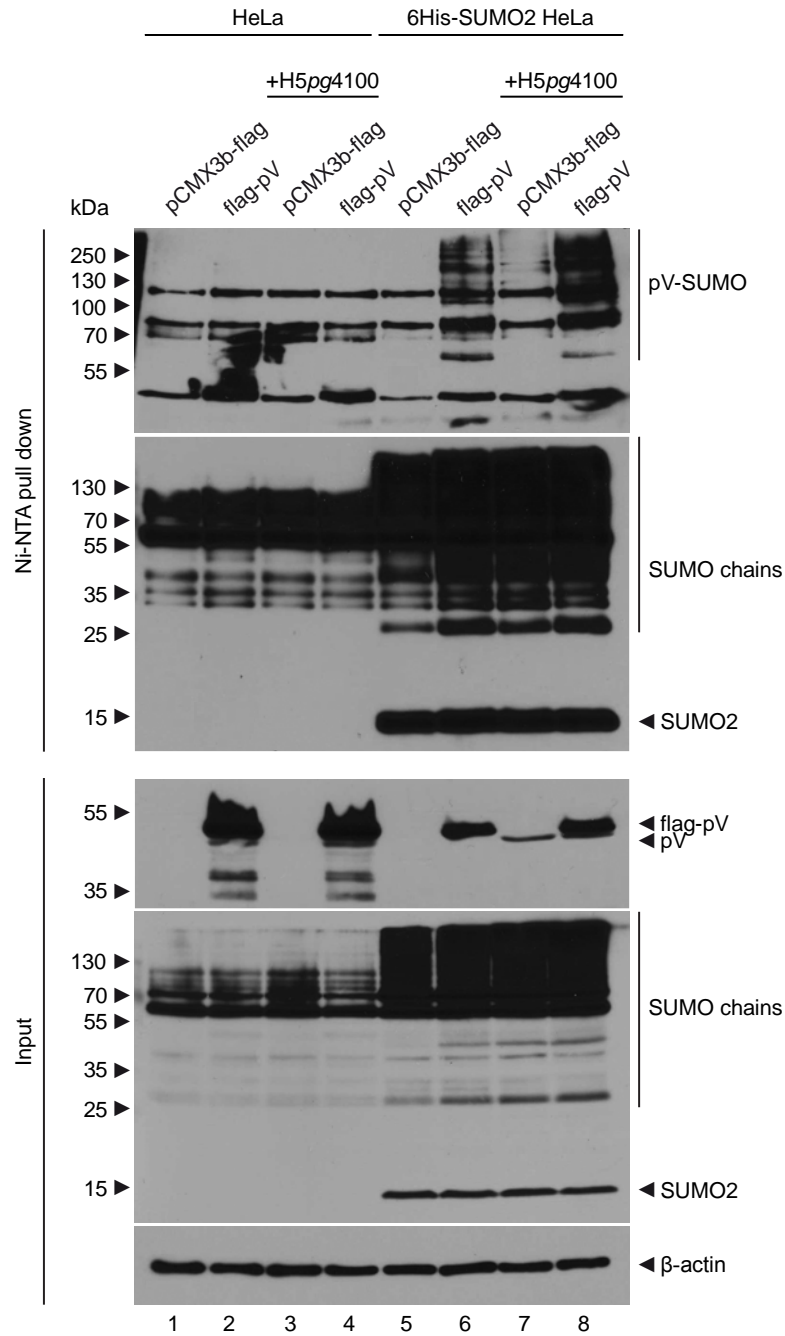


**Figure 18: SUMOylation of pV is not counteracted during HAdV-C5 infection in HeLa cells.**

HeLa cells or HeLa cells stably expressing 6His-SUMO2 were transfected with 10  $\mu$ g of a flag-pV expression plasmid (#2738) or its empty vector control pCMX3b-flag (#152) and superinfected with HAdV-C5 (H5pg4100, moi 20) 24 h p.t. The cells were harvested 24 h p.i. and subjected to a guanidinium chloride buffer. 6His-SUMO conjugates were purified by usage of a Ni-NTA-matrix, resolved with total-cell lysates as input control by 10-12 % SDS-PAGE and visualized by immunoblotting (400 mA, 90 min, nitrocellulose  $\phi = 0.45 \mu$ m). Ni-NTA purified and input proteins were detected by using pab  $\alpha$ -pV (25  $\mu$ g input), mab  $\alpha$ -6His (50  $\mu$ g input) and AC-15 ( $\alpha$ - $\beta$ -actin, 25  $\mu$ g input). Molecular weights in kDa are indicated on the *left*, while corresponding proteins are labeled on the *right*.

If the presence of other viral proteins really acts against the SUMOylation of pV, this modification should be reduced compared to cells that were transiently transfected with a flag-pV expression plasmid (Fig. 16). However, this is not the case. Again, pV-SUMOylation

appears weaker in 6His-SUMO2 HeLa cells expressing pV only due to HAdV-C5 infection, compared to cells transiently overexpressing flag-pV (Fig. 18, upper panel, lanes 6-7). In contrast, 6His-SUMO2 HeLa cells, which were infected in the presence of flag-pV, reveal an even stronger SUMOylation of pV (Fig. 18, upper panel, lanes 6 and 8).

#### 4.3.1.3. HAdV-C5 pV can be modified with SUMO1 *in vitro*.

HAdV-C5 pV steady-state concentrations were very low in HeLa cells stably expressing 6His-SUMO1, regardless of whether the cells were transiently transfected with a flag-pV expression plasmid (Fig. 16C, lane 5) or infected with HAdV-C5 (Fig. 17B, lane 5). Consequently, an investigation of SUMO1 conjugation to HAdV-C5 pV, was not truly possible. In order to shed light on this open question, HA-pV and flag-pV were translated *in vitro* by usage of a wheat germ translation kit (Fig. 19A-B) and subjected to an *in vitro* SUMOylation kit for SUMO1 modification (Fig. 19C-E). The translation efficiency was controlled by Western Blotting, after separation of the reaction mixture by SDS-PAGE (Fig. 19A-B). Interestingly, the HA-staining revealed additional slower migrating bands (Fig. 19A), which are comparable to those detected in total-cell lysates of human origin (compare Fig. 15B). Thus, post-translational modification of the protein might already start under the conditions of its *in vitro* translation. In contrast, flag-pV shows only one distinct band after translation in a separate experiment (Fig. 19B), which could reflect its lower concentration.

Subsequently, both translated proteins were subjected to *in vitro* modification with SUMO1 where the modification of HAdV-C5 pV with SUMO1 could be finally visualized (Fig. 19C and D). The experiments were performed separately, resulting in stronger signals of SUMO1 modification for HA-pV (Fig. 19C, lane 1). However, the signal with a size of 65-70 kDa, matching the size of HAdV-C5 pV bound with one SUMO1 protein, was detectable for flag-pV as well (Fig. 19D, lane 1). These results indicate that HAdV-C5 pV can be actually modified with SUMO1. In the latter experiment, a portion of the *in vitro* reaction was stained for SUMO1, as a control (Fig. 19E). This blot proves that the SUMO1 mutant cannot be conjugated to target proteins any more (Fig. 19E, lane 2). Unfortunately, it further shows a huge amount of proteins in the translation reaction, which are competing with the protein of interest to become SUMOylated (Fig. 19E, lane 1). This last finding explains the low reaction efficiency of the desired SUMO1 modification.

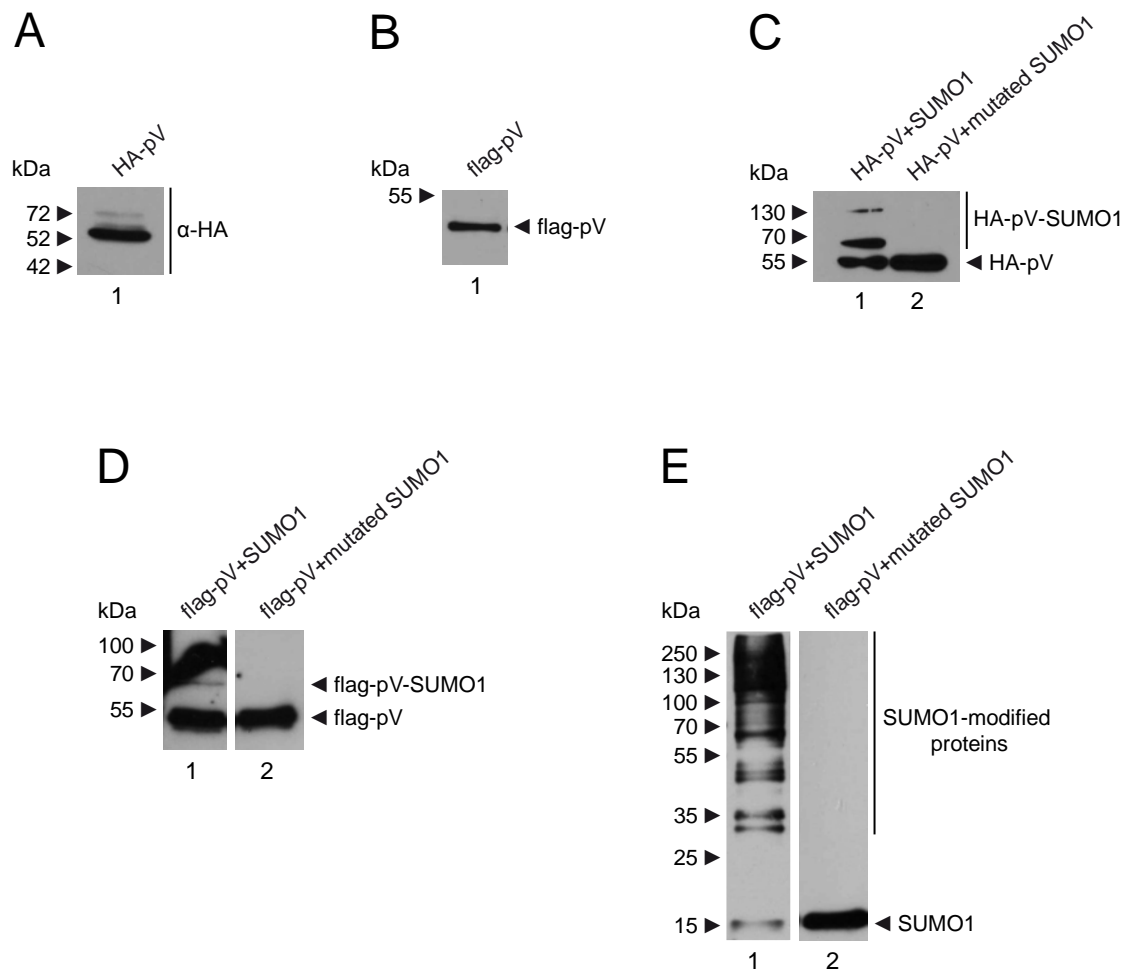


**Figure 19: HAdV-C5 pV can be modified with SUMO1 *in vitro*.**

**A-B** Independent *in vitro* translations of the proteins HA-pV and flag-pV by use of a wheat germ translation kit, according to the manufactures' protocol. The cds were derived from plasmids expressing HA-pV (#2635) or flag-pV (#2738) under the control of a CMV-promoter. 1  $\mu$ l of each product were resolved by 12 % SDS-PAGE. **C-E** SUMOylation of *in vitro* translated proteins (A-B) in independent experiments and without further purification by use of an *in vitro* SUMOylation kit for SUMO1 modification according to the manufactures' protocol. A mutated SUMO1 protein, which cannot be conjugated to target proteins anymore, serves as a negative target (provided by the kit). **C** Reaction performed with 2  $\mu$ l HA-pV translation mix, **D-E** reaction performed with 3  $\mu$ l flag-pV translation mix. All proteins were visualized by immunoblotting (400 mA, 90 min, nitrocellulose  $\varnothing = 0.45 \mu$ m) and detected by using mab 3F10 ( $\alpha$ -HA), mab M2 ( $\alpha$ -flag) and  $\alpha$ -SUMO1 (provided by the kit). Molecular weights in kDa are indicated on the *left*, while corresponding proteins are labeled on the *right*.

#### 4.3.2. *In silico* analysis reveals several SCM within HAdV-C5 pV, enabling the generation of putative pV SUMO mutants

Post-translational modification of proteins is an important regulatory tool of the cell to manifold the functions of its proteins. Since pV was shown to be extensively modified with SUMO proteins in the previous experiments (Fig. 15-19), an *in silico* analysis of pV was performed in order to find the putative SUMO conjugation and/or SUMO interacting motifs (Fig. 20A).

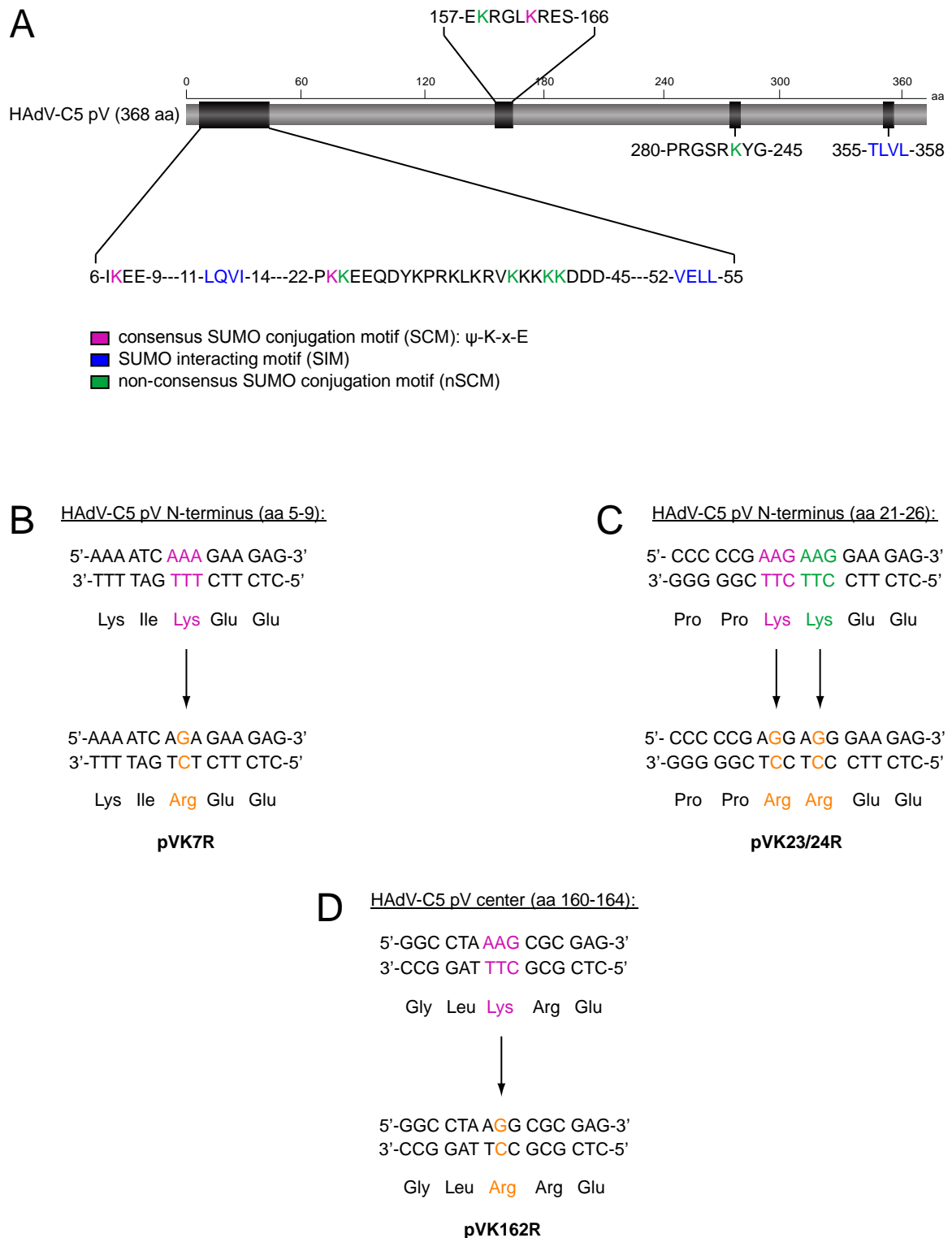


**Figure 20: HAAdV-C5 pV contains several SCM, nSCM and SIM.**

**A** *In silico* analysis of HAAdV-C5 pV to determine its potential SUMO conjugation or interaction motifs, using the algorithms *SUMOPlot*<sup>TM</sup> (<http://www.abgent.com/sumoplot>), *GPS-SUMO* (Ren *et al.*, 2009; Zhao *et al.*, 2014) and *Jassa* (Beauchair *et al.*, 2015). **B-D** The nucleotide exchange A→G (depicted in yellow), in three different fragments of the pV-cds by site-directed mutagenesis leads to a substitution of the respective K by R, retaining the charge of the proteins primary sequence. Thereby three SCM and one neighboring nSCM were either mutated individually or combined. The flag-pV expression plasmid (# 2738) was used as template in quick-change PCRs.

Three different algorithms, based on numerous published SUMOylation sites within a multitude of different proteins, were compared in this approach *SUMOPlot*<sup>TM</sup> (<http://www.abgent.com/sumoplot>), *GPS-SUMO* (Ren *et al.*, 2009; Zhao *et al.*, 2014) and *Jassa* (Joined Advanced Sumoylation Site and Sim Analyser; Beauclair *et al.*, 2015). All of the algorithms found three consensus SUMO conjugation motifs (SCM) with high probability within pV, namely K7, K23 and K162 (Fig. 20A, depicted in pink). Additionally, one non-consensus SUMO conjugation site (nSCM) was predicted with high probability at K24 and several nSCM with low or medium probabilities were found (Fig. 20A, depicted in green). Furthermore, three SUMO interacting motifs (SIM) were predicted within pV, although they have low probability and appear only with use of low thresholds (Fig. 20A, depicted in blue).

Based on these findings, different putative SUMO conjugation mutants of HAdV-C5 pV were generated by site-directed mutagenesis to determine the actual sites of pV-SUMOylation. As a start, the three SCM within the coding sequence of pV were modified in a way that leads to the substitution of the lysine residue within the motif with an arginine. This retains the local as well as the net charge of the protein and thereby reduces the unwanted possibility of conformational changes, which could cause a change or even a loss of function. To obtain those mutants, single nucleotides of the pV coding sequence were exchanged by quick-change (QC)-PCR, using the flag-pV expression plasmid as template (Fig. 20B-D, depicted in yellow). This results in a lysine to arginine exchange within the primary protein sequence of pV. Hence, the mutants were named pVK7R (Fig. 20B and Fig. 22A) and pVK162R (Fig. 20D and Fig. 22A). In case of the third SCM, containing K23, the neighboring K24, which was predicted with low probability as nSCM, was substituted as well, leading to a double mutant named pVK23/24R (Fig. 20C and Fig. 22A). Next to these pV mutants, containing one modified SCM, additional plasmids were generated, having only one intact SCM within pV, instead (pVK7/23/24R, pVK23/24/162R and pVK7/162R; Fig. 23A). The last pV mutant, termed pV4xKR, has alterations in all three SCM and the nSCM, containing K24.

To get an impression of the structural impact of the introduced point mutations on HAdV-C5 pV, a comparison of predicted protein structures was run with *I-TASSER* (Iterative Threading ASSEmblY Refinement) for HAdV-C5 pV and for HAdV-C5 pV4xKR (Fig. 21) (Roy *et al.*, 2010; Yang *et al.*, 2015; Yang & Zhang, 2015; Zhang, 2008). Despite the exchange of four amino acids, depicted in orange, the predicted secondary structure of pV4xKR was almost identical to the one found for wildtype pV (Fig. 21A). The same holds true for residues expected to be exposed to the surrounding solvent, which are indicated by an E. Those comprise around



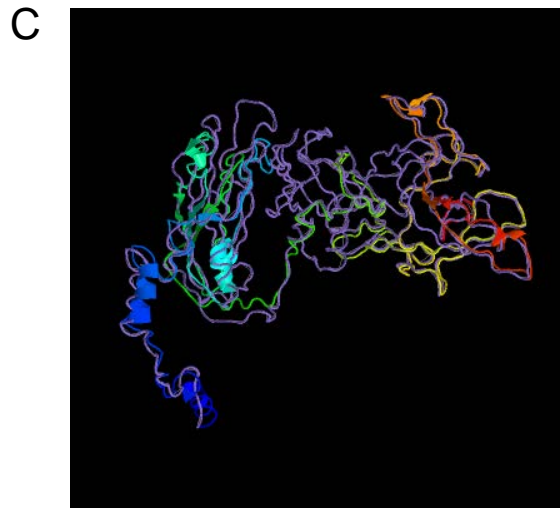


**Figure 21: Comparison of structural elements within HAdV-C5 pV and pV4xKR.**

*In silico* analysis of structural elements within HAdV-C5 pV and pV4xKR by use of *I-TASSER* (Roy *et al.*, 2010; Yang *et al.*, 2015; Yang & Zhang, 2015; Zhang, 2008). **A** Alignment of predicted secondary structure elements with primary structures of HAdV-C5 pV and pV4xKR. Helices (H) are depicted in red, strands (S) are depicted in blue, buried residues (B) are depicted in pink and random coiled residues (C) or solvent exposed residues (E) are depicted in black. K→R substitutions are indicated in yellow. **B** Predicted tertiary structures of HAdV-C5 pV and pV4xKR. The N-terminus is depicted in blue and the C-terminus is shown in red. The spatial orientation is indicated by a transparent cube. **C** Top-hit of a TM-align of the *I-TASSER* model with the PDB (protein database) library, showing the structural analogy of the capsid protein VP1 from rabbit hemorrhagic disease virus (RHDV) to HAdV-C5 pV4xKR (TM-score = 0.881, RMSD = 2.18, identity = 0.067, coverage = 0.938). C-score means confidence score, TM means template modeling and RMSD means root-mean-square deviation of atoms, measured in Ångstrom (Å).

It has to be taken into account though, that the accuracy of these three-dimensional protein models is rather weak. The confidence score (C-score) is typically in the range of [-5,2] and is supposed to be greater than -1.5 to give an accurate global protein structure. Additionally, the template modeling score (TM-score) should be at least 0.5. Both are only fulfilled for the structure prediction of the pV-mutant (pV4xKR; Fig. 21B, right panel). Hence, the predicted differences in tertiary structure of both HAdV-C5 pV proteins are not reliable and could be artificial, due to the computational approximation used.

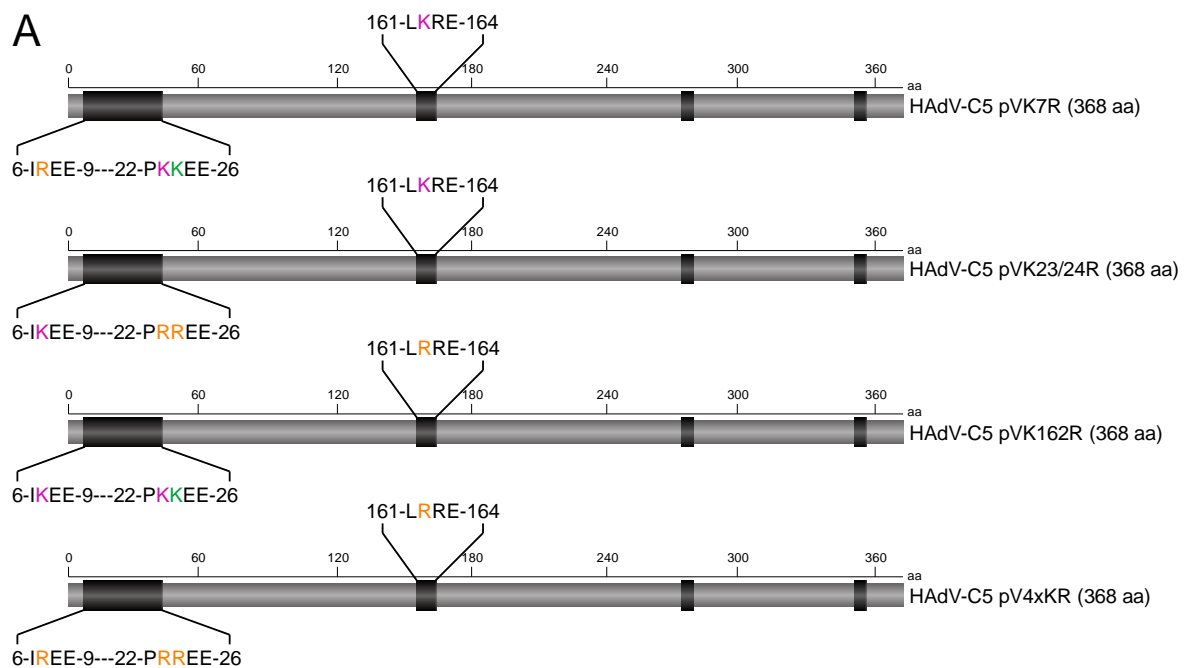
Taken together, there is no strong hint towards a structural change of HAdV-C5 pV after substitution of the four specific lysine residues by arginine.

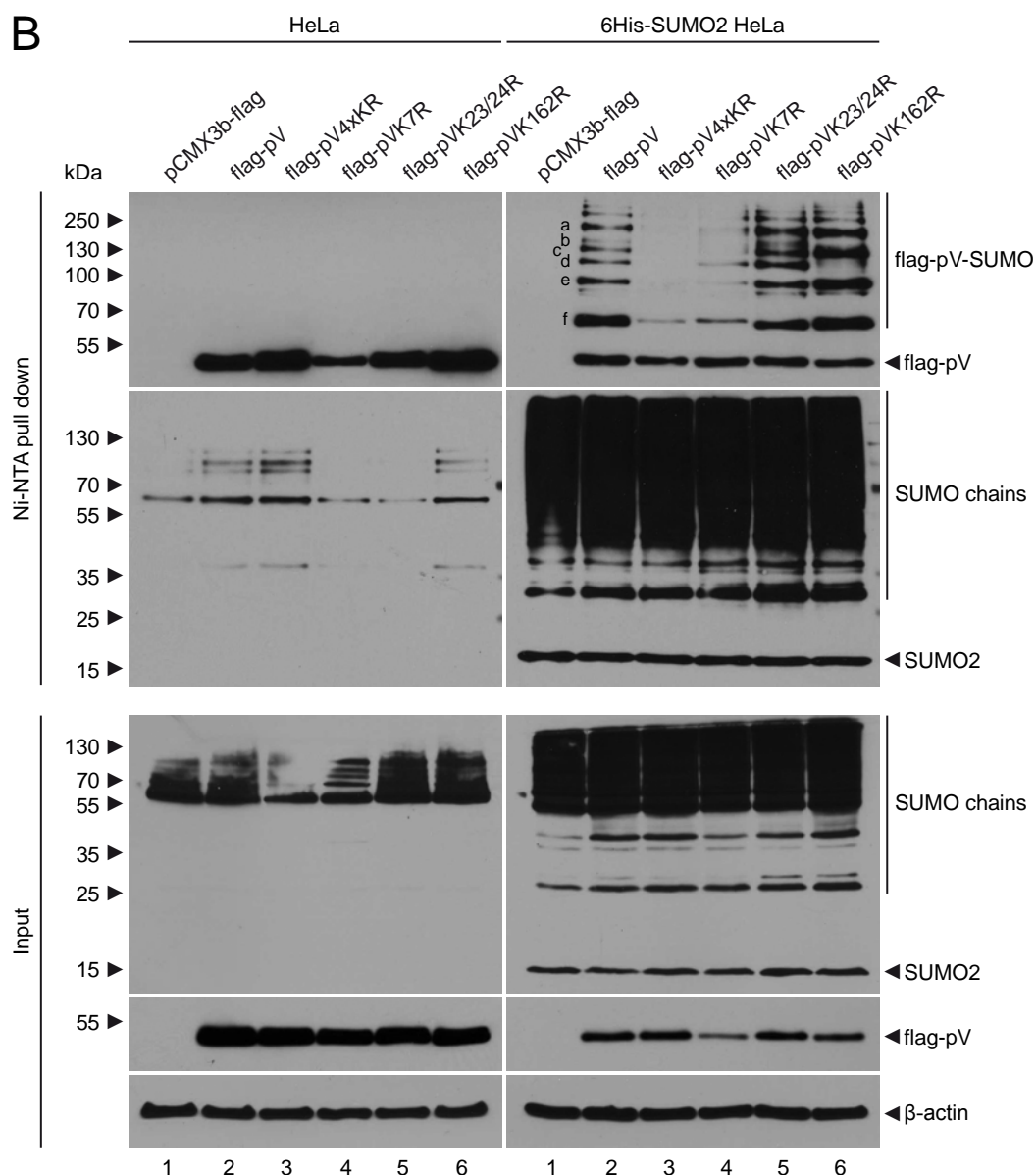
Interestingly however, the proposed tertiary structure of HAdV-C5 pV4xKR, which appears to be more accurate, shares great structural similarities with another viral capsid protein, namely virion protein 1 (VP1), former VP60, of the *calicivirus* RHDV (rabbit hemorrhagic disease virus) (Luque *et al.*, 2012) (Fig. 21C). Likewise, adenoviruses, caliciviruses are non-enveloped, icosahedral viruses, albeit with a poly-adenylated, positive-sensed, single-stranded RNA genome of only ~7.5 kb. Their diameter is only around 40 nm compared to an 80-120 nm sized adenovirus (Hansman *et al.*, 2010; van Oostrum & Burnett, 1985). The whole capsid is built of

VP1-dimers arranged with  $T = 3$  symmetry, while each monomer has three known domains. The N-terminal arm (NTA) resembles the predicted N-terminus of HAdV-C5 pV4xKR very well. It is followed by the shell (S), which is composed of an eight-stranded  $\beta$ -sandwich and therewith larger than the equivalent region of pV4xKR. Yet, the flexible protruding domain (P) closely matches the C-terminus of pV4xKR again (Fig. 21B, right panel and 21C). Interactions among the highly conserved  $\beta$ -barrel interfaces of VP1 are mainly hydrophobic, whereas the NTA  $\alpha$ -helices form a network of interactions beneath the capsid surface of caliciviruses that increases capsid stability (Hansman *et al.*, 2010; Luque *et al.*, 2012). Interestingly, calicivirus capsids are built out of only one structural protein, VP1. The prerequisite for this is the possibility of a molecular switch among quasiaequivalent conformations. In case of VP1, this function is dictated by the first 29 N-terminal residues (Bárcena *et al.*, 2004; Dokland, 2000).

#### 4.3.3. Mutation of the three SCM within HAdV-C5 pV alters the pattern of the proteins SUMO2 chain modification

In the following experiments, the influence of the SCM mutations on the pV-SUMOylation was investigated. Therefore, HeLa or 6His-SUMO2 HeLa cells were transfected with the flag-pV expression plasmid or the different SCM mutants and prepared for Ni-NTA purification 48 h p.t. In the first experimental set up only the pV mutants with a single altered SCM were used in comparison to flag-pV wt and flag-pV4xKR, which has no intact SCM anymore (Fig. 22A).



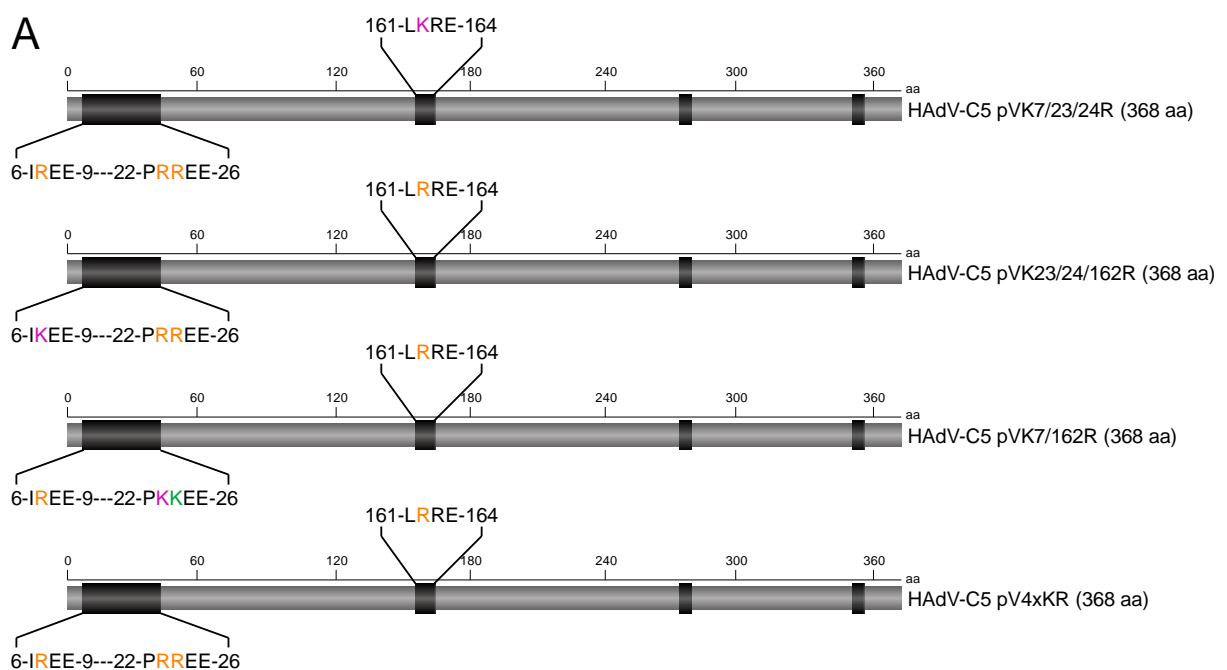


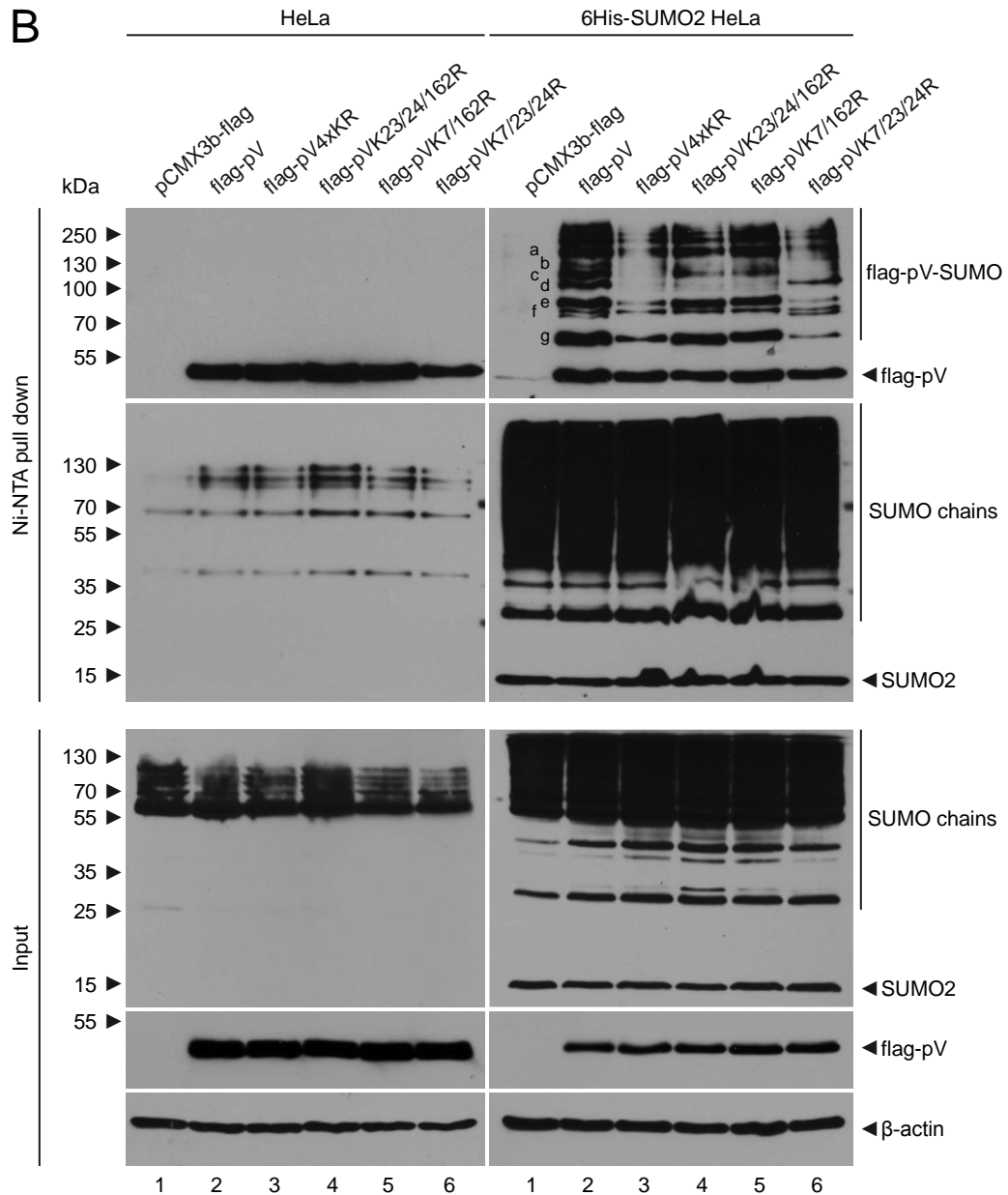
**Figure 22: Mutation of single SCM in HAdV-C5 pV alters the SUMO2 modification pattern of the protein.** A Schematic illustration of the HAdV-C5 pV-SCM mutants used in the experiment (B), SCM are depicted in pink, nSCM in green and K $\rightarrow$ R exchanges in yellow. B HeLa cells or HeLa cells, stably expressing 6His-SUMO2, were transfected with 10  $\mu$ g of a flag-pV expression plasmid (#2738), 10  $\mu$ g of the flag-pV-SCM mutants indicated in A or 10  $\mu$ g of the empty vector control pCMX3b-flag (#152). All cells were harvested 48 h p.t. and subjected to a guanidinium chloride buffer. 6His-SUMO conjugates were purified by usage of a Ni-NTA-matrix, resolved with total-cell lysates as input control by 10-12 % SDS-PAGE and visualized by immunoblotting (400 mA, 90 min, nitrocellulose  $\phi$  = 0.45  $\mu$ m). Ni-NTA purified and input proteins were detected by using mab M2 ( $\alpha$ -flag, 50  $\mu$ g input), mab  $\alpha$ -6His (75  $\mu$ g input) and AC-15 ( $\alpha$ - $\beta$ -actin, 25  $\mu$ g input). Molecular weights in kDa are indicated on the left, while corresponding proteins are labeled on the right.

Figure 22B reveals the expected pattern of SUMO2 chain modification for flag-pV wt (Fig. 22B, upper right panel, lane 2), which is already known from Figure 16B. Strikingly, pV4xKR lost almost every modification larger than 65 kDa and also this band (f) is much weaker than for pV-wt, although the amount of pulled SUMO-conjugates and the input levels of pV are comparable (Fig. 22B, upper right panels, lanes 2-3). In contrast, the single SCM

mutants, apart from pVK7R, do not show such strong alteration of SUMO2 modification (Fig. 22B, upper right panel, lanes 4-6). The pattern of flag-pVK23/24R is identical to the one of flag-pV wt (Fig. 22B, upper right panel, lanes 2 and 5), whereas in case of flag-pVK162R certain bands (b and d) do not clearly appear, although the overall signal of the other bands is even stronger than for flag-pV wt (Fig. 22B, upper right panel, lanes 2 and 6). Interestingly, flag-pVK7R shows a reduction of SUMO2 modification almost as strong as pV4xKR, although the amount of pulled down SUMO-conjugates is slightly higher than for pV wt (Fig. 22B, upper right panels, lanes 2-4). This indicates a major role of lysine residue K7 for the SUMO conjugation to protein V. Noteworthy, the input concentration of pVK7R was reduced, though (Fig. 22B, lower right panel, lane 4).

The reverse experiment further clarifies the picture (Fig. 23). This time, the pV mutants with only one intact SCM were compared to pV wt and pV4xKR (Fig. 23A). As a whole, the signal intensity of the Ni-NTA purification was stronger than in the previous experiment, leading to the occurrence of a new double band for flag-pV wt at approximately 70 kDa (Fig. 23B, upper right panel, lane 2). The upper of those bands was already visible in Figure 22B, but not for every pV mutant. Here, only the appearance of the lower band (f) differs. It can clearly be assigned to K162, since it is not visible if this residue is substituted by arginine (Fig. 23B, upper right panel, lanes 3-5 and Fig. 23C). The same is true for SUMO band d, which matches the result of the previous experiment (Fig. 22B and Fig. 23B, upper right panel, lanes 4-6 and Fig. 23C).





**C**

Experiment 1 (Fig. 22):		Experiment 2 (Fig. 23):	
SUMO-band	K	SUMO-band	K
a	7 ?	a	7, 23/24 > 162
b	162, 7 ?	b	7, 23/24, 162
c	7 ?	c	7, 23/24
d	162	d	162
e	7 ?	e	7, 23/24 > 162
f	7 ?	f	162
		g	7, 23/24 > 162

**Figure 23: Combined mutation of different SCM reveals specificity of certain SUMO2 conjugations to HAdV-C5 pV.**

**A** Schematic illustration of the HAdV-C5 pV-SCM mutants used in the experiment (B). SCM are depicted in pink, nSCM in green and K→R exchanges in yellow. **B** HeLa cells or HeLa cells stably expressing 6His-SUMO2 were transfected with 10 µg of a flag-pV expression plasmid (#2738), 10 µg of the flag-pV-SCM mutants indicated in A or 10 µg of the empty vector control pCMX3b-flag (#152). All cells were harvested 48 h p.t. and subjected to a guanidinium chloride buffer. 6His-SUMO conjugates were purified by usage of a Ni-NTA-matrix, resolved with

total-cell lysates as input control by 10-12 % SDS-PAGE and visualized by immunoblotting (400 mA, 90 min, nitrocellulose  $\phi = 0.45 \mu\text{m}$ ). Ni-NTA purified and input proteins were detected by using mab M2 ( $\alpha$ -flag, 50  $\mu\text{g}$  input), mab  $\alpha$ -6His (75  $\mu\text{g}$  input) and AC-15 ( $\alpha$ - $\beta$ -actin, 25  $\mu\text{g}$  input). Molecular weights in kDa are indicated on the *left*, while corresponding proteins are labeled on the *right*. **C** Summary of the appearing SUMO-bands in Fig. 22B and 23B with the lysine residue K they can be assigned to.

In contrast to the previous experiment, it does not make a difference, whether K7 or K23/24 were exchanged. If one site is still intact, the pattern of SUMO2 modification is identical (Fig. 23B, upper right panels, lanes 4-5). If both conjugation sites are missing and only SCM K162 is present, band c disappears, though (Fig. 23B, upper right panel, lane 6). Additionally, bands a, e and g are less intense, indicating a greater dependence of these SUMO signals on K7, K23 and K24 than K162 (Fig. 23C). Band b is not clearly visible in all of the pV-SCM mutants (Fig. 23B, upper right panel, lanes 3-6). The combination of these observations results in the SUMO2 pattern of pV4xKR where four SUMO bands (b-d and f) are not detectable anymore and the others are reduced in signal (Fig. 23B upper right panel, lanes 2-3).

Taken together, only two bands of the pV SUMO2 pattern can be precisely assigned to a certain SCM, which are d and f belonging to K162. Furthermore, K7 seems to be more important than K23/24 for the occurrence or signal intensity of the other bands, since the mutation of only K23/24 had no effect on the pV-SUMOylation, whereas it was dramatically decreased in the absence of K7 (Fig. 22B and Fig. 23C). However, K23/24 seems to be able to compensate the lack of K7, since there is no change of the pV-SUMOylation pattern if one or the other residue is substituted. Only a mutation of both sites leads to the clear loss of band c (Fig. 23B and C). Band b seems to depend on K7 and K162, although the lack of K7 can be compensated by K23/24 again (Fig. 23C). Remarkably, pV still shows SUMO2 modification if all its SCM are altered, although significantly reduced (Fig. 22B and Fig. 23B, lane 3). These results point to the fact that HAdV-C5 pV is modified with SUMO proteins not only at one, but also at different SCM and that even further nSCM must be involved.

#### **4.3.4. Mutation of the three SCM within HAdV-C5 pV alters the subcellular distribution of the viral protein**

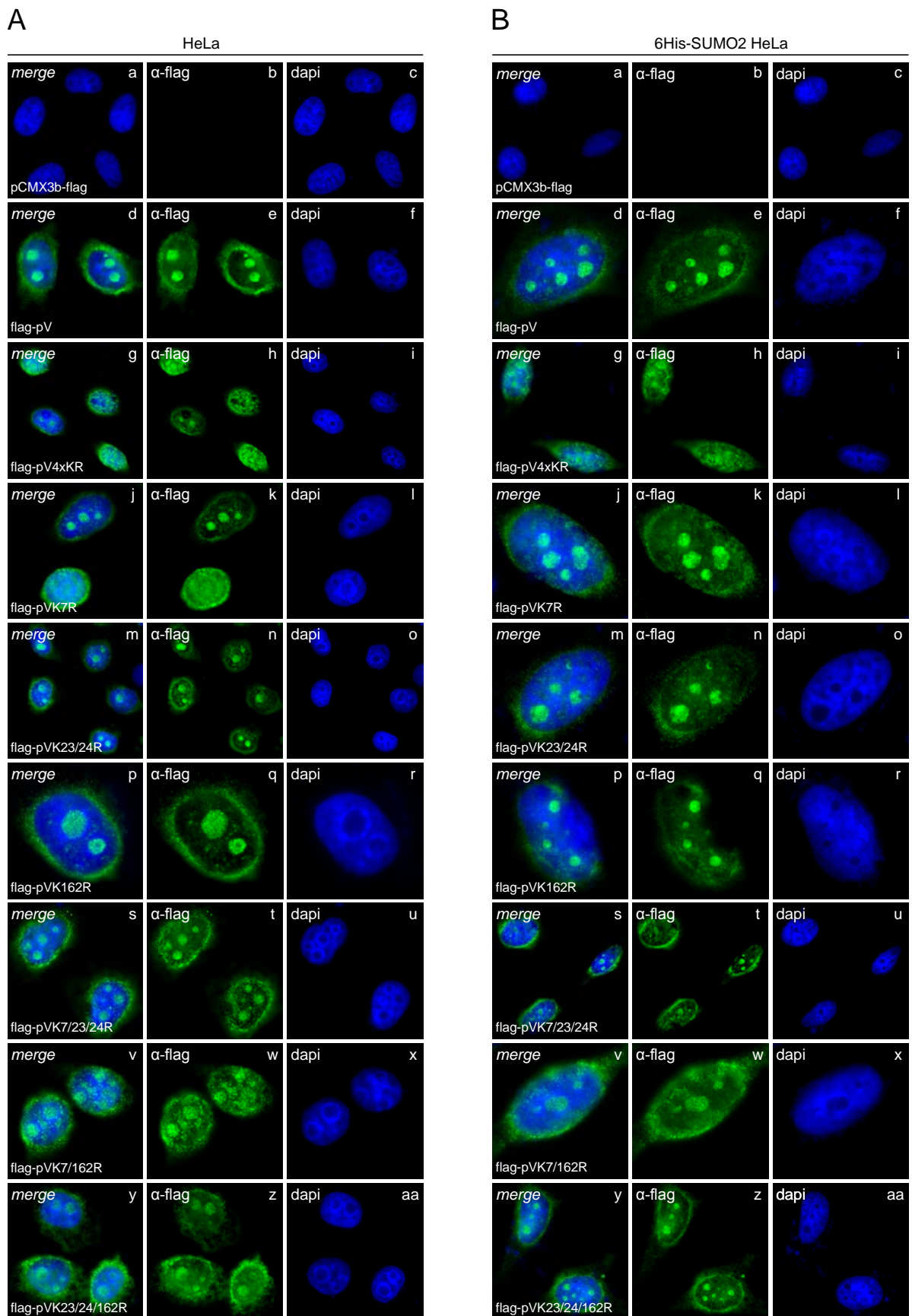
SUMOylation is a posttranslational modification of proteins, which can influence their subcellular localization (van Damme *et al.*, 2010; Shen *et al.*, 2006a; Zhong *et al.*, 2000b). We and others already found different fractions of HAdV-C5 pV in the nucleus during immunofluorescence analysis where it accumulates at the nucleoli and has an additional diffuse distribution in the nucleoplasm (Fig. 10) (Matthews, 2001; Matthews & Russell, 1998a).

Furthermore, it partially co-localizes with PML-NBs in transiently transfected HepaRG cells (Fig. 11). These nuclear structures could represent the spots where pV is actually modified with SUMO proteins (compare sections 1.2.1-1.2.1.1).

To elucidate whether SUMOylated pV localizes in distinct fractions within the nucleus, immunofluorescence of the protein and its SCM mutants was analyzed in HeLa cells and HeLa cells stably expressing 6His-SUMO2 (Fig. 24). As expected, in HeLa cells the most abundant phenotype of flag-pV shows clear accumulations in the nucleus and a weak diffuse signal in the nucleoplasm (Fig. 24A, panels d-e and 24C). It is surrounded by a cytoplasmic sphere, which might be a consequence of MeOH fixation, since it was not observed in cells fixed with PFA (Fig. 10A-D). A similar distribution was observed for the single SCM mutant flag-pVK7R (Fig. 24A, panels i-k and 24C). In case of flag-pVK23/24R, flag-pVK162R and flag-pVK7/23/24R even a higher percentage of this phenotype was found (Fig. 24C), indicating that these mutations do not truly influence the localization of HAdV-C5 pV. Obviously, the amount of cells, showing distinct accumulations at the nucleoli, ranges from approximately 60-80 %. Flag-pV4xKR, on the contrary, has a greater portion of diffuse signal (Fig. 24A, panels g-h and 24C). Even though the accumulations remain visible in the majority of transfected cells, they are often blurry and melt with the diffuse fraction of pV in the nucleoplasm. This type of subcellular distribution was also detected in the majority of HeLa cells positive for flag-pVK23/24/162R or flag-pVK7/162R (Fig. 24A, panels v-z). Overall, these findings indicate that the lack of certain SCM within HAdV-C5 pV leads to less accumulation of the protein at the host nucleoli. In this regard especially K162 seems to be important, if it is altered in combination with one of the other SCM K7 or K23. Its solitary absence does not show any influences, though (Fig. 24C).

In a HeLa cell line, which is stably overexpressing SUMO2, a greater fraction of HAdV-C5 pV is expected to be SUMOylated, if the SUMO conjugation sites are available. Consequently, the differences between accumulation patterns of flag-pV and its SCM mutants should increase in 6His-SUMO2 HeLa cells (Fig. 24B and 24D), if they should actually depend on the SUMOylation of pV. Indeed, the percentage of cells showing clear accumulations in pV4xKR almost did not change with 43 % of cells containing blurred accumulations in comparison to HeLa cells (Fig. 24D). As observed in HeLa cells, flag-pVK7R shares the highest similarity with flag-pV wt (Fig. 24C-D). Moreover, the phenotypes of flag-pVK23/24R, flag-pVK162R and flag-pVK7/23/24R are almost identical again (Fig. 24B, panels m-t and 24D). In opposite to HeLa cells as well as to flag-pV wildtype, they show a lower percentage of clear accumulations than flag-pV though, ranging from 56 to 75 % (Fig. 24D). Flag-pVK23/24/162R

and flag-pVK7/162R resemble the distribution of flag-pV4xKR the most (Fig. 24B, panels v-z and 24D), which was already found in HeLa cells before.



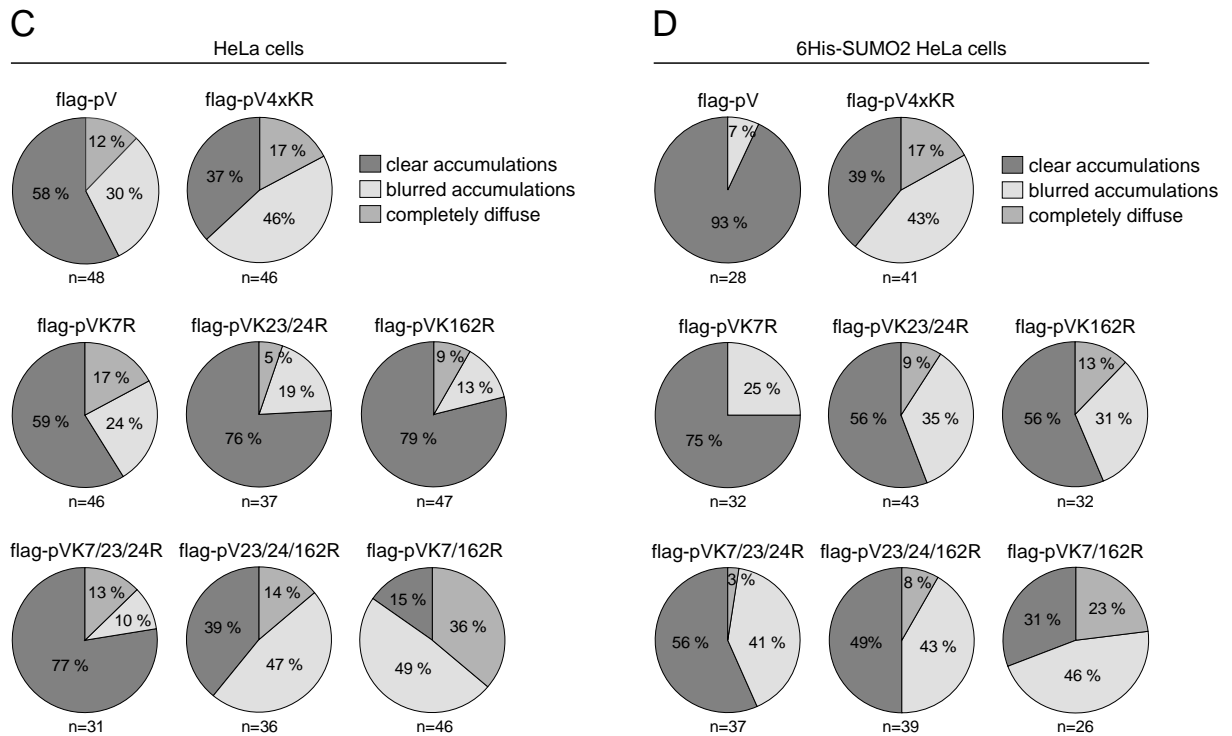


**Figure 24: HAdV-C5 pV4xKR accumulates less in the nucleus of transiently transfected HeLa cells compared to pV.**

**A-B** HeLa or HeLa cells stably expressing 6His-SUMO2 were transfected with 2  $\mu$ g of a flag-pV expression plasmid (#2738), the different flag-pV-SCM mutants or the empty vector control pCMX3b-flag (#152) and fixed with MeOH 48 h p.t. The cells were stained with pab  $\alpha$ -pV, which was detected with an Alexa488-conjugated (green) secondary antibody, while nuclei were stained with dapi (blue). *Merge* indicates the overlay of single images in each row. Images were captured with a Leica fluorescence wide field microscope. **C-D** Statistical summary of captured phenotypes (n), the most abundant one of each transfection is shown in A-B.

To validate these results the immunofluorescence analysis was repeated in HepaRG cells (Fig. 25). These cells are termed ‘pseudo-primary’. Therefore, they offer the possibility to investigate the subcellular localization of HAdV-C5 pV in a less modified system. The distribution of flag-pV was comparable to the one in parental HeLa cells (Fig. 24A, panels d-e, 24C and Fig. 25A, panels d-e, 25C). In contrast, no distinct nuclear accumulations were found in flag-pV4xKR positive cells (Fig. 25A, panels g and h and 25C). Hence, the loss of nucleoli association with lack of SCM within pV was even more pronounced in HepaRG cells. Unfortunately, the phenotypic distribution of other flag-pV-SCM mutants differed from the previous experiment. Although flag-pVK7R, flag-pVK162R and flag-pVK7/162R showed very similar localization patterns in HeLa cells, all mutants containing an alteration at K23 behaved almost the opposite (Fig. 24C and Fig. 25B-C). In this experiment, flag-pVK23/24R, flag-pVK7/23/24R and flag-pVK7/162R variants of the viral protein share the closest relation to flag-pV4xKR (Fig. 25C), which allows no sure identification of the lysine residue mainly responsible.

In summary the previous experiments revealed that only the lack of all three SCM within

HAdV-C5 pV causes a significant reduction of its accumulation at the nucleoli in different transiently transfected human cell lines.

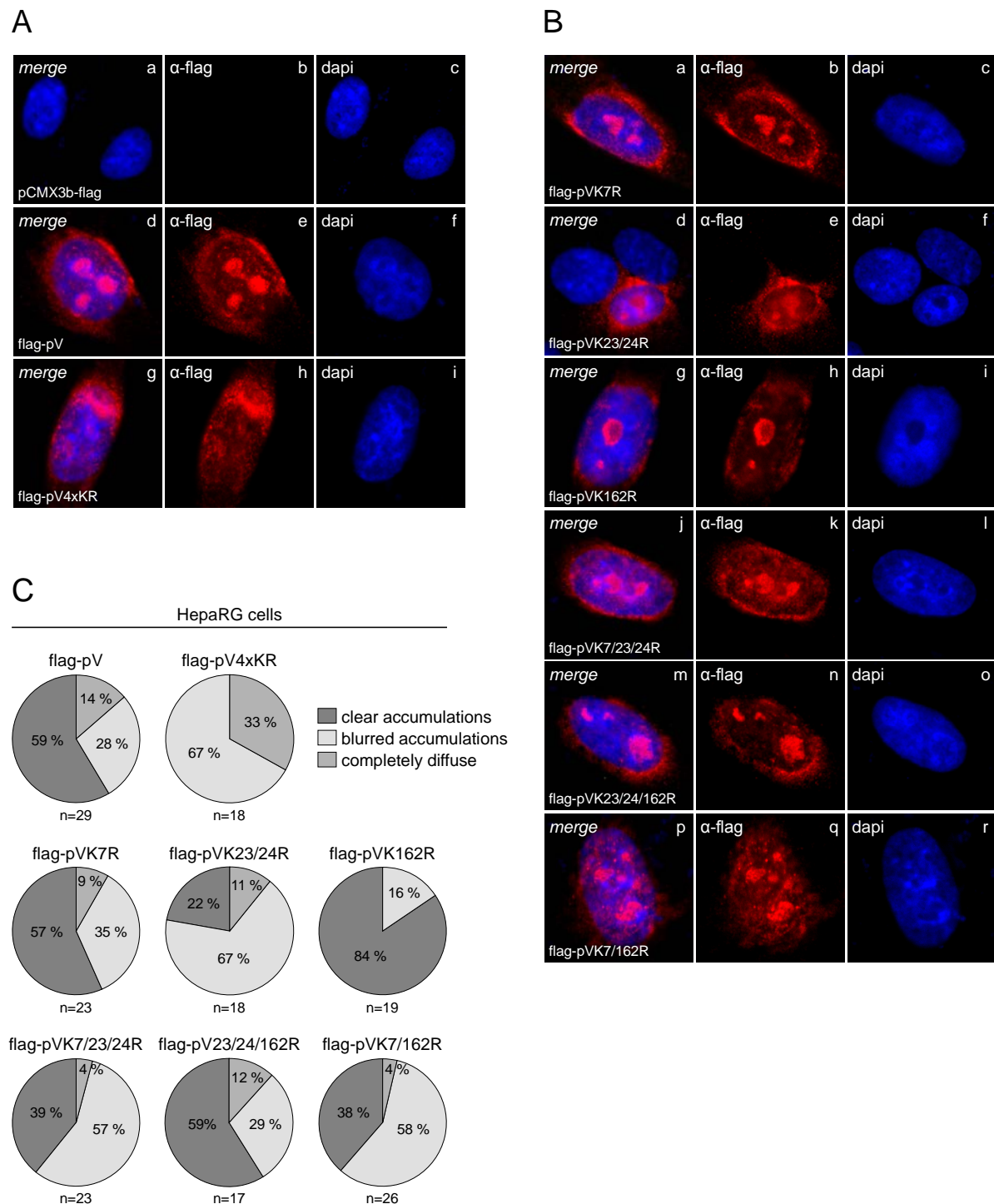


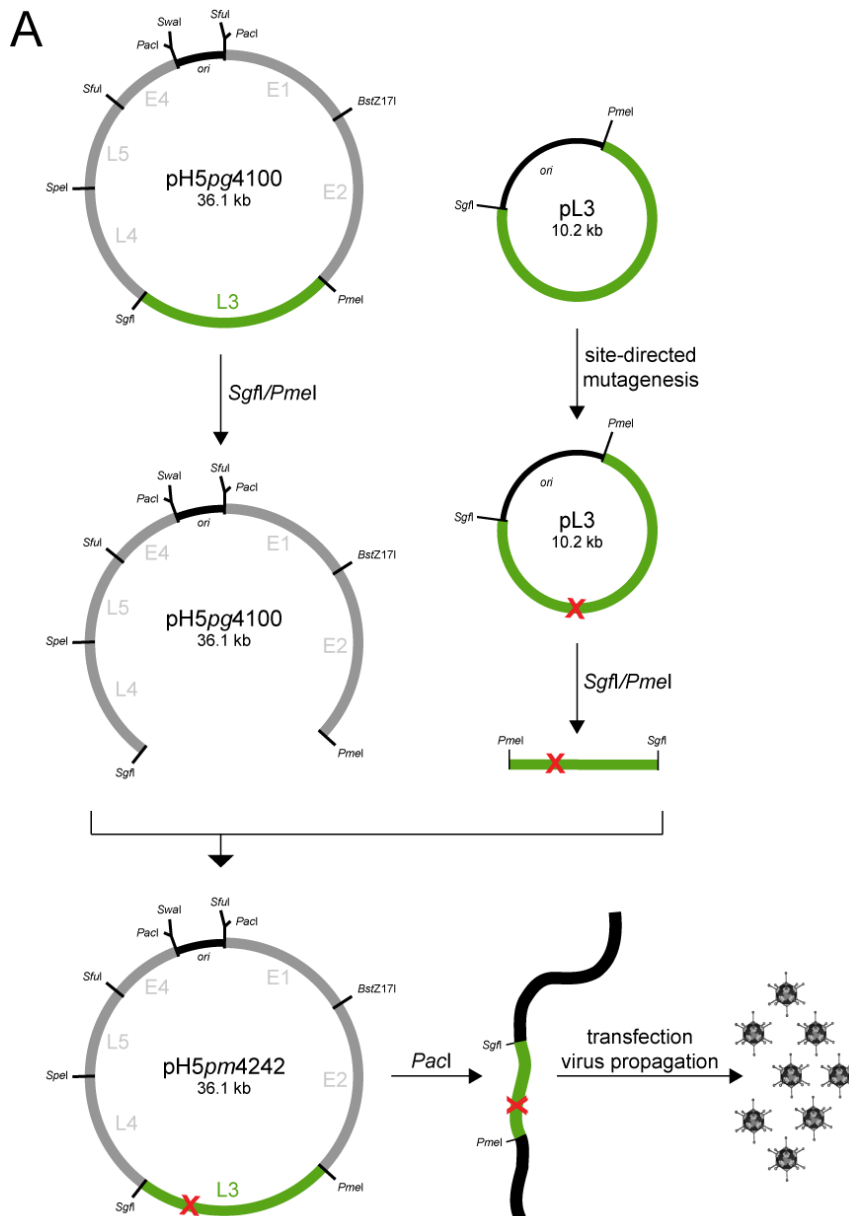
**Figure 25: HAdV-C5 pV4xKR accumulates significantly less in the nucleus of transiently transfected HepaRG cells compared to pV.**

**A-B** HepaRG cells were transfected with 2  $\mu$ g of a flag-expression plasmid (#2738), the different flag-pV-SCM mutants or the empty vector plasmid pCMX3b-flag (#152) and fixed with MeOH 48 h p.t. The cells were stained with pab  $\alpha$ -pV, the primary antibody was detected with a Cy3-conjugated (red) secondary antibody and nuclei were stained with dapi (blue). *Merge* indicates the overlay of single images in each row. Images were captured with a Leica fluorescence wide field microscope. **C** Statistical summary of captured phenotypes (n). The most abundant one of each transfection is shown in A-B.

#### 4.4. The role of pV-SUMOylation during the course of HAdV-C5 infection

##### 4.4.1. Alterations in the three SCM within pV leads to reduced SUMO2-modifications of the protein during HAdV-C5 infection

In section 4.3.1.2, it was already depicted that the modification of pV with SUMO2 proteins occurs not only in transient transfection experiments of the protein, but also in HAdV-C5 infection, albeit not as pronounced. In order to get insight into the role of this pV-SUMOylation during the course of adenoviral infection, a mutant virus was generated in which the lysine residues K7, K23 and K162 of the SCM as well as K24, being part of a neighboring nSCM, are substituted by an arginine R, as before in the mutant flag-pV4xKR (see Fig. 20 and Fig. 22A).



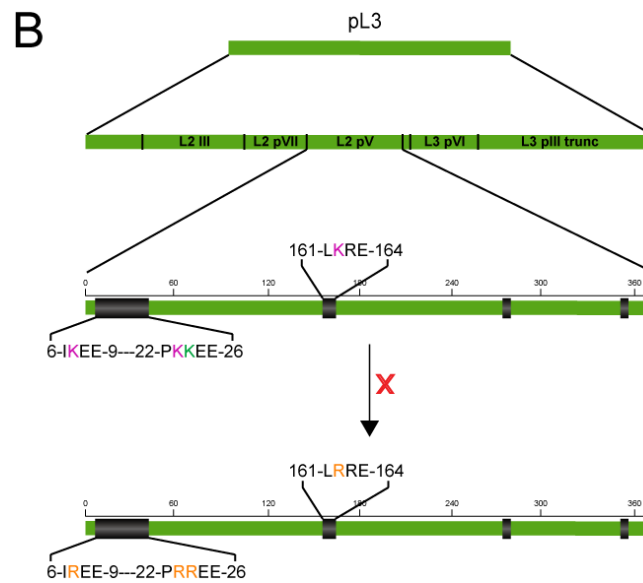


**Figure 26: Generation of a replication competent HAdV-C5 mutant containing four K→R exchanges in the SCM of the pV coding region.**

**A** The plasmid pL3 (#1547) was modified by site-directed mutagenesis to introduce point mutations in the SCM within the coding sequence of HAdV-C5 pV (indicated by a red cross). Afterwards, it was digested with the single-cutter restriction enzymes *SgfI* and *PmeI*, together with the bacmid pH5pg4100 (#1154), containing the whole HAdV-C5 genome. This allows the directed ligation of the modified pL3, as substitute of the original L3 fragment, into the open bacmid DNA. To allow the production of new infectious particles, the modified viral genome had to be linearized and freed from the bacterial part with help of the restriction enzyme *PacI*. Afterwards, the viral genome was transfected into H1299 cells for production of the new mutant virus H5pm4242. **B** The nucleotide exchange A→G in three different fragments of the pV-cds by three quick-change PCRs in a row leads to a substitution of the respective K by R (depicted in yellow) within protein V. Thereby the three SCM (depicted in pink) and one nSCM (depicted in green) were mutated, retaining the local and net charge of the protein. pL3 was used as first template.

The idea behind the mutation of several putative SUMOylation sites at once, is to increase the chance of a detectable functional change of protein V during HAdV-C5 infection. Consequently, any visible effect in further experiments can either be a global result of the four mutations or actually rely on single mutated SCM. The underlying cloning strategy is visualized in Figure 26.

In previous work, a bacmid containing the whole genome of HAdV-C5 (pH5pg4100), was divided into seven smaller parts by restriction enzymes cutting only one unique site of the viral genome. The resulting fragments of the viral genome were sub cloned into vector plasmids again. These have a final size, which allows the introduction of point mutations or other alterations by site-directed mutagenesis with the help of QC-PCRs (Groitl & Dobner, 2007). A following treatment of the modified plasmid and the original bacmid DNA, containing the whole viral genome, with the restriction enzymes, corresponding to the modified fragment of viral DNA, cuts out the fragment of interest and enables the directed ligation of the modified DNA fragment into the viral genome. The newly derived bacmid DNA can be multiplied in

bacteria and linearized after purification with the restriction enzyme *PacI*, whereby the non-viral part is cut out as well. The linearized, ds viral genome is finally transfected with Lipofectamin<sup>®</sup> 2000 into human cells to produce infectious particles of the designed virus mutant (Fig. 26A). The cds of HAdV-C5 pV is part of the genome fragment L3 (Fig. 26B), thus the plasmid pL3 was subjected to three QC-PCRs in a row, each introducing a new nucleotide exchange A→G, as already depicted in Figure 20B-D. This causes four K→R exchanges within the three SCM and one neighboring nSCM in the translated protein V (Fig. 26B). Each product sequence was confirmed by Sanger-sequencing. After successful production of infectious mutant virus particles (H5pm4242) in H1299 cells, genomic DNA was isolated from these cells and the presence of the introduced mutations within adenoviral pV was validated again by Sanger-sequencing.

The first experiment done with the new HAdV-C5 mutant virus was to review the modification pattern of pV with SUMO2 in 6His-SUMO2 expressing HeLa cells (Fig. 27). Therefore, the cells were infected either with HAdV-C5 wt (H5pg4100) or with the pV-SCM mutant virus (H5pm4242).

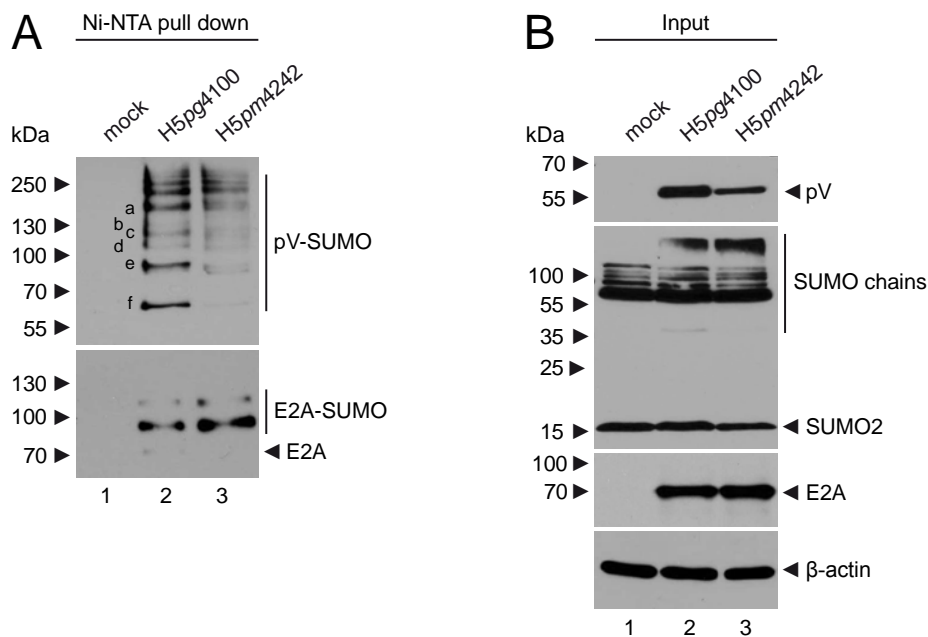


**Figure 27: SUMO2 modification of HAdV-C5 pV is reduced during pV-SCM mutant virus infection in 6His-SUMO2 HeLa cells.**

HeLa cells stably expressing 6His-SUMO2 were infected with HAdV-C5 wt (H5pg4100, moi 5) or the HAdV-C5 pV-SCM mutant (H5pm4242, moi 5). The cells were harvested 24 h p.i. and subjected to a guanidinium chloride buffer. **A** 6His-SUMO conjugates were purified by usage of a Ni-NTA-matrix, resolved with **B** total-cell lysates as input control by 10-12 % SDS-PAGE and visualized by immunoblotting (400 mA, 90 min, nitrocellulose  $\varnothing = 0.45 \mu\text{m}$ ). Ni-NTA purified and input proteins were detected by using pab  $\alpha$ -pV, (20  $\mu\text{g}$  input), mab  $\alpha$ -6His (75  $\mu\text{g}$  input), mab B6-8 ( $\alpha$ -E2A, 25  $\mu\text{g}$  input) and AC-15 ( $\alpha$ - $\beta$ -actin, 25  $\mu\text{g}$  input). Molecular weights in kDa are indicated on the *left*, while corresponding proteins are labeled on the *right*. Mock means uninfected control.

Resulting total-cell lysates were subsequently purified with a Ni-NTA matrix to pull down 6His-SUMO2 conjugates. Indeed, the pull down of pV from mutant virus infected cells shows a SUMO2 ladder with severely reduced signal intensities, compared to the pull down from HAdV-C5 wt infected cells (Fig. 27A, upper panel, lanes 2-3). To control whether the used amounts of protein are comparable, the same pull down samples were split and additionally stained for E2A, which is another viral protein known to be modified with SUMO2 (Terzic, 2014). The result clarifies that the pulled amounts of SUMO2 conjugates are comparable in both samples (Fig. 27A, lower panel, lanes 2-3). As already observed in the transient transfection experiments (Fig. 22B and Fig. 23B), bands a, c, e and f in Figure 27A (upper panel, lanes 2-3) almost completely disappear in pV-SCM mutant virus infected cells, whereas bands b and d occur already very weakly in HAdV-C5 wt infected cells (Fig. 27A, upper panel, lanes 2-3). It cannot be ruled out though, that the faint appearance of pV-SUMOylation in mutant virus infection is partially caused by lower concentrations of pV compared to HAdV-C5 wt infection (Fig. 27B, upper panel, lanes 2-3).

#### 4.4.2. Viral replication is not significantly influenced by the lack of SCM within HAdV-C5 pV in H1299 cells

In order to reveal the importance of pV-SUMOylation during the course of adenoviral infection, the production of new infectious particles was monitored over three days in H1299 cells infected either with HAdV-C5 wt or with the pV-SCM mutant virus.

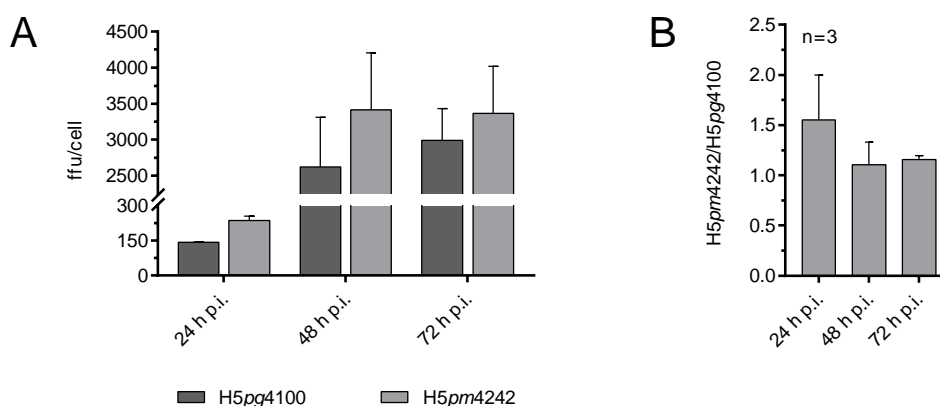


**Figure 28: Viral progeny production is slightly enhanced during pV-SCM mutant virus infection compared to HAdV-C5 wt infection in H1299 cells.**

H1299 cells were infected with HAdV-C5 wt (H5pg4100, moi 20) or pV-SCM mutant virus (H5pm4242, moi 20) and harvested 24, 48 or 72 h p.i. The viral progeny was isolated and titrated on H1299 cells by visualizing the infected cells via immunofluorescence to determine the yield. **A** Experiment with three technical replicates where the average is plotted. Error bars indicate the standard deviation and ffu means fluorescence forming units. **B** Average of  $n = 3$  independent experiments, each done in triplicates, emphasizing the ratio of the pV-SCM mutant virus and HAdV-C5 wt (H5pm4242/H5pg4100) at each time point investigated.

The difference in viral replication was not significant at any time point, though (Fig. 28A). Nevertheless, the mutant virus showed a tendency to produce more viral progeny than HAdV-C5 wt. This tendency declines and has its maximum at the earliest time point investigated, which is 24 h p.i. where 1.5-fold more particles that are infectious were produced during pV-SCM mutant virus infection than during HAdV-C5 wt infection (Fig. 28B).

#### **4.4.3. The concentrations of different viral proteins are elevated during HAdV-C5 pV-SCM mutant infection in H1299 cells**

In case of a true replication benefit of the pV-SCM mutant virus, it could be expected that also certain viral proteins be expressed to a higher extent than during HAdV-C5 wt infection. For example E2A, which is essential for viral DNA-replication, might be a candidate (van Breukelen *et al.*, 2003; Friefeld *et al.*, 1983, 1984; de Jong *et al.*, 2003; Lindembaum *et al.*, 1986; Vliet & Sussenbach, 1975). In addition, E1A proteins, which are able to enhance the transcription of different adenoviral promoters (Berk, 1986; Berk *et al.*, 1979; Berscheminski *et al.*, 2013; Jones & Shenk, 1979; Nevins, 1981). On the other hand, it was already observed that pV lacking its SCM is present in lower amounts than pV in HAdV-C5 wt infection (Fig. 27).

In order to examine the behavior of known viral proteins during HAdV-C5 pV-SCM mutant infection compared to HAdV-C5 wt infection, another time course experiment was performed in H1299 cells. The cells were harvested for lysis at different time points between 8 and 72 h p.i. and their protein content was further analyzed by immunoblotting (Fig. 29). The results match the tendency of the previous experiment (Fig. 28). Especially, the early viral proteins under investigation, namely E1A, E1B-19K, E1B-55K, E2A and E4orf6 (Fig. 29, lanes 2-3 and 8-9), appear in higher steady state concentrations in pV-SCM mutant virus infected cells compared to those infected with HAdV-C5 wt. This difference is particularly pronounced at early time points after infection. Additionally, the late protein L4-100K can be detected earlier during mutant virus infection (Fig. 29, lanes 4 and 10), whereas the late capsid proteins show comparable levels at all time points (Fig. 29, lanes 4-6 and 10-12). For the intermediate protein IX (pIX) no differences can be visualized (Fig. 29, lanes 5-6 and 11-12) and the only investigated protein present in lower amounts during mutant virus infection is the modified pV itself (Fig. 29, lanes 4-6 and 11-12), as it was already seen in Figure 27.

RESULTS

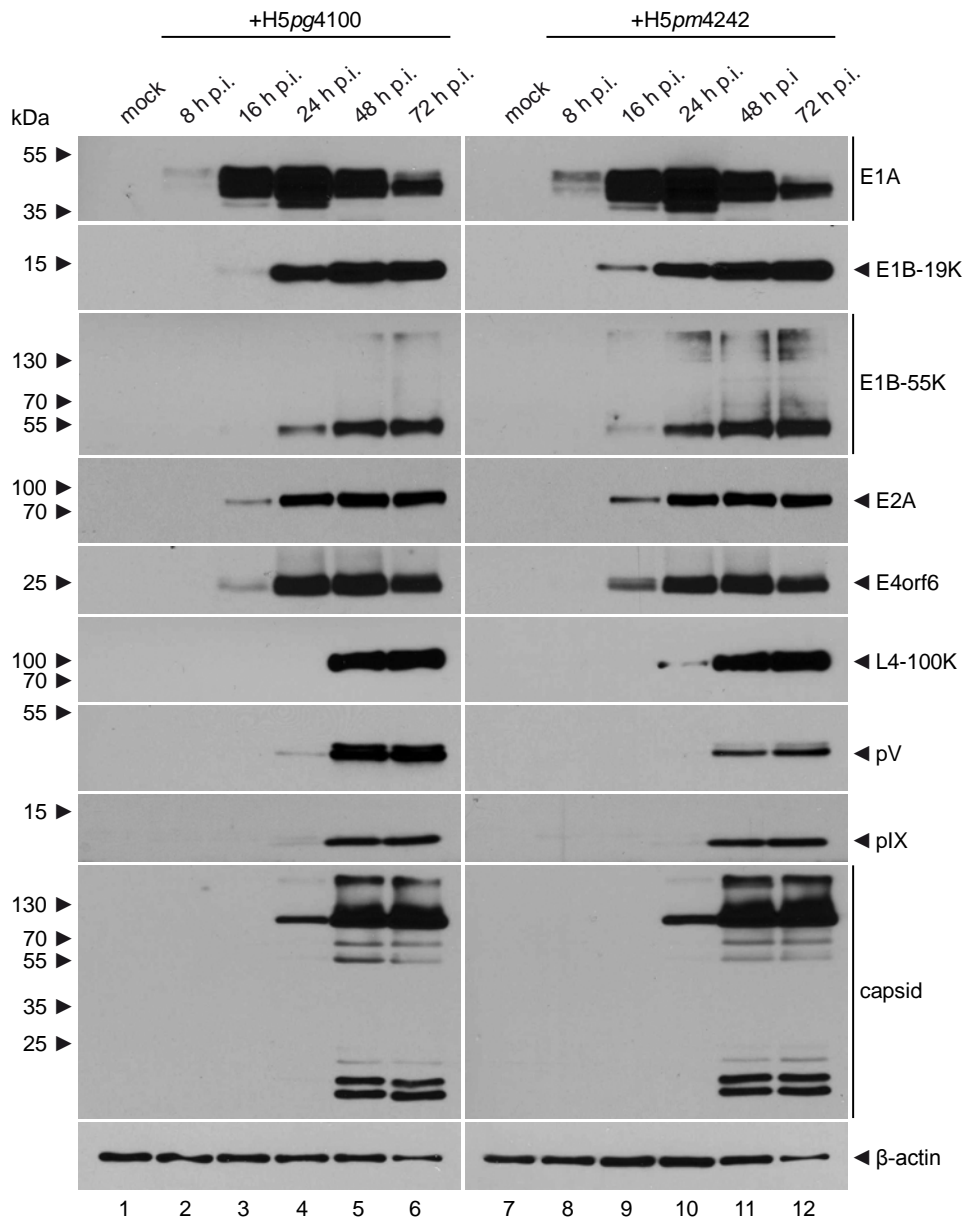


**Figure 29: Viral protein levels increase faster during pV-SCM mutant virus infection compared to HAdV-C5 wt infection in H1299 cells.**

H1299 cells were infected with HAdV-C5 wt (H5pg4100, moi 20) or pV-SCM mutant virus (H5pm4242, moi 20) and harvested 8, 16, 24, 48 or 72 h p.i. Total-cell lysates were resolved by 10-12% SDS-PAGE and visualized by immunoblotting (400 mA, 90 min, nitrocellulose  $\phi = 0.45 \mu\text{m}$ ). Input levels of proteins were detected by using mab M73 ( $\alpha$ -E1A, 50  $\mu\text{g}$  input), pab  $\alpha$ -19K (10  $\mu\text{g}$  input), mab 2A6 ( $\alpha$ -E1B-55K, 25  $\mu\text{g}$  input), mab B6-8 ( $\alpha$ -E2A, 10  $\mu\text{g}$  input), mab RSA3 ( $\alpha$ -E4orf6, 100  $\mu\text{g}$  input), mab 6B10 ( $\alpha$ -L4100K, 10  $\mu\text{g}$  input), pab  $\alpha$ -pV (10  $\mu\text{g}$  input), pab  $\alpha$ -pIX (100  $\mu\text{g}$  input), pab L133 ( $\alpha$ -capsid, 25  $\mu\text{g}$  input), pab  $\alpha$ -Mre11 (50  $\mu\text{g}$  input) and mab AC-15 ( $\alpha$ - $\beta$ -actin, 25  $\mu\text{g}$  input). Molecular weights in kDa are indicated on the *left*, while corresponding proteins are labeled on the *right*. Mock means uninfected control.

An obvious resulting question is, whether pV might be capable to regulate viral transcription processes and if so, whether this function depends on the SUMOylation status of the protein. To shed light on this idea H1299 cells were co-transfected with a flag-pV or a flag-pV4xKR expressing plasmid together with a construct, which expresses a reporter gene under the control

of an adenoviral promoter. Additionally, a plasmid expressing an independent reporter gene is co-transfected as internal transfection control. 24 h p.t. the cells were subjected to a dual luciferase assay. However, the comparison of HAdV-C5 pV with pV lacking its SCM did not show any enhancing activity on all viral promoters investigated (Fig. 30A). There might be a small activating influence of pV in general on the early promoters E2 (E2E) and E3, albeit it is not even 2-fold and cannot explain the earlier occurrence of E1A or E1B proteins during pV-SCM mutant virus infection (Fig. 29).

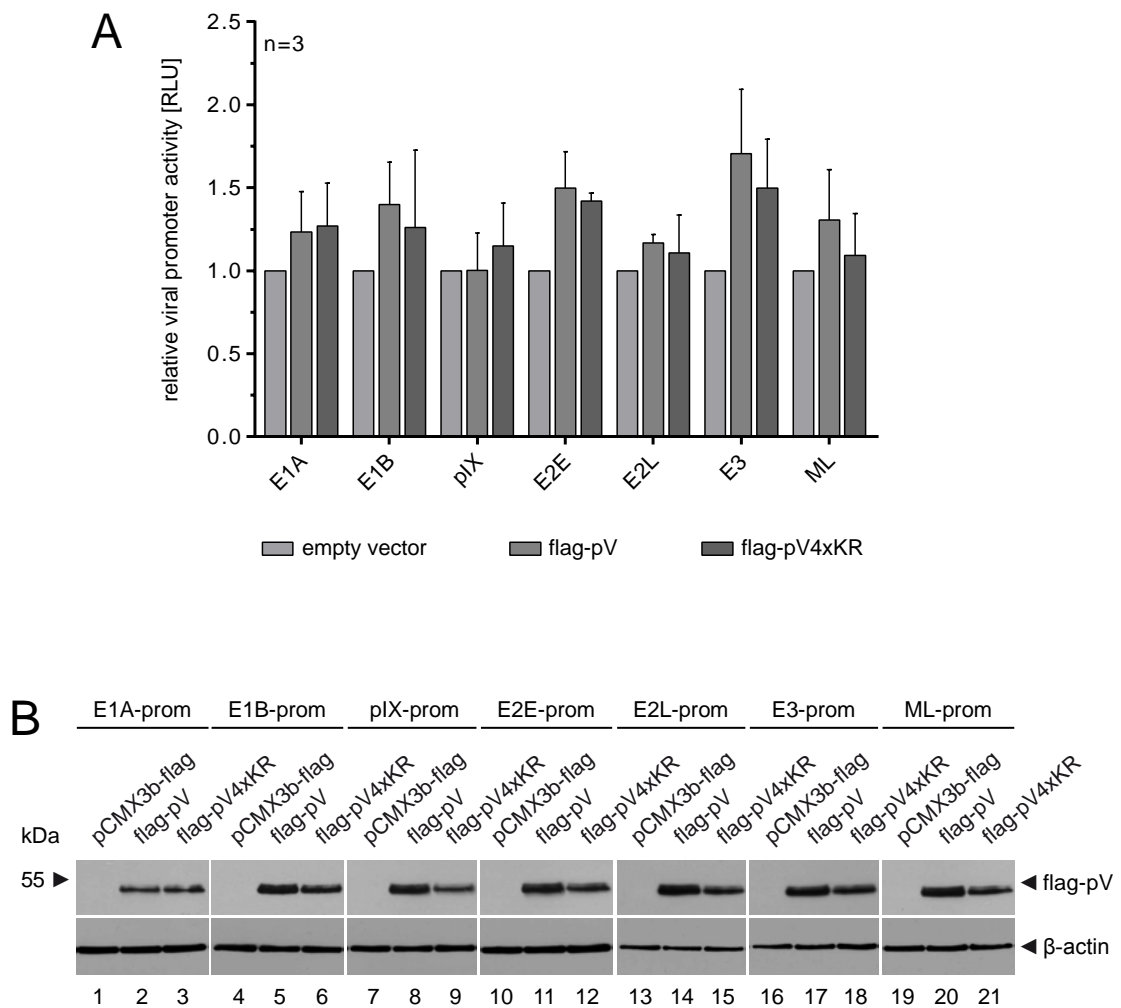


**Figure 30: Flag-pV4xKR does not enhance the activity of adenoviral promoters in transiently transfected H1299 cells.**

H1299 cells were transfected with 0.5  $\mu$ g of a flag-pV (#2738), a flag-pV4xKR (#2969) expressing plasmid or the empty vector pCMX3b-flag (#152) in combination with 0,5  $\mu$ g of a plasmid expressing the *firefly* luciferase gene under control of different adenoviral promoters (E1A, E1B, pIX, E2 early (E2E), E2 late (E2L) or Major late (ML)) and additionally 0,5  $\mu$ g of a *renilla* luciferase expression plasmid (#180). The activities of both luciferases were measured in a dual luciferase assay 24 h p.t. **A** The viral promoter activity ( $LU_{\text{firefly}}/LU_{\text{renilla}}$ ) in the presence of flag-pV or flag-pV4xKR relative to the empty vector control was determined in  $n = 3$  independent experiments, each performed in triplicates. The empty vector control was set to 1 and the resulting averages for each condition are depicted with corresponding standard deviations. RLU means relative luciferase unit. **B** Total-cell lysates were resolved by 10% SDS-PAGE and visualized by immunoblotting (400 mA, 90 min, nitrocellulose ( $\varnothing = 0.45 \mu\text{m}$ )). Input levels of proteins were detected by using mab M2 ( $\alpha$ -flag) and mab AC-15 ( $\alpha$ - $\beta$ -actin). Molecular weights in kDa are indicated on the *left*, while corresponding proteins are labeled on the *right*. Prom means promoter.

To rule out that the steady state concentrations of proteins differ between samples to be compared, a Western Blot analysis of total-cell lysates was performed. It convincingly shows that both pV proteins were expressed in the presence of a certain viral promoter (Fig. 30B). In case of the viral promoters pIX, E2E, E2L and ML, the concentration of flag-pV4xKR is slightly lower compared to flag-pV (Fig. 30B, lanes 7-15 and 19-21), whereas both protein concentrations are comparable in the presence of the E1A, E1B and E3 promoters (Fig. 30B, lanes 1-6 and 16-18). Consequently, the pV-SCM mutant does not seem to have a direct influence on the activity of adenoviral promoters, although the possibility remains that another viral factor is needed to mediate an enhanced transcription.

#### **4.4.4. The replication cycle of the HAdV-C5 pV-SCM mutant is accelerated compared to the wildtype virus in HepaRG cells**

To validate these first characterization results of the HAdV-C5 pV-SCM mutant, additional experiments were performed in the ‘pseudo-primary’ cell line HepaRG. In contrast to other transformed cell lines, like HeLa or H1299, they offer the advantage of having only few major chromosomal rearrangements (Gripon *et al.*, 2002). Furthermore, they are less infectable with HAdV-C5 and the progression of the viral life cycle is slower than in HeLa, H1299 or A549 cells. This might allow a better visualization of the differences between HAdV-C5 wt and the pV-SCM mutant. In fact, the replication efficiency of the mutant virus was superior more clearly in HepaRG cells (Fig. 31A) compared to H1299 cells (Fig. 29). An average of three independent experiments amounted to an approximately 2.5-fold increase of viral progeny produced 24 h p.i. in mutant virus infected cells (Fig. 31B). This benefit over HAdV-C5 wt declines within 72 h p.i., but the ratio remains greater than one.

This tendency of the mutant virus to replicate faster was also reflected by the equilibrium concentrations of different adenoviral proteins, found in another time course experiment in HepaRG cells (Fig. 31C). The procedure was the same as for the previous study in H1299 cells (Fig. 29). As expected, HAdV-C5 wt infection proceeded a little slower than in H1299 cells, whereas no severe difference was detectable for the pV-SCM mutant virus infection (compare Fig. 29 and 31C). Consequently, the early proteins E1A, E1B-19K and E1B-55K appeared 8 h earlier during pV-SCM mutant virus infection compared to HAdV-C5 wt infected cells (Fig. 31C, lanes 2-4 and 7-9). The gene products E2A and E4orf6 were present in higher concentrations at corresponding time points (Fig. 31C, lanes 3-4 and 8-9). Similarly, the late protein L4-100K occurred 8 h earlier in HepaRG cells infected with the pV mutant virus

(Fig. 31C, lanes 4 and 8) and other than in H1299, also many of the capsid proteins show a stronger signal than in wildtype infected cells (Fig. 31C, lanes 5-6 and 9-11 and Fig. 29). Only the mutated pV is less concentrated again during HAdV-C5 pV-SCM mutant infection (Fig. 31C, lanes 5-6 and 10-11). Furthermore, the levels of the cellular tumor suppressor p53 are decreasing slightly faster during mutant virus infection (Fig. 31C, lanes 4-6 and 9-11).

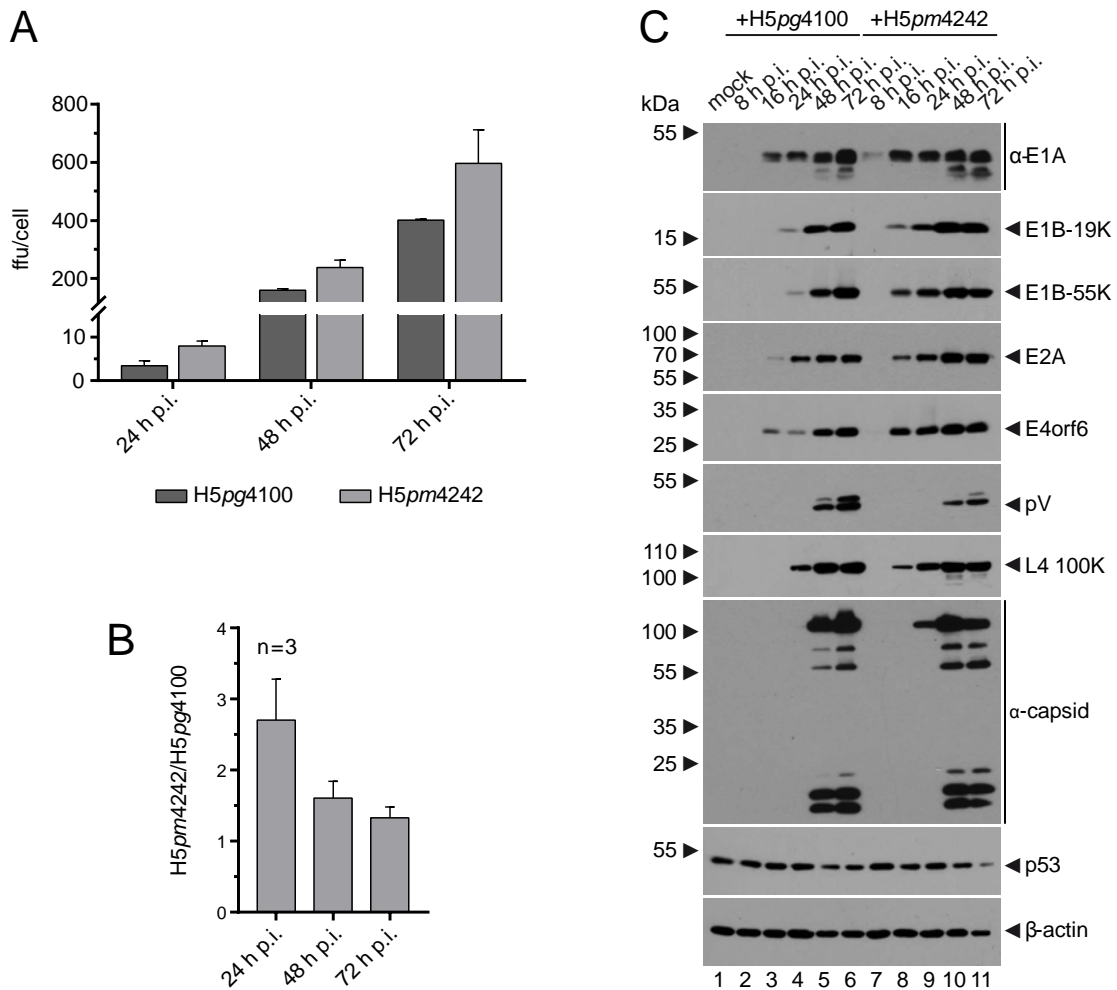


**Figure 31: The replication cycle of the virus mutant HAdV-C5 pV-SCM benefits from the lack of SCM within pV in HepaRG cells.**

**A-B** HepaRG cells were infected with HAdV-C5 wt (H5pg4100, moi 20) or pV-SCM mutant virus (H5pm4242, moi 20) and harvested 24, 48 or 72 h.p.i. The viral progeny was isolated and titrated on H1299 cells by visualizing the infected cells via immunofluorescence to determine the yield. **A** Experiment with three technical replicates where the average is plotted. Error bars indicate the standard deviation and ffu means fluorescence forming units. **B** Average of  $n = 3$  independent experiments, each done in triplicates, emphasizing the ratio of the pV-SCM mutant virus and HAdV-C5 wt (H5pm4242/H5pg4100) at each time point investigated. **C** HepaRG cells were infected with HAdV-C5 wt (H5pg4100, moi 20) or pV-SCM mutant virus (H5pm4242, moi 20) and harvested 8, 16, 24, 48 or 72 h.p.i. Total-cell lysates were resolved by 10-12% SDS-PAGE and visualized by immunoblotting (400 mA, 90 min, nitrocellulose  $\varnothing = 0.45 \mu\text{m}$ ). Input levels of proteins were detected by using mab M73 ( $\alpha$ -E1A, 75  $\mu\text{g}$  input), pab  $\alpha$ -19K (10  $\mu\text{g}$  input), mab 2A6 ( $\alpha$ -E1B-55K, 25  $\mu\text{g}$  input), mab B6-8 ( $\alpha$ -E2A, 5  $\mu\text{g}$  input), mab RSA3 ( $\alpha$ -E4orf6, 25  $\mu\text{g}$  input), mab 6B10 ( $\alpha$ -L4-100K, 10  $\mu\text{g}$  input), pab  $\alpha$ -pV (10  $\mu\text{g}$  input), pab L133 ( $\alpha$ -capsid, 25  $\mu\text{g}$  input), mab Do-1 ( $\alpha$ -p53, 30  $\mu\text{g}$  input) and mab AC-15 ( $\alpha$ - $\beta$ -actin, 15  $\mu\text{g}$  input). Molecular weights in kDa are indicated on the *left*, while corresponding proteins are labeled on the *right*. Mock means uninfected control.

This is in accordance with the earlier presence of the adenoviral proteins E1B-55K and E4orf6, which form an E3-ubiquitin ligase complex together with different cellular proteins (see section 1.1.3.2). This complex induces a polyubiquitination of different cellular substrates, such as Mre11 and p53, leading to their proteasomal degradation (Blanchette *et al.*, 2004; Querido *et al.*, 2001a, b; Stracker *et al.*, 2002).

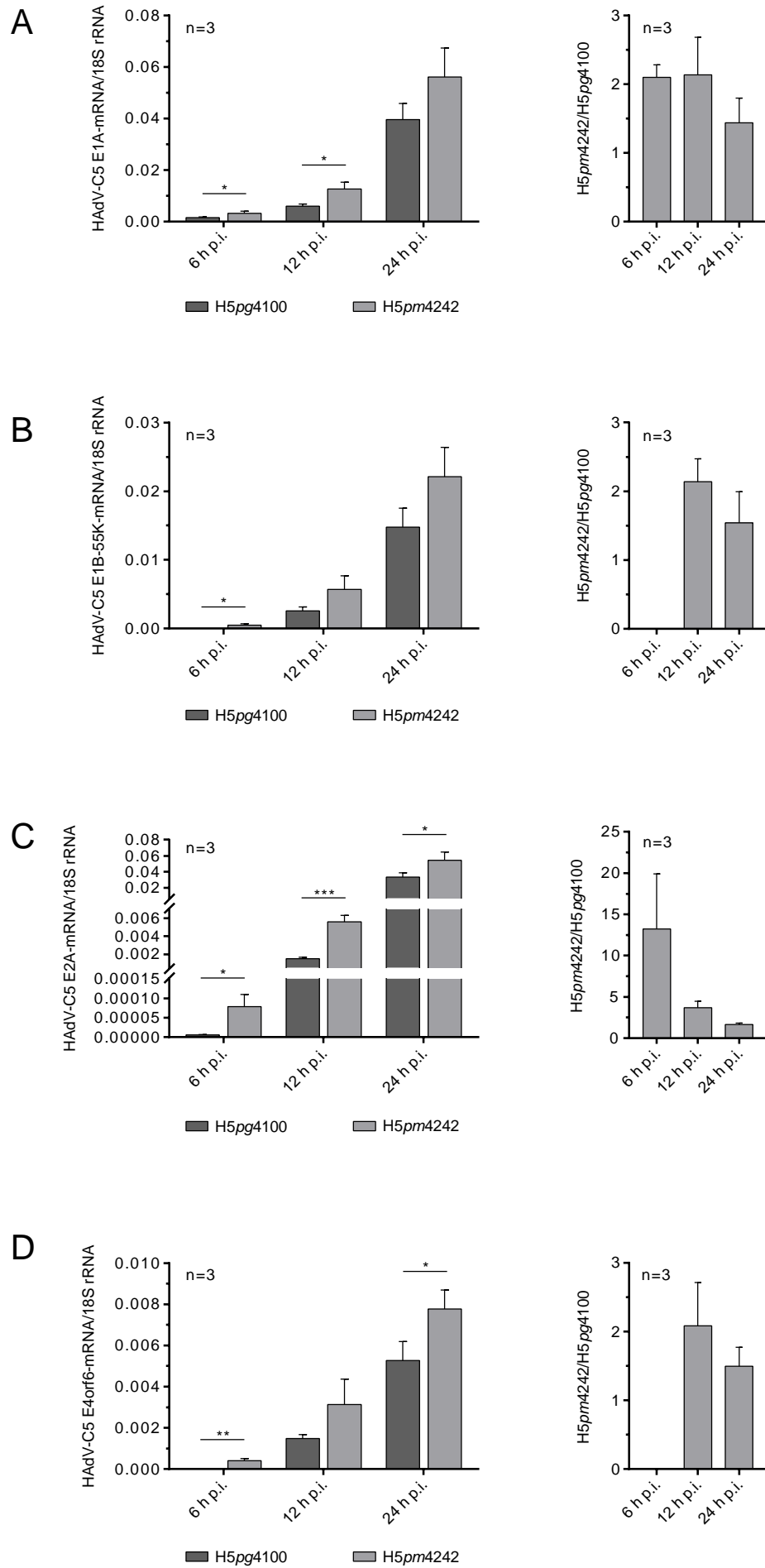
In conclusion, the acceleration of the HAdV-C5 pV-SCM mutant replication cycle could be confirmed in HepaRG cells. It turned out to be even more pronounced in these ‘pseudo-primary’ cells. Thus, HepaRG cells provide a suitable model system to characterize the HAdV-C5 pV-SCM mutant further in comparison to the wildtype virus.

#### **4.4.4.1. Viral mRNA concentrations are elevated during HAdV-C5 pV-SCM mutant virus infection**

Although the pV-SCM mutant (flag-pV4xKR) did not show an activating effect on adenoviral promoters in transiently transfected H1299 cells (Fig. 30), viral transcription was additionally monitored for one day in infected HepaRG cells. Therefore, the cells were infected either with HAdV-C5 wt or with the pV-SCM mutant virus and harvested 6, 12 or 24 h p.i. The total-RNA was isolated and contained mRNAs were reversely transcribed. The resulting cDNA was amplified by RT-PCR with primer pairs matching different regions of the adenoviral genome to reveal the relation between early as well as late mRNAs in the differently infected HepaRG cells. The primer pairs used in this study are not exon-specific. Consequently, they would amplify traces of viral DNA as well. To prove that the samples did not contain interfering contaminations of viral DNA, the RT-PCR products were subjected to an agarose gel and visualized with ethidium bromide. As an example, the amplified cDNA of a pV-cds fragment is shown in Figure 32G. This DNA is not detectable earlier than 12 h after pV-SCM mutant virus infection and only 24 h after HAdV-C5 wt infection in three independent experiments, indicating a high purity of the isolated RNA samples with reliable ratios of both viruses.

In accordance with the previous time course experiments on protein level, all viral mRNAs investigated occurred earlier or with enhanced concentrations at a certain time point in pV-SCM mutant virus infected cells (Fig. 32). Interestingly, E1A-mRNA concentrations were already ~2-fold higher at the early time points 6 and 12 h p.i. (Fig. 32A), although E1A is the first adenoviral gene expressed. This observation was similar for the early viral mRNAs encoding E1B-55K (Fig. 32B) and E4orf6 (Fig. 32D), albeit they were exclusively detected in pV-SCM mutant virus infected cells at the earliest time point measured, which is 6 h p.i.

RESULTS



RESULTS

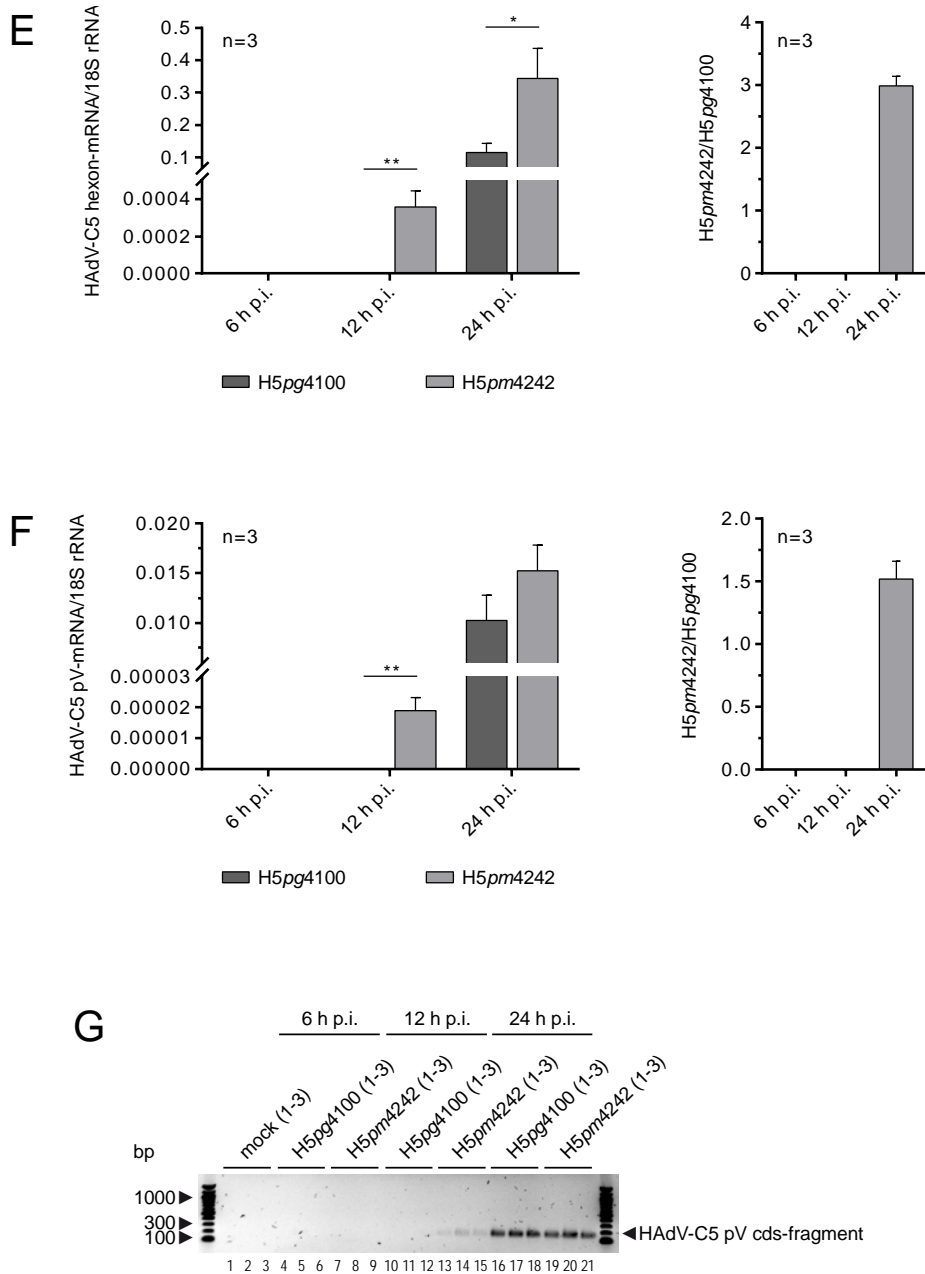


**Figure 32: Viral mRNAs accumulate faster during pV-SCM mutant viral infection in HepaRG cells in comparison with HAdV-C5 wt infection.**

HepaRG cells were infected with HAdV-C5 wt (H5pg4100, moi 20) or pV-SCM mutant virus (H5pm4242, moi 20) and harvested 6, 12 or 24 h p.i. Total-RNA was isolated from the cells, contained mRNA was reversely transcribed and the resulting cDNA was amplified by RT-PCR with primer pairs specific for a certain viral cds-fragment and primer pairs against a cds-fragment of cellular 18S rRNA. **A-F** On the *left*, HAdV-C5 mRNA amounts are depicted relative to the amounts of cellular 18S rRNA as an average of  $n = 3$  independent experiments. Error bars indicate the standard deviation. RT-PCR was performed in technical duplicates for each experiment and the statistics were calculated with a 2-tailed, unpaired t-test for each time point. P-value  $< 0.05$  means \*,  $p < 0.01$  means \*\*,  $p < 0.001$  means \*\*\*. On the *right*, the ratio of the pV-SCM mutant virus and HAdV-C5 wt (H5pm4242/H5pg4100) is emphasized for each time point investigated. **G** shows an agarose gel (0.8 %) of the RT-PCR products obtained with a primer pair specific for a DNA-fragment within the pV-cds from the same three experiments. Contained DNA was visualized with ethidium bromide during UV-exposure; nucleic acid sizes in bp are indicated on the *left*, while corresponding DNA-fragments are labeled on the *right*. Mock means uninfected control and HAdV-C5 mRNA/18S rRNA means

$$f(h \text{ p. i.}) = \frac{E_{\text{viral mRNA primer pair}}^{-Ct(\text{viral mRNA}(h \text{ p.i.}))}}{E_{18S \text{ rRNA primer pair}}^{-Ct(18S \text{ rRNA}(h \text{ p.i.}))}}$$

with  $E$  = efficiency of the corresponding primer pair.

Due to higher variations between the independent experiments, the p-value was greater than 0.5 at 12 h p.i., nevertheless the same trend towards higher mRNA concentrations in pV-SCM mutant virus infected cells is visible at this time point. The elevated mRNA concentrations of E2A were even more pronounced (Fig. 32C). Already 6 h p.i. an approximately 12.5-fold excess of E2A-mRNA could be detected, which declined later on, as it was found for the other viral mRNAs too (Fig. 32A-F).

Comparable to the steady state concentrations of adenoviral proteins, not only early, but also late viral mRNAs were influenced (Fig. 32E-F). Interestingly, besides hexon-mRNA (Fig. 32E) also pV-mRNA (Fig. 32F) occurred already 12 h after pV-SCM mutant virus infection, whereas it cannot be detected earlier than 24 h after HAdV-C5 wt infection. However, pV-SCM was the only protein with reduced steady state concentrations in the previous time course experiment (Fig. 31C). Hence, the underlying cause cannot be found on transcriptional level, but the protein is likely to be affected directly.

Taken together, these results further underline a benefit of the HAdV-C5 pV-SCM mutant virus early during infection, which is occurring definitely prior to translation of adenoviral proteins.

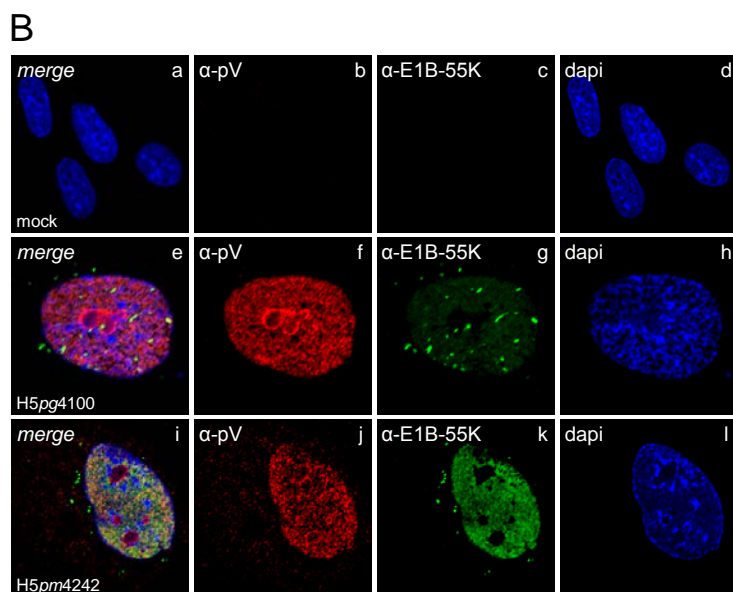
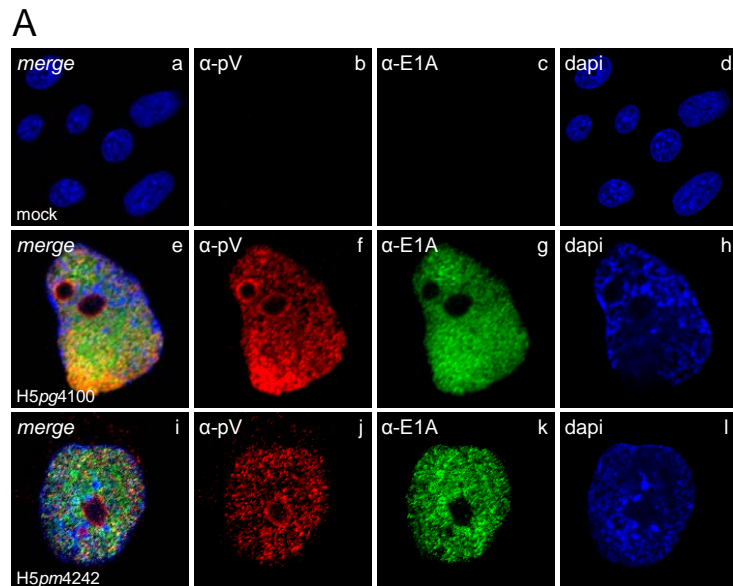
#### **4.4.4.2. The lack of SCM within HAdV-C5 pV does not influence the subcellular distribution of early adenoviral proteins, whereas mutated pV shows a lower affinity to host nucleoli**

The expression level of many viral proteins was altered during HAdV-C5 pV-SCM mutant infection in HepaRG cells (Fig. 31C and Fig. 32). To elucidate, whether not only the amount of essential viral proteins changes, but also their subcellular distribution, HepaRG cells were infected with HAdV-C5 wt or the pV-SCM mutant virus and prepared for immunofluorescence analysis 24 h p.i. The cells were double stained for pV and either E1A, E1B-55K or E2A (Fig. 33), which are all regulatory, adenoviral proteins showing higher concentrations at early time points during pV-SCM mutant virus infection (Fig. 31C). The results reveal that neither the localization of E1A (Fig. 33A), nor the distribution of E1B-55K (Fig. 33B) or E2A (Fig. 33C) is altered in comparison to HAdV-C5 wt infected HepaRG cells.

As usual, E1A was diffusely distributed throughout the whole nucleus of all captured, infected cells sparing the nucleoli (Fig. 33A, panels g and k) (Berscheminski *et al.*, 2013; White *et al.*, 1988). On the other hand, E1B-55K accumulated in speckled fractions of different size and shape within the cytoplasm and showed an additional diffuse signal in the nucleus. The latter can be more or less intense and excludes the nucleoli like E1A (Fig. 33B, panels g and k)

(Ornelles & Shenk, 1991). Consequently, none of the two proteins showed a remarkable co-localization with pV at the nucleoli. Only parts of their diffuse fractions overlap with diffuse portions of pV (Fig. 33A-B, panels e and i).

E2A forms spherical structures within the nucleus, which are known to be the sites of viral replication (Puvion-Dutilleul *et al.*, 1984; Voelkerding & Klessig, 1986). They appeared from small filled dots to huge hollow spheres, which holds true for cells infected either with HAdV-C5 wt or with the pV-SCM mutant virus (Fig. 33C, panels g and k). Hence, no difference in the localization of essential early viral proteins can be detected between HAdV-C5 wt and pV-SCM mutant virus infected HepaRG cells.



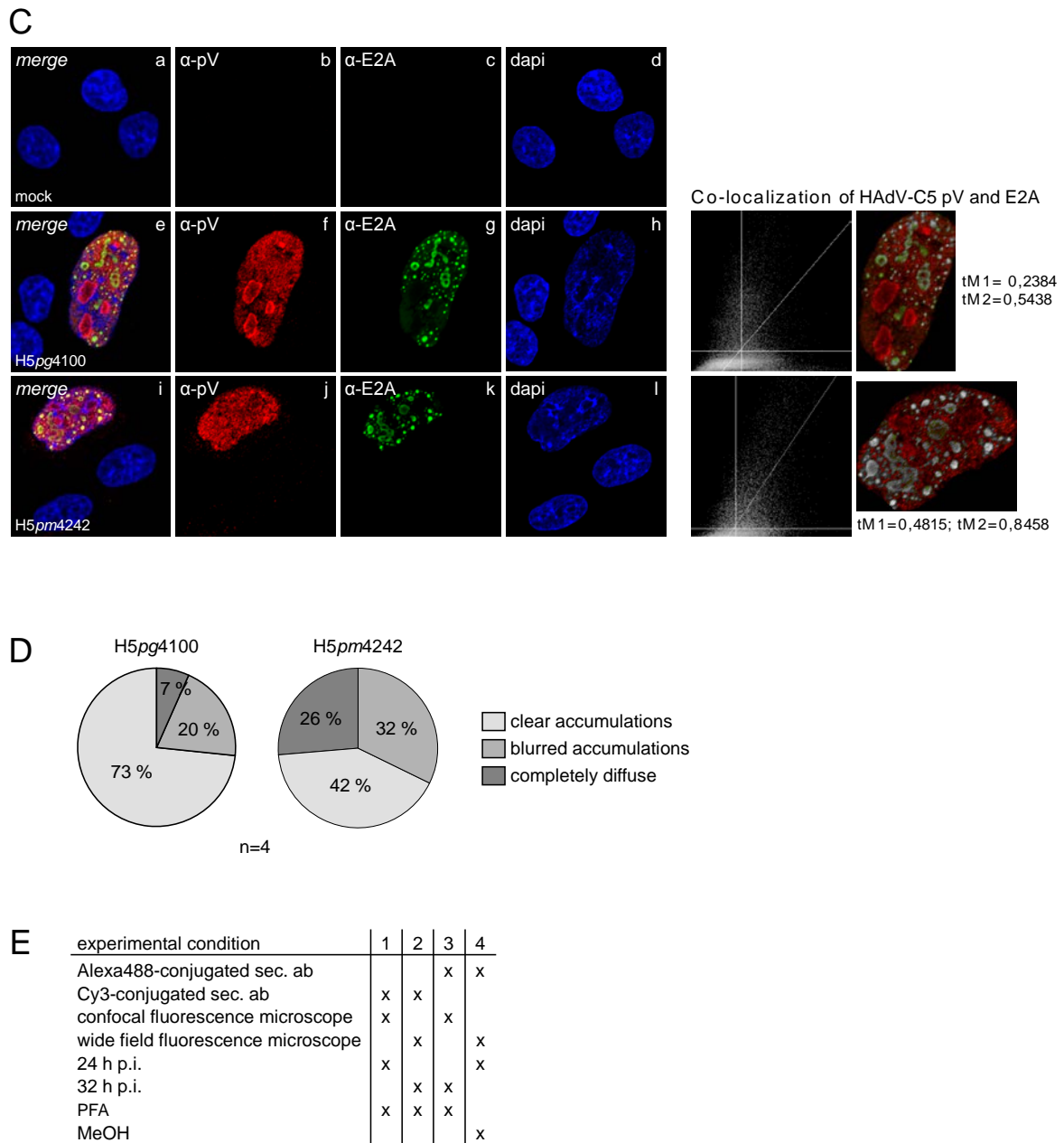


**Figure 33: The subcellular localization of the early viral proteins E1A, E1B-55K and E2A is not influenced by the lack of SCM within HAdV-C5 pV. Protein V lacking its SCM accumulates less at host nucleoli, though.**

HepaRG cells were infected with HAdV-C5 wt (H5pg4100, moi 20) or a HAdV-C5 pV-SCM mutant (H5pm4242, moi 20) and fixed with 4% PFA 24 h p.i. To visualize pV the cells were treated with pab  $\alpha$ -pV. **A** E1A was visualized with mab M73 ( $\alpha$ -E1A), **B** E1B-55K was visualized with mab 2A6 ( $\alpha$ -E1B-55K) and **C** E2A was visualized with mab B6-8 ( $\alpha$ -E2A). Primary antibodies were detected with Alexa488- (green) or Cy3- (red) conjugated secondary antibodies and nuclei were stained with dapi (blue). *Merge* indicates the overlay of single images of each row and mock means uninfected control. Images were captured with a Nikon confocal microscope. The co-localization of HAdV-C5 pV and E2A is depicted the by 2D-histograms, which are correlating the pixel intensities of two channels, on the one side and the corresponding channel overlay of the analyzed regions of interest (ROI) on the other side, tM means thresholded Mander's split coefficient where the number indicates the channel, 1 corresponds to the red channel (pV) and 2 corresponds to the green channel (E2A). **D** Statistical summary of captured phenotypes in n = 4 independent experiments, the most abundant ones of experiment 1 (**E**) are shown in A-C. **E** Table of the differences in experimental conditions for individual experiments 1-4.

Furthermore, the sites of viral replication and the host nucleoli where pV accumulates are excluding each other. This leads to separate fractions of pV and E2A during wildtype infection, apart from the diffuse portion of pV (Fig. 33C, panel e) (Matthews & Russell, 1998a). This finding was confirmed in a co-localization study of panels e-f where the thresholded Mander's split coefficients resulted in  $tM1 = 0.24$  for the red channel (pV) and  $tM2 = 0.54$  for the green channel (E2A). This phenomenon was less pronounced in 42 % of pV-SCM mutant virus infected HepaRG cells ( $n = 12$ ) where some portion of pV accumulated in small dots at the periphery of the nucleus, close to the nuclear membrane (Fig. 33C, panel j). According to the intensity overlay of red and green channels in the nuclear area these spherical structures indeed co-localize with corresponding dots of E2A, leading to a grey signal (Fig. 33C, lower right panel). On the contrary, the green intensity corresponding to E2A clearly dominates the red signal in wildtype infected cell nuclei (Fig. 33C, upper right panel). In pV-SCM mutant virus infected cells, E2A signal-intensities co-localize with those of pV ( $tM2 = 0.85$ ) and a greater nuclear portion of pV correlates with E2A signals ( $tM1 = 0.48$ ) compared to wildtype infected cells ( $tM1 = 0.24$ ). To gain certainty, the analysis of a larger amount of infected cells would be necessary, though.

Another interesting observation was already made in HeLa and HepaRG cells, transiently transfected with flag-pV or its different SCM mutants. It was noticeable that pV4xKR accumulated less clearly within the nucleus than pV wt (Fig. 24 and Fig. 25). The same phenotype was now evident in HepaRG cells infected with the HAdV-C5 pV-SCM mutant virus (Fig. 33A-D). An average of four independent immunofluorescence analysis in which pV was stained yielded in 73 % of HAdV-C5 wt infected cells where pV clearly accumulates at host nucleoli. In contrast, this phenotype was only seen in 42 % of HepaRG cells infected with the pV-SCM mutant virus (Fig. 33D). This tendency of pV-SCM being more diffusely distributed in the host nucleus was seen in each individual experiment as well (see representatively Fig. 33A-C, panels f and j), although the experimental conditions differed slightly. In two of four analysis, the primary pV antibody was detected with a Cy3-conjugated secondary antibody and in the other two experiments with an Alexa488-conjugated secondary antibody. Moreover, the time point investigated varied between 24 and 32 h p.i. Two experiments were analyzed with a confocal and the other two with a wide field fluorescence microscope. Additionally, in one experiment, the cells were fixed with MeOH instead of PFA (Fig. 33E). Nevertheless, the result of these different experiments remained similar, underlining the previous findings from transient transfection experiments (Fig. 24 and Fig. 25). In conclusion, the lack of SCM within HAdV-C5 pV seems to reduce the affinity of the protein to accumulate at the host nucleoli.

In one experiment, HAdV-C5 pV was co-stained with nucleophosmin 1 (NPM1, B23.1) as already depicted in Figure 10D. In accordance with previous publications, showing the relocalization of NPM1 during adenoviral infection most likely as a consequence of present pV (Matthews, 2001; Ugai *et al.*, 2012; Walton *et al.*, 1989), the subcellular distribution of NPM1 was predominantly nucleolar in mock infected HepaRG cells (53-68 % of captured cells, n = 60 and n = 40). Upon infection with HAdV-C5, this distribution shifted to 50-60 % of captured cells (n = 16 and n = 10) showing a nucleolar and nucleoplasmic localization, whereas only in 20-25 % of the cells NPM1 was exclusively detected at the nucleoli. However, this distribution of NPM1 was completely the same in HepaRG cells infected with the HAdV-C5 pV-SCM mutant (n = 17 and n = 14). Consequently, the reduced affinity of pV, lacking its SCM, to localize at the nucleoli does not seem to be accompanied by an increased translocation of NPM1 to the nucleoplasm.

#### **4.4.4.3. Viral DNA-replication is significantly enhanced at early time points during HAdV-C5 pV-SCM mutant virus infection**

As a consequence of earlier viral protein expression during HAdV-C5 pV-SCM mutant virus infection compared to wildtype infection, it was already expected that the onset of viral DNA-replication might be accelerated as well. In order to pursue this idea, HepaRG cells were infected again either with the HAdV-C5 pV-SCM mutant or with the wildtype virus and harvested 1, 16, 24 and 48 h p.i. The genomic DNA of collected samples was isolated and purified to be analyzed by RT-PCR where the time point 1 h p.i. was supposed to define the baseline of infectious particles entering the cell and thereby the amount of incoming adenoviral DNA. At each time point, the HAdV-C5 DNA was determined relative to the one-copy gene  $\beta$ 2-microglobuline to avoid false differences due to varying DNA contents of the samples.

This approach indeed confirmed an accelerated viral DNA-replication during pV-SCM mutant virus infection (Fig. 34A), showing its greatest advantage 16 h p.i. (Fig. 34B) and therewith shortly after the onset of viral DNA-replication. As already observed in previous experiments (Fig. 31-32), this difference decreased with proceeding infection and equaled out two days after infection (Fig. 34). Interestingly, already 1 h p.i. more viral DNA was isolated from mutant virus infected HepaRG cells compared to those infected with HAdV-C5 wt in four independent experiments (Fig. 34). Since the cause of this dissimilarity between both viruses has not been clarified yet, later time points were not normalized to this early time point, prior to the onset of viral DNA-replication, as it was initially planned.

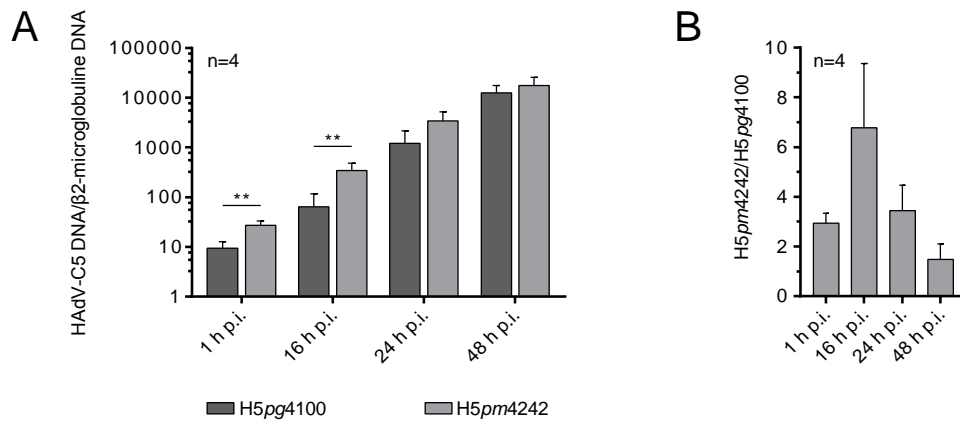


**Figure 34: Viral DNA-replication is significantly accelerated early after its onset during HAdV-C5 pV-SCM mutant virus infected compared to wildtype infected HepaRG cells.**

HepaRG cells were infected with HAdV-C5 wt (H5pg4100, moi 20) or pV-SCM mutant virus (H5pm4242, moi 20) and harvested 1, 16, 24 or 48 h p.i. Genomic DNA was isolated from the cells and amplified by RT-PCR with primer pairs specific for a HAdV-C5 hexon-cds fragment (#1441/1442) or specific for a fragment of the cellular single-copy gene  $\beta$ 2-microglobuline (#2775/2776). **A** HAdV-C5 DNA amounts are depicted relative to the amounts of the cellular single-copy gene as an average of  $n = 4$  independent experiments. Error bars indicate the standard deviation. RT-PCR was performed in technical duplicates for each experiment and statistics were calculated with a 2-tailed, unpaired t-test. P-value  $< 0.01$  means \*\*. **B** emphasizes the ratio of the pV-SCM mutant virus and HAdV-C5 wt (H5pm4242/H5pg4100) at each time point investigated.

HAdV-C5 DNA/  $\beta$ 2-microglobuline DNA means  $f(h p. i.) = \frac{E^{-Ct}(\text{viral DNA } (h p. i.))}{E_{\text{hexon primer pair}}^{-Ct}} / \frac{E^{-Ct}(\beta 2\text{-micro DNA } (h p. i.))}{E_{\beta 2\text{-micro primer pair}}^{-Ct}}$ , with  $E$  = efficiency of the corresponding primer pair.

#### 4.5. The role of HAdV-C5 pV in oncogenic transformation processes

Human adenoviruses have not been classified as tumor viruses to date, since there is no existing proof of their tumorigenicity in humans so far. Adenoviral genomes could be found in infiltrating lymphocytes of human sarcoma, which were interestingly predominantly of species C, a group of adenoviruses not being classified as tumorigenic (Kosulin *et al.*, 2013). Consequently, a contribution of HAdVs to the emergence of tumors in human beings cannot be excluded (see section 1.1.5). Furthermore, it has been known for decades that the presence of viral DNA fragments encoding the E1-region from various adenovirus species are sufficient to transform primary rodent cells in vitro (Endter & Dobner, 2004; Graham *et al.*, 1984; Graham, 1984). Since one of the greatest interests in adenovirus research is the generation of new vectors for gene therapy and the generation of oncolytic viruses, it is of essential importance for the safety of their usage to gain further knowledge on the contribution of the incoming adenoviral proteins to tumorigenicity as well.

#### 4.5.1. The presence of HAdV-C5 pV represses the transformation of primary BRK cells mediated by the E1A proteins and E1B-55K of HAdV-C5

In order to determine the oncogenic potential of the HAdV-C5 pV-cds transformation assays were performed in primary baby rat kidney (pBRK) cells. The cells were either transiently transfected with plasmids expressing HAdV-C5 E1A-gene products, E1B-55 K or pV. Alternatively, they were co-transfected with two of those plasmids to create all possible combinations. After several weeks of propagation, the cell cultures were fixed and stained with crystal violet to analyze the formed foci (Fig. 35A).

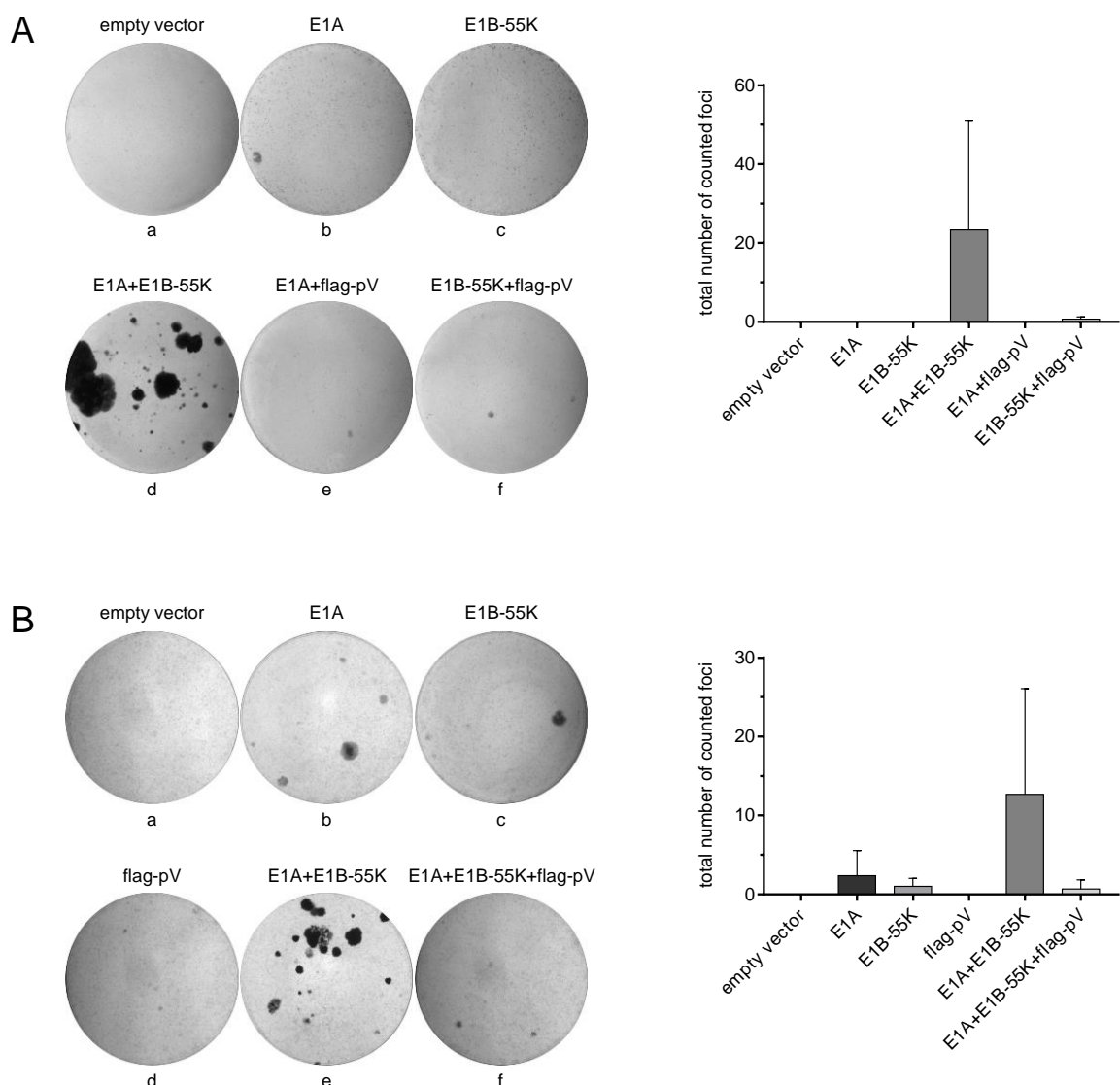


**Figure 35: HAdV-C5 pV inhibits the colony formation mediated by E1A-proteins and E1B-55K.**

Primary BRK cells were transfected with 2  $\mu$ g of a HAdV-C5 flag-pV expression plasmid (#2738), a plasmid expressing E1A proteins (#737), a plasmid expressing E1B-55K (#1319) or **A** co-transfected with combinations of two of these plasmids (2  $\mu$ g each) and **B** co-transfected with either E1-expressing plasmids or E1- and pV-expressing plasmids (2  $\mu$ g each). All DNA amounts were adjusted with corresponding empty vector plasmids, which were also co-transfected as a negative control (A-B). Both experiments were performed in triplicates. The

---

cells were propagated **A** eight weeks or **B** six weeks and fixed with a solution containing 25 % MeOH and 1 % crystal violet in H<sub>2</sub>O. Thereby grown foci of BRK cells were visualized to be counted subsequently. For both experiments, one example of the triplicates is shown on the *left*, while corresponding averages are indicated on the *right*. Error bars depict the standard deviation of replicates.

In contrast to the cells expressing a combination of E1A isoforms and E1B-55K (Fig. 35A, panel d), neither a combination of E1A proteins with pV (Fig. 35A, panel e) nor the expression of E1B-55K and pV (Fig. 35A, panel f) resulted in the formation of proliferating cell colonies. Hence, pV is not able to compensate the loss of E1A or E1B-55K functions in order to promote an immortalized or transformed cell phenotype.

Furthermore, HAdV-C5 pV is not capable to boost the cell transformation mediated by E1A gene products and E1B-55K as it was shown for the early proteins E4orf3 and E4orf6 (Nevels *et al.*, 1997, 1999a). In fact, exactly the opposite was observed in pBRK cells co-transfected with plasmids expressing E1A isoforms, E1B-55K or pV (Fig. 35B, panel f). In these cells, the focus formation was almost completely inhibited compared to cells expressing only E1-proteins (Fig. 35B, panel e). In regard of the previous findings (Fig. 35A), it was already expected that HAdV-C5 pV alone could not induce uncontrolled cell proliferation either (Fig. 35B, panel d).

This severe influence of HAdV-C5 pV on the E1-mediated oncogenic transformation of pBRK cells was unexpected. Therefore, an immunofluorescence analysis of the E1A proteins, E1B-55K and pV was performed in transiently transfected pBRK cells to confirm that all transfected plasmids initially express their corresponding gene products in those cells (Fig. 36). The experiment revealed that E1A isoforms (Fig. 36, panels h and r) as well as E1B-55K (Fig. 36, panels i and s) and pV (Fig. 36, panels o and t) were well-expressed 48 h p.t. Furthermore, the subcellular distribution of each protein was not influenced by the presence of the other proteins (Fig. 36, panels f-t) and the localization pattern of all three proteins is comparable to the one observed in transformed human epithelial cells (compare Fig. 10 and Fig. 33). Consequently, there is no lack of HAdV-C5 E1-oncoproteins, which would explain the strong repression of cell colony formation in the presence of pV.

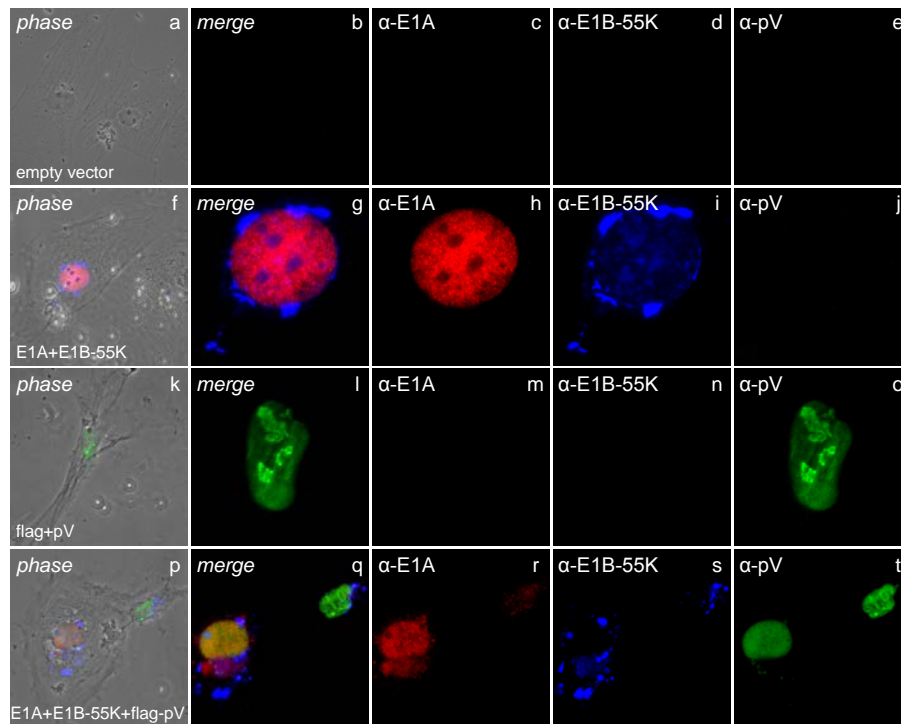


**Figure 36: The expression of HAdV-C5 E1A-proteins, E1B-55K and pV is not impaired in transiently transfected pBRK cells and their subcellular distribution is comparable to transformed human epithelial cells.**

Primary BRK cells were transfected with 2  $\mu$ g of a HAdV-C5 flag-pV expression plasmid (#2738) or co-transfected with either HAdV-C5 E1 expressing plasmids (#737 and #1319), E1 and pV expressing plasmids (#737, #1319 and #2738) or the corresponding empty vector controls (2  $\mu$ g each). These were further used to adjust all DNA amounts. The cells were fixed with PFA 48 h p.t. and triple stained with pab  $\alpha$ -pV, mab M73 ( $\alpha$ -E1A) and mab 4E8 ( $\alpha$ -E1B-55K). Primary antibodies were detected with Alexa488- (green), Cy3- (red) or Cy5- (blue) conjugated secondary antibodies. Nuclei and cytoplasmic areas are indicated by phase contrast images (phase). *Phase* and *merge* depict the overlay of single images in each row. Columns two to four show enlarged nuclei of the corresponding *phase* image. All images were captured with a Leica fluorescence wide field microscope.

#### 4.5.1.1. A cell line BRK-ABV derived by pBRK cells co-transfected with HAdV-C5 E1A, E1B-55K and pV expressing plasmids shows no sign of a classical E1-mediated transformation

To elucidate the mechanism of how pV is inhibiting the oncogenic transformation of pBRK cells by the E1-oncoproteins, stable cell lines were generated by transfecting pBRK cells with HAdV-C5 E1-region expressing plasmids (named BRK-AB) or E1-region expressing plasmids in combination with a plasmid expressing HAdV-C5 pV (named BRK-ABV). After cultivation of the transfected cells for eight weeks, the grown cell colonies were collected (Polyclonal) and propagated further. In case of pBRKs, initially transfected with E1-region and pV expressing plasmids, only two colonies could be found, though. These hardly grew and were difficult to get to confluency, matching the previous findings (Fig. 35). A comparison between the growth behavior of BRK-AB and BRK-ABV cells with two additional control cell lines AB120, which

are established BRK cells transformed by E1A and E1B proteins and H1299, which is an E1A, E1B-negative human tumor cell line, further underlined this observation (Fig. 37B). Although the fully transformed control cell lines AB120 and H1299 were still proliferating more rapidly than low passage BRK-AB cells, they showed a comparable growth behavior. In contrast, BRK-ABV cells hardly grew at all (Fig. 37B).

In order to take the different growth rates of BRK-AB and BRK-ABV into account, the morphology of both generated cell lines was compared at the same passage (p4). This comparison revealed a difference between BRK-ABV and BRK-AB cells in size and shape (Fig. 37A). BRK-ABV cells were bigger and more stretched than BRK-AB cells (Fig. 37A, panels a and c). They remind of the morphology of pBRK cells shortly after transfection, which are assumed to become senescent predominantly. BRK-AB cells on the other hand were smaller and kept their morphology in formed foci (Fig. 37A, panels b and d).

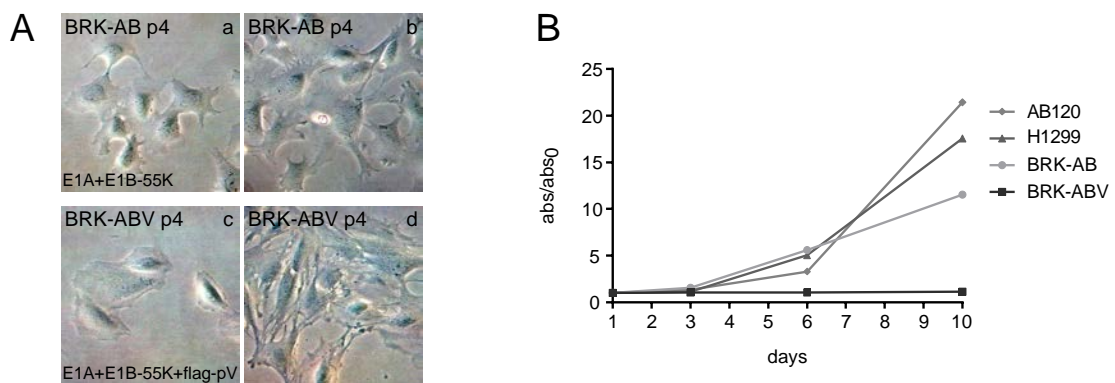


**Figure 37: The generated stable cell lines BRK-AB and BRK-ABV differ in morphology and growth rate.** Primary BRK cells were co-transfected with plasmids expressing HAdV-C5 E1A proteins (#737) or E1B-55K (#1319, 2  $\mu$ g each) to generate a stable cell line BRK-AB or co-transfected with the same E1 expression plasmids plus a HAdV-C5 flag-pV expression plasmid (#2738, 2  $\mu$ g each) to generate a stable cell line BRK-ABV. The DNA amounts were adjusted with corresponding empty vector plasmids and the cells were cultivated for eight weeks prior to collecting grown cell colonies (polyclonal) for further propagation. **A** The morphology of both cell lines was compared at passage four (p4). Images were captured with DFC 320 camera at a Leica DMIL light microscope. **B** The growth behavior of both generated cell lines was monitored by a MTT-assay over 10 days in comparison to fully transformed cell lines AB120 and H1299. The measured absorbance (abs) was normalized to day 1 after seeding the cells ( $abs_0$ ) for each cell line. The MTT-assay was performed in technical triplicates approximately three months p.t.

To characterize the generated cell lines further they were prepared for immunofluorescence analysis approximately three months p.t. The classical E1-region mediated transformation of rodent cells is denoted by retention of the E1-coding region and the expression of corresponding gene products as well (Flint *et al.*, 1976; Gallimore, 1974; Johansson *et al.*, 1977).

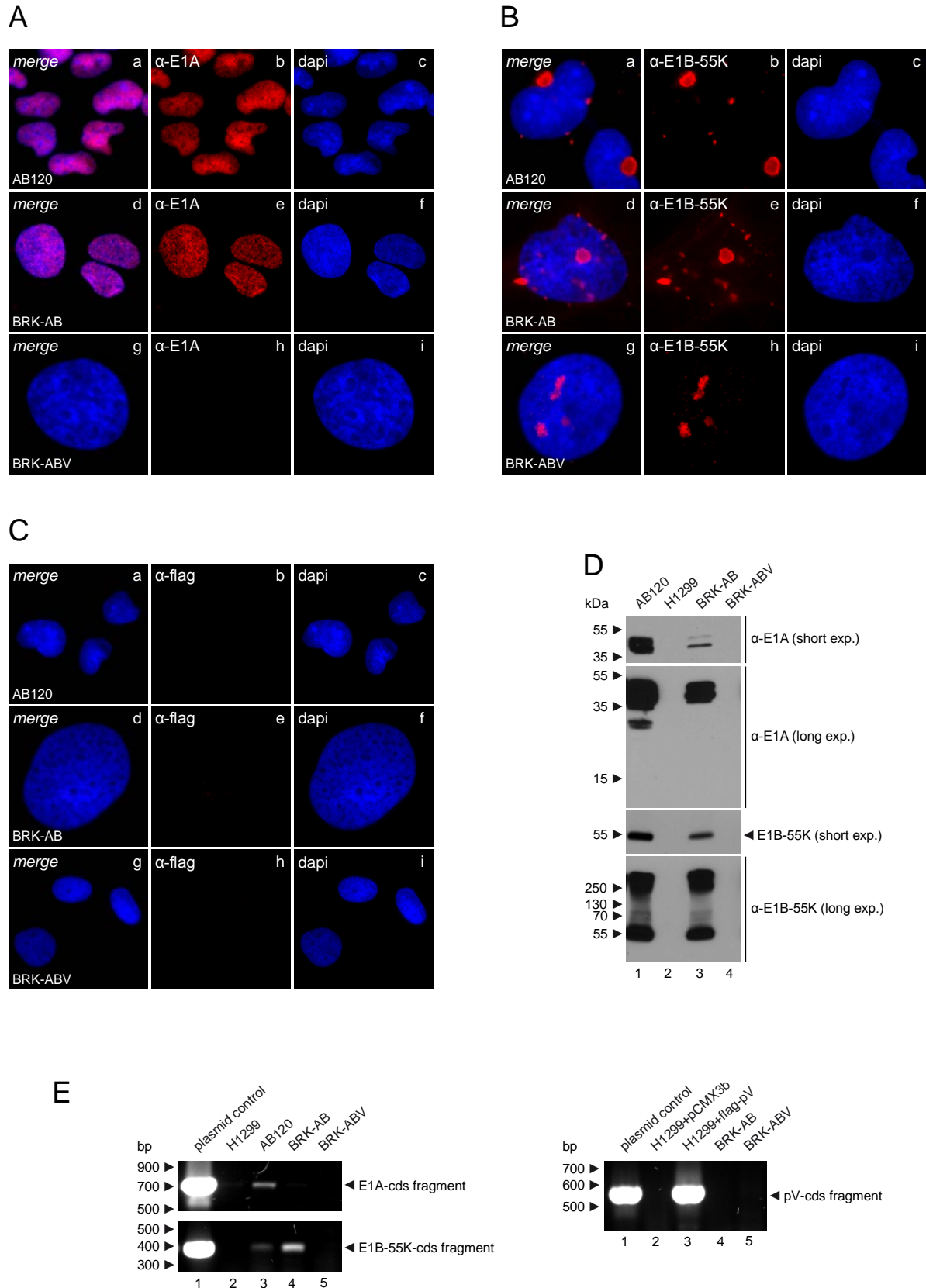


**Figure 38: The generated cell line BRK-ABV neither contains HA $\Delta$ V-C5 proteins E1A, E1B-55K and pV nor the corresponding viral DNA.**

**A-C** The cell lines AB120, BRK-AB and BRK-ABV were fixed with 4 % PFA 48 h after seeding and stained with **A** mab M73 ( $\alpha$ -E1A), **B** mab 4E8 ( $\alpha$ -E1B-55K) and **C** mab M2 ( $\alpha$ -flag). The primary antibodies were detected with a Cy3-conjugated (red) secondary antibody and nuclei were stained with dapi (blue). *Merge* indicates the overlay of single images in each row, which were captured with a Leica fluorescence wide field microscope.

**D-E** The cell lines AB120, H1299, BRK-AB and BRK-ABV were harvested 48 h after seeding. Total-cell lysates were split and one half **D** was resolved by 12 % SDS-PAGE. The contained proteins were visualized by immunoblotting (400mA, 90 min, nitrocellulose  $\varnothing = 0.45 \mu\text{m}$ ). Input levels of E1A (50  $\mu\text{g}$ ) were detected by using mab M73 ( $\alpha$ -E1A) and input levels of E1B-55K (50  $\mu\text{g}$ ) were detected by using mab 4E8 ( $\alpha$ -E1B-55K). Molecular weights in kDa are indicated on the *left*, while corresponding proteins are labelled on the *right*. Exp. means exposure. **E** Total-proteins (5  $\mu\text{g}$  each) of the remaining lysates were digested with proteinase K and subjected to PCR with primer pairs specific for a fragment within the HAdV-C5 E1A-cds (#330/332) or specific for a fragment within the HAdV-C5 E1B-55K-cds (#64/110). Moreover, the plasmids expressing E1A proteins (#737) or E1B-55K (#1319) were included. For the detection of HAdV-C5 pV DNA, 5  $\mu\text{g}$  of total-cell lysates derived from H1299 cells either transfected with 10  $\mu\text{g}$  of a flag-pV expression plasmid (#2738) or 10  $\mu\text{g}$  of its empty vector control pCMX3b-flag (#152) were digested with proteinase K in addition to the lysates of BRK-AB and BRK-ABV (5  $\mu\text{g}$  each). The samples and the corresponding plasmid control (#2738) were subjected to PCR with primer pairs specific for a fragment within the HAdV-C5 pV-cds (#811/3397). All reactions were resolved by agarose-gel (0.66%) electrophoreses where contained DNA was visualized with ethidium bromide by UV-exposure. Nucleic acid sizes in bp are indicated on the *left*, while corresponding DNA-fragments are labeled on the *right*.

In accordance with the literature the established control cell line AB120 as well as the generated cell line BRK-AB expressed both HAdV-C5 E1A proteins (Fig. 38A, panels a-f) and E1B-55K (Fig. 38B, panels a-f) in the expected subcellular distribution. BRK-ABV cells on the other hand were negative for E1A and E1B-55K proteins (Fig. 38A, panels g-i and 38B, panels g-i). The same results were obtained by immunoblotting of total-cell lysates derived from BRK-AB and BRK-ABV cells in comparison to total-cell lysates of the control cell lines AB120 and H1299 (Fig. 38D). These data further confirmed the expected sizes of the isoforms E1A-12S and -13S as well as the correct size of E1B-55K. All adenoviral oncoproteins were expressed in AB120 and BRK-AB cells (Fig. 38D, lanes 1 and 3), but not in H1299 or BRK-ABV cells (Fig. 38D, lanes 2 and 4), indicating that the generated cell line BRK-ABV has not been classically transformed by the adenoviral E1-oncoproteins.

In accordance with these observations, immunofluorescence of HAdV-C5 flag-pV could be detected neither in AB120, BRK-AB nor in BRK-ABV cells using a monoclonal  $\alpha$ -flag antibody (Fig. 38C, panels a-i). To exclude a loss of the flag-tag during propagation of pBRK cells, a PCR analysis should reveal the presence of viral DNA. Therefore, genomic DNA was isolated from BRK-AB and BRK-ABV cells as well as from AB120 and H1299 cells as positive and negative controls for E1A- and E1B-55K-cds, respectively. Additionally, genomic DNA derived from H1299 cells, transiently transfected with either the flag-pV expression plasmid or its empty vector control for 48 h, served as positive and negative controls for the presence of flag-pV DNA. The obtained DNA was subjected to PCR in comparison to the original plasmid DNA and the results confirmed the findings of the immunofluorescence analysis (Fig. 38A-C and 38E). Only the flag-pV positive controls (Fig. 38E, right panel, lanes 1 and 3) showed an amplified fragment of the pV-cds, whereas no trace was detectable in the BRK-AB or BRK-ABV cell lysates (Fig. 38E, right panel, lanes 4-5).

Fragments of the E1A- and E1B-55K-coding regions were amplified from DNA samples of H1299, AB120, BRK-AB and BRK-ABV cells (Fig. 38E, left panels). BRK-ABV cells, as well as the negative control H1299 cells, were negative for E1A- or E1B-cds DNA (Fig. 38E, left panels, lanes 2 and 5). However, the signals of E1A and E1B DNA-fragments amplified from cell line AB120 and BRK-AB samples were very weak as well (Fig. 38E, left panels, lanes 1 and 3-4). Hence, a possibility remains that the amount of pV-DNA is beneath the detection limit of the method.

In regard of the combined characterization results in Figures 37 and 38, it seems more likely however, that the stable cell line BRK-ABV is a result of spontaneous immortalization rather than being a consequence of the presence of E1A, E1B-55K and pV proteins. This further indicates the strong repression of pBRK cell transformation by E1-gene products in the presence of HAdV-C5 pV.

#### **4.5.2. Inclusion of the whole HAdV-C5 E1-region cannot prevent the inhibitory effect of pV on the focus formation of pBRK cells**

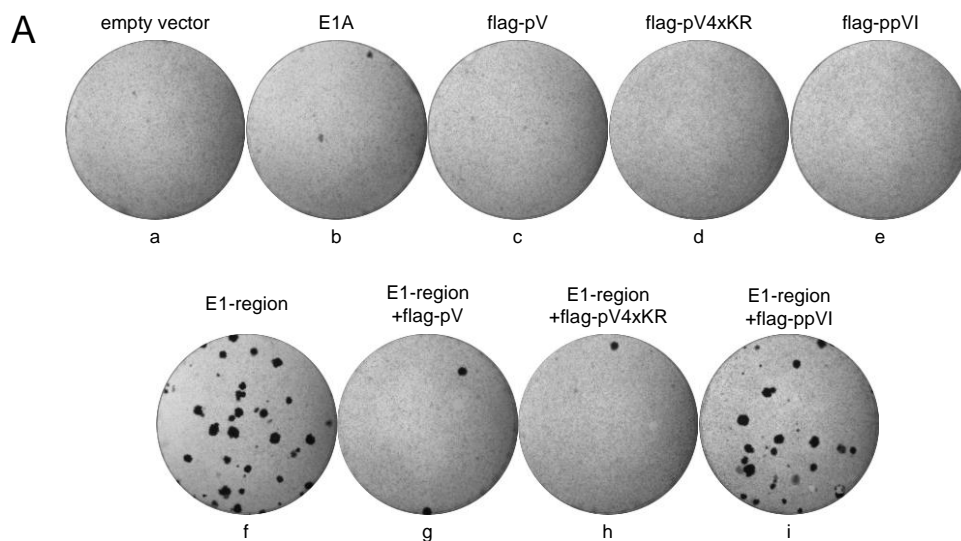
In the previous section, the whole E1A coding region of HAdV-C5 was used to immortalize pBRK cells, however, not in combination with the complete E1B-region. A combination with the E1B-55K-cds afforded the transfection of two plasmid-DNAs. Consequently, the additional expression of HAdV-C5 pV resulted in the transfection of three separate plasmids, leading to a statistical distribution of seven different types of co-transfected cells. This experimental set up led to large standard deviations within replicates, a low number of total grown colonies and long propagation times of the pBRK cells (Fig. 35). In order to optimize the experimental conditions, pBRK cells were subsequently transfected with a plasmid encoding the whole HAdV-C5 E1-region in combination with pV expression plasmids or the corresponding empty vector controls. Moreover, less toxic calcium phosphate was chosen as transfection reagent. This approach offers several advantages. In contrast to the separate expression plasmids, both E1A and E1B proteins are expressed under control of their viral promoters. Furthermore, always both factors needed to promote the transformation of rodent cells are present in a single transfected pBRK cell and since the whole E1B-region is expressed, the additional anti-apoptotic factor E1B-19K is present, whose function is independent of E1B-55K (see section 1.1.3.2).

#### 4.5.2.1. Colony formation of pBRK cells is not inhibited due to SCM within HAdV-C5 pV

To elucidate, whether the SUMOylation status of HAdV-C5 pV might be important for the inhibition of the E1-region-mediated transformation, the pV-SCM mutant (flag-pV4xKR) was included in the following transformation assay (Fig. 39). The results prove that the use of only one plasmid encoding the whole E1-region of HAdV-C5 improved the efficiency of the transformation assay considerably. The number of grown colonies increased, propagation time of the pBRK cells decreased and most importantly, reproducibility increased, which is indicated by smaller standard deviations between independent experiments (Fig. 39B).

In this experimental set up, the observed phenotype is even more pronounced than before (Fig. 35). On average, around forty foci were formed of pBRK cells in the presence of the E1 expression plasmid (Fig. 39A, panel f and 39B). In contrast, less than five colonies could be found in the presence of flag-pV again (Fig. 39A, panel g and 39B). Accordingly, the presence of E1B-19K could not prevent the inhibition of colony formation by HAdV-C5 pV. The same holds true in the presence of the pV-SCM mutant (Fig. 39A, panel h and 39B), which means, that the lack of SCM within pV and therefore the SUMO modification at these sites does not regulate this phenotype either.

The possibility remains however, that the observed loss of foci formation is a consequence of an unbalanced DNA-uptake of the pBRK cells, due to the co-transfection of different sized DNA-plasmids.



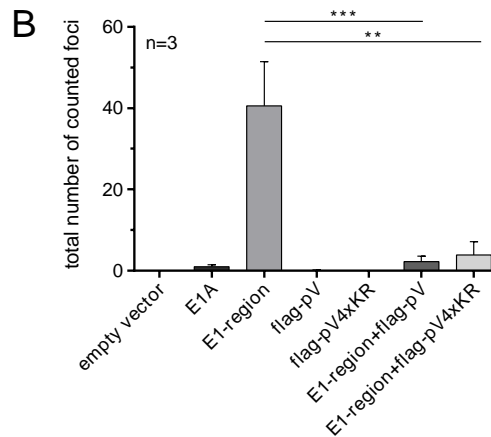


**Figure 39: The inhibition of pBRK focus formation mediated by E1-oncoproteins is not dependent on SCM within HAdV-C5 pV.**

Primary BRK cells were transfected with 2  $\mu$ g of a HAdV-C5 E1-region expressing plasmid (#608), a plasmid expressing only E1A-proteins (#737), a flag-pV expression plasmid (#2738) or its SCM mutant (#2969) and co-transfected with #608 and #2738, #608 and #2969 or the empty vector controls respectively. All DNA amounts were adjusted with corresponding empty vector plasmids and the experiments were performed in triplicates. The cells were propagated four weeks and fixed with a solution containing 25 % MeOH and 1 % crystal violet in H<sub>2</sub>O. Thereby grown foci of BRK are visualized to be assessed subsequently. **A** One experimental replicate is shown representatively. The shown experiment included additionally a flag-ppVI expression plasmid (#2739). **B** The average of three independent experiments, each performed in triplicates, is depicted with error bars indicating the standard deviation. The statistics were calculated with a 2-tailed, unpaired t-test for each comparison. P-value < 0.05 means \*, p < 0.01 means \*\*, p < 0.001 means \*\*\*.

Therefore, another expression plasmid was included in one of the transformation assays as a transfection control (Fig. 39A, panels e and i). It is the same vector-backbone (pCMX3b-flag) as for HAdV-C5 pV, however, containing the coding sequence of HAdV-C5 capsid protein VI in its unprocessed form (ppVI). The results clearly reveal that the inhibition of colony formation by E1 oncoproteins is specific for HAdV-C5 pV, since the co-expression of ppVI with E1 gene products did not alter this capacity.

#### 4.5.2.2. The focus formation of pBRK cells induced by HAdV-C5 E1-gene products depends on the concentration of present pV

In another approach, the relation between co-transfected plasmid DNAs should be investigated to reveal, whether the phenotype of the previous experiment (Fig. 39) is dependent on the dose of HAdV-C5 pV. Therefore, the concentration of the E1-region expressing plasmid was held constant, whereas the amount of the flag-pV expression plasmid was reduced 10-fold from sample to sample. If both plasmids were transfected in equal amounts, the transformation assay result was similar to the previously described phenotype (Fig. 40, panel e and 40B). A decreasing portion of HAdV-C5 pV led to an increase in pBRK focus formation, though. A 10-fold excess of the E1-expressing plasmid is hardly counteracting the pV influence (Fig. 40A,

panel f and 40B), whereas a 1000-fold excess resulted in a number of grown colonies comparable to the pBRK cells only transfected with the E1 expressing plasmid (Fig. 40A, panels d and h and 40B). Hence, the HAdV-C5 pV-mediated inhibition of pBRK cell transformation by the E1-oncogenes is dose-dependent.

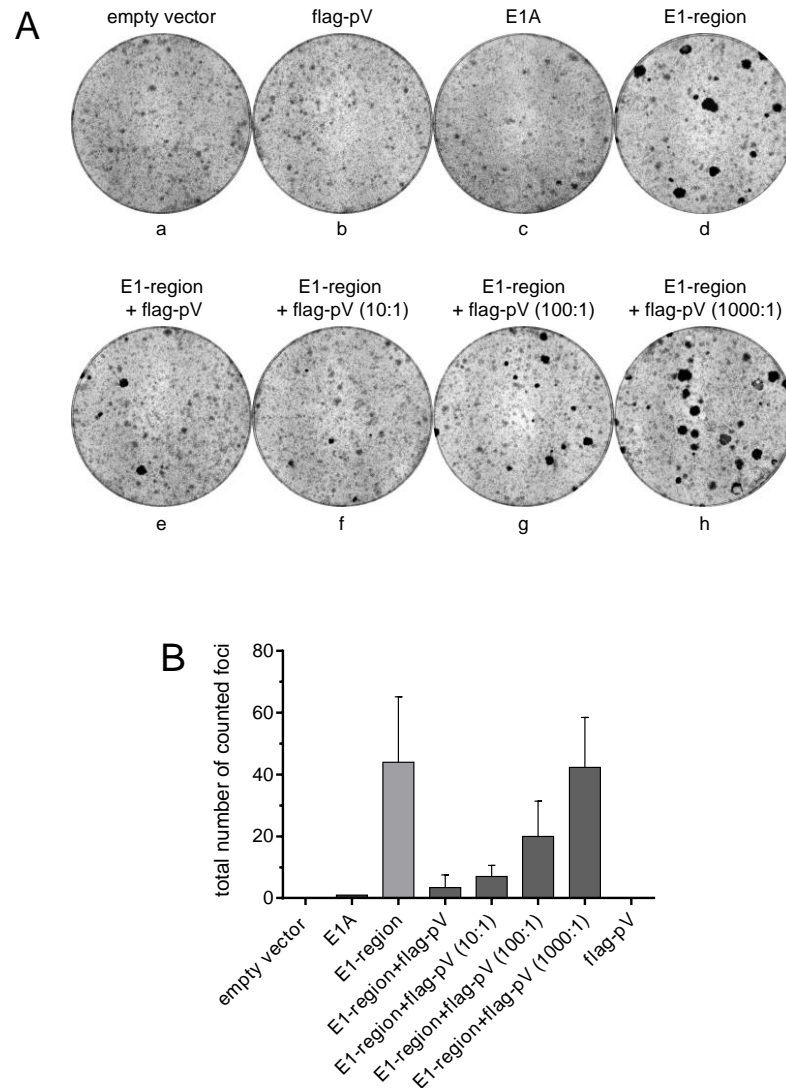


**Figure 40: The HAdV-C5 pV-mediated inhibition of pBRK cell transformation by the E1-oncogenes is dose-dependent.**

Primary BRK cells were transfected with 2  $\mu$ g of a HAdV-C5 E1-region expressing plasmid (#608), a plasmid expressing only E1A-proteins (#737), a flag-pV expression plasmid (#2738) or co-transfected with #608 and #2738 with a 10-fold decreasing dose of #2738 in each sample or the empty vector controls. These were further used to adjust all DNA amounts. The experiments were performed in triplicates. The cells were propagated four weeks and fixed with a solution containing 25 % MeOH and 1 % crystal violet in H<sub>2</sub>O. Thereby grown foci of BRK are visualized to be assessed subsequently. **A** One example of each triplicate is shown representatively. **B** The average of replicates is depicted with error bars indicating the standard deviation.

#### 4.5.2.3. The flag-tag fused to HAdV-C5 pV is not responsible for its inhibitory effect on pBRK cell transformation in the presence of adenoviral E1-oncogenes

All the HAdV-C5 pV encoding plasmids used in previous transformation assays express a N-terminally flag-tagged pV (compare Fig. 9). In order to exclude that the observed inhibitory effect of pV on pBRK cell transformation actually depends on its flag-tag, other pV encoding plasmids expressing either a N-terminal HA-tag or no tag at all are included in further transformation assays.

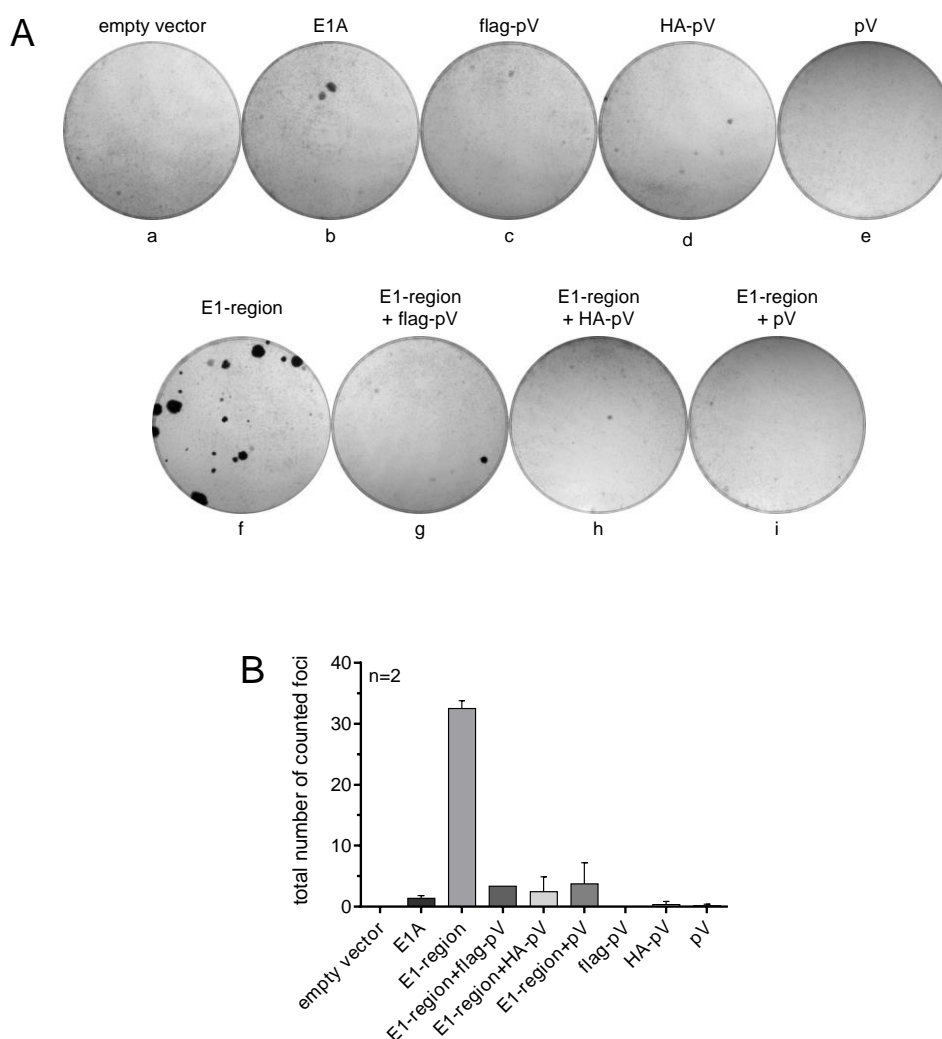


**Figure 41: The oncogenic transformation of pBRK cells by HAdV-C5 E1A and E1B proteins is efficiently prevented by pV in a tag-independent manner.**

Primary BRK cells were transfected with 2  $\mu$ g of a HAdV-C5 E1-region expressing plasmid (#608), a plasmid expressing only E1A-proteins (#737), plasmids expressing different tags (HA-(#2635), flag- (#2738)) or no tag (#2970) at the N-terminus of HAdV-C5 pV or co-transfected with #608 and one of the different pV proteins. All DNA amounts were adjusted with the corresponding empty vector plasmids. Two independent experiments were performed in triplicates, where the pBRK cells were propagated four weeks and fixed afterwards with a solution containing 25 % MeOH and 1 % crystal violet in H<sub>2</sub>O. Thereby grown foci of BRK are visualized to be assessed subsequently. **A** One experimental replicate is shown representatively. **B** The average of two independent experiments, each performed in triplicates, is depicted with error bars indicating the standard deviation.

The results of two independent experiments convincingly reveal that the tag does not influence the observed phenotype, though (Fig. 41). Oncogenic transformation of pBRK cells by E1A and E1B proteins (Fig. 41A, panel f and 41B) is efficiently prevented, no matter which pV protein is present (Fig. 41A, panels g-i and 41B).

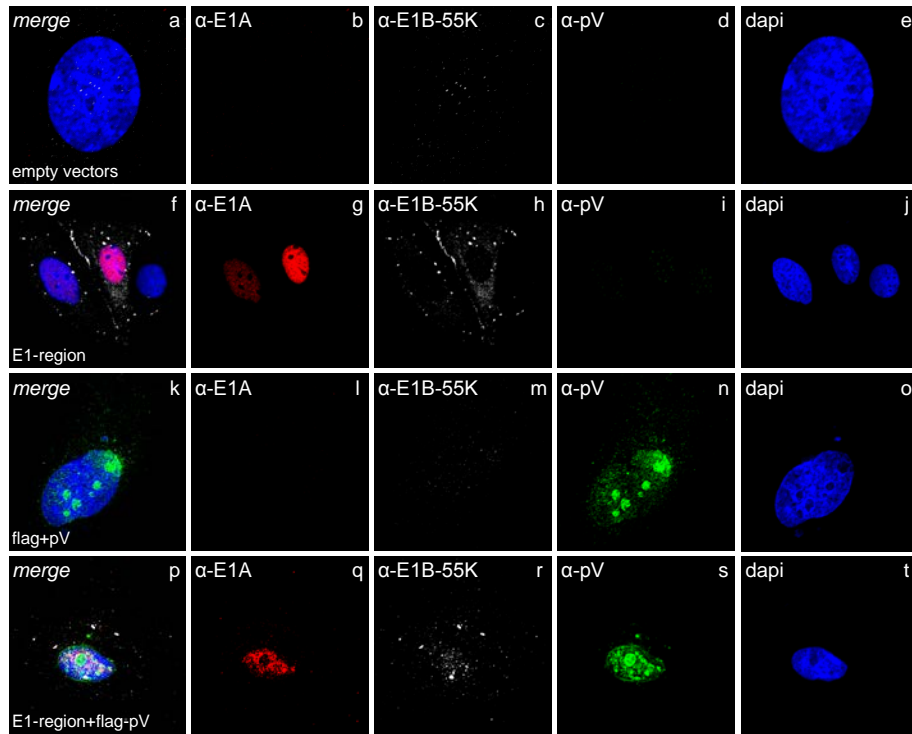
#### **4.5.3. The number of pBRK cells positive for the HAdV-C5 proteins E1A, E1B-55K and pV remains low during the first 10 d p.t.**

How is HAdV-C5 pV inhibiting the induction of colony formation by the adenoviral oncoproteins E1A and E1B, which is usually occurring during the first two weeks after transfection of the cells? To shed light on this question, a time course experiment was performed where pBRK cells were transfected with E1-region expressing plasmids, flag-pV expression plasmids or co-transfected with both plasmids in equal amounts, as it was done in the transformation assays before (Fig. 39-41). The cells were fixed 2, 4, 7 or 10 d p.t. and were subsequently prepared for immunofluorescence analysis together (Fig. 42). Two days after transfection the protein expression was comparable to the first experimental set up, in which three individual plasmids were co-transfected (compare Fig. 36 and Fig. 42A). Primary BRK cells transfected only with an E1-region expression plasmid showed the expected distribution of E1A proteins and E1B-55K. E1A is diffusely distributed throughout the whole nucleus only sparing the nucleoli and E1B-55K can be observed in small cytoplasmic dots. In some cells, also a faint and diffuse nuclear staining is visible, whereas no signal was distinguishable from background with an  $\alpha$ -pV antibody (Fig. 42A, panels f-j). The opposite was seen in cells transfected only with a flag-pV expression plasmid (Fig. 42A, panels k-o). Flag-pV accumulates in the nucleoli of pBRK cells and shows a faint diffuse portion in the nucleoplasm as well. Sometimes certain accumulations can be even detected in the cytoplasm as it was already seen in previous experiments, where the cells had been fixed with methanol (compare Fig. 10B and Fig. 24-25). Furthermore, a distinct pV-portion seems to accumulate at the nuclear membrane (Fig. 42B, panel n). In only few of the co-transfected pBRK cells, all products of transfected genes could be detected where they show the same distribution as in the absence of the other proteins (Fig. 42A, panels p-t).

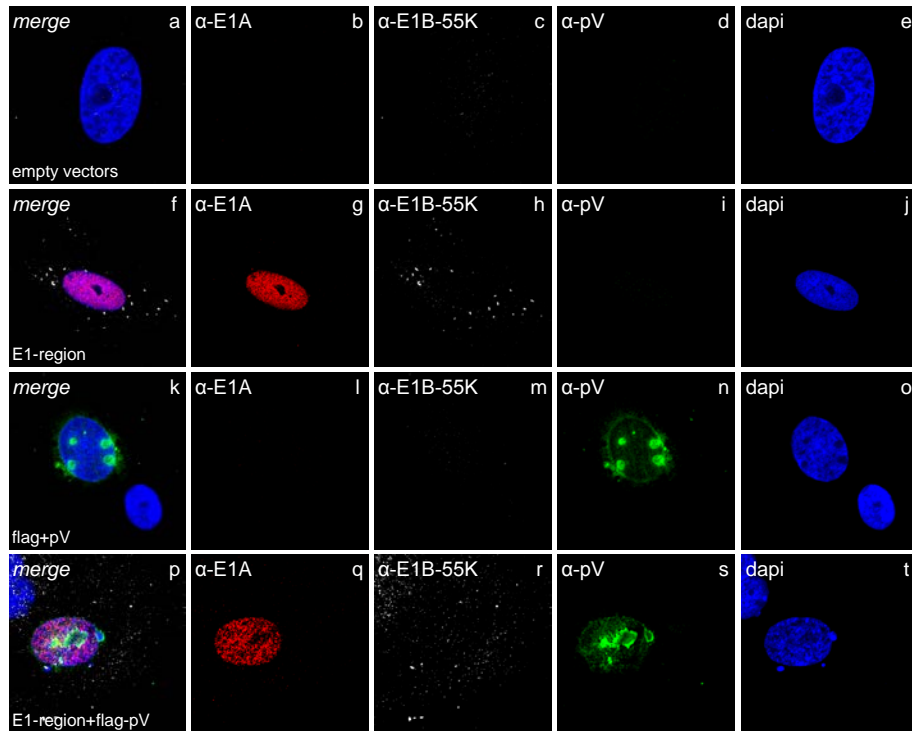
A quantification of total fluorescent cells revealed that more cells express flag-pV (green) than E1A (red) or that E1A is not always expressed in sufficient amounts to be detected (Fig. 42E, upper left panel). The same is true for E1B-55K expression (white), which has not been quantified separately, since it is transcribed from the same plasmid as E1A proteins. In case of

co-transfected pBRK cells, much more cells emitted only green fluorescence as well.

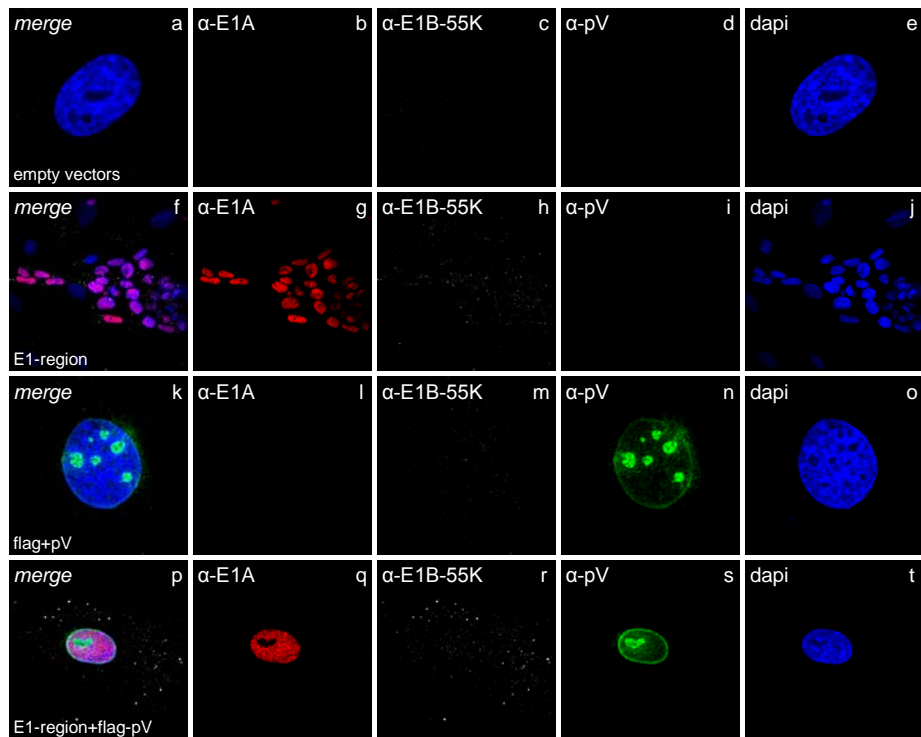
A 2 d p.t.



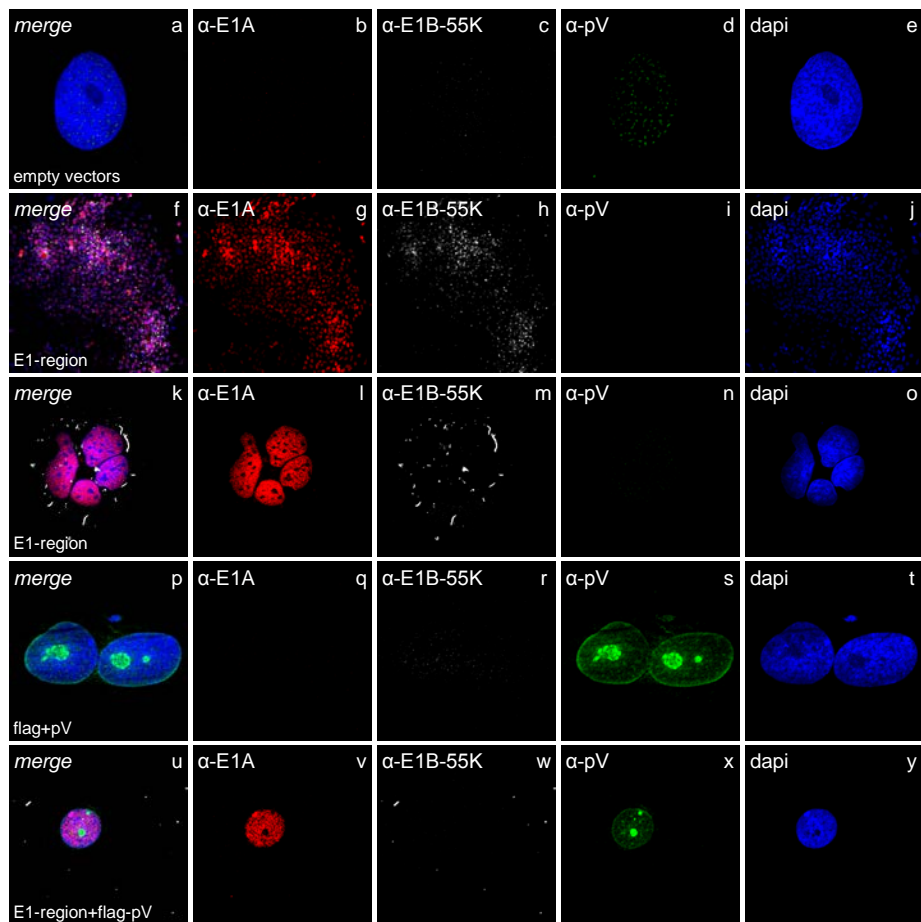
B 4 d p.t.



## C 7 d p.t.



## D 10 d p.t.



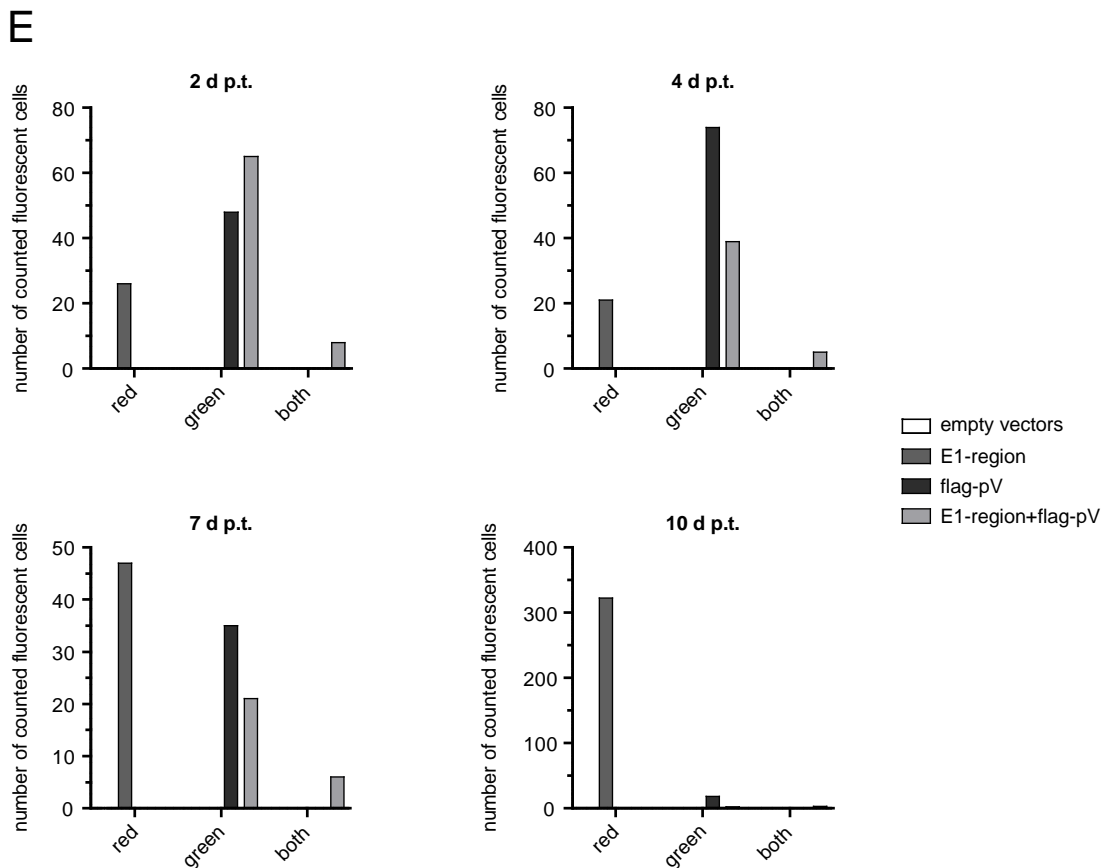


**Figure 42: The amount of pBRK cells expressing HAdV-C5 E1-proteins and pV is remarkably low during the first 10 d p.t.**

**A-D** Primary BRK cells were transfected with 2  $\mu$ g of a HAdV-C5 E1-region expression plasmid (#608), a HAdV-C5 flag-pV expression plasmid (#2738) or co-transfected with both plasmids and the corresponding empty vector controls (2  $\mu$ g each). These were further used to adjust all DNA amounts. The cells were fixed with MeOH 2, 4, 7 or 10 d p.t. and stored at -20°C until they were triple stained together with pab  $\alpha$ -pV, mab M73 ( $\alpha$ -E1A) and mab 4E8 ( $\alpha$ -E1B-55K). Primary antibodies were detected with Alexa488- (green), Cy3- (red) or Cy5- (white) conjugated secondary antibodies, while nuclei were stained with dapi (blue). *Merge* depicts the overlay of single images in each row. All images were captured with a Nikon confocal fluorescence microscope. **E** Quantification of fluorescent cells in the depicted experiment (A-D) at each time point and each combination of transfected plasmids investigated. E1-region expressing plasmids are quantified by the appearance of red-fluorescence. In case of the co-transfected samples (E1-region+flag-pV) only the amount of cells emitting red and green fluorescence (both) and the amount of cells emitting only green fluorescence (green) were determined, not the amount of cells emitting only red fluorescence (red), which appeared rarely.

All in all, the number of fluorescent and therewith the number of efficiently transfected pBRK cells was remarkably low ( $n = 26$  for pBRKs transfected with E1-expressing plasmids,  $n = 48$  for pBRKs transfected with flag-pV expressing plasmids and  $n = 73$  for co-transfected pBRKs of which 65 appear green and only 8 were positive for both colors). 200 000 cells were seeded in one well of a six-well plate containing coverslips (18x18 mm), which were used for the immunofluorescence analysis. Consequently, these coverslips were covered with approximately 67 000 pBRK cells and the transfection efficiencies can be expressed as 0.004 % ( $n = 26$ ), 0.072 % ( $n = 48$ ) and 0.109 % ( $n = 73$ ) of which 89 % are only positive for pV in the latter case. In regard of the average number of approximately 40 grown pBRK cell colonies per

transformation assay, this low transfection efficiency was already expected, although it exacerbates a statistical interpretation of this protein-time course analysis.

Nonetheless, the remaining time points were assessed and revealed an interesting tendency. 4 d p.t. the picture has not changed much in comparison to 2 d p.t. (Fig. 42B). The subcellular distribution of all the stained proteins (E1A, E1B-55K and flag-pV) has not changed. The same holds true for the number observed fluorescent cells (Fig. 42E, upper right panel). 21 pBRK cells were positive for E1A proteins (red), whereas the number of cells expressing flag-pV (green) slightly increased ( $n = 74$ ). Again only five of the co-transfected pBRK cells were positive for both proteins, while 39 were only emitting green fluorescence. Hence, they are presumably only positive for flag-pV.

7 d p.t. the amount of E1-expressing pBRK cells (red) already doubled ( $n = 47$ ; Fig. 42E, lower left panel). This reflected the observation of first grown cell colonies, which were still small, but showed a homogeneous expression of E1A proteins and E1B-55K (Fig. 42C, panels f-j). In contrast, the number of flag-pV positive cells (green) decreased, regardless of whether the corresponding plasmid was transfected alone ( $n = 35$ ) or together with the E1-region expression plasmid ( $n = 21$ ; Fig. 42E, lower left panel). Moreover, most of the green cells appeared individually or in smaller groups of not more than five cells in close proximity, but they were never detected as homogenous colonies (Fig. 42C, panels k-o). The latter was similar for the co-transfected pBRK cells. Those, expressing all stained proteins were always captured individually (Fig. 42C, panels p-t). Furthermore, no increase in their number could be observed ( $n = 6$ ; Fig. 42E, lower left panel).

The last time point underlined this tendency. 10 d p.t. a notable number of small colonies had started to grow in pBRK cells transfected with an E1-region expressing plasmid and some bigger ones could be already captured as well (Fig. 42D, panels f-o). The amount of red-emitting cells was estimated greater than 300 on that coverslip (Fig. 42E, lower right panel). This amount of proliferating cells exceeded the amount of single remaining green cells, which express flag-pV ( $n = 18$ ) by far (Fig. 42D, panels p-t and 42E, lower right panel). On the coverslip carrying the co-transfected pBRK cells only three cells expressing all stained proteins remained. Additionally, only two cells were still positive for flag-pV (green) alone (Fig. 42D, panels u-y and 42E, lower right panel).

Taken together, this experiment plausibly reflected the foci development of pBRK cells expressing the E1-proteins of HAdV-C5. Flag-pV might be expressed in higher amounts than the E1-oncogenes initially. It cannot promote the proliferation of transfected rat cells though,

which leads to the decline of pV-positive cells over time. Most interestingly, the co-transfection of E1-region expressing plasmids and flag-pV expression plasmids results in a much higher number of cells, which seem to be only positive for pV, whereas the amount of cells expressing both, E1-proteins and pV, is remarkably low. Moreover, these double positive cells remain low during the first two weeks after transfection. This observation perfectly matches the lack of pBRK cell colonies in transformation assays as soon as HAdV-C5 pV is present.

#### **4.5.4. The number of human tumor cells HEK293 and HeLa is drastically reduced after transient transfection with a flag-pV expression plasmid**

To evaluate whether this interesting phenotype detected in primary rat cells is transferrable to the human system, a comparative assay was designed for transformed human cells as well. The observed phenotype described in sections 4.5.1-4.5.3 was restricted to pBRK cells expressing HAdV-C5 E1-gene products in combination with pV. Therefore, the cell line HEK293, which has been derived from human embryonic kidney (HEK) cells stably expressing HAdV-C5 E1A and E1B oncoproteins (Graham *et al.*, 1977), was chosen as well as HeLa cells, a human cervix carcinoma cell line (Ehrmann & Gey, 1953; Gey, 1958), which is stably expressing the proteins E6 and E7 of HPV-18. Both of these proteins share functional similarities with the adenoviral E1A and E1B proteins (Davies & Vousden, 1992; Phelps *et al.*, 1988; Sato *et al.*, 1989; Scheffner *et al.*, 1994; Steinwaerder *et al.*, 2001). The two cell lines were co-transfected with a vector plasmid containing a puromycin selection marker (pBabePuro) and a flag-pV expression plasmid, its empty vector control or an EGFP expressing plasmid (Fig. 43). This procedure allows for a subsequent selection of transiently transfected cells, since the flag-vector plasmid does not contain any required sequence for drug selection. Due to the rapid proliferation of both chosen cell lines, the selection of transfected cells is required, though.

Puromycin selection was started 3 d p.t. and the remaining cells were fixed and stained with a crystal violet-solution 10 d p.t. At this time, the control cells, which were not co-transfected with the pBabePuro plasmid, had died (Fig. 43A-B, panels a-c). In the presence of flag-pV, remaining colonies of both HEK293 (Fig. 43A, panel e) and HeLa cells (Fig. 43B, panel e) were remarkably reduced in comparison to the empty vector control (Fig. 43A-B, panel d). In contrast, the presence of EGFP only led to a slight decrease of surviving cell colonies (Fig. 43A-B, panel f). Hence, the reduction of cell survival seems to be specific for the presence of HAdV-C5 pV. Strikingly, these results resembled the previous findings in pBRK cells (sections 4.5.1-4.5.3).

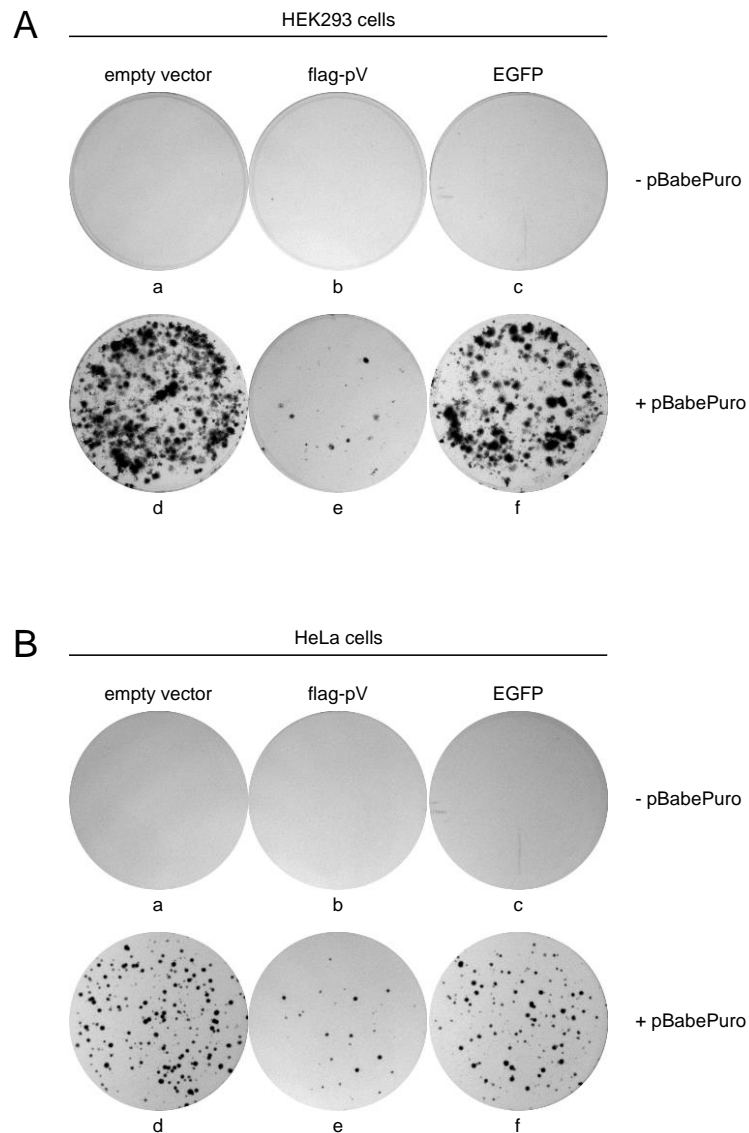


**Figure 43: The number of human tumor cells HEK293 and HeLa is drastically reduced after transient transfection with a flag-pV expression plasmid, followed by drug selection.**

Human **A** HEK293 or **B** HeLa cells were transfected with 2  $\mu\text{g}$  of a flag-pV expression plasmid (#2738), its empty vector control pCMX3b-flag (#152) or an EGFP-expressing vector plasmid (#146) and co-transfected with one of those plasmids in combination with pBabePuro (#96), a vector plasmid with a puromycin selection marker. All DNA amounts were adjusted with corresponding empty vector plasmids and the experiments were performed in triplicates. The puromycin selection was started 2 d p.t. and the cells were propagated ten days in total, prior to their fixation with a solution, containing 25 % MeOH and 1 % crystal violet in  $\text{H}_2\text{O}$ . Thereby grown colonies of puromycin-resistant cells are visualized. One experimental replicate is shown representatively for experiments A and B, which were reproduced two times.

## 5 Discussion

---

### 5.1. The lack of consensus SUMO conjugation motifs within HAdV-C5 pV accelerates viral replication

Post-translational modifications of proteins are an enormously important tool of cells to extend their functional repertoire and to regulate it strictly. During the last decade, an increasing research interest in this topic could be registered, since it offers a huge variety of new regulatory mechanisms, which contribute to a better understanding of the complex cell biology. PTMs can occur on the amino acid side chain or at the termini of a protein (Voet *et al.*, 2006; Walsh, 2006). Whereby, sites that carry a nucleophilic, functional group are the main targets of post-translational modification. Those can be the hydroxyl groups of serine, threonine and tyrosine; the side chain amines of lysine, arginine and histidine; the thiolate anion of cysteine or the carboxylate of aspartate and glutamate, for instance (Walsh, 2006). The most common PTM is phosphorylation, which adds a phosphate group to either serine, tyrosine or threonine residues (Bingham & Farrell, 1977; Krebs & Beavo, 1979; Langan, 1970; Matthews & Huebner, 1984). This modification is often involved in the regulation of enzyme activities (Khoury *et al.*, 2011). Moreover, many eukaryotic proteins are modified with carbohydrate molecules, a process called glycosylation (Parodi & Leloir, 1979; Schachter, 1974), which can promote protein folding, improve protein stability as well as it can serve regulatory functions. Attachment of lipid molecules, known as lipidation (prenylation, N-myristoylation, S-palmitoylation, GPI (glycosylphosphatidylinositol)-anchors; Hentschel *et al.*, 2016; Nadolski & Linder, 2007; Schmidt, 1983), often targets proteins, which are attached to the cell membrane. Of course, the interplay of viruses with infected host cells is influenced by such PTMs as well concerning both viral and cellular proteins. In this regard, the SUMOylation of proteins has emerged as one key post-translational modification. SUMO proteins, which belong to the family of ubiquitin-like modifiers (UBLs), can be covalently bound to target proteins or non-covalently interact with SIM motifs of other proteins to affect their function (see section 1.2.1.1). The SUMOylation machinery is widely exploited by DNA as well as RNA viruses, whose proteins can either modify and/or be modified by the SUMOylation system (Everett *et al.*, 2013). For instance, there is growing evidence that SUMOylation regulates several cellular proteins involved in intrinsic and innate immunity (Hannoun *et al.*, 2016, Mattoscio *et al.*, 2013).

In case of HAdV-C5 pV, the lack of consensus SUMO conjugation motifs (SCM) resulted in a global acceleration of viral replication, which was visible on transcriptional level, on protein level, during viral DNA-replication as well as in release of viral progeny (section 4.4). This acceleration of the HAdV-C5 pV-SCM mutant replication cycle was more pronounced in the ‘pseudo-primary’ cell line HepaRG than in fully transformed H1299 cells. That, in turn could be a consequence of their slower propagation, accompanied by a slower proceeding of the adenoviral life cycle (compare sections 4.4.1-4.4.4).

Contradictory at first view, the overall SUMOylation pattern of pV was faint 24 h after HAdV-C5 wildtype infection, indicating that the modification might not play a crucial role during adenoviral infection. On the other hand, it might be even actively counteracted by the virus (Fig. 17). The latter would be a very interesting phenotype, since it could match the emerging hypothesis of a SUMOylation dependent regulation of proteins involved in intrinsic and innate immunity (Hannoun *et al.*, 2016; Mattosco *et al.*, 2013). However, 6His-SUMO2 HeLa cells, transiently transfected with pV and superinfected with HAdV-C5, showed no decrease in pV-SUMOylation compared to 6His-SUMO2 HeLa cells only transfected with pV (Fig. 18). Hence, the weak pV-SUMOylation during HAdV-C5 infection might rather be a result of less protein available than in transiently transfected or superinfected 6His-SUMO2 HeLa cells. Moreover, the SUMOylation pattern of pV could depend on and vary with the adenoviral life cycle. There could be a rapid deSUMOylation of pV during HAdV-C5 infection, resulting in low equilibrium concentrations of the SUMOylated protein. In regard of its weak signal intensity, it is challenging though to narrow down these different possibilities.

Mutation of the three SCM within HAdV-C5 pV allowed further insight. It caused a loss of distinct SUMO signals and an overall intensity reduction of the remaining ones (Fig. 22, 23 and 27). This significant reduction of pV-SUMOylation during pV-SCM mutant virus infection could be partially caused by lower amounts of the protein compared to HAdV-C5 wt infection (sections 4.4.1-4.4.4). However, this does not seem to be the predominant reason, since the loss of signal intensity is not even. It is more pronounced for certain SUMO signals, as it was already the case in transfection experiments with HAdV-C5 pV-SCM mutants (Fig. 22-23).

Taken together, the lack of SCM within pV indeed reduces the SUMOylation of the protein during transient transfection studies as well as in HAdV-C5 infection. Hence, the loss of certain SUMO signals could be the actual cause of the observed pV-SCM mutant viral life cycle acceleration. To clarify, whether this observed phenotype rather depends on the lack of specific SCM than on the combined loss of SCM within HAdV-C5 pV, mutant viruses would have to

be generated, which contain single SCM-mutations within the pV-cds, as the plasmids in section 4.3.2.

Several hints have been revealed by phenotypic analysis of the pV-SCM mutant virus (section 4.4). Interestingly, already the equilibrium concentrations of early viral proteins were elevated during infection with the HAdV-C5 pV-SCM mutant (Fig. 29 and 31). Newly translated pV, lacking its SCM, cannot be the cause of this phenotype though, since it is only expressed in the late phase of adenoviral infection (section 1.1.2). Thus, incoming modified pV seems to influence early viral protein levels. In accordance with this hypothesis, also adenoviral mRNA concentrations are already influenced at a time point where viral transcription has just started and only incoming virion proteins of HAdV-C5 can be present (Fig. 32). Especially, in case of E1A-mRNA this is striking, as it is known to be the first adenoviral protein expressed.

In reporter gene assays where HAdV-C5 pV or its SCM mutant was transiently transfected, no SUMO-dependent influence on the activity of adenoviral promoters could be observed (Fig. 30). Nevertheless, the possibility remains that another viral factor is needed to mediate an enhanced transcription of adenoviral promoters. Whether viral transcription is influenced directly or whether the viral mRNAs might rather be stabilized post-transcriptionally, remains to be clarified in future experiments. So far, pV has not been identified as RNA-binding protein (RBP). Also the alignment of its primary structure with known RNA-recognition motifs (RRM), zinc fingers or the KH-domain (Stefl *et al.*, 2005; Valverde *et al.*, 2008) did not point to the opposite, since no matches could be identified ([https://blast.ncbi.nlm.nih.gov/Blast.cgi?PROGRAM=blastp&PAGE\\_TYPE=BlastSearch&LINK\\_LOC=blasthome](https://blast.ncbi.nlm.nih.gov/Blast.cgi?PROGRAM=blastp&PAGE_TYPE=BlastSearch&LINK_LOC=blasthome)). Still, pV could act on RNA in a complex with other cellular or even viral RBPs.

Another explanation for the accelerated pV-SCM mutant virus phenotype would be a benefit in the immediate early phase of infection; meaning viral entry and nuclear uptake of the viral core (see section 1.1.3.1). This possibility is supported by the monitoring of viral DNA-replication where already 1 h p.i. more viral DNA could be detected in pV-SCM mutant virus infected cells (Fig. 34). This DNA can only reflect the amount of incoming particles. It was supposed to be used for normalization of later time points, since both viruses were applied with the same moi. The used viral stocks were titered by fluorescent staining of infected cells in which viral replication occurs. Consequently, only infectious particles are compared with this method and the viral stocks are not purified further. In this experimental approach however, defective particles, which might enter the cells and contain viral DNA, but are not able to replicate later on, would have been captured as well at this early time point after infection. These particles

could not enhance later adenoviral DNA-replication, but the levels of incoming viral DNA. In this case, the acceleration of pV-SCM mutant virus replication would rather depend on another origin than a more efficient entry of the virus.

In order to gain more insight into this complex situation, it would be beneficial to purify the infectious particles further before they are used in comparative experiments. Moreover, a synchronization of the human cells to be infected could be of advantage. In future experiments, the tracking of both HAdV-C5 genomes, wildtype and pV-SCM mutant, with life-cell imaging might be the method of choice to obtain comparative viral entry kinetics. Another possibility would be the use of azide-alkyne ‘click’ cycloadditions to label the viral DNA. In this experimental approach, the virus is propagated in the presence of an alkyne-modified nucleoside, such as EdC, which can be ‘clicked’ in following experiments to a fluorophore or another signaling molecule carrying an azide group. Thereby viral DNA can be labelled directly, highly chemoselective and with high sensitivity, which allows the tracking of incoming viral genomes through newly infected host cells. This experimental set up, however, does not enable the use of life-cell imaging (Wang et al., 2013).

### **5.1.1. Mutational alteration of the pV primary structure could result in conformational changes within the protein, which might further influence its function and HAdV-C5 virion integrity**

If the HAdV-C5 pV-SCM mutant virus really enters permissive host cells more efficient, it could be related to a structural change within the virion, which might be even independent of pV-SUMOylation. Immunoblotting of proteins originating from three different infected cell lines elucidated that pV, lacking its SCM, occurs in lower steady state concentrations than wildtype pV (Fig. 27, 29 and 31). Since pV-mRNA expression is accelerated during pV-SCM mutant virus infection, as all adenoviral mRNAs investigated (Fig. 32), the protein is likely to be affected directly. Among the reasons for lower pV levels could be a lower protein stability, relocalization of pV-SCM to insoluble fractions such as the nuclear matrix or even degradation of the protein. The latter possibility does not seem likely though, since the pV concentration was still increasing over time (Fig. 29 and 31).

SUMO-conjugation to a protein is linked to an increase of the proteins stability, because competitive ubiquitination is prevented at the corresponding lysine residue and polyubiquitination represents a signal for proteasomal degradation (Desterro *et al.*, 1998). A decrease of pV-stability could be conceivable, upon lack of certain SUMO conjugation sites.

However, not because of increasing ubiquitination, as the corresponding lysine residues were substituted by arginine in the pV-SCM mutant virus. In fact, this amino acid substitution itself, at four individual positions of protein V, could affect the protein conformation and thereby its stability, function or both.

To minimize the probability of such an unwanted side effect, specifically arginine was chosen as a substitute for lysine, since it retains the local as well as the net charge of the altered protein (Fig. 20). In addition, the impact of these point mutations within the primary structure of HAdV-C5 pV on structural elements of the protein was evaluated by *I-TASSER* (Iterative Threading ASSEmbly Refinement) (Roy *et al.*, 2010; Yang *et al.*, 2015; Yang & Zhang, 2015; Zhang, 2008). Since there was no change in any secondary structure element and the accuracy of tertiary structure predictions was weak (Fig. 21), the probability of structural changes within pV was assessed low. Nevertheless, they cannot be excluded.

In this regard it is important to notice that HAdV-C5 pV has been predicted to be a protein of low structural order by different algorithms *APSSP 2* (Advanced Protein Secondary Structure Prediction Server) (Raghava, 2002), *PSIPRED V3.3* (Pérez-Vargas *et al.*, 2014) and *I-TASSER*. Intrinsically disordered proteins (IDPs) often contain a combination of disordered regions (IDRs) and structured domains (van der Lee *et al.*, 2014), as it was predicted for HAdV-C5 pV (Fig. 21). The high degree of disorder results in a large flexibility of the proteins and allows for a dynamic switch between conformational changes. This makes IDPs available for the interaction with a variety of different target molecules, such as DNA, other proteins, complexes or PTMs. Upon binding to different targets many IDPs form well-defined structures, which depend to a high degree on the binding partner (Berlow *et al.*, 2015; Wright & Dyson, 2015). The binding of HAdV-C5 pV to DNA in solution, for instance, was shown to be sequence independent, but mainly dependent on the soluble N-terminus of the protein (aa 1-200) (Chatterjee *et al.*, 1986a; Pérez-Vargas *et al.*, 2014). Inside adenoviral virions, however, fewer regions of pV contact the viral genome, indicating that the other DNA-binding regions are masked sterically or through interactions with other viral proteins. This results in a complex of higher order, which is destabilized during capsid disassembly (Pérez-Vargas *et al.*, 2014).

In general, a complex containing IDPs is often highly dynamic and short lived. This facilitates a rapid exchange of binding sites between multiple interacting partners. Partner recognition often occurs through short linear sequence motifs, such as the conserved LxCxE motif within adenoviral E1A, E7 of HPV or the T antigen of SV40 (Berlow *et al.*, 2015; Chellappan *et al.*, 1992; Van Roey *et al.*, 2014). Due to their variability, intrinsically disordered proteins play

important roles in many cellular, regulatory processes. Since viruses only dispose of few different proteins, intrinsic disorder offers a great opportunity to manifold their protein functions. Furthermore, multiple sites of PTM are often located in disordered regions of IDPs where they can act synergistically (Berlow *et al.*, 2015; Radivojac *et al.*, 2007).

The accumulation of certain PTMs can alter the charge distribution within a protein and consequently its conformational state. This can further influence the interaction with other proteins, also within protein complexes, or favor and disfavor molecular recognition processes, respectively (Berlow *et al.*, 2015; Das & Pappu, 2013; Mitrea *et al.*, 2014). Hence, it is almost impossible to exclude that a specific protein-protein, protein-RNA or protein-DNA interaction is not influenced by the alteration of the primary sequence of intrinsically disordered HAdV-C5 pV. The mutation of consensus SUMO conjugation motifs could lead to dynamic conformational changes, which are unpredictable. These can either be a direct result of the loss of protein SUMOylation or completely independent of this modification.

The high similarity between the tertiary structure of RHDV's capsid protein VP1 and the predicted tertiary structure of HAdV-C5 pV4xKR (Fig. 21C) further underlines a putative conformational flexibility of pV. Although the capsid organization of adenoviruses is different from caliciviruses, which are built of quasiequivalent conformations of VP1 proteins, the correlation between VP1 and pV4xKR is very interesting. A conformational flexibility of pV could allow different orientations of pV inside the adenoviral particles, when it comes to the nucleosome-like organization of the adenoviral core or the bridging with the surrounding capsid via interaction with capsid protein VI (Anderson *et al.*, 1989; Brown *et al.*, 1975; Chatterjee *et al.*, 1985, 1986a; Everitt *et al.*, 1975; Matthews & Russell, 1998a; van Oostrum & Burnett, 1985; Vayda *et al.*, 1983).

In recent studies, pV is even speculated to form a ternary complex with pVI and pVIII underneath the vertex region of mature capsids, which is still a subject of debate, though (Condezo *et al.*, 2015; Liu *et al.*, 2010; Reddy & Nemerow, 2014a). As already mentioned, the contribution of IDPs to protein complexes can depend on their state of PTM and/or protein conformation. For instance, it could be shown that SUMO1 modification of PML is essential for maintaining the 3D-structure of PML-NBs (Muller *et al.*, 1998; Muller & Dejean, 1999; Sternsdorf *et al.*, 1997; Zhong *et al.*, 2000a). Consequently, the lack of SCM within HAdV-C5 pV and/or the resulting prevention of the SUMO modification of certain pV sites could interfere with the formation of specific protein complexes during the course of adenoviral infection.

Taken together, HAdV-C5 pV, lacking its SCM, could change its behavior within mature

adenoviral particles and thereby pV could affect their stability. A pre-weakening of adenoviral virions might facilitate viral uptake and disassembly, which starts already at the cell surface (Burckhardt *et al.*, 2011; Suomalainen *et al.*, 2013).

If the presence of less protein V should be the cause of reduced pV-signals after immunoblotting of pV-SCM mutant virus infected cells (Fig. 27, 29 and 31), also a lack of pV incorporation into new infectious particles would be imaginable. In this regard, it would be very interesting to investigate, whether SUMOylated proteins might be incorporated into new infectious particles during virion assembly and whether SUMOylated adenoviral proteins can be still detected in mature virions. Only few studies investigating post-translational modifications within viral particles have been published so far. A very early one was done in the eighties to reveal the presence of phosphorylated, adenoviral proteins. Indeed, phosphorylated protein IIIa could be found in mature particles, whereas pV-phosphorylation disappeared during virion maturation (Weber & Khittoo, 1983). Other PTMs of adenoviral proteins within viral particles, however, have never been reported. Very recently, it could be shown that the major core protein VII is acetylated at specific sites, however, solely in cell extracts and not within purified viruses (Avgousti *et al.*, 2016).

Conclusively, the possibility remains that a change of pV-SUMOylation already influences the stability within adenoviral virions and facilitates their uptake into host cells.

### **5.1.2. Post-translational modification of HAdV-C5 pV might not be restricted to SUMOylation**

In section 4.3, we reported the extensive modification of HAdV-C5 pV with SUMO2 chains (Fig. 16-18) and the possibility of a SUMO1 conjugation to the protein *in vitro* (Fig. 19). However, only two bands of the pV-SUMO2 pattern could be precisely assigned to a certain SCM within pV. This SCM is K162 and therewith only one of 26 lysine residues within the whole protein. K7 seems to be important for a variety of the other pV-SUMO2 signals, although its loss can obviously be compensated by K23 or K24 (Fig. 23C). Interestingly, even the lack of all three SCM within HAdV-C5 pV does not result in a non-SUMOylated protein (Fig. 22B and Fig. 23B), indicating that other lysine residues rescue the loss of certain SCM or that they function as nSCM and so far unknown SUMOylation sites, respectively. Most certainly, these results point to the fact that HAdV-C5 pV is modified with SUMO proteins at different lysine residues, which do not always have to be part of a consensus SUMO conjugation motif. These findings indicate that pV might be a highly regulated protein.

In this regard, other post-translational modifications come into mind. Phosphorylation of pV has been first reported in 1983 (Weber & Khittoo, 1983), as already mentioned in the previous section (5.1.1). The role of this modification during productive infection with HAdV-C5, however, has never been addressed further. Moreover, there is a variety of molecules, such as acetyl groups or methyl (alkyl) groups (Allfrey *et al.*, 1964; Comb *et al.*, 1966; Gershey *et al.*, 1969; Lipmann, 1946; Perry *et al.*, 1969; Polgar, 1964) and other proteins like ubiquitin (Ciechanover *et al.*, 1980; Hershko, 1983; Hershko *et al.*, 1980, 1984, Hershko & Ciechanover, 1982, 1986; Hershko & Heller, 1985; Suresh *et al.*, 2016), Nedd8 (Enchev *et al.*, 2015; Parry & Estelle, 2004) or ISG15 (Staub, 2004; Zhang & Zhang, 2011), which can be reversibly attached to the  $\epsilon$ -amino group of lysine residues, likewise SUMO proteins. Recently, it could be shown that lysine residues can be even modified by inorganic polyphosphate, a process referred to as polyphosphorylation (Azevedo *et al.*, 2015).

An extended *in silico* analysis of HAdV-C5 pV (Fig. 44) confirmed that the 26 lysine residues within the protein offer lots of possibilities to modify pV, apart from SUMOylation. Next to putative sites of acetylation, which were predicted at 22 of the lysine residues (Li *et al.*, 2012, 2014; Shao *et al.*, 2012; Wang *et al.*, 2012), few sites of methylation were found as well, although with much lower probability (Shao *et al.*, 2009; Wang *et al.*, 2011). Therefore, it is questionable, whether methylation of pV is indeed occurring. However, ubiquitination could be a competing modification to SUMOylation at lysine 7, 24 and 42 of which two have been substituted by arginine in the HAdV-C5 pV-SCM mutant virus (Fig. 20). Moreover, lysine residues 158, 124, 3 and 188 have been proposed as putative sites of ubiquitination with probabilities  $> 0.65$  (Xiang Chen *et al.*, 2013).

Additionally, the cross talk between different PTMs is possible. SUMOylation can be dependent on adjacent phosphorylation (Hietakangas *et al.*, 2006). In turn, it was demonstrated that protein tyrosine phosphorylation was positively correlated with SUMOylation (Yao *et al.*, 2011). This cross-talk between phosphorylation and SUMOylation was also identified to regulate the functions of another adenoviral protein, E1B-55K (Wimmer *et al.*, 2013). Moreover, phosphorylation of a protein can also be a signal for subsequent poly-ubiquitination to induce proteasomal degradation of the target (Swaney *et al.*, 2013) to mention only few possibilities how PTMs can influence each other. By use of different algorithms, more than 30 putative sites of phosphorylation were identified within the primary sequence of HAdV-C5 pV (Blom *et al.*, 1999; Dinkel *et al.*, 2016). For convenience, only those predicted with high confidence in proximity to potentially modified lysine residues are depicted in Figure 44.

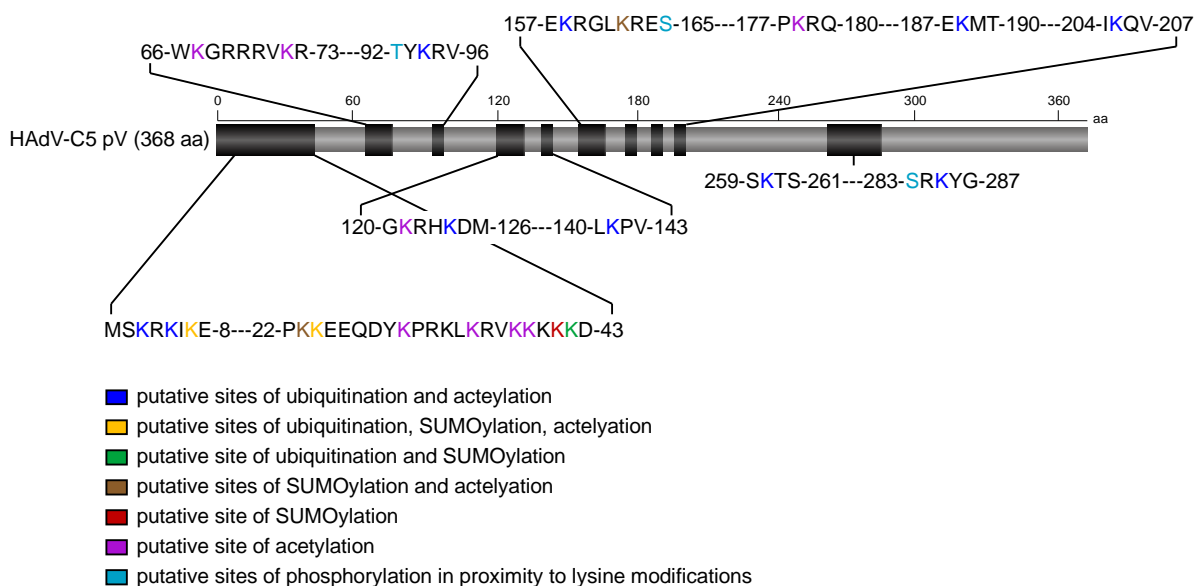


**Figure 44: *In silico* analysis of HAdV-C5 pV reveals multiple putative modifications of lysine residues.**

*In silico* analysis of HAdV-C5 pV to determine all possible post-translational modifications at its lysine residues K. Different algorithms were used: *SUMOPlot*<sup>TM</sup> (<http://www.abgent.com/sumoplot>), *GPS-SUMO* (Ren *et al.*, 2009; Zhao *et al.*, 2014), *Jassa* (Beauclair *et al.*, 2015), *iUbiq-Lys* (Qiu *et al.*, 2015), *UbiProber* (Xiang Chen *et al.*, 2013), *iMethyl-PseAAC* (Wang *et al.*, 2011), *BPB-PPMS* (Shao *et al.*, 2009), *ASEB* (Li *et al.*, 2012, 2014; Wang *et al.*, 2012), *BRABS-PHKA* (Shao *et al.*, 2012), *NetPhos 2.0* (Blom *et al.*, 1999), *Scanprosite* (<http://prosite.expasy.org/cgi-bin/prosite/ScanView.cgi?scanfile=716334427602.scan.gz>) and *The Eukaryotic Linear Motif (ELM) resource* (Dinkel *et al.*, 2016). Putative combinations of modifications are depicted in different colors. The probability of certain residues to be modified is highly depend on the algorithm used. Only results are depicted that score > 0.6 in one or more search algorithms.

Another form of PTM is the cleavage of peptide bonds, as in processing a propeptide to its mature form (Walsh, 2006). The same holds true for the deconjugation of UBL modifiers from target proteins. This process depends on the activity of specific cysteine-proteases, the ULPs (Müller *et al.*, 2001). Consequently, in the presence of cysteine-protease inhibitors, HAdV-C5 pV shows slower migrating bands or a slower migrating smear after immunoblotting (Fig. 15). Interestingly however, even a faster migrating portion was found (Fig. 15B), which could indicate an unknown, C-terminally shortened isoform of HAdV-5 pV, because of proteolytic cleavage. This band was occurring after immunoblotting of HAdV-C2 infected HeLa cells in earlier work of Russell and Matthews as well. Interestingly, it could not be detected in purified HAdV-C2 virus particles (Matthews & Russell, 1998a). However, it could be a sign of protein degradation as well. In a more recent work of Pérez-Vargas and co-workers the faster migrating portion of pV was interpreted as a product of proteolytic degradation, since the protein shows two consistent features of high proteolysis rates, the interconversion between monomer and dimer as well as the presence of intrinsically disordered regions (Pérez-Vargas *et al.*, 2014).

Obviously, HAdV-C5 pV has a high potential to be modified with various functional groups and/or proteins during the adenoviral life cycle in eukaryotic cells, indicating a tight regulation

of the protein by either the virus, the host or both. Hence, the accelerated replication of the pV--SCM mutant virus cannot be clearly assigned to the loss of specific SUMO moieties, since other modifications at these sites could be affected as well. Moreover, an influence of conformational changes cannot be excluded (compare section 5.1.1). Nonetheless, a modification of pV with SUMO proteins during productive HAdV-C5 infection has been convincingly shown in this work (sections 4.3-4.4).

## **5.2. HAdV-C5 pV associates with nucleoli of the infected host**

The hypothesis of HAdV-C5 pV being a strictly regulated protein fits the finding that pV is necessary for viral progeny production. A HAdV-C5 mutant virus, depleted of pV, could only be rescued through acquirement of three additional point mutations in the coding region of protein  $\mu$ . Otherwise, the production of infectious progeny failed (Ugai *et al.*, 2007).

Interestingly, also the knockdown of the cellular factor nucleophosmin 1 (B23.1, NPM1) strongly restricts viral progeny production in primary human pulmonary endothelial cells (HPAEC) (Ugai *et al.*, 2012) as well as in tumor derived HeLa cells (Samad *et al.*, 2012) (section 1.1.4.1). NPM1 is a nucleolar phosphoprotein, which is only modestly expressed in human primary cells (Nozawa *et al.*, 1996). On the contrary, it is overexpressed in various types of human tumors (Grisendi *et al.*, 2006) where it is localized in the nucleoli as well as in the nucleoplasm (Subong *et al.*, 1999) (section 1.2.2.1).

In an early work of Matthews and Russell it was shown that HAdV-C2 pV associates with host nucleoli as well, besides its diffuse distribution throughout the nucleoplasm (Matthews, 2001; Matthews & Russell, 1998a). This subcellular localization could be confirmed in this work for HAdV-C5 pV (Fig. 10). Later on, it was revealed that transiently transfected pV-EGFP is able to translocate NPM1 as well as another nucleolar protein, nucleolin (C23), to the cytoplasm of HeLa cells (Matthews, 2001). In this regard, pV was shown to interact with NPM1 through its N-terminus (aa 1-78) and its C-terminus (aa 314-369) (Samad *et al.*, 2012), which seem to mediate the translocation of B23 and C23 cooperatively (Matthews, 2001). The balance between cellular B23.1 and adenoviral pV was shown to be crucial for efficient viral particle assembly, since loss of either B23.1 or pV (Samad *et al.*, 2012; Ugai *et al.*, 2012) as well as overexpression of pV (Freudenberger, 2012) strongly suppressed infectious particle formation. This phenotype could be rescued in every case by transient expression of the missing protein.

Interestingly, viral DNA-replication and late gene expression are not significantly influenced (Samad *et al.*, 2012; Ugai *et al.*, 2012). Likewise adenoviral pV, B23.1 is able to bind DNA, which leads to an association of the viral genome with B23.1 in a sequence unspecific manner (Samad *et al.*, 2007, 2012). Moreover, B23.1 was shown to restrict the access of adenoviral core proteins VII and V as well as cellular histone 3 (H3) to the viral chromatin. Hence, it is assumed to function as a chaperone during assembly of the adenoviral core to mediate proper viral chromatin formation for an efficient encapsidation into new viral particles (Samad *et al.*, 2007, 2012).

The mutation of SCM within the coding sequence of HAdV-C5 pV led to a decrease of the overall protein signal after immunoblotting (Fig. 27, 29 and 31) as well as in immunofluorescence analysis of infected cells, compared to cells infected with HAdV-C5 wildtype. However, not only the amounts of detected pV differed between viral infections. Protein V, lacking its SCM, seems to have a reduced affinity to accumulate at host nucleoli (Fig. 33). This behavior was already observed during transient transfection experiments in HeLa (Fig. 24) as well as in HepaRG cells (Fig. 25). Thus, it seems to occur independent of the tumor cell line used. The transfection experiments further revealed that the mutation of single SCM within HAdV-C5 pV does not have a significant impact on the localization of the protein in both cell lines. Only if all three SCM are altered, pV accumulations are significantly less pronounced.

However, the accumulation of wildtype pV at host nucleoli is remarkably increased, if SUMO2 proteins are stably overexpressed in HeLa cells (Fig. 24B and D). Since a greater portion of pV is expected to be SUMOylated in cells overexpressing SUMO proteins, this could indicate that the SUMO modified pool of pV is the one directed to nucleoli. This is a very interesting thought, since the SUMO proteases SENP3 and SENP5 are known to be located at nucleoli as well (Di Bacco *et al.*, 2006; Gong & Yeh, 2006; Mukhopadhyay & Dasso, 2007). Both proteases show enzymatic activity against SUMO2- and SUMO3-modified substrates, such as HAdV-C5 pV (see section 1.2.1.1) and their combined knockdown results in a nucleolar accumulation of SUMO2/3, which both are usually found in the nucleoplasm (Yun *et al.*, 2008).

Interestingly, a knock-down of B23 resulted in the same phenotype, as it is accompanied by the loss of SENP3 and SENP5, presumably through proteasomal degradation (Yun *et al.*, 2008). Mammalian cells lacking B23 show defects in ribosome biogenesis (Itahana *et al.*, 2003). Yun *et al.* speculate that B23 might regulate the SUMOylation of factors involved in ribosome biogenesis through SENP3 and SENP5. They further hypothesize that the control of

SUMOylation through SENP3 and SENP5 might be a unifying mechanism, which could explain the huge variety of B23 functions (Yun *et al.*, 2008).

To take the same line, it is imaginable that the perturbation of adenoviral assembly in the absence of B23.1 is actually caused by the accompanied loss of SENP3 and/or SENP5. These proteases might usually deSUMOylate pV, which is located at nucleoli in order to activate a function critical for proper capsid assembly.

### **5.2.1. HAdV-C5 pV might interact with PML containing structures like PML-NBs or centrosomes**

Most certainly, there are different pV-fractions existing in the host nucleus. Next to its well-documented localization at host nucleoli, there is also a large pV-portion distributed over the whole nucleoplasm and furthermore we detected a partial co-localization of HAdV-C5pV with PML in transient transfection experiments (Fig. 11). However, these aggregates do not have the typical size and shape of PML-NBs. They are larger and typically localize in proximity to the nuclear envelope. Moreover, pV could not be co-precipitated with one of the constituent PML-NB factors PML, Sp100 or Daxx (Fig. 12). Since the composition of PML-NBs is dynamic, an interaction with temporary factors of the PML-NBs remains a possibility, though. So far, at least 166 interaction partners of the PML-NBs are described in literature (van Damme *et al.*, 2010).

A well represented functional group of PML-NBs interaction partners comprise proteins involved in virus-host interactions (see section 1.2.1.2). We were able to co-precipitate two adenoviral proteins with HAdV-C5 pV, pVI and E1B-55K, both known to partially associate with PML-NBs (Fig. 13). Protein VI was already previously described as interaction partner of pV by early cross-linking studies (Chatterjee *et al.*, 1985; Everitt *et al.*, 1975) and more recently by West-Western (Matthews & Russell, 1998a) and pulldown assays (Pérez-Vargas *et al.*, 2014). In case of E1B-55 K, the immunoprecipitation result was equivocal (Fig. 14). Hence, the interaction between HAdV-C5 pV and E1B-55K cannot be stated with certainty.

The observed co-localization spots of HAdV-C5 pV and PML could represent the centrosomes as well, since the PML isoform III was shown to localize to these structures during various stages of the cell cycle (Xu *et al.*, 2005). The centrosome is central to the control of cytokinesis. Its dysregulation causes genome instability and aneuploidy (Carroll *et al.*, 1999; Lingle & Salisbury, 1999; Nigg, 2002; Pihan *et al.*, 1998; Weber *et al.*, 1998), whereby the loss of PML III function is sufficient to induce centrosome amplification (Xu *et al.*, 2005). In normal cells,

the doubling of centrosomes occurs during late G1- to S-phase with the cell cycle-dependent kinase cdk2 as one of the major initiation regulators (Edward H Hinchcliffe, 2002).

Interestingly, one of the major targets of cdk2/cyclin E is NPM1, which is associated with the unduplicated centrosome in the early G1-phase (see section 1.2.2.1). It can only dissociate from the centrosomes upon phosphorylation at Thr<sup>199</sup> to enable their subsequent duplication (Okuda *et al.*, 2000; Tokuyama *et al.*, 2001). The kinase activity of cdk2 is regulated through PML III in turn by inhibition of the centrosome associated kinase Aurora A (Xu *et al.*, 2005). It is assumed that the formation of monopolar mitotic cells due to a continuous association of NPM1 with the centrosome induces cell death (Tokuyama *et al.*, 2001), whereas an upregulation of cdk2/cyclin E activity results in centrosome amplification and genome instability (Xu *et al.*, 2005).

Many of the cellular processes to which NPM/B23 is linked involve large multiprotein complexes, such as nucleoli or centrosomes. HAdV-C5 pV has the ability to interact with NPM1 and both proteins have been co-detected in the nucleoli of adenoviral infected host cells. Hence, there is a realistic possibility of pV being co-located with NPM1 to centrosomes as well, which would explain the detected co-localization of pV and PML, presumably PML III. However, the possibility remains that the partial co-localization of pV with PML is exclusive for HepaRG cells or even a consequence of stress, induced by the cytotoxicity of the transfection reagent PEI.

### **5.3. HAdV-C5 pV prevents E1-region mediated transformation of primary rat cells**

Most adenovirus derived tumors, tumor cell lines and transformed cell lines are characterized by the persistence of viral DNA in a chromosomally integrated form and the expression of virus-specific antigens. The transforming capacity of human adenoviruses is mainly mediated by the gene products of the E1-coding region containing the two transcription units E1A and E1B. This is also the only region of the adenoviral genome, which is almost consistently retained in an integrated state in adenovirus transformed cell lines of human or rodent origin (Graham, 1984).

Adenoviral vectors for gene therapy usually lack the E1-region, which makes them replication-incompetent, thus indicating their safe application. The typical adenoviral vector contains additional deletions in the E3-coding region to create enough space for the insertion of foreign genes (Crystal, 2014; Rosenfeld *et al.*, 1991). Most of the early adenoviral vectors originated

from species C. Unfortunately, these vectors provoke a strong adaptive immune response of the infected host. Already in the late 90s, it was proposed that this immunity is independent of active viral replication or *de novo* protein synthesis. It was argued by the authors that high titers of the incoming viral proteins are sufficient to induce and recruit specific CTLs (Kafri *et al.*, 1998). This might also explain the short effective expression of adenovirus vectors *in vivo*, which is limited to about two weeks (Jooss & Chirmule, 2003; Yang *et al.*, 1994, 1996). What seems to be a strong limitation at first makes adenovirus vectors ideal, if a short-term expression is desired as in vaccine development or the specific killing of cancer-cells by delivery of cytotoxic genes. Also the immunogenicity of adenovirus vectors can be advantageous when it comes to the design of oncolytic viruses (Crystal, 2014). According to the Journal of Gene Medicine (Ginn *et al.*, 2013), adenoviral vectors emerged to one of the most commonly used vectors worldwide. Hence, it is of great importance for safety reasons to improve the understanding of adenoviral biology. In this regard, especially the incoming virion proteins are of interest, which seem to be able to influence the host even if viral replication is completely shut off (Kafri *et al.*, 1998).

In this study, we addressed the transforming capacity of the HAdV-C5 minor core protein V (section 4.5). Unexpectedly, this protein was able to prevent the oncogenic transformation of pBRK cells mediated by the E1-region of HAdV-C5 almost completely (Fig. 35 and Fig. 39-42). This phenotype was shown to be independent of the epitope tag, fused to the N-terminus of pV (Fig. 41), but largely dependent on the dose of the transfected pV expression plasmid (Fig. 40). All products of transfected genes were initially expressed in pBRK cells (Fig. 36 and Fig. 42A). Nevertheless, a stable cell line BRK-ABV generated by transient transfection of E1-region and pV expression plasmids, did not show any sign of viral protein expression or the presence of viral DNA-fragments. In contrast, pBRK cells BRK-AB, which were initially transfected only with E1A and E1B expressing plasmids, could be propagated for months without losing the transfected viral DNAs. Moreover, they showed continuous expression of the E1 oncoproteins (Fig. 38) as described in literature (Flint *et al.*, 1976; Gallimore, 1974; Graham *et al.*, 1984, 1977; Graham, 1984; Johansson *et al.*, 1978). These BRK-AB cells grew comparable to established, stably transformed rat cells as well as HEK293 cells, whereas BRK-ABV cells hardly grew at all (Fig. 37).

In conclusion, evidence predominates that these cells might rather be a result of spontaneous immortalization than a result of the initial transfection of adenoviral oncogenes.

### **5.3.1. The inhibitory capacity of HAdV-C5 pV does not rely on the SUMOylation of the protein**

In section 4.3, we presented HAdV-C5 pV as a novel target of the host SUMOylation machinery. Interestingly, the SUMO-modification of another viral protein, the E1B-55K oncoprotein, was proposed to be necessary for the ability of E1B-55K to participate in the transformation of pBRK cell. Point mutations within the SCM of E1B-55K lead to the cytoplasmic accumulation of the protein, which is usually able to shuttle between nucleus and cytoplasm. Moreover, these mutants are no longer able to block the p53-mediated transcription (Endter *et al.*, 2001) or to efficiently interact with PML-IV (Wimmer *et al.*, 2010, 2015). Consequently, SUMO-1 is assumed to regulate the subcellular localization of E1B-55K, which seems to be crucial for its inhibitory activity on p53 and for its contribution to cell transformation of pBRKs (Endter *et al.*, 2001).

Recently, a C-terminal mutant of E1B-55K was shown to be unable to interact with another PML-isoform, PML-V. Interestingly, this E1B-55K mutant lost its SUMO modification as well and is concomitantly localized exclusively to the cytoplasm (Wimmer *et al.*, 2015). Both unSUMOylated E1B-55K mutants, which are also deficient in the interaction with PML-IV/V, could not efficiently contribute to the transformation of pBRK cells. In addition, the SUMO modification of p53 was almost lost in their presence (Wimmer *et al.*, 2015), which is consistent with the hypothesis that E1B-55K is a SUMO1 E3 ligase for p53 (Müller & Dobner, 2008; Pennella *et al.*, 2010). Apart from the interference of E1B-55K with p53 functions, the inactivation of the SUMO conjugation site within E1B-55K inhibits the proteasomal degradation of the human tumor suppressor protein Daxx (Schreiner *et al.*, 2010, 2011).

In sum, these observations highlight the importance of the SUMO-modification for the interplay of viral and cellular factors, which obviously influences the transforming capacity of oncoproteins or the function of cellular tumor suppressor proteins. In case of HAdV-C5 pV, however, the alteration of four SCM within the protein had no effect on its ability to suppress the E1-region mediated oncogenic transformation of pBRK cells. In this regard, the inhibitory efficiency of the protein was comparable to HAdV-C5 pV wildtype (Fig. 39).

### **5.3.2. The co-expression of adenoviral E1-oncoproteins and pV might be lethal to mammalian cells**

To get a better impression of the adenoviral protein behavior during the development of propagating cell colonies we performed an immunofluorescence analysis at different time

points during the first 10 days after transfection of the primary BRK cells (Fig. 42). This time course matches the observations from previous transformations assays perfectly. The colony growth of cells, which were transfected only with E1-oncogenes, could be actually monitored. In contrast, the growth of cells transfected only with a pV-expression plasmid almost did not change. Surprisingly however, the number of cells being positive for E1 gene products in the presence of pV was very low from the beginning and remained low, showing no signs of proliferating cell colonies (Fig. 42). The simple co-transfection of different plasmids is unlikely to be the underlying cause, because a co-transfection of the E1-coding region with other plasmids encoding adenoviral proteins does not result in such an inhibition of colony formation (Fig. 39A). Another explanation would be a disturbance of protein expression either on transcriptional or on translational level. In addition, a subsequent degradation of the adenoviral proteins would be a possibility. Since all adenoviral proteins are affected at the same time, although being expressed under the control of different promoters, it seems more probable that the cells might die upon co-transfection with E1 and pV expressing plasmids.

Regarding the low transfection efficiency of pBRK cells (see section 4.5.3), this is a challenging question to address. Strikingly however, the same phenotype was observed in fully transformed human cell lines HEK293 and HeLa, which were transiently transfected with a flag-pV expression plasmid and propagated further under selection pressure (Fig. 43). In comparison to cells transfected with an empty vector control, only very few cell colonies survived a puromycin selection in the presence of HAdV-C5 pV, indicating that the pV-expressing cells actually die. HEK293 cells are stably transformed by adenoviral DNA. Moreover, they continuously express E1A and E1B proteins, whereas HeLa cells express the functional related oncoproteins E6 and E7 of HPV-18. Hence, the observations in those human cell lines resemble the findings in pBRK cells completely.

It remains to be investigated however, which kind of cell death is mediated. Can it be apoptosis despite the presence of two independent adenoviral inhibitors of the programmed cell death, which are E1B-19K and E1B-55K? Moreover, is the observed phenotype actually dependent on the expression of adenoviral E1A and E1B proteins, their functional homologs or completely independent of these proteins? In fact, the solitary presence of HAdV-C5 pV seems improbable to be the underlying reason, since pBRK cells expressing only pV are much higher in number than those expressing additionally E1A and E1B proteins (Fig. 43E). Moreover, there is evidence for an interaction between HAdV-C5 pV and E1B-55K, although this remains uncertain (section 4.2.3).

An interesting possibility however, could be the lack of DNA integration events after transient co-transfection of the coding-plasmids. Integration of adenoviral DNA encoding the E1-region is a prerequisite for the classical route of adenovirus mediated cell transformation (Graham, 1984). In general, the risk of DNA-integration events depends on the level of DNA-damage, as ds-breaks are required for an efficient integration in both host and foreign DNA (Pett & Coleman, 2007; Würtele *et al.*, 2003). DNA-integration occurs predominantly randomly (Hsiung *et al.*, 1980; Kato *et al.*, 1986; Pellicer *et al.*, 1978; Robins *et al.*, 1981), but frequently common fragile sites (CFSs) are targeted (Wentzensen *et al.*, 2004). Importantly, such integration sites are often accompanied by an instability increase (Butner & Lo, 1986; Heartlein *et al.*, 1988; Perucho *et al.*, 1980).

During productive HAdV-C5 infection, E1B-55K is known to counteract the DDR. In collaboration with adenoviral E4orf6, it mediates the proteasomal degradation of the MRN component Mre11 (Querido *et al.*, 2001a; Schwartz *et al.*, 2008; Stracker *et al.*, 2002). Moreover, E1B-55K accumulates in large, cytoplasmic inclusions, if transiently transfected or in transformed BRK cells (see Fig. 38) (Zantema *et al.*, 1985). These E1B-55K-bodies match the criteria of aggresomes and contain MRN-components also in the absence of E4orf6 (Liu *et al.*, 2005), reflecting the observation that E1B-55K can bind to Mre11 independently (Carson *et al.*, 2003). Such aggresomes are proposed to increase the rate of proteasomal degradation of misfolded proteins by concentrating suitable substrates with components of the ubiquitin-proteasome system around the centrosome (Garcia-Mata *et al.*, 2002; Kopito, 2000). Hence, E1B-55K might be capable to interfere with the DDR on its own, paving the way for DNA-integration events because of increased DNA-damage.

This idea is supported by an earlier publication in which E1B-55K was shown to be required for the retention of transfected adenoviral DNA in BRK cells. If those cells were transformed by cooperative effects of E1A and E4orf3 or E4orf6, they did not contain the initially transfected adenoviral DNA anymore, in most of the cases (Nevels *et al.*, 2001). Consequently, HAdV-C5 pV would have to interfere with the function of E1B-55K, which is able to facilitate DNA-damage within the cell without ending up in an apoptotic state.

In section 1.1.4.1, the close correlation of HAdV-C5 pV and NPM1 has been addressed. In addition to its various functions (see section 1.2.2.1), NPM1 has been revealed to participate in the DDR as well. Following the induction of DNA ds-breaks, NPM1 becomes phosphorylated at Thr<sup>199</sup> leading to its localization at sites of DNA-damage (Lee *et al.*, 2005). This is the same phosphorylation, which is required for the release of NPM1 from the centrosome to enable its

duplication. As a result, cells containing mutated NPM1 T199A acquire increased DNA lesions (Koike *et al.*, 2010) and a high frequency of aberrant mitosis with monopolar spindles (Tokuyama *et al.*, 2001). It is assumed by the authors that monopolar mitotic cells do not undergo cytokinesis, which should result in an increase of cells with an abnormal genome amplification. However, this was not the case, indicating that the aberrant mitosis might trigger cell death instead (Tokuyama *et al.*, 2001; Xu *et al.*, 2005).

Although highly speculative at this point, HAdV-C5 pV, localized to the centrosome (compare section 5.2.1), might be able to prevent phosphorylation of NPM1 at Thr<sup>199</sup>, which would block the duplication of centrosomes and promote cell death through aberrant mitosis. This function of protein V might be elicited as a response to uncontrolled cell growth or provoked by the global DDR. The latter was recently proposed to be triggered by the formation of viral replication centers but independent of MRN (Shah & O'Shea, 2015). This way, HAdV-C5 pV could contribute to the route of a lytic adenoviral infection and provide a late viral checkpoint to avoid the unwanted survival of infected cells, which would prevent the release of adenoviral progeny. In this scenario, pV would not actively prevent DNA-integration; it rather ensures the death of uncontrolled growing cells, being an 'adenoviral tumor suppressor protein'.

Protein V is specific for *Mastadenoviruses* (Davison *et al.*, 2003), which could reflect a perfect adaptation to their host. Examining this hypothesis could contribute to the efficacy and safety of future oncolytic viruses and vectors for gene therapy, in cases where a short-term expression of delivered material is favored.

## 6 Literature

---

- Ahmad, Y., Boisvert, F.-M., Gregor, P., Cobley, A. & Lamond, A. I. (2009). NOPdb: Nucleolar Proteome Database - 2008 update. *Nucleic Acids Res* **37**, D181–D184.
- Akey, C. W. & Luger, K. (2003). Histone chaperones and nucleosome assembly. *Curr Opin Struct Biol* **13**, 6–14.
- Akusjarvi, G. (2008). Temporal regulation of adenovirus major late alternative RNA splicing. *Front Biosci A J virtual Libr* **13**, 5006–5015.
- Alestrom, P., Akusjarvi, G., Lager, M., Yeh-Kai, L. & Pettersson, U. (1984). Genes encoding the core proteins of adenovirus type 2. *J Biol Chem* **259**, 13980–13985.
- Allfrey, V. G., Faulkner, R. & Mirsky, A. E. (1964). Acetylation and Methylation of Histones and their possible Role in the Regulation of RNA Synthesis. *Proc Natl Acad Sci U S A* **51**, 786–794.
- Amin, M. A., Matsunaga, S., Uchiyama, S. & Fukui, K. (2008a). Depletion of nucleophosmin leads to distortion of nucleolar and nuclear structures in HeLa cells. *Biochem J* **415**, 345–351.
- Amin, M. A., Matsunaga, S., Uchiyama, S. & Fukui, K. (2008b). Nucleophosmin is required for chromosome congression, proper mitotic spindle formation and kinetochore-microtubule attachment in HeLa cells. *FEBS Lett* **582**, 3839–3844.
- Andersen, J. S., Lam, Y. W., Leung, A. K. L., Ong, S.-E., Lyon, C. E., Lamond, A. I. & Mann, M. (2005). Nucleolar proteome dynamics. *Nature* **433**, 77–83.
- Anderson, C. W., Baum, P. R. & Gesteland, R. F. (1973). Processing of adenovirus 2-induced proteins. *J Virol* **12**, 241–252.
- Anderson, C. W., Young, M. E. & Flint, S. J. (1989). Characterization of the adenovirus 2 virion protein, mu. *Virology* **172**, 506–512.
- Aninat, C., Piton, A., Glaise, D., Le Charpentier, T., Langouet, S., Morel, F., Guguen-Guillouzo, C. & Guillouzo, A. (2006). Expression of cytochromes P450, conjugating enzymes and nuclear receptors in human hepatoma HepaRG cells. *Drug Metab Dispos* **34**, 75–83.
- Ankerst, J. & Jonsson, N. (1989). Adenovirus type 9-induced tumorigenesis in the rat mammary gland related to sex hormonal state. *J Natl Cancer Inst* **81**, 294–298.
- Antoniali, G., Lirussi, L., Poletto, M. & Tell, G. (2014). Emerging roles of the nucleolus in regulating the DNA damage response: The noncanonical DNA repair enzyme APE1/Ref-1 as a paradigmatical example. *Antioxid Redox Signal* **20**, 621–639.
- Aoki, K., Benkő, M., Davison, A. J., Echavarría, M., Erdman, D. D., Harrach, B., Kajon, A. E., Schnurr, D., Wadell, G. & Members of the Adenovirus Research Community, M. of the A. R. (2011). Toward an integrated human adenovirus designation system that utilizes molecular and serological data and serves both clinical and fundamental virology. *J Virol* **85**, 5703–5704.
- Ascoli, C. A. & Maul, G. G. (1991). Identification of a novel nuclear domain. *J Cell Biol* **112**, 785–795.
- Avgousti, D. C., Herrmann, C., Kulej, K., Pancholi, N. J., Sekulic, N., Petrescu, J., Molden, R. C., Blumenthal, D., Paris, A. J., Reyes, E. D., Ostapchuk, P., Hearing, P., Seeholzer, S. H., Worthen, G. S., Black, B. E., Garcia, B. A. & Weitzman, M. D. (2016). A core viral protein binds host nucleosomes to sequester immune danger signals. *Nature* **535**, 173–177.
- Azevedo, C., Livermore, T. & Saiardi, A. (2015). Protein polyphosphorylation of lysine residues by inorganic polyphosphate. *Mol Cell* **58**, 71–82.
- Babich, A. & Nevins, J. R. (1981). The stability of early adenovirus mRNA is controlled by the viral 72 kd DNA-binding protein. *Cell* **26**, 371–379.
- Di Bacco, A., Ouyang, J., Lee, H.-Y., Catic, A., Ploegh, H. & Gill, G. (2006). The SUMO-specific protease SENP5 is required for cell division. *Mol Cell Biol* **26**, 4489–4498.
- Bachemheimer, S. & Darnell, J. E. (1975). Adenovirus-2 mRNA is transcribed as part of a high-molecular-weight precursor RNA. *Proc Natl Acad Sci U S A* **72**, 4445–4449.
- Bagchi, S., Raychaudhuri, P. & Nevins, J. R. (1990). Adenovirus E1A proteins can dissociate heteromeric complexes involving the E2F transcription factor: A novel mechanism for E1A transactivation. *Cell* **62**, 659–669.

- Bagchi, S., Weinmann, R. & Raychaudhuri, P. (1991).** The retinoblastoma protein copurifies with E2F-I, an E1A-regulated inhibitor of the transcription factor E2F. *Cell* **65**, 1063–1072.
- Bailey, A. & Mautner, V. (1994).** Phylogenetic Relationships among Adenovirus Serotypes. *Virology* **205**, 438–452.
- Baker, C. C. & Ziff, E. B. (1981).** Promoters and heterogeneous 5' termini of the messenger RNAs of adenovirus serotype 2. *J Mol Biol* **149**, 189–221.
- Bandara, L. R. & La Thangue, N. B. (1991).** Adenovirus E1a prevents the retinoblastoma gene product from complexing with a cellular transcription factor. *Nature* **351**, 494–497.
- Bárcena, J., Verdaguer, N., Roca, R., Morales, M., Angulo, I., Risco, C., Carrascosa, J. L., Torres, J. M. & Castón, J. R. (2004).** The coat protein of Rabbit hemorrhagic disease virus contains a molecular switch at the N-terminal region facing the inner surface of the capsid. *Virology* **322**, 118–134.
- Beauclair, G., Bridier-Nahmias, A., Zagury, J.-F., Saib, A. & Zamborlini, A. (2015).** JASSA: A comprehensive tool for prediction of SUMOylation sites and SIMs. *Bioinformatics* **31**, 3483–3491.
- Beer, A. (1852).** Bestimmung der Absorption des rothen Lichts in farbigen Flüssigkeiten. *Ann der Phys und Chemie* **162**, 78–88.
- Bellgrau, D., Walker, T. A. & Cook, J. L. (1988).** Recognition of adenovirus E1A gene products on immortalized cell surfaces by cytotoxic T lymphocytes. *J Virol* **62**, 1513–1519.
- Benchimol, S. (2001).** P53-Dependent Pathways of Apoptosis. *Cell Death Differ* **8**, 1049–1051.
- Benevento, M., Di Palma, S., Snijder, J., Moyer, C. L., Reddy, V. S., Nemerow, G. R. & Heck, A. J. R. (2014).** Adenovirus composition, proteolysis and disassembly studied by in-depth qualitative and quantitative proteomics. *J Biol Chem* **289**, 11421–11430.
- Benkö, M. & Harrach, B. (1998).** A proposal for a new (third) genus within the family Adenoviridae. *Arch Virol* **143**, 829–837.
- Benkö, M. & Harrach, B. (2003).** Molecular evolution of adenoviruses. *Curr Top Microbiol Immunol* **272**, 3–35.
- Benkó, M., Elo, P., Ursu, K., Ahne, W., LaPatra, S. E., Thomson, D. & Harrach, B. (2002).** First molecular evidence for the existence of distinct fish and snake adenoviruses. *J Virol* **76**, 10056–10059.
- Berciaud, S., Rayne, F., Kassab, S., Jubert, C., Faure-Della Corte, M., Salin, F., Wodrich, H., Lafon, M. E. & Members, T. S. (2012).** Adenovirus infections in Bordeaux University Hospital 2008-2010: clinical and virological features. *J Clin Virol Off Publ Pan Am Soc Clin Virol* **54**, 302–307.
- Bergelson, J. M., Cunningham, J. A., Droguett, G., Kurt-Jones, E. A., Krithivas, A., Hong, J. S., Horwitz, M. S., Crowell, R. L. & Finberg, R. W. (1997).** Isolation of a common receptor for Coxsackie B viruses and adenoviruses 2 and 5. *Science* **275**, 1320–1323.
- Berget, S. M. & Sharp, P. A. (1977).** A spliced sequence at the 5'-terminus of adenovirus late mRNA. *Brookhaven Symp Biol* **74**, 332–344.
- Berk, A. J. (2007).** Adenoviridae: The viruses and their replication. In *Fields Virol*, 5th edn., pp. 2355–2394. Edited by D. Knipe, P. Howley, D. Griffin, R. Lamb, M. Martin, B. Roizman & S. Straus. Philadelphia, PA: Lippincott Williams & Wilkins.
- Berk, A. J. (1986).** Adenovirus promoters and E1A transactivation. *Annu Rev Genet* **20**, 45–79.
- Berk, A. J. & Sharp, P. A. (1978).** Structure of the adenovirus 2 early mRNAs. *Cell* **14**, 695–711.
- Berk, A. J., Lee, F., Harrison, T., Williams, J. & Sharp, P. A. (1979).** Pre-early adenovirus 5 gene product regulates synthesis of early viral messenger RNAs. *Cell* **17**, 935–944.
- Berlow, R. B., Dyson, H. J. & Wright, P. E. (2015).** Functional advantages of dynamic protein disorder. *FEBS Lett* **589**, 2433–2440.
- Bernardi, R., Papa, A. & Pandolfi, P. P. (2008).** Regulation of apoptosis by PML and the PML-NBs. *Oncogene* **27**, 6299–6312.
- Bernardi, R. & Pandolfi, P. P. (2007).** Structure, dynamics and functions of promyelocytic leukaemia nuclear bodies. *Nat Rev Mol Cell Biol* **8**, 1006–1016.
- Bernardi, R. & Pandolfi, P. P. (2014).** A Dialog on the First 20 Years of PML Research and the Next 20 Ahead. *Front Oncol* **4**, 1–6.
- Bernards, R., Schrier, P. I., Houweling, A., Bos, J. L., van der Eb, A. J., Zijlstra, M. & Melief, C. J. (1983).** Tumorigenicity of cells transformed by adenovirus type 12 by evasion of T-cell immunity. *Nature* **305**, 776–779.

- Bernier-Villamor, V., Sampson, D. A., Matunis, M. J. & Lima, C. D. (2002).** Structural basis for E2-mediated SUMO conjugation revealed by a complex between ubiquitin-conjugating enzyme Ubc9 and RanGAP1. *Cell* **108**, 345–356.
- Berscheminski, J., Wimmer, P., Brun, J., Ip, W. H., Groitl, P., Horlacher, T., Jaffray, E., Hay, R. T., Dobner, T. & Schreiner, S. (2014).** Sp100 isoform-specific regulation of human adenovirus 5 gene expression. *J Virol* **88**, 6076–6092.
- Berscheminski, J., Groitl, P., Dobner, T., Wimmer, P. & Schreiner, S. (2013).** The adenoviral oncogene E1A-13S interacts with a specific isoform of the tumor suppressor PML to enhance viral transcription. *J Virol* **87**, 965–977.
- den Besten, W., Kuo, M. L., Tago, K., Williams, R. T. & Sherr, C. J. (2006).** Ubiquitination of and sumoylation by, the Arf tumor suppressor. *Isr Med Assoc J* **8**, 249–251.
- Bhat, G., Sivaraman, L., Murthy, S., Domer, P. & Thimmappaya, B. (1987).** In vivo identification of multiple promoter domains of adenovirus E1A-late promoter. *EMBO J* **6**, 2045–2052.
- Biasiotto, R. & Akusjärvi, G. (2015).** Regulation of human adenovirus alternative RNA splicing by the adenoviral L4-33K and L4-22K proteins. *Int J Mol Sci* **16**, 2893–2912.
- Bingham, E. W. & Farrell, H. M. J. (1977).** Phosphorylation of casein by the lactating mammary gland: a review. *J Dairy Sci* **60**, 1199–1207.
- Bischof, O., Kim, S. H., Irving, J., Beresten, S., Ellis, N. A. & Campisi, J. (2001).** Regulation and localization of the Bloom syndrome protein in response to DNA damage. *J Cell Biol* **153**, 367–380.
- Bischof, O., Kirsh, O., Pearson, M., Itahana, K., Pelicci, P. G. & Dejean, A. (2002).** Deconstructing PML-induced premature senescence. *EMBO J* **21**, 3358–3369.
- Blais, A. & Dynlacht, B. D. (2004).** Hitting their targets: An emerging picture of E2F and cell cycle control. *Curr Opin Genet Dev* **14**, 527–532.
- Blanchette, P., Cheng, C. Y., Yan, Q., Ketner, G., Ornelles, D. A., Dobner, T., Conaway, R. C., Conaway, J. W. & Branton, P. E. (2004).** Both BC-box motifs of adenovirus protein E4orf6 are required to efficiently assemble an E3 ligase complex that degrades p53. *Mol Cell Biol* **24**, 9619–9629.
- Blom, N., Gammeltoft, S. & Brunak, S. (1999).** Sequence and structure-based prediction of eukaryotic protein phosphorylation sites. *J Mol Biol* **294**, 1351–1362.
- Blomster, H. A., Imanishi, S. Y., Siimes, J., Kastu, J., Morrice, N. A., Eriksson, J. E. & Sistonen, L. (2010).** In vivo identification of sumoylation sites by a signature tag and cysteine-targeted affinity purification. *J Biol Chem* **285**, 19324–19329.
- Bohren, K. M., Nadkarni, V., Song, J. H., Gabbay, K. H. & Owerbach, D. (2004).** A M55V Polymorphism in a Novel SUMO Gene (SUMO-4) Differentially Activates Heat Shock Transcription Factors and Is Associated with Susceptibility to Type I Diabetes Mellitus. *J Biol Chem* **279**, 27233–27238.
- Boisvert, F. M., Hendzel, M. J. & Bazett-Jones, D. P. (2000).** Promyelocytic leukemia (PML) nuclear bodies are protein structures that do not accumulate RNA. *J Cell Biol* **148**, 283–292.
- Boisvert, F.-M., van Koningsbruggen, S., Navascués, J. & Lamond, A. I. (2007).** The multifunctional nucleolus. *Nat Rev Mol Cell Biol* **8**, 574–585.
- Borer, R. A., Lehner, C. F., Eppenberger, H. M. & Nigg, E. A. (1989).** Major nucleolar proteins shuttle between nucleus and cytoplasm. *Cell* **56**, 379–390.
- Borrow, J., Goddard, A. D., Gibbons, B., Katz, F., Swirsky, D., Fioretos, T., Dube, I., Winfield, D. A., Kingston, J. & Hagemeijer, A. (1992).** Diagnosis of acute promyelocytic leukaemia by RT-PCR: Detection of PML-RARA and RARA-PML fusion transcripts. *Br J Haematol* **82**, 529–540.
- Boulon, S., Westman, B. J., Hutten, S., Boisvert, F.-M. & Lamond, A. I. (2010).** The Nucleolus under Stress. *Mol Cell* **40**, 216–227.
- Box, J. K., Paquet, N., Adams, M. N., Boucher, D., Bolderson, E., Byrne, K. J. O. & Richard, D. J. (2016).** Nucleophosmin: From structure and function to disease development. *BMC Mol Biol* **17**, 1–12.
- Boyer, G. S., Denny, F. W. & Ginsberg, H. S. (1959).** Sequential cellular changes produced by types 5 and 7 adenoviruses in HeLa cells and in human amniotic cells; cytological studies aided by fluorescein-labelled antibody. *J Exp Med* **110**, 827–844.
- Bradford, M. M. (1976).** A rapid and sensitive method for the quantitation of microgram quantities of protein utilizing the principle of protein-dye binding. *Anal Biochem* **72**, 248–254.

- Brand, P., Lenser, T. & Hemmerich, P. (2010).** Assembly dynamics of PML nuclear bodies in living cells. *PMC Biophys* **3**, 3.
- Brangwynne, C. P., Mitchison, T. J. & Hyman, A. A. (2011).** Active liquid-like behavior of nucleoli determines their size and shape in *Xenopus laevis* oocytes. *Proc Natl Acad Sci U S A* **108**, 4334–4339.
- Bremner, K. H., Scherer, J., Yi, J., Vershinin, M., Gross, S. P. & Vallee, R. B. (2009).** Adenovirus Transport via Direct Interaction of Cytoplasmic Dynein with the Viral Capsid Hexon Subunit. *Cell Host Microbe* **6**, 523–535.
- van Breukelen, B., Brenkman, A. B., Holthuisen, P. E. & van der Vliet, P. C. (2003).** Adenovirus type 5 DNA binding protein stimulates binding of DNA polymerase to the replication origin. *J Virol* **77**, 915–922.
- Brown, D. T., Westphal, M., Burlingham, B. T., Winterhoff, U. & Doerfler, W. (1975).** Structure and composition of the adenovirus type 2 core. *J Virol* **16**, 366–387.
- Burckhardt, C. J., Suomalainen, M., Schoenenberger, P., Boucke, K., Hemmi, S. & Greber, U. F. (2011).** Drifting Motions of the Adenovirus Receptor CAR and Immobile Integrins Initiate Virus Uncoating and Membrane Lytic Protein Exposure. *Cell Host Microbe* **10**, 105–117.
- Burg, J. L., Schweitzer, J. & Daniell, E. (1983).** Introduction of superhelical turns into DNA by adenoviral core proteins and chromatin assembly factors. *J Virol* **46**, 749–755.
- Burgert, H. G., Maryanski, J. L. & Kvist, S. (1987).** ‘E3/19’ protein of adenovirus type 2 inhibits lysis of cytolytic T lymphocytes by blocking cell-surface expression of histocompatibility class I antigens. *Proc Natl Acad Sci U S A* **84**, 1356–1360.
- Burnett, R. M., Grütter, M. G. & White, J. L. (1985).** The structure of the adenovirus capsid. I. An envelope model of hexon at 6 Å resolution. *J Mol Biol* **185**, 105–123.
- Butner, K. A. & Lo, C. W. (1986).** High frequency DNA rearrangements associated with mouse centromeric satellite DNA. *J Mol Biol* **187**, 547–556.
- Campos, S. K. (2014).** New structural model of adenoviral cement proteins is not yet concrete. *Proc Natl Acad Sci U S A* **111**, 2–3.
- Carbone, R., Pearson, M., Minucci, S. & Pelicci, P. G. (2002).** PML NBs associate with the hMre11 complex and p53 at sites of irradiation induced DNA damage. *Oncogene* **21**, 1633–1640.
- Carroll, P. E., Okuda, M., Horn, H. F., Biddinger, P., Stambrook, P. J., Gleich, L. L., Li, Y. Q., Tarapore, P. & Fukasawa, K. (1999).** Centrosome hyperamplification in human cancer: chromosome instability induced by p53 mutation and/or Mdm2 overexpression. *Oncogene* **18**, 1935–1944.
- Carson, C. T., Schwartz, R. A., Stracker, T. H., Lilley, C. E., Lee, D. V & Weitzman, M. D. (2003).** The Mre11 complex is required for ATM activation and the G2/M checkpoint. *EMBO J* **22**, 6610–6620.
- Carvalho, T., Seeler, J. S., Öhman, K., Jordan, P., Pettersson, U., Akusjärvi, G., Carmo-Fonseca, M. & Dejean, A. (1995).** Targeting of adenovirus E1A and E4-ORF3 proteins to nuclear matrix-associated PML bodies. *J Cell Biol* **131**, 45–56.
- Castiglia, C. L. & Flint, S. J. (1983).** Effects of adenovirus infection on rRNA synthesis and maturation in HeLa cells. *Mol Cell Biol* **3**, 662–671.
- Castro, M. E., Leal, J. F. M., Leonart, M. E., Ramon y Cajal, S. & Carnero, A. (2008).** Loss-of-function genetic screening identifies a cluster of ribosomal proteins regulating p53 function. *Carcinogenesis* **29**, 1343–1350.
- Celik, C., Gozel, M. G., Turkay, H., Bakici, M. Z., Güven, A. S. & Elaldi, N. (2015).** Rotavirus and adenovirus gastroenteritis: Time series analysis. *Pediatr Int* **57**, 590–596.
- Centers for Disease, C. & P. (2013).** Adenovirus-associated epidemic keratoconjunctivitis outbreaks—four states, 2008–2010. *MMWR Morb Mortal Wkly Rep* **62**, 637–641.
- Challberg, M. D., Ostrove, J. M. & Kelly, T. J. J. (1982).** Initiation of adenovirus DNA replication: Detection of covalent complexes between nucleotide and the 80-kilodalton terminal protein. *J Virol* **41**, 265–270.
- Chang, J. H., Lin, J. Y., Wu, M. H. & Yung, B. Y. (1998).** Evidence for the ability of nucleophosmin/B23 to bind ATP. *Biochem J* **339**, 539–544.
- Chatterjee, P. K., Vayda, M. E. & Flint, S. J. (1985).** Interactions among the three adenovirus core proteins. *J Virol* **55**, 379–386.
- Chatterjee, P. K., Vayda, M. E. & Flint, S. J. (1986a).** Identification of proteins and protein domains

- that contact DNA within adenovirus nucleoprotein cores by ultraviolet light crosslinking of oligonucleotides 32P-labelled in vivo. *J Mol Biol* **188**, 23–37.
- Chatterjee, P. K., Yang, U. C. & Flint, S. J. (1986b)**. Comparison of the interaction of the adenovirus type 2 major core protein and its precursor with DNA. *Nucleic Acids Res* **14**, 2721–2735.
- Chatterjee, P. K., Vaydal, M. E. & Flint, S. J. (1986c)**. Adenoviral protein VII packages intracellular viral DNA throughout the early phase of infection. *EMBO J* **5**, 1633–1644.
- Chaudhuri, S., Vyas, K., Kapasi, P., Komar, A. A., Dinman, J. D., Barik, S. & Mazumder, B. (2007)**. Human ribosomal protein L13a is dispensable for canonical ribosome function but indispensable for efficient rRNA methylation. *RNA* **13**, 2224–2237.
- Chellappan, S., Kraus, V. B., Kroger, B., Munger, K., Howley, P. M., Phelps, W. C. & Nevins, J. R. (1992)**. Adenovirus E1A, simian virus 40 tumor antigen and human papillomavirus E7 protein share the capacity to disrupt the interaction between transcription factor E2F and the retinoblastoma gene product. *Proc Natl Acad Sci U S A* **89**, 4549–4553.
- Chen, D., Shan, J., Zhu, W.-G., Qin, J. & Gu, W. (2010)**. Transcription-independent ARF regulation in oncogenic stress-mediated p53 responses. *Nature* **464**, 624–627.
- Chen, S.-P., Huang, Y.-C., Chiu, C.-H., Wong, K.-S., Huang, Y.-L., Huang, C.-G., Tsao, K.-C. & Lin, T.-Y. (2013)**. Clinical features of radiologically confirmed pneumonia due to adenovirus in children. *J Clin Virol* **56**, 7–12.
- Chen, Y., Wright, J., Meng, X. & Leppard, K. N. (2015)**. Promyelocytic Leukemia Protein Isoform II Promotes Transcription Factor Recruitment To Activate Interferon Beta and Interferon-Responsive Gene Expression. *Mol Cell Biol* **35**, 1660–1672.
- Chen, Z. & Chen, S.-J. (1992)**. RARA and PML Genes in Acute Promyelocytic Leukemia. *Leuk Lymphoma* **8**, 253–260.
- Cheng, X. & Kao, H.-Y. (2012)**. Post-translational modifications of PML: Consequences and implications. *Front Oncol* **2**, 1–10.
- Chhabra, P., Payne, D. C., Szilagyi, P. G., Edwards, K. M., Staat, M. A., Shirley, S. H., Wikswo, M., Nix, W. A., Lu, X., Parashar, U. D. & Vinjé, J. (2013)**. Etiology of viral gastroenteritis in children. *J Infect Dis* **208**, 790–800.
- Choi, J. W., Lee, S. B., Kim, C. K., Lee, K.-H., Cho, S.-W. & Ahn, J.-Y. (2008)**. Lysine 263 residue of NPM/B23 is essential for regulating ATP binding and B23 stability. *FEBS Lett* **582**, 1073–1080.
- Chow, L. T., Gelinis, R. E., Broker, T. R. & Roberts, R. J. (1977)**. An amazing sequence arrangement at the 5' ends of adenovirus 2 messenger RNA. *Rev Med Virol* **10**, 362–371.
- Chow, L. T., Broker, T. R. & Lewis, J. B. (1979)**. Complex splicing patterns of RNAs from the early regions of adenovirus-2. *J Mol Biol* **134**, 265–303.
- Christensen, J. B., Byrd, S. A., Walker, A. K., Strahler, J. R., Andrews, P. C. & Imperiale, M. J. (2008)**. Presence of the adenovirus IVa2 protein at a single vertex of the mature virion. *J Virol* **82**, 9086–9093.
- Ciechanover, A., Heller, H., Elias, S., Haas, A. L. & Hershko, A. (1980)**. ATP-dependent conjugation of reticulocyte proteins with the polypeptide required for protein degradation. *Proc Natl Acad Sci U S A* **77**, 1365–1368.
- Cleat, P. H. & Hay, R. T. (1989)**. Co-operative interactions between NFI and the adenovirus DNA binding protein at the adenovirus origin of replication. *EMBO J* **8**, 1841–1848.
- Colby, W. W. & Shenk, T. (1981)**. Adenovirus Type 5 Virions Can Be Assembled In Vivo in the Absence of Detectable Polypeptide IX. *J Virol* **39**, 977–980.
- Colombo, E., Marine, J.-C., Danovi, D., Falini, B. & Pelicci, P. G. (2002)**. Nucleophosmin regulates the stability and transcriptional activity of p53. *Nat Cell Biol* **4**, 529–533.
- Comb, D. G., Sarkar, N. & Pinzino, C. J. (1966)**. The methylation of lysine residues in protein. *J Biol Chem* **241**, 1857–1862.
- Condemine, W., Takahashi, Y., Zhu, J., Puvion-Dutilleul, F., Guegan, S., Janin, A. & de Thé, H. (2006)**. Characterization of Endogenous Human Promyelocytic Leukemia Isoforms. *Cancer Res* **66**, 6192–6198.
- Condezo, G. N., Marabini, R., Ayora, S., Carazo, J. M. J. M. J. M., Alba, R. R., Chillón, M., San Martín, C., Chillón, M. & San Martín, C. (2015)**. Structures of Adenovirus Incomplete Particles Clarify Capsid Architecture and Show Maturation Changes of Packaging Protein L1 52/55k. *J Virol* **89**, 9653–9664.
- Cook, J. L., May, D. L., Lewis, A. M. & Walker, T. A. (1987)**. Adenovirus E1A gene induction of

- susceptibility to lysis by natural killer cells and activated macrophages in infected rodent cells. *J Virol* **61**, 3510–3520.
- Corden, J., Engelking, H. M. & Pearson, G. D. (1976).** Chromatin-like organization of the adenovirus chromosome. *Proc Natl Acad Sci U S A* **73**, 401–404.
- Cory, S., Huang, D. C. S. & Adams, J. M. (2003).** The Bcl-2 family: Roles in cell survival and oncogenesis. *Oncogene* **22**, 8590–8607.
- Costes, S. V., Daelemans, D., Cho, E. H., Dobbins, Z., Pavlakis, G. & Lockett, S. (2004).** Automatic and Quantitative Measurement of Protein-Protein Colocalization in Live Cells. *Biophys J* **86**, 3993–4003.
- Crosby, C. M. & Barry, M. A. (2014).** IIIa deleted adenovirus as a single-cycle genome replicating vector. *Virology* **462–463**, 158–165.
- Crystal, R. G. (2014).** Adenovirus: The First Effective In Vivo Gene Delivery Vector. *Hum Gene Ther* **25**, 3–11.
- Cuccurese, M., Russo, G., Russo, A. & Pietropaolo, C. (2005).** Alternative splicing and nonsense-mediated mRNA decay regulate mammalian ribosomal gene expression. *Nucleic Acids Res* **33**, 5965–5977.
- Cuconati, A. & White, E. (2002).** Viral homologs of BCL-2: Role of apoptosis in the regulation of virus infection. *Genes Dev* **16**, 2465–2478.
- Cuconati, A., Degenhardt, K., Sundararajan, R., Ansel, A. & White, E. (2002).** Bak and Bax function to limit adenovirus replication through apoptosis induction. *J Virol* **76**, 4547–4558.
- Cuesta, R., Xi, Q. & Schneider, R. J. (2001).** Preferential translation of adenovirus mRNAs in infected cells. *Cold Spring Harb Symp Quant Biol* **66**, 259–267.
- Dales, S. & Chardonnet, Y. (1973).** Early events in the interaction of adenoviruses with HeLa cells. IV. Association with microtubules and the nuclear pore complex during vectorial movement of the inoculum. *Virology* **56**, 465–483.
- van Damme, E., Laukens, K., Dang, T. H. & van Ostade, X. (2010).** A manually curated network of the pml nuclear body interactome reveals an important role for PML-NBs in SUMOylation dynamics. *Int J Biol Sci* **6**, 51–67.
- Das, R. K. & Pappu, R. V. (2013).** Conformations of intrinsically disordered proteins are influenced by linear sequence distributions of oppositely charged residues. *Proc Natl Acad Sci U S A* **110**, 13392–13397.
- Davies, R. C. & Vousden, K. H. (1992).** Functional analysis of human papillomavirus type 16 E7 by complementation with adenovirus E1A mutants. *J Gen Virol* **73 (Pt 8)**, 2135–2139.
- Davison, A. J., Benkö, M. & Harrach, B. (2003).** Genetic content and evolution of adenoviruses. *J Gen Virol* **84**, 2895–2908.
- Dellaire, G., Eskiw, C. H., Dehghani, H., Ching, R. W. & Bazett-Jones, D. P. (2006a).** Mitotic accumulations of PML protein contribute to the re-establishment of PML nuclear bodies in G1. *J Cell Sci* **119**, 1034–1042.
- Dellaire, G., Ching, R. W., Dehghani, H., Ren, Y. & Bazett-Jones, D. P. (2006b).** The number of PML nuclear bodies increases in early S phase by a fission mechanism. *J Cell Sci* **119**, 1026–1033.
- Dellaire, G. & Bazett-Jones, D. P. (2004).** PML nuclear bodies: Dynamic sensors of DNA damage and cellular stress. *BioEssays* **26**, 963–977.
- Dery, C. V., Herrmann, C. H. & Mathews, M. B. (1987).** Response of individual adenovirus promoters to the products of the E1A gene. *Oncogene* **2**, 15–23.
- Desterro, J. M., Thomson, J. & Hay, R. T. (1997).** Ubc9 conjugates SUMO but not ubiquitin. *FEBS Lett* **417**, 297–300.
- Desterro, J. M., Rodriguez, M. S. & Hay, R. T. (1998).** SUMO-1 modification of IkappaBalpha inhibits NF-kappaB activation. *Mol Cell* **2**, 233–239.
- Desterro, J. M., Rodriguez, M. S., Kemp, G. D. & Hay, R. T. (1999).** Identification of the enzyme required for activation of the small ubiquitin-like protein SUMO-1. *J Biol Chem* **274**, 10618–10624.
- Detrait, M., De Prophetis, S., Delville, J.-P. & Komuta, M. (2015).** Fulminant isolated adenovirus hepatitis 5 months after haplo-identical HSCT for AML. *Clin case reports* **3**, 802–805.
- Dhar, S. K. & St. Clair, D. K. (2009).** Nucleophosmin blocks mitochondrial localization of p53 and apoptosis. *J Biol Chem* **284**, 16409–16418.
- Dijk, M., Typas, D., Mullenders, L. & Pines, A. (2014).** Insight in the multilevel regulation of NER.

- Exp Cell Res* **329**, 116–123.
- Dingle, J. H. & Langmuir, A. D. (1968).** Epidemiology of acute, respiratory disease in military recruits. *Am Rev Respir Dis* **97**, Suppl:1-65.
- Dinkel, H., Van Roey, K., Michael, S., Kumar, M., Uyar, B., Altenberg, B., Milchevskaya, V., Schneider, M., Kuhn, H., Behrendt, A., Dahl, S. L., Damerell, V., Diebel, S., Kalman, S., Klein, S., Knudsen, A. C., Mader, C., Merrill, S., Staudt, A., Thiel, V., Welti, L., Davey, N. E., Diella, F. & Gibson, T. J. (2016).** ELM 2016-data update and new functionality of the eukaryotic linear motif resource. *Nucleic Acids Res* **44**, D294–D300.
- Dobner, T., Horikoshi, N., Rubenwolf, S. & Shenk, T. (1996).** Blockage by adenovirus E4orf6 of transcriptional activation by the p53 tumor suppressor. *Science* **272**, 1470–1473.
- Dokland, T. (2000).** Freedom and restraint: Themes in virus capsid assembly. *Structure* **8**, 157–162.
- Douglas, W. & Nevins, J. R. (1994).** Interacting Domains of E2F1, DPi and the Adenovirus E4 Protein. *J Virol* **68**, 4212–4219.
- Drygin, D., Rice, W. G. & Grummt, I. (2010).** The RNA Polymerase I Transcription Machinery: An Emerging Target for the Treatment of Cancer. *Annu Rev Pharmacol Toxicol* **50**, 131–156.
- Dulbecco, R. & Freeman, G. (1959).** Plaque production by the polyoma virus. *Virology* **8**, 396–397.
- Dumbar, T. S., Gentry, G. A. & Olson, M. O. (1989).** Interaction of nucleolar phosphoprotein B23 with nucleic acids. *Biochemistry* **28**, 9495–9501.
- Duprez, E., Saurin, A. J., Desterro, J. M., Lallemand-Breitenbach, V., Howe, K., Boddy, M. N., Solomon, E., de Thé, H., Hay, R. T. & Freemont, P. S. (1999).** SUMO-1 modification of the acute promyelocytic leukaemia protein PML: Implications for nuclear localisation. *J Cell Sci* 381–393.
- Dyck, J. A., Maul, G. G., Miller, W. H. J., Chen, J. D., Kakizuka, A. & Evans, R. M. (1994).** A novel macromolecular structure is a target of the promyelocyte-retinoic acid receptor oncoprotein. *Cell* **76**, 333–343.
- Edward H Hinchcliffe, G. S. (2002).** Two for two: Cdk2 and its role in centrosome doubling. *Oncogene* 6154–6160.
- Ehrmann, R. L. & Gey, G. O. (1953).** The use of cell colonies on glass for evaluating nutrition and growth in roller-tube cultures. *J Natl Cancer Inst* **13**, 1099–1121.
- Eirin-Lopez, J. M., Frehlick, L. J. & Ausió, J. (2006).** Long-Term Evolution and Functional Diversification in the Members of the Nucleophosmin/Nucleoplasmin Family of Nuclear Chaperones. *Genetics* **173**, 1835–1850.
- Emmott, E. & Hiscox, J. A. (2009).** Nucleolar targeting: The hub of the matter. *EMBO Rep* **10**, 231–238.
- Enchev, R. I., Schulman, B. A. & Peter, M. (2015).** Protein neddylation: Beyond cullin-RING ligases. *Nat Rev Mol Cell Biol* **16**, 30–44.
- Enders, J. F., Bell, J. A., Dingle, J. H., Francis, T., Hilleman, M. R., Huebner, R. J. & Payne, A. M. M. (1956).** Adenoviruses-Group Name Proposed for New Respiratory-Tract Viruses. *Science* (80- ) **124**, 119–120.
- Endo, A., Kitamura, N. & Komada, M. (2009).** Nucleophosmin/B23 regulates ubiquitin dynamics in nucleoli by recruiting deubiquitylating enzyme USP36. *J Biol Chem* **284**, 27918–27923.
- Endter, C. & Dobner, T. (2004).** Cell transformation by human adenoviruses. *Curr Top Microbiol Immunol* **273**, 164–214.
- Endter, C., Kzhyshkowska, J., Stauber, R. & Dobner, T. (2001).** SUMO-1 modification required for transformation by adenovirus type 5 early region 1B 55-kDa oncoprotein. *Proc Natl Acad Sci U S A* **98**, 11312–11317.
- Enomoto, T., Lindstrom, M. S., Jin, A., Ke, H. & Zhang, Y. (2006).** Essential Role of the B23/NPM Core Domain in Regulating ARF Binding and B23 Stability. *J Biol Chem* **281**, 18463–18472.
- Erster, S., Mihara, M., Kim, R. H., Petrenko, O. & Moll, U. M. (2004).** In vivo mitochondrial p53 translocation triggers a rapid first wave of cell death in response to DNA damage that can precede p53 target gene activation. *Mol Cell Biol* **24**, 6728–6741.
- Esposito, S., Preti, V., Consolo, S., Nazzari, E. & Principi, N. (2012).** Adenovirus 36 infection and obesity. *J Clin Virol* **55**, 95–100.
- Esposito, S., Daleno, C., Prunotto, G., Scala, A., Tagliabue, C., Borzani, I., Fossali, E., Pelucchi, C. & Principi, N. (2013).** Impact of viral infections in children with community-acquired pneumonia: Results of a study of 17 respiratory viruses. *Influenza Other Respi Viruses* **7**, 18–26.

- Evans, J. D. & Hearing, P. (2005). Relocalization of the Mre11-Rad50-Nbs1 Complex by the Adenovirus E4 ORF3 Protein Is Required for Viral Replication. *J Virol* **79**, 6207–6215.
- Everett, R. D. (2001). DNA viruses and viral proteins that interact with PML nuclear bodies. *Oncogene* **20**, 7266–7273.
- Everett, R. D., Lomonte, P., Sternsdorf, T., van Driel, R. & Orr, A. (1999). Cell cycle regulation of PML modification and ND10 composition. *J Cell Sci* **112** ( Pt 2), 4581–4588.
- Everett, R. D. & Chelbi-Alix, M. K. (2007). PML and PML nuclear bodies: Implications in antiviral defence. *Biochimie* **89**, 819–830.
- Everett, R. D., Boutell, C. & Hale, B. G. (2013). Interplay between viruses and host sumoylation pathways. *Nat Rev Microbiol* **11**, 400–411.
- Everitt, E., Lutter, L. & Philipson, L. (1975). Structural proteins of adenoviruses. XII. Location and neighbor relationship among proteins of adenovirion type 2 as revealed by enzymatic iodination, immunoprecipitation and chemical cross-linking. *Virology* **67**, 197–208.
- Everitt, E., Sundquist, B. O., Pettersson, U. L. V & Philipson, L. (1973). Structural Proteins of Adenoviruses X. Isolation and topography of low molecular weight antigens from the virion of adenovirus type 2. *Virology* **52**, 130–147.
- Fabry, C. M. S., Rosa-Calatrava, M., Conway, J. F., Zubietta, C., Cusack, S., Ruigrok, R. W. H. & Schoehn, G. (2005). A quasi-atomic model of human adenovirus type 5 capsid. *EMBO J* **24**, 1645–1654.
- Fagioli, M., Alcalay, M., Pandolfi, P. P., Venturini, L., Mencarelli, A., Simeone, A., Acampora, D., Grignani, F. & Pelicci, P. G. (1992). Alternative splicing of PML transcripts predicts coexpression of several carboxy-terminally different protein isoforms. *Oncogene* **7**, 1083–1091.
- Fankhauser, C., Izaurralde, E., Adachi, Y., Wingfield, P. & Laemmli, U. K. (1991). Specific complex of human immunodeficiency virus type 1 rev and nucleolar B23 proteins: Dissociation by the Rev response element. *Mol Cell Biol* **11**, 2567–2575.
- Fatica, A. & Tollervey, D. (2002). Making ribosomes. *Curr Opin Cell Biol* **14**, 313–318.
- Ferbeyre, G., de Stanchina, E., Querido, E., Baptiste, N., Prives, C. & Lowe, S. W. (2000). PML is induced by oncogenic ras and promotes premature senescence. *Genes Dev* **14**, 2015–2027.
- Ferguson, B., Krippel, B., Andrisani, O., Jones, N., Westphal, H. & Rosenberg, M. (1985). E1A 13S and 12S mRNA products made in Escherichia coli both function as nucleus-localized transcription activators but do not directly bind DNA. *Mol Cell Biol* **5**, 2653–2661.
- Ferrari, R., Pellegrini, M., Horwitz, G. A., Xie, W., Berk, A. J. & Kurdistani, S. K. (2008). Epigenetic reprogramming by adenovirus e1a. *Science* **321**, 1086–1088.
- Ferrari, R., Su, T., Li, B., Bonora, G., Oberai, A., Chan, Y., Sasidharan, R., Berk, A. J., Pellegrini, M. & Kurdistani, S. K. (2012). Reorganization of the host epigenome by a viral oncogene. *Genome Res* **22**, 1212–1221.
- Ferrari, R., Gou, D., Jawdekar, G., Johnson, S. A., Nava, M., Su, T., Yousef, A. F., Zemke, N. R., Pellegrini, M., Kurdistani, S. K. & Berk, A. J. (2014). Adenovirus Small E1A Employs the Lysine Acetylases p300/CBP and Tumor Suppressor Rb to Repress Select Host Genes and Promote Productive Virus Infection. *Cell Host Microbe* **16**, 663–676.
- Field, J., Nikawa, J., Broek, D., MacDonald, B., Rodgers, L., Wilson, I. A., Lerner, R. A. & Wigler, M. (1988). Purification of a RAS-responsive adenylyl cyclase complex from Saccharomyces cerevisiae by use of an epitope addition method. *Mol Cell Biol* **8**, 2159–2165.
- Firat-Karalar, E. N. & Stearns, T. (2014). The centriole duplication cycle. *Philos Trans R Soc Lond B Biol Sci* **369**, 1–10.
- Flint, S. J., Sambrook, J., Williams, J. F. & Sharp, P. A. (1976). Viral nucleic acid sequences in transformed cells. IV. A study of the sequences of adenovirus 5 DNA and RNA in four lines of adenovirus 5-transformed rodent cells using specific fragments of the viral genome. *Virology* **72**, 456–470.
- Freimuth P, Anderson, C. W. (1993). Human Adenovirus Serotype 12 Virion Precursors pMu and pVI Are Cleaved at Amino-Terminal and Carboxy-Terminal sites That Conform to the Adenovirus 2 Endoproteinase Cleavage Consensus Sequence. *Virology* **193**, 348–355.
- Freudenberger, N. (2012). *Funktionelle Analysen der Strukturproteine pVII, pV und pμ des humanen Adenovirus Typ 5*. Humboldt-Universität zu Berlin.
- Friefeld, B. R., Krevolin, M. D. & Horwitz, M. S. (1983). Effects of the adenovirus H5ts125 and H5ts107 DNA binding proteins on DNA replication in vitro. *Virology* **124**, 380–389.

- Friefeld, B. R., Lichy, J. H., Field, J., Gronostajski, R. M., Guggenheimer, R. A., Krevolin, M. D., Nagata, K., Hurwitz, J. & Horwitz, M. S. (1984). The in vitro replication of adenovirus DNA. *Curr Top Microbiol Immunol* **110**, 221–255.
- Frisch, S. M. & Mymryk, J. S. (2002). Adenovirus-5 E1A: Paradox and paradigm. *Nat Rev Mol Cell Biol* **3**, 441–452.
- Furcinitti, P. S., van Oostrum, J. & Burnett, R. M. (1989). Adenovirus polypeptide IX revealed as capsid cement by difference images from electron microscopy and crystallography. *EMBO J* **8**, 3563–3570.
- Gadad, S. S., Senapati, P., Syed, S. H., Rajan, R. E., Shandilya, J., Swaminathan, V., Chatterjee, S., Colombo, E., Dimitrov, S., Pelicci, P. G., Ranga, U. & Kundu, T. K. (2011). The Multifunctional Protein Nucleophosmin (NPM1) Is a Human Linker Histone H1 Chaperone. *Biochemistry* **50**, 2780–2789.
- Galisson, F., Mahrouche, L., Courcelles, M., Bonneil, E., Meloche, S., Chelbi-Alix, M. K. & Thibault, P. (2011). A novel proteomics approach to identify SUMOylated proteins and their modification sites in human cells. *Mol Cell Proteomics* **10**, M110.004796.
- Gallimore, P. H. (1974). Viral DNA in transformed cells. II. A study of the sequences of adenovirus 2 DNA in nine lines of transformed rat cells using specific fragments of the viral genome. *J Mol Biol* **89**, 49–72.
- Garcia-Mata, R., Gao, Y.-S. & Sztul, E. (2002). Hassles with taking out the garbage: Aggravating aggregates. *Traffic* **3**, 388–396.
- Garnett, C. T., Erdman, D., Xu, W. & Gooding, L. R. (2002). Prevalence and quantitation of species C adenovirus DNA in human mucosal lymphocytes. *J Virol* **76**, 10608–10616.
- Garnett, C. T., Talekar, G., Mahr, J. A., Huang, W., Zhang, Y., Ornelles, D. A. & Gooding, L. R. (2009). Latent species C adenoviruses in human tonsil tissues. *J Virol* **83**, 2417–2428.
- Geng, Y., Monajembashi, S., Shao, A., Cui, D., He, W., Chen, Z., Hemmerich, P. & Tang, J. (2012). Contribution of the C-terminal Regions of Promyelocytic Leukemia Protein (PML) Isoforms II and V to PML Nuclear Body Formation. *J Biol Chem* **287**, 30729–30742.
- Gerd Liebert, U., Bergs, S., Ganzenmueller, T., Hage, E. & Heim, A. (2015). Human mastadenovirus type 70: A novel, multiple recombinant species D mastadenovirus isolated from diarrhoeal faeces of a haematopoietic stem cell transplantation recipient. *J Gen Virol* **96**, 2734–2742.
- Gershay, E. L., Haslett, G. W., Vidali, G. & Allfrey, V. G. (1969). Chemical studies of histone methylation. Evidence for the occurrence of 3-methylhistidine in avian erythrocyte histone fractions. *J Biol Chem* **244**, 4871–4877.
- Gey, G. O. (1958). Normal and malignant cells in tissue culture. *Ann N Y Acad Sci* **76**, 547–549.
- Ghosh, M. K. & Harter, M. L. (2003). A Viral Mechanism for Remodeling Chromatin Structure in G0 Cells. *Mol Cell* **12**, 255–260.
- Giard, D. J., Aaronson, S. A., Todaro, G. J., Arnstein, P., Kersey, J. H., Dosik, H. & Parks, W. P. (1973). In vitro cultivation of human tumors: Establishment of cell lines derived from a series of solid tumors. *J Natl Cancer Inst* **51**, 1417–1423.
- Giberson, A. N., Davidson, A. R. & Parks, R. J. (2011). Chromatin structure of adenovirus DNA throughout infection. *Nucleic Acids Res* **40**, 2369–2376.
- Ginn, S. L., Alexander, I. E., Edelstein, M. L., Abedi, M. R. & Wixon, J. (2013). Gene therapy clinical trials worldwide to 2012 - an update. *J Gene Med* **15**, 65–77.
- Ginsberg, H. S., Badger, G. F., Dingle, J. H., Jordan, W. S. & Katz, S. (1955). Etiologic relationship of the RI-67 agent to acute respiratory disease (ARD). *J Clin Invest* **34**, 820–831.
- Ginsberg, H. S., Pereira, H. G., Valentine, R. C. & Wilcox, W. C. (1966). A proposed terminology for the adenovirus antigens and virion morphological subunits. *Virology* **28**, 782–783.
- Ginsberg, H. S., Lundholm-Beauchamp, U., Horswood, R. L., Pernis, B., Wold, W. S., Chanock, R. M. & Prince, G. A. (1989). Role of early region 3 (E3) in pathogenesis of adenovirus disease. *Proc Natl Acad Sci U S A* **86**, 3823–3827.
- Girard, M., Bouche, J., Marty, L., Revet, B. & Berthelot, N. (1977). Circular adenovirus DNA-protein complexes from infected cell nuclei. *Virology* **83**, 34–55.
- Girdwood, D., Bumpass, D., Vaughan, O. A., Thain, A., Anderson, L. A., Snowden, A. W., Garcia-Wilson, E., Perkins, N. D. & Hay, R. T. (2003). p300 Transcriptional Repression Is Mediated by SUMO Modification allele knockouts of p300 and CBP display distinct transcriptional phenotypes indicate that DNA bound transcription factors are likely to be in competition for lim. *Mol Cell*

- 11, 1043–1054.
- Gong, L. & Yeh, E. T. H. (2006).** Characterization of a family of nucleolar SUMO-specific proteases with preference for SUMO-2 or SUMO-3. *J Biol Chem* **281**, 15869–15877.
- Gonzalez-Prieto, R., Cuijpers, S. A., Luijsterburg, M. S., van Attikum, H. & Vertegaal, A. C. (2015).** SUMOylation and PARylation cooperate to recruit and stabilize SLX4 at DNA damage sites. *EMBO Rep* **16**, 512–519.
- Gräble, M. & Hearing, P. (1992).** cis and trans requirements for the selective packaging of adenovirus type 5 DNA. *J Virol* **66**, 723–731.
- Graham, F. L. (1984).** Transformation by and Oncogenicity of Human Adenoviruses. In *The Adenoviruses*, pp. 339–398. Boston, MA: Springer US.
- Graham, F. L., Smiley, J., Russell, W. C. & Nairn, R. (1977).** Characteristics of a human cell line transformed by DNA from human adenovirus type 5. *J Gen Virol* **36**, 59–74.
- Graham, F., Rowe, D. T., Mckinnon, R., Bacchetti, S., Ruben, M. & Branton, P. E. (1984).** Transformation by Human Adenoviruses. *J Cell Physiol Suppl* **3**, 151–163.
- Greber, U. F., Willetts, M., Webster, P. & Helenius, A. (1993).** Stepwise dismantling of adenovirus 2 during entry into cells. *Cell* **75**, 477–486.
- Greber, U. F. & Way, M. (2006).** A Superhighway to Virus Infection. *Cell* **124**, 741–754.
- Greber, U. F., Suomalainen, M., Stidwill, R. P., Boucke, K., Ebersold, M. W. & Helenius, A. (1997).** The role of the nuclear pore complex in adenovirus DNA entry. *EMBO J* **16**, 5998–6007.
- Green, M. & Daesch, G. E. (1961).** Biochemical studies on adenovirus multiplication. II. Kinetics of nucleic acid and protein synthesis in suspension cultures. *Virology* **13**, 169–176.
- Gripon, P., Rumin, S., Urban, S., Le Seyec, J., Glaise, D., Cannie, I., Guyomard, C., Lucas, J., Trepo, C. & Guguen-Guillouzo, C. (2002).** Infection of a human hepatoma cell line by hepatitis B virus. *Proc Natl Acad Sci U S A* **99**, 15655–15660.
- Grisendi, S., Bernardi, R., Rossi, M., Cheng, K., Khandker, L., Manova, K. & Pandolfi, P. P. (2005).** Role of nucleophosmin in embryonic development and tumorigenesis. *Nature* **437**, 147–153.
- Grisendi, S., Mecucci, C., Falini, B. & Pandolfi, P. P. (2006).** Nucleophosmin and cancer. *Nat Rev Cancer* **6**, 493–505.
- Groitel, P. & Dobner, T. (2007).** Construction of adenovirus type 5 early region 1 and 4 virus mutants. *Methods Mol Med* **130**, 29–39.
- Grötzinger, T., Jensen, K. & Will, H. (1996).** The interferon (IFN)-stimulated gene Sp100 promoter contains an IFN-gamma activation site and an imperfect IFN-stimulated response element which mediate type I IFN inducibility. *J Biol Chem* **271**, 25253–25260.
- Grummt, I. (2013).** The nucleolus - guardian of cellular homeostasis and genome integrity. *Chromosoma* **122**, 487–497.
- Grummt, I. & Längst, G. (2013).** Epigenetic control of RNA polymerase I transcription in mammalian cells. *Biochim Biophys Acta - Gene Regul Mech* **1829**, 393–404.
- Grummt, I. & Pikaard, C. S. (2003).** Epigenetic silencing of RNA polymerase I transcription. *Nat Rev Mol Cell Biol* **4**, 641–649.
- Gründemann, D. & Schömig, E. (1996).** Protection of DNA during preparative agarose gel electrophoresis against damage induced by ultraviolet light. *Biotechniques* **21**, 898–903.
- Guan, D. & Kao, H.-Y. (2015).** The function, regulation and therapeutic implications of the tumor suppressor protein, PML. *Cell Biosci* **5**, 1–14.
- Guillouzo, A., Corlu, A., Aninat, C., Glaise, D., Morel, F. & Guguen-Guillouzo, C. (2007).** The human hepatoma HepaRG cells: A highly differentiated model for studies of liver metabolism and toxicity of xenobiotics. *Chem Biol Interact* **168**, 66–73.
- Guimet, D. & Hearing, P. (2013).** The adenovirus L4-22K protein has distinct functions in the posttranscriptional regulation of gene expression and encapsidation of the viral genome. *J Virol* **87**, 7688–7699.
- Guldner, H. H., Szosteki, C., Grötzinger, T. & Will, H. (1992).** IFN enhance expression of Sp100, an autoantigen in primary biliary cirrhosis. *J Immunol* **149**, 4067–4073.
- Gustin, K. E. & Imperiale, M. J. (1998).** Encapsidation of viral DNA requires the adenovirus L1 52/55-kilodalton protein. *J Virol* **72**, 7860–7870.
- Hahn, W. C., Dessain, S. K., Brooks, M. W., King, J. E., Elenbaas, B., Sabatini, D. M., DeCaprio, J. A. & Weinberg, R. A. (2002).** Enumeration of the simian virus 40 early region elements

- necessary for human cell transformation. *Mol Cell Biol* **22**, 2111–2123.
- Haindl, M., Harasim, T., Eick, D. & Muller, S. (2008).** The nucleolar SUMO-specific protease SENP3 reverses SUMO modification of nucleophosmin and is required for rRNA processing. *EMBO Rep* **9**, 273–279.
- Han, T. W., Kato, M., Xie, S., Wu, L. C., Mirzaei, H., Pei, J., Chen, M., Xie, Y., Allen, J., Xiao, G. & McKnight, S. L. (2012).** Cell-free Formation of RNA Granules: Bound RNAs Identify Features and Components of Cellular Assemblies. *Cell* **149**, 768–779.
- Hanahan, D. & Meselson, M. (1983).** Plasmid screening at high colony density. *Methods Enzymol* **100**, 333–342.
- Handwerger, K. E., Cordero, J. A. & Gall, J. G. (2005).** Cajal bodies, nucleoli and speckles in the *Xenopus* oocyte nucleus have a low-density, sponge-like structure. *Mol Biol Cell* **16**, 202–211.
- Hang, J. & Dasso, M. (2002).** Association of the human SUMO-1 protease SENP2 with the nuclear pore. *J Biol Chem* **277**, 19961–19966.
- Hannoun, Z., Maarifi, G. & Chelbi-Alix, M. K. (2016).** The implication of SUMO in intrinsic and innate immunity. *Cytokine Growth Factor Rev* **29**, 3–16.
- Hansman, G. S., Jiang, X. J. & Green, K. Y. (Eds.). (2010).** *Caliciviruses: Molecular and Cellular Virology*. Norwich: Caister Academic Press.
- Harlow, E., Whyte, P., Franza, B. R. & Schley, C. (1986).** Association of adenovirus early-region 1A proteins with cellular polypeptides. *Mol Cell Biol* **6**, 1579–1589.
- Harlow, E., Williamson, N. M., Ralston, R., Helfman, D. M. & Adams, T. E. (1985).** Molecular Cloning and In Vitro Expression of a cDNA Clone for Human Cellular Tumor Antigen p53. *Mol Cell Biol* **5**, 1601–1610.
- Harlow, E. & Lane, D. (1988).** *Antibodies: A laboratory manual*. Cold Spring Harbor Laboratory.
- Harrach, B., Benkö, M., Both, G., Brown, M., Davison, A., Echavarria, M., Hess, M., Jones, M., Kajon, A., Lehmkuhl, H. D., Mautner, V., Mittal, S. K. & Wadell, G. (2012).** Adenoviridae - ninth report of the International Committee on Taxonomy of Viruses. In *Virus Taxon*, pp. 125–141. Edited by A. M. Q. King, M. J. Adams, E. B. Carstens & Lefkowitz Elliot J. Oxford: Elsevier.
- Harvey, A. C. & Downs, J. A. (2004).** What functions do linker histones provide? *Mol Microbiol* **53**, 771–775.
- Hasson, T. B., Soloway, P. D., Ornelles, D. A., Doerfler, W. & Shenk, T. (1989).** Adenovirus L1 52- and 55-kilodalton proteins are required for assembly of virions. *J Virol* **63**, 3612–3621.
- Hasson, T. B., Ornelles, D. A. & Shenk, T. (1992).** Adenovirus L1 52- and 55-kilodalton proteins are present within assembling virions and colocalize with nuclear structures distinct from replication centers. *J Virol* **66**, 6133–6142.
- Hattersley, N., Shen, L., Jaffray, E. G. & Hay, R. T. (2011).** The SUMO protease SENP6 is a direct regulator of PML nuclear bodies. *Mol Biol Cell* **22**, 78–90.
- Hay, R. T. (1996).** Adenovirus DNA Replication. In *DNA Replication Eukaryot Cells*, pp. 699–719. Cold Spring Harbor Laboratory Press.
- Hay, R. T. (2005).** Sumo: A History of Modification. *Mol Cell* **18**, 1–12.
- Hay, R. T. (2007).** SUMO-specific proteases: a twist in the tail. *Trends Cell Biol* **17**, 370–376.
- Hearing, P., Samulski, R. J., Wishart, W. L. & Shenk, T. (1987).** Identification of a repeated sequence element required for efficient encapsidation of the adenovirus type 5 chromosome. *J Virol* **61**, 2555–2558.
- Heartlein, M. W., Knoll, J. H. & Latt, S. a. (1988).** Chromosome instability associated with human alphoid DNA transfected into the Chinese hamster genome. *Mol Cell Biol* **8**, 3611–3618.
- Hecker, C.-M., Rabiller, M., Haglund, K., Bayer, P. & Dikic, I. (2006).** Specification of SUMO1- and SUMO2-interacting Motifs. *J Biol Chem* **281**, 16117–16127.
- Hendriks, I. A., D'Souza, R. C., Yang, B., Verlaan-de Vries, M., Mann, M. & Vertegaal, A. C. (2014).** Uncovering global SUMOylation signaling networks in a site-specific manner. *Nat Struct Mol Biol* **21**, 927–936.
- Hendriks, I. A. & Vertegaal, A. C. O. (2016).** A comprehensive compilation of SUMO proteomics. *Nat Rev Mol Cell Biol* **17**, 581–595.
- Hendriks, I. A., Treffers, L. W., Verlaan-deVries, M., Olsen, J. V. & Vertegaal, A. C. O. (2015).** SUMO-2 Orchestrates Chromatin Modifiers in Response to DNA Damage. *Cell Rep* **10**, 1778–1791.
- Hentschel, A., Zahedi, R. P. & Ahrends, R. (2016).** Protein lipid modifications - More than just a

- greasy ballast. *Proteomics* **16**, 759–782.
- Hernandez-Verdun, D. (2011).** Assembly and disassembly of the nucleolus during the cell cycle. *Nucleus* **2**, 189–194.
- Hershko, A. (1983).** Ubiquitin: Roles in protein modification and breakdown. *Cell* **34**, 11–12.
- Hershko, A. & Ciechanover, A. (1982).** Mechanisms of intracellular protein breakdown. *Annu Rev Biochem* **51**, 335–364.
- Hershko, A. & Ciechanover, A. (1986).** The ubiquitin pathway for the degradation of intracellular proteins. *Prog Nucleic Acid Res Mol Biol* **33**, 19–56.
- Hershko, A. & Heller, H. (1985).** Occurrence of a polyubiquitin structure in ubiquitin-protein conjugates. *Biochem Biophys Res Commun* **128**, 1079–1086.
- Hershko, A., Ciechanover, A., Heller, H., Haas, A. L. & Rose, I. A. (1980).** Proposed role of ATP in protein breakdown: Conjugation of protein with multiple chains of the polypeptide of ATP-dependent proteolysis. *Proc Natl Acad Sci U S A* **77**, 1783–1786.
- Hershko, A., Heller, H., Eytan, E., Kaklij, G. & Rose, I. A. (1984).** Role of the alpha-amino group of protein in ubiquitin-mediated protein breakdown. *Proc Natl Acad Sci U S A* **81**, 7021–7025.
- Hierholzer, J. C. (1992).** Adenoviruses in the immunocompromised host. *Clin Microbiol Rev* **5**, 262–274.
- Hietakangas, V., Anckar, J., Blomster, H. A., Fujimoto, M., Palvimo, J. J., Nakai, A. & Sistonen, L. (2006).** PDSM, a motif for phosphorylation-dependent SUMO modification. *Proc Natl Acad Sci U S A* **103**, 45–50.
- Higashino, F., Pipas, J. M. & Shenk, T. (1998).** Adenovirus E4orf6 oncoprotein modulates the function of the p53-related protein, p73. *Proc Natl Acad Sci U S A* **95**, 15683–15687.
- Hillemann, M. R. & Werner, J. H. (1954).** Recovery of new agent from patients with acute respiratory illness. *Proc Soc Exp Biol Med* **85**, 183–188.
- Hindley, C. E., Lawrence, F. J. & Matthews, D. A. (2007a).** A Role for Transportin in the Nuclear Import of Adenovirus Core Proteins and DNA. *Traffic* **8**, 1313–1322.
- Hindley, C. E., Davidson, A. D. & Matthews, D. A. (2007b).** Relationship between adenovirus DNA replication proteins and nucleolar proteins B23.1 and B23.2. *J Gen Virol* **88**, 3244–3248.
- Hingorani, K., Szebeni, A. & Olson, M. O. J. (2000).** Mapping the functional domains of nucleolar protein B23. *J Biol Chem* **275**, 24451–24457.
- Hodges, M., Tissot, C., Howe, K., Grimwade, D. & Freemont, P. S. (1998).** NUCLEAR STRUCTURE '98 Structure, Organization and Dynamics of Promyelocytic Leukemia Protein Nuclear Bodies. *Am J Hum Genet* **63**, 297–304.
- Hofland, C. A., Eron, L. J. & Washecka, R. M. (2004).** Hemorrhagic adenovirus cystitis after renal transplantation. *Transplant Proc* **36**, 3025–3027.
- Hofmann, T. G. & Will, H. (2003).** Body language: The function of PML nuclear bodies in apoptosis regulation. *Cell Death Differ* **10**, 1290–1299.
- Holmberg Olausson, K., Nistér, M. & Lindström, M. (2012).** p53 -Dependent and -Independent Nucleolar Stress Responses. *Cells* **1**, 774–798.
- Hong, S. S., Szolajaska, E., Schoehn, G., Franqueville, L., Myhre, S., Lindholm, L., Ruigrok, R. W. H., Boulanger, P. & Chroboczek, J. (2005).** The 100K-Chaperone Protein from Adenovirus Serotype 2 (Subgroup C) Assists in Trimerization and Nuclear Localization of Hexons from Subgroups C and B Adenoviruses. *J Mol Biol* **352**, 125–138.
- Hopp, T. P., Prickett, K. S., Price, V. L., Libby, R. T., March, C. J., Pat Cerretti, D., Urdal, D. L. & Conlon, P. J. (1988).** A Short Polypeptide Marker Sequence Useful for Recombinant Protein Identification and Purification. *Nat Biotech* **6**, 1204–1210.
- Hoppe, A., Beech, S. J., Dimmock, J. & Leppard, K. N. (2006).** Interaction of the adenovirus type 5 E4 Orf3 protein with promyelocytic leukemia protein isoform II is required for ND10 disruption. *J Virol* **80**, 3042–3049.
- Horne, R. W., Brenner, S., Waterson, A. P. & Wildy, P. (1959).** The icosahedral form of an adenovirus. *J Mol Biol* **1**, 84–86.
- Horwitz, M. S., Scharff, M. D. & Maizel, J. V. J. (1969).** Synthesis and assembly of adenovirus 2. I. Polypeptide synthesis, assembly of capsomeres and morphogenesis of the virion. *Virology* **39**, 682–694.
- Howe, J. A. & Bayley, S. T. (1992).** Effects of Ad5 E1A mutant viruses on the cell cycle in relation to the binding of cellular proteins including the retinoblastoma protein and cyclin A. *Virology* **186**,

- 15–24.
- Hsiung, N., Warrick, H., DeRiel, J. K., Tuan, D., Forget, B. G., Skoultchi, A. & Kucherlapati, R. (1980).** Cotransfer of circular and linear prokaryotic and eukaryotic DNA sequences into mouse cells. *Proc Natl Acad Sci U S A* **77**, 4852–4856.
- Huang, J. T. & Schneider, R. J. (1991).** Adenovirus inhibition of cellular protein synthesis involves inactivation of cap-binding protein. *Cell* **65**, 271–280.
- Huang, W. & Flint, S. J. (1998).** The tripartite leader sequence of subgroup C adenovirus major late mRNAs can increase the efficiency of mRNA export. *J Virol* **72**, 225–235.
- Ishibashi, M. & Maizel, J. V. (1974).** The polypeptides of adenovirus. V. Young virions, structural intermediate between top components and aged virions. *Virology* **57**, 409–424.
- Ishov, A. M., Sotnikov, A. G., Negorev, D., Vladimirova, O. V., Neff, N., Kamitani, T., Yeh, E. T., Strauss, J. F. & Maul, G. G. (1999).** PML is critical for ND10 formation and recruits the PML-interacting protein daxx to this nuclear structure when modified by SUMO-1. *J Cell Biol* **147**, 221–234.
- Itahana, K., Bhat, K. P., Jin, A., Itahana, Y., Hawke, D., Kobayashi, R. & Zhang, Y. (2003).** Tumor suppressor ARF degrades B23, a nucleolar protein involved in ribosome biogenesis and cell proliferation. *Mol Cell* **12**, 1151–1164.
- Jacob, M. D., Audas, T. E., Uniacke, J., Trinkle-Mulcahy, L. & Lee, S. (2013).** Environmental cues induce a long noncoding RNA-dependent remodeling of the nucleolus. *Mol Biol Cell* **24**, 2943–2953.
- Javier, R. & Shenk, T. (1996).** Mammary tumors induced by human adenovirus type 9: A role for the viral early region 4 gene. *Breast Cancer Res Treat* **39**, 57–67.
- Javier, R. T. (1994).** Adenovirus type 9 E4 open reading frame 1 encodes a transforming protein required for the production of mammary tumors in rats. *J Virol* **68**, 3917–3924.
- Jawetz, E. (1959).** The story of shipyard eye. *Br Med J* **1**, 873–876.
- Jensen, K., Shiels, C. & Freemont, P. S. (2001).** PML protein isoforms and the RBCC/TRIM motif. *Oncogene* **20**, 7223–7233.
- Johansson, K., Pettersson, U., Philipson, L. & Tibbetts, C. (1977).** Reassociation of complementary strand-specific adenovirus type 2 DNA with viral DNA sequences of transformed cells. *J Virol* **23**, 29–35.
- Johansson, K., Persson, H., Lewis, A. M., Pettersson, U., Tibbetts, C. & Philipson, L. (1978).** Viral DNA sequences and gene products in hamster cells transformed by adenovirus type 2. *J Virol* **27**, 628–639.
- Johnson, E. S., Schwienhorst, I., Dohmen, R. J. & Blobel, G. (1997).** The ubiquitin-like protein Smt3p is activated for conjugation to other proteins by an Aos1p/Uba2p heterodimer. *EMBO J* **16**, 5509–5519.
- Jones, M. S., Harrach, B., Ganac, R. D., Gozum, M. M. A., Dela Cruz, W. P., Riedel, B., Pan, C., Delwart, E. L. & Schnurr, D. P. (2007).** New adenovirus species found in a patient presenting with gastroenteritis. *J Virol* **81**, 5978–5984.
- Jones, N. & Shenk, T. (1979).** An adenovirus type 5 early gene function regulates expression of other early viral genes. *Proc Natl Acad Sci U S A* **76**, 3665–3669.
- de Jong, R. N., van der Vliet, P. C. & Brenkman, A. B. (2003).** Adenovirus DNA replication: Protein priming, jumping back and the role of the DNA binding protein DBP. *Curr Top Microbiol Immunol* **272**, 187–211.
- Jooss, K. & Chirmule, N. (2003).** Immunity to adenovirus and adeno-associated viral vectors: Implications for gene therapy. *Gene Ther* **10**, 955–963.
- Kafri, T., Morgan, D., Krahl, T., Sarvetnick, N., Sherman, L. & Verma, I. (1998).** Cellular immune response to adenoviral vector infected cells does not require de novo viral gene expression: Implications for gene therapy. *Proc Natl Acad Sci U S A* **95**, 11377–11382.
- Kato, M., Han, T. W., Xie, S., Shi, K., Du, X., Wu, L. C., Mirzaei, H., Goldsmith, E. J., Longgood, J., Pei, J., Grishin, N. V., Frantz, D. E., Schneider, J. W., Chen, S., Li, L., Sawaya, M. R., Eisenberg, D., Tycko, R. & McKnight, S. L. (2012).** Cell-free Formation of RNA Granules: Low Complexity Sequence Domains Form Dynamic Fibers within Hydrogels. *Cell* **149**, 753–767.
- Kato, S., Anderson, R. A. & Camerini-Otero, R. D. (1986).** Foreign DNA introduced by calcium phosphate is integrated into repetitive DNA elements of the mouse L cell genome. *Mol Cell Biol* **6**, 1787–1795.

- Keller, M., Tagawa, T., Preuss, M. & Miller, A. D. (2002). Biophysical characterization of the DNA binding and condensing properties of adenoviral core peptide  $\mu$  (mu). *Biochemistry* **41**, 652–659.
- Keusekotten, K., Bade, V. N., Meyer-Teschendorf, K., Sriramachandran, A. M., Fischer-Schrader, K., Krause, A., Horst, C., Schwarz, G., Hofmann, K., Dohmen, R. J. & Praefcke, G. J. K. (2014). Multivalent interactions of the SUMO-interaction motifs in RING finger protein 4 determine the specificity for chains of the SUMO. *Biochem J* **457**, 207–214.
- Khittoo, G. & Weber, J. (1977). Genetic analysis of adenovirus type 2 VI. A temperature-sensitive mutant defective for DNA encapsidation. *Virology* **81**, 126–137.
- Khoury, G. A., Baliban, R. C. & Floudas, C. A. (2011). Proteome-wide post-translational modification statistics: Frequency analysis and curation of the swiss-prot database. *Sci Rep* **1**, 1–5.
- Kim, Y.-E. & Ahn, J.-H. (2015). Positive Role of Promyelocytic Leukemia Protein in Type I Interferon Response and Its Regulation by Human Cytomegalovirus. *PLOS Pathog* **11**, 1–24.
- Kimelman, D., Miller, J. S., Porter, D. & Roberts, B. E. (1985). E1a regions of the human adenoviruses and of the highly oncogenic simian adenovirus 7 are closely related. *J Virol* **53**, 399–409.
- Kindsmüller, K., Groitl, P., Hartl, B., Blanchette, P., Hauber, J. & Dobner, T. (2007). Intranuclear targeting and nuclear export of the adenovirus E1B-55K protein are regulated by SUMO1 conjugation. *Proc Natl Acad Sci U S A* **104**, 6684–6689.
- Kindsmüller, K., Schreiner, S., Leinenkugel, F., Groitl, P., Kremmer, E. & Dobner, T. (2009). A 49-kilodalton isoform of the adenovirus type 5 early region 1B 55-kilodalton protein is sufficient to support virus replication. *J Virol* **83**, 9045–9056.
- Koike, A., Nishikawa, H., Wu, W., Okada, Y., Venkitaraman, A. R. & Ohta, T. (2010). Recruitment of Phosphorylated NPM1 to Sites of DNA Damage through RNF8-Dependent Ubiquitin Conjugates. *Cancer Res* **70**, 6746–6756.
- Koken, M. H., Puvion-Dutilleul, F., Guillemain, M. C., Viron, A., Linares-Cruz, G., Stuurman, N., de Jong, L., Szosteki, C., Calvo, F. & Chomienne, C. (1994). The t(15;17) translocation alters a nuclear body in a retinoic acid-reversible fashion. *EMBO J* **13**, 1073–1083.
- Komatsu, T., Dacheux, D., Kreppel, F., Nagata, K. & Wodrich, H. (2015). A Method for Visualization of Incoming Adenovirus Chromatin Complexes in Fixed and Living Cells. *PLoS One* **10**, 1–11.
- Koonin, E. V. (1993). A common set of conserved motifs in a vast variety of putative nucleic acid-dependent ATPases including MCM proteins involved in the initiation of eukaryotic DNA replication. *Nucleic Acids Res* **21**, 2541–2547.
- Kopito, R. R. (2000). Aggresomes, inclusion bodies and protein aggregation. *Trends Cell Biol* **10**, 524–530.
- Kosulin, K., Haberler, C., Hainfellner, J. A., Amann, G., Lang, S. & Lion, T. (2007). Investigation of adenovirus occurrence in pediatric tumor entities. *J Virol* **81**, 7629–7635.
- Kosulin, K., Hoffmann, F., Clauditz, T. S., Wilczak, W. & Dobner, T. (2013). Presence of Adenovirus Species C in Infiltrating Lymphocytes of Human Sarcoma. *PLoS One* **8**, 1–8.
- Krebs, E. G. & Beavo, J. A. (1979). Phosphorylation-dephosphorylation of enzymes. *Annu Rev Biochem* **48**, 923–959.
- Krilov, L. R. (2005). Adenovirus infections in the immunocompromised host. *Pediatr Infect Dis J* **24**, 555–556.
- Kuo, M. L., den Besten, W., Thomas, M. C. & Sherr, C. J. (2008). Arf-induced turnover of the nucleolar nucleophosmin-associated SUMO-2/3 protease Senp3. *Cell Cycle* **7**, 3378–3387.
- Kurki, S., Peltonen, K., Latonen, L., Kiviharju, T., Ojala, P., Meek, D. & Laiho, M. (2004). Nucleolar protein NPM interacts with HDM2 and protects tumor suppressor protein p53 from HDM2-mediated degradation. *Cancer Cell* **5**, 465–475.
- Kzhyshkowska, J., Kremmer, E., Hofmann, M., Wolf, H. & Dobner, T. (2004). Protein arginine methylation during lytic adenovirus infection. *Biochem J* **383**, 259–265.
- Laemmli, U. K. (1970). Cleavage of Structural Proteins during the Assembly of the Head of Bacteriophage T4. *Nature* **227**, 680–685.
- Lallemant-Breitenbach, V., Zhu, J., Puvion, F., Koken, M., Honoré, N., Dubeikovsky, A., Duprez, E., Pandolfi, P. P., Puvion, E., Freemont, P. & de Thé, H. (2001). Role of promyelocytic leukemia (PML) sumolation in nuclear body formation, 11S proteasome

- recruitment and As<sub>2</sub>O<sub>3</sub>-induced PML or PML/retinoic acid receptor alpha degradation. *J Exp Med* **193**, 1361–1371.
- Lallemand-Breitenbach, V. & de Thé, H. (2010).** PML nuclear bodies. *Cold Spring Harb Perspect Biol* **2**, 1–17.
- Lam, Y. W., Trinkle-Mulcahy, L. & Lamond, A. I. (2005).** The nucleolus. *J Cell Sci* **118**, 1335–1337.
- Lam, Y. W., Evans, V. C., Heesom, K. J., Lamond, A. I. & Matthews, D. A. (2010).** Proteomics Analysis of the Nucleolus in Adenovirus-infected Cells. *Mol Cell Proteomics* **9**, 117–130.
- Lam, Y. W. & Trinkle-Mulcahy, L. (2015).** New insights into nucleolar structure and function. *F1000Prime Rep* **7**, 48.
- Lang, M., Jegou, T., Chung, I., Richter, K., Münch, S., Udvarhelyi, A., Cremer, C., Hemmerich, P., Engelhardt, J., Hell, S. W. & Rippe, K. (2010).** Three-dimensional organization of promyelocytic leukemia nuclear bodies. *J Cell Sci* **123**, 392–400.
- Langan, T. A. (1970).** Phosphorylation of histones in vivo under the control of cyclic AMP and hormones. *Adv Biochem Psychopharmacol* **3**, 307–323.
- Lawrence, F. J., McStay, B. & Matthews, D. A. (2006).** Nucleolar protein upstream binding factor is sequestered into adenovirus DNA replication centres during infection without affecting RNA polymerase I location or ablating rRNA synthesis. *J Cell Sci* **119**, 2621–2631.
- Le, L. P., Le, H. N., Nelson, A. R., Matthews, D. A., Yamamoto, M. & Curiel, D. T. (2006).** Core labeling of adenovirus with EGFP. *Virology* **351**, 291–302.
- Lee, J.-O., Russo, A. A. & Pavletich, N. P. (1998).** Structure of the retinoblastoma tumour-suppressor pocket domain bound to a peptide from HPV E7. *Nature* **391**, 859–865.
- van der Lee, R., Buljan, M., Lang, B., Weatheritt, R. J., Daughdrill, G. W., Dunker, A. K., Fuxreiter, M., Gough, J., Gsponer, J., Jones, D. T., Kim, P. M., Kriwacki, R. W., Oldfield, C. J., Pappu, R. V., Tompa, P., Uversky, V. N., Wright, P. E. & Babu, M. M. (2014).** Classification of intrinsically disordered regions and proteins. *Chem Rev* **114**, 6589–6631.
- Lee, S. Y., Park, J.-H., Kim, S., Park, E.-J., Yun, Y. & Kwon, J. (2005).** A proteomics approach for the identification of nucleophosmin and heterogeneous nuclear ribonucleoprotein C1/C2 as chromatin-binding proteins in response to DNA double-strand breaks. *Biochem J* **388**, 7–15.
- Lee, T. W., Lawrence, F. J., Dauksaite, V., Akusjarvi, G., Blair, G. E. & Matthews, D. A. (2004).** Precursor of human adenovirus core polypeptide Mu targets the nucleolus and modulates the expression of E2 proteins. *J Gen Virol* **85**, 185–196.
- Lee, T. W. R., Blair, G. E. & Matthews, D. A. (2003).** Adenovirus core protein VII contains distinct sequences that mediate targeting to the nucleus and nucleolus and colocalization with human chromosomes. *J Gen Virol* **84**, 3423–3428.
- Lenaerts, L., De Clercq, E. & Naesens, L. (2008).** Clinical features and treatment of adenovirus infections. *Rev Med Virol* **18**, 357–374.
- Leopold, P. L., Kreitzer, G., Miyazawa, N., Rempel, S., Pfister, K. K., Rodriguez-Boulan, E. & Crystal, R. G. (2000).** Dynein- and Microtubule-Mediated Translocation of Adenovirus Serotype 5 Occurs after Endosomal Lysis. *Hum Gene Ther* **11**, 151–165.
- Leppard, K. N. & Everett, R. D. (1999).** The adenovirus type 5 E1b 55K and E4 Orf3 proteins associate in infected cells and affect ND10 components. *J Gen Virol* **80** (Pt 4), 997–1008.
- Lewis, P. F., Schmidt, M. A., Lu, X., Erdman, D. D., Campbell, M., Thomas, A., Cieslak, P. R., Grenz, L. D., Tsaknardis, L., Gleaves, C., Kendall, B. & Gilbert, D. (2009).** A community-based outbreak of severe respiratory illness caused by human adenovirus serotype 14. *J Infect Dis* **199**, 1427–1434.
- Li, E., Stupack, D., Bokoch, G. M. & Nemerow, G. R. (1998a).** Adenovirus endocytosis requires actin cytoskeleton reorganization mediated by Rho family GTPases. *J Virol* **72**, 8806–8812.
- Li, E., Stupack, D., Klemke, R., Cheresch, D. A. & Nemerow, G. R. (1998b).** Adenovirus endocytosis via alpha(v) integrins requires phosphoinositide-3-OH kinase. *J Virol* **72**, 2055–2061.
- Li, H., Leo, C., Zhu, J., Wu, X., O’Neil, J., Park, E. J. & Chen, J. D. (2000).** Sequestration and inhibition of Daxx-mediated transcriptional repression by PML. *Mol Cell Biol* **20**, 1784–1796.
- Li, T., Du, Y., Wang, L., Huang, L., Li, W., Lu, M., Zhang, X. & Zhu, W.-G. (2012).** Characterization and prediction of lysine (K)-acetyl-transferase specific acetylation sites. *Mol Cell proteomics MCP* **11**, 1–9.
- Li, T., Song, B., Wu, Z., Lu, M. & Zhu, W.-G. (2014).** Systematic identification of Class I HDAC substrates. *Brief Bioinform* **15**, 963–972.

- Liang, Y.-C., Lee, C.-C., Yao, Y.-L., Lai, C.-C., Schmitz, M. L. & Yang, W.-M. (2016). SUMO5, a Novel Poly-SUMO Isoform, Regulates PML Nuclear Bodies. *Sci Rep* **6**, 1–15.
- Lichy, J. H., Field, J., Horwitz, M. S. & Hurwitz, J. (1982). Separation of the adenovirus terminal protein precursor from its associated DNA polymerase: Role of both proteins in the initiation of adenovirus DNA replication. *Proc Natl Acad Sci U S A* **79**, 5225–5229.
- Lillie, J. W. & Green, M. R. (1989). Transcription activation by the adenovirus E1a protein. *Nature* **338**, 39–44.
- Lim, M. J. & Wang, X. W. (2006). Nucleophosmin and human cancer. *Cancer Detect Prev* **30**, 481–490.
- Lin, C. Y., Tan, B. C.-M., Liu, H., Shih, C.-J., Chien, K.-Y., Lin, C.-L. & Yung, B. Y.-M. (2010). Dephosphorylation of nucleophosmin by PP1 $\beta$  facilitates pRB binding and consequent E2F1-dependent DNA repair. *Mol Biol Cell* **21**, 4409–4417.
- Lin, D.-Y., Huang, Y.-S., Jeng, J.-C., Kuo, H.-Y., Chang, C.-C., Chao, T.-T., Ho, C.-C., Chen, Y.-C., Lin, T.-P., Fang, H.-I., Hung, C.-C., Suen, C.-S., Hwang, M.-J., Chang, K.-S., Maul, G. G. & Shih, H.-M. (2006). Role of SUMO-interacting motif in Daxx SUMO modification, subnuclear localization and repression of sumoylated transcription factors. *Mol Cell* **24**, 341–354.
- Lindembaum, J. O., Field, J. & Hurwitz, J. (1986). The adenovirus DNA binding protein and adenovirus DNA polymerase interact to catalyze elongation of primed DNA templates. *J Biol Chem* **261**, 10218–10227.
- Lindström, M. S. (2011). NPM1/B23: A Multifunctional Chaperone in Ribosome Biogenesis and Chromatin Remodeling. *Biochem Res Int* **2011**, 1–16.
- Lingle, W. L. & Salisbury, J. L. (1999). Altered Centrosome Structure Is Associated with Abnormal Mitoses in Human Breast Tumors. *Am J Pathol* **155**, 1941–1951.
- Lion, T., Kosulin, K., Landlinger, C., Rauch, M., Preuner, S., Jugovic, D., Pötschger, U., Lawitschka, A., Peters, C., Fritsch, G. & Matthes-Martin, S. (2010). Monitoring of adenovirus load in stool by real-time PCR permits early detection of impending invasive infection in patients after allogeneic stem cell transplantation. *Leukemia* **24**, 706–714.
- Lion, T., Baumgartinger, R., Watzinger, F., Matthes-Martin, S., Suda, M., Preuner, S., Futterknecht, B., Lawitschka, A., Peters, C., Pötschger, U. & Gadner, H. (2003). Molecular monitoring of adenovirus in peripheral blood after allogeneic bone marrow transplantation permits early diagnosis of disseminated disease. *Blood* **102**, 1114–1120.
- Lion, T. (2014). Adenovirus infections in immunocompetent and immunocompromised patients. *Clin Microbiol Rev* **27**.
- Lipmann, F. (1946). Enzymatic acetylation and the coenzyme of acetylation. *Biol Bull* **91**, 239.
- Lischwe, M. A. & Sung, M. T. (1977). A histone-like protein from adenovirus chromatin. *Nature* **267**, 552–554.
- Liu, E. B., Ferreyra, L., Fischer, S. L., Pavan, J. V., Nates, S. V., Hudson, N. R., Tirado, D., Dyer, D. W., Chodosh, J., Seto, D. & Jones, M. S. (2011). Genetic Analysis of a Novel Human Adenovirus with a Serologically Unique Hexon and a Recombinant Fiber Gene. *PLoS One* **6**, e24491.
- Liu, F. & Green, M. R. (1994). Promoter targeting by adenovirus E1a through interaction with different cellular DNA-binding domains. *Nature* **368**, 520–525.
- Liu, G. Q., Babiss, L. E., Volkert, F. C., Young, C. S. & Ginsberg, H. S. (1985). A thermolabile mutant of adenovirus 5 resulting from a substitution mutation in the protein VIII gene. *J Virol* **53**, 920–925.
- Liu, H., Naismith, J. H. & Hay, R. T. (2003). Adenovirus DNA replication. *Curr Top Microbiol Immunol* **272**, 131–164.
- Liu, H., Jin, L., Koh, S. B. S., Atanasov, I., Schein, S., Wu, L. & Zhou, Z. H. (2010). Atomic structure of human adenovirus by cryo-EM reveals interactions among protein networks. *Science (80- )* **329**, 1038–1043.
- Liu, X. & Marmorstein, R. (2007). Structure of the retinoblastoma protein bound to adenovirus E1A reveals the molecular basis for viral oncoprotein inactivation of a tumor suppressor. *Genes Dev* **21**, 2711–2716.
- Liu, X., Liu, Z., Jang, S.-W., Ma, Z., Shinmura, K., Kang, S., Dong, S., Chen, J., Fukasawa, K. & Ye, K. (2007). Sumoylation of nucleophosmin/B23 regulates its subcellular localization, mediating cell proliferation and survival. *Proc Natl Acad Sci U S A* **104**, 9679–9684.

- Liu, Y., Shevchenko, A. & Berk, A. J. (2005).** Adenovirus exploits the cellular aggresome response to accelerate inactivation of the MRN complex. *J Virol* **79**, 14004–14016.
- Lois, L. M. & Lima, C. D. (2005).** Structures of the SUMO E1 provide mechanistic insights into SUMO activation and E2 recruitment to E1. *EMBO J* **24**, 439–451.
- Lomonosova, E., Subramanian, T. & Chinnadurai, G. (2005).** Mitochondrial localization of p53 during adenovirus infection and regulation of its activity by E1B-19K. *Oncogene* **24**, 6796–6808.
- Lonberg-Holm, K. & Philipson, L. (1969).** Early events of virus-cell interaction in an adenovirus system. *J Virol* **4**, 323–338.
- Luijsterburg, M. S., White, M. F., van Driel, R. & Dame, R. T. (2008).** The Major Architects of Chromatin: Architectural Proteins in Bacteria, Archaea and Eukaryotes. *Crit Rev Biochem Mol Biol* **43**, 393–418.
- Lunardi, A., Gaboli, M., Giorgio, M., Rivi, R., Bygrave, A., Antoniou, M., Drabek, D., Dzierzak, E., Fagioli, M., Salmena, L., Botto, M., Cordon-Cardo, C., Luzzatto, L., Pelicci, P. G., Grosveld, F. & Pandolfi, P. P. (2011).** A Role for PML in Innate Immunity. *Genes Cancer* **2**, 10–19.
- Luque, D., Gonzalez, J. M., Gomez-Blanco, J., Marabini, R., Chichon, J., Mena, I., Angulo, I., Carrascosa, J. L., Verdaguer, N., Trus, B. L., Barcena, J. & Caston, J. R. (2012).** Epitope Insertion at the N-Terminal Molecular Switch of the Rabbit Hemorrhagic Disease Virus T=3 Capsid Protein Leads to Larger T=4 Capsids. *J Virol* **86**, 6470–6480.
- Lutz, P., Puvion-Dutilleul, F., Lutz, Y. & Kedinger, C. (1996).** Nucleoplasmic and nucleolar distribution of the adenovirus IVa2 gene product. *J Virol* **70**, 3449–3460.
- Lutz, P., Rosa-Calatrava, M. & Kedinger, C. (1997).** The product of the adenovirus intermediate gene IX is a transcriptional activator. *J Virol* **71**, 5102–5109.
- Ma, H.-C. & Hearing, P. (2011).** Adenovirus structural protein IIIa is involved in the serotype specificity of viral DNA packaging. *J Virol* **85**, 7849–7855.
- Maier, O. & Wiethoff, C. M. (2010).** N-terminal  $\alpha$ -helix-independent membrane interactions facilitate adenovirus protein VI induction of membrane tubule formation. *Virology* **408**, 31–38.
- Maier, O., Galan, D. L., Wodrich, H. & Wiethoff, C. M. (2010).** An N-terminal domain of adenovirus protein VI fragments membranes by inducing positive membrane curvature. *Virology* **402**, 11–19.
- Maizel, J. V., White, D. O. & Scharff, M. D. (1968).** The polypeptides of adenovirus. I. Evidence for multiple protein components in the virion and a comparison of types 2, 7A and 12. *Virology* **36**, 115–125.
- Manders, E. M. M., Verbeek, F. J. & Aten, J. A. (1993).** Measurement of co-localization of objects in dual-colour confocal images. *J Microsc* **169**, 375–382.
- Mangel, W. F. & Initiative, N. (2014).** Structure, Function and Dynamics in Adenovirus Maturation. *Viruses* **6**, 4536–4570.
- Marchenko, N. D., Zaika, A. & Moll, U. M. (2000).** Death signal-induced localization of p53 protein to mitochondria. A potential role in apoptotic signaling. *J Biol Chem* **275**, 16202–16212.
- Marko, J. F. (2012).** The liquid drop nature of nucleoli. *Nucleus* **3**, 115–117.
- Martin-Fernandez, M., Longshaw, S. V., Kirby, I., Santis, G., Tobin, M. J., Clarke, D. T. & Jones, G. R. (2004).** Adenovirus Type-5 Entry and Disassembly Followed in Living Cells by FRET, Fluorescence Anisotropy and FLIM. *Biophys J* **87**, 1316–1327.
- Martinez, R., Schellenberger, P., Vasishtan, D., Akin, C., Austin, S., Dacheux, D., Rayne, F., Siebert, A., Ruzsics, Z., Gruenewald, K. & Wodrich, H. (2015).** The amphipathic helix of adenovirus capsid protein VI contributes to penton release and postentry sorting. *J Virol* **89**, 2121–2135.
- Marton, M. J., Baim, S. B., Ornelles, D. A. & Shenk, T. (1990).** The adenovirus E4 17-kilodalton protein complexes with the cellular transcription factor E2F, altering its DNA-binding properties and stimulating E1A-independent accumulation of E2 mRNA. *J Virol* **64**, 2345–2359.
- Matic, I., van Hagen, M., Schimmel, J., Macek, B., Ogg, S. C., Tatham, M. H., Hay, R. T., Lamond, A. I., Mann, M. & Vertegaal, A. C. O. (2007).** In Vivo Identification of Human Small Ubiquitin-like Modifier Polymerization Sites by High Accuracy Mass Spectrometry and an in Vitro to in Vivo Strategy. *Mol Cell Proteomics* **7**, 132–144.
- Matic, I., Schimmel, J., Hendriks, I. A., van Santen, M. A., van de Rijke, F., van Dam, H., Gnad, F., Mann, M. & Vertegaal, A. C. O. (2010).** Site-Specific Identification of SUMO-2 Targets in Cells Reveals an Inverted SUMOylation Motif and a Hydrophobic Cluster SUMOylation Motif.

- Mol Cell* **39**, 641–652.
- Matthews, D. A. (2001).** Adenovirus protein V induces redistribution of nucleolin and B23 from nucleolus to cytoplasm. *J Virol* **75**, 1031–1038.
- Matthews, D. A. & Russell, W. C. (1995).** Adenovirus protein-protein interactions: Molecular parameters governing the binding of protein VI to hexon and the activation of the adenovirus 23K protease. *J Gen Virol* **76**, 1959–1969.
- Matthews, D. A. & Russell, W. C. (1998a).** Adenovirus core protein V is delivered by the invading virus to the nucleus of the infected cell and later in infection is associated with nucleoli. *J Gen Virol* **79 (Pt 7)**, 1671–1675.
- Matthews, D. A. & Russell, W. C. (1994).** Adenovirus protein-protein interactions: Hexon and protein VI. *J Gen Virol* **75 (Pt 12)**, 3365–3374.
- Matthews, D. A. & Russell, W. C. (1998b).** Adenovirus core protein V interacts with p32 - a protein which is associated with both the mitochondria and the nucleus. *J Gen Virol* **79 (Pt 7)**, 1677–1685.
- Matthews, H. R. & Huebner, V. D. (1984).** Nuclear protein kinases. *Mol Cell Biochem* **59**, 81–99.
- Mattosio, D., Segré, C. V & Chiocca, S. (2013).** Viral manipulation of cellular protein conjugation pathways: The SUMO lesson. *World J Virol* **2**, 79–90.
- Maul, G. G., Yu, E., Ishov, A. M. & Epstein, A. L. (1995).** Nuclear domain 10 (ND10) associated proteins are also present in nuclear bodies and redistribute to hundreds of nuclear sites after stress. *J Cell Biochem* **59**, 498–513.
- McGuffin, L. J., Bryson, K. & Jones, D. T. (2000).** The PSIPRED protein structure prediction server. *Bioinformatics* **16**, 404–405.
- Melchior, F., Schergaut, M. & Pichler, A. (2003).** SUMO: Ligases, isopeptidases and nuclear pores. *Trends Biochem Sci* **28**, 612–618.
- Meroni, G. & Diez-Roux, G. (2005).** TRIM/RBCC, a novel class of ‘single protein RING finger’ E3 ubiquitin ligases. *BioEssays News Rev Mol Cell Dev Biol* **27**, 1147–1157.
- Mills, I., Cvitas, T., Homann, K., Kallay, N. & Kuchitsu, K. (2010).** *IUPAC Green Book by Simply Chemistry*, 2nd edn.
- Mirza, M. A. & Weber, J. (1982).** Structure of adenovirus chromatin. *Biochim Biophys Acta* **696**, 76–86.
- Misteli, T. (2001).** The concept of self-organization in cellular architecture. *J Cell Biol* **155**, 181–186.
- Mitreá, D. M., Grace, C. R., Buljan, M., Yun, M.-K., Pytel, N. J., Satumba, J., Nourse, A., Park, C.-G., Madan Babu, M., White, S. W. & Kriwacki, R. W. (2014).** Structural polymorphism in the N-terminal oligomerization domain of NPM1. *Proc Natl Acad Sci U S A* **111**, 4466–4471.
- Mitsudomi, T., Steinberg, S. M., Nau, M. M., Carbone, D., D’Amico, D., Bodner, S., Oie, H. K., Linnoila, R. I., Mulshine, J. L. & Minna, J. D. (1992).** p53 gene mutations in non-small-cell lung cancer cell lines and their correlation with the presence of ras mutations and clinical features. *Oncogene* **7**, 171–180.
- Miyashita, T. & Reed, J. C. (1995).** Tumor suppressor p53 is a direct transcriptional activator of the human bax gene. *Cell* **80**, 293–299.
- Montell, C., Fisher, E. F., Caruthers, M. H. & Berk, A. J. (1982).** Resolving the functions of overlapping viral genes by site-specific mutagenesis at a mRNA splice site. *Nature* **295**, 380–384.
- Moore, M., Horikoshi, N. & Shenk, T. (1996).** Oncogenic potential of the adenovirus E4orf6 protein. *Proc Natl Acad Sci U S A* **93**, 11295–11301.
- Morgenstern, J. P. & Land, H. (1990).** Advanced mammalian gene transfer: High titre retroviral vectors with multiple drug selection markers and a complementary helper-free packaging cell line. *Nucleic Acids Res* **18**, 3587–3596.
- Morris, S. J. & Leppard, K. N. (2009).** Adenovirus serotype 5 L4-22K and L4-33K proteins have distinct functions in regulating late gene expression. *J Virol* **83**, 3049–3058.
- Moyer, C. L. & Nemerow, G. R. (2012).** Disulfide-bond formation by a single cysteine mutation in adenovirus protein VI impairs capsid release and membrane lysis. *Virology* **428**, 41–47.
- Moyer, C. L., Wiethoff, C. M., Maier, O., Smith, J. G. & Nemerow, G. R. (2011).** Functional genetic and biophysical analyses of membrane disruption by human adenovirus. *J Virol* **85**, 2631–2641.
- Mukhopadhyay, D. & Dasso, M. (2007).** Modification in reverse: The SUMO proteases. *Trends Biochem Sci* **32**, 286–295.
- Muller, S. & Dejean, A. (1999).** Viral immediate-early proteins abrogate the modification by SUMO-1 of PML and Sp100 proteins, correlating with nuclear body disruption. *J Virol* **73**, 5137–5143.

- Muller, S., Matunis, M. J. & Dejean, A. (1998). Conjugation with the ubiquitin-related modifier SUMO-1 regulates the partitioning of PML within the nucleus. *EMBO J* **17**, 61–70.
- Müller, S. & Dobner, T. (2008). The adenovirus E1B-55K oncoprotein induces SUMO modification of p53. *Cell Cycle* **7**, 754–758.
- Müller, S., Hoegge, C., Pyrowolakis, G. & Jentsch, S. (2001). SUMO, ubiquitin's mysterious cousin. *Nat Rev Mol Cell Biol* **2**, 202–210.
- Murano, K., Okuwaki, M., Hisaoka, M. & Nagata, K. (2008). Transcription Regulation of the rRNA Gene by a Multifunctional Nucleolar Protein, B23/Nucleophosmin, through Its Histone Chaperone Activity. *Mol Cell Biol* **28**, 3114–3126.
- Nadolski, M. J. & Linder, M. E. (2007). Protein lipidation. *FEBS J* **274**, 5202–5210.
- Nathan, D., Sterner, D. E. & Berger, S. L. (2003). Histone modifications: Now summoning sumoylation. *Proc Natl Acad Sci U S A* **100**, 13118–13120.
- Nayak, A. & Müller, S. (2014). SUMO-specific proteases/isopeptidases: SENPs and beyond. *Genome Biol* **15**, 422.
- Negi, S. S. & Olson, M. O. J. (2006). Effects of interphase and mitotic phosphorylation on the mobility and location of nucleolar protein B23. *J Cell Sci* **119**, 3676–3685.
- Neill, S. D. & Nevins, J. R. (1991). Genetic analysis of the adenovirus E4 6/7 trans activator: Interaction with E2F and induction of a stable DNA-protein complex are critical for activity. *J Virol* **65**, 5364–5373.
- Neill, S. D., Hemstrom, C., Virtanen, A. & Nevins, J. R. (1990). An adenovirus E4 gene product trans-activates E2 transcription and stimulates stable E2F binding through a direct association with E2F. *Proc Natl Acad Sci U S A* **87**, 2008–2012.
- Neo, S. H., Itahana, Y., Alagu, J., Kitagawa, M., Guo, A. K., Lee, S. H., Tang, K. & Itahana, K. (2015). TRIM28 Is an E3 Ligase for ARF-Mediated NPM1/B23 SUMOylation That Represses Centrosome Amplification. *Mol Cell Biol* **35**, 2851–2863.
- Nermut, M. V. (1979). Structural elements in adenovirus cores. Evidence for a 'core shell' and linear structures in 'relaxed' cores. *Arch Virol* **62**, 101–116.
- Nervi, C., Poindexter, E. C., Grignani, F., Pandolfi, P. P., Lo Coco, F., Avvisati, G., Pelicci, P. G. & Jetten, A. M. (1992). Characterization of the PML-RAR alpha chimeric product of the acute promyelocytic leukemia-specific t(15;17) translocation. *Cancer Res* **52**, 3687–3692.
- Nevels, M., Rubenwolf, S., Spruss, T., Wolf, H. & Dobner, T. (1997). The adenovirus E4orf6 protein can promote E1A/E1B-induced focus formation by interfering with p53 tumor suppressor function. *Proc Natl Acad Sci U S A* **94**, 1206–1211.
- Nevels, M., Täuber, B., Kremmer, E., Spruss, T., Wolf, H. & Dobner, T. (1999a). Transforming potential of the adenovirus type 5 E4orf3 protein. *J Virol* **73**, 1591–1600.
- Nevels, M., Spruss, T., Wolf, H. & Dobner, T. (1999b). The adenovirus E4orf6 protein contributes to malignant transformation by antagonizing E1A-induced accumulation of the tumor suppressor protein p53. *Oncogene* **18**, 9–17.
- Nevels, M., Rubenwolf, S., Spruss, T., Wolf, H. & Dobner, T. (2000). Two distinct activities contribute to the oncogenic potential of the adenovirus type 5 E4orf6 protein. *J Virol* **74**, 5168–5181.
- Nevels, M., Täuber, B., Spruss, T., Wolf, H. & Dobner, T. (2001). "Hit-and-Run" Transformation by Adenovirus Oncogenes. *J Virol* **75**, 3089–3094.
- Nevins, J. R. (1981). Mechanism of activation of early viral transcription by the adenovirus E1A gene product. *Cell* **26**, 213–220.
- Nevins, J. R., Ginsberg, H. S., Blanchard, J. M., Wilson, M. C. & Darnell, J. E. (1979). Regulation of the primary expression of the early adenovirus transcription units. *J Virol* **32**, 727–733.
- Newcomb, W. W., Boring, J. W. & Brown, J. C. (1984). Ion Etching of Human Adenovirus 2: Structure of the Core. *J Virol* **51**, 52–56.
- Nguyen, E. K., Nemerow, G. R. & Smith, J. G. (2010). Direct evidence from single-cell analysis that human {alpha}-defensins block adenovirus uncoating to neutralize infection. *J Virol* **84**, 4041–4049.
- Nigg, E. A. (2002). Centrosome aberrations: Cause or consequence of cancer progression? *Nat Rev Cancer* **2**, 815–825.
- Nishida, T. & Yamada, Y. (2008). SMT3IP1, a nucleolar SUMO-specific protease, deconjugates SUMO-2 from nucleolar and cytoplasmic nucleophosmin. *Biochem Biophys Res Commun* **374**,

- 382–387.
- Nisole, S., Maroui, M. A., Mascle, X. H., Aubry, M. & Chelbi-Alix, M. K. (2013). Differential Roles of PML Isoforms. *Front Oncol* **3**, 125.
- Nozawa, Y., Van Belzen, N., Van der Made, A. C., Dinjens, W. N. & Bosman, F. T. (1996). Expression of nucleophosmin/B23 in normal and neoplastic colorectal mucosa. *J Pathol* **178**, 48–52.
- Numazaki, Y., Kumasaka, T., Yano, N., Yamanaka, M., Miyazawa, T., Takai, S. & Ishida, N. (1973). Further Study on Acute Hemorrhagic Cystitis Due to Adenovirus Type 11. *N Engl J Med* **289**, 344–347.
- Nunes, V. S. & Moretti, N. S. (2016). Nuclear subcompartments: An overview. *Cell Biol Int* **41**, 2–7.
- Obert, S., O'Connor, R. J., Schmid, S. & Hearing, P. (1994). The adenovirus E4-6/7 protein transactivates the E2 promoter by inducing dimerization of a heteromeric E2F complex. *Mol Cell Biol* **14**, 1333–1346.
- Oda, E., Ohki, R., Murasawa, H., Nemoto, J., Shibue, T., Yamashita, T., Tokino, T., Taniguchi, T. & Tanaka, N. (2000). Noxa, a BH3-only member of the Bcl-2 family and candidate mediator of p53-induced apoptosis. *Science* **288**, 1053–1058.
- Ogawa, L. M. & Baserga, S. J. (2017). Crosstalk between the nucleolus and the DNA damage response. *Mol BioSyst* **1803**, 673–683.
- Okuda, M., Horn, H. F., Tarapore, P., Tokuyama, Y., Smulian, A. G., Chan, P. K., Knudsen, E. S., Hofmann, I. A., Snyder, J. D., Bove, K. E. & Fukasawa, K. (2000). Nucleophosmin/B23 is a target of CDK2/cyclin E in centrosome duplication. *Cell* **103**, 127–140.
- Okuma, T., Honda, R., Ichikawa, G., Tsumagari, N. & Yasuda, H. (1999). In Vitro SUMO-1 Modification Requires Two Enzymatic Steps, E1 and E2. *Biochem Biophys Res Commun* **254**, 693–698.
- Okuwaki, M. (2008). The Structure and Functions of NPM1/Nucleophosmin/B23, a Multifunctional Nucleolar Acidic Protein. *J Biochem* **143**, 441–448.
- Okuwaki, M., Iwamatsu, A., Tsujimoto, M. & Nagata, K. (2001). Identification of nucleophosmin/B23, an acidic nucleolar protein, as a stimulatory factor for in vitro replication of adenovirus DNA complexed with viral basic core proteins. *J Mol Biol* **311**, 41–55.
- Olson, M. O., Dunder, M. & Szebeni, A. (2000). The nucleolus: An old factory with unexpected capabilities. *Trends Cell Biol* **10**, 189–196.
- van Oostrum, J. & Burnett, R. M. (1985). Molecular composition of the adenovirus type 2 virion. *J Virol* **56**, 439–448.
- van Ormondt, H., Maat, J. & van Beveren, C. P. (1980). The nucleotide sequence of the transforming early region E1 of adenovirus type 5 DNA. *Gene* **11**, 299–309.
- Ornelles, D. A. & Shenk, T. (1991). Localization of the adenovirus early region 1B 55-kilodalton protein during lytic infection: association with nuclear viral inclusions requires the early region 4 34-kilodalton protein. *J Virol* **65**, 424–429.
- Ortega-Esteban, A., Condezo, G. N., Perez-Berna, A. J., Chillon, M., Flint, S. J., Reguera, D., San Martín, C. & de Pablo, P. J. (2015). Mechanics of Viral Chromatin Reveals the Pressurization of Human Adenovirus. *ACS Nano* **9**, 10826–10833.
- de Ory, F., Avellón, A., Echevarría, J. E., Sánchez-Seco, M. P., Trallero, G., Cabrerizo, M., Casas, I., Pozo, F., Fedele, G., Vicente, D., Pena, M. J., Moreno, A., Niubo, J., Rabella, N., Rubio, G., Pérez-Ruiz, M., Rodríguez-Iglesias, M., Gimeno, C., Eiros, J. M., Melón, S., Blasco, M., López-Miragaya, I., Varela, E., Martínez-Sapiña, A., Rodríguez, G., Marcos, M. Á., Gegúndez, M. I., Cilla, G., Gabilondo, I., Navarro, J. M., Torres, J., Aznar, C., Castellanos, A., Guisasaola, M. E., Negro, A. I., Tenorio, A. & Vázquez-Morón, S. (2013). Viral infections of the central nervous system in Spain: A prospective study. *J Med Virol* **85**, 554–562.
- Ostapchuk, P. & Hearing, P. (2008). Adenovirus IVa2 protein binds ATP. *J Virol* **82**, 10290–10294.
- Ostapchuk, P., Almond, M. & Hearing, P. (2011). Characterization of Empty adenovirus particles assembled in the absence of a functional adenovirus IVa2 protein. *J Virol* **85**, 5524–5531.
- Ou, H. D., Kwiatkowski, W., Deerinck, T. J., Noske, A., Blain, K. Y., Land, H. S., Soria, C., Powers, C. J., May, A. P., Shu, X., Tsien, R. Y., Fitzpatrick, J. A. J., Long, J. A., Ellisman, M. H., Choe, S. & O'Shea, C. C. (2012). A structural basis for the assembly and functions of a viral polymer that inactivates multiple tumor suppressors. *Cell* **151**, 304–319.
- Owerbach, D., McKay, E. M., Yeh, E. T. H., Gabbay, K. H. & Bohren, K. M. (2005). A proline-90

- residue unique to SUMO-4 prevents maturation and sumoylation. *Biochem Biophys Res Commun* **337**, 517–520.
- Pandolfi, P. P., Alcalay, M., Fagioli, M., Zangrilli, D., Mencarelli, A., Diverio, D., Biondi, A., Lo Coco, F., Rambaldi, A. & Grignani, F. (1992).** Genomic variability and alternative splicing generate multiple PML/RAR alpha transcripts that encode aberrant PML proteins and PML/RAR alpha isoforms in acute promyelocytic leukaemia. *EMBO J* **11**, 1397–1407.
- Pardo-Mateos, A. & Young, C. S. H. (2004).** Adenovirus IVa2 protein plays an important role in transcription from the major late promoter in vivo. *Virology* **327**, 50–59.
- Parks, C. L. & Shenk, T. (1997).** Activation of the adenovirus major late promoter by transcription factors MAZ and Sp1. *J Virol* **71**, 9600–9607.
- Parks, R. J. (2005).** Adenovirus protein IX: A new look at an old protein. *Mol Ther* **11**, 19–25.
- Parlato, R. & Liss, B. (2014).** How Parkinson's disease meets nucleolar stress. *Biochim Biophys Acta - Mol Basis Dis* **1842**, 791–797.
- Parodi, A. J. & Leloir, L. F. (1979).** The role of lipid intermediates in the glycosylation of proteins in the eucaryotic cell. *Biochim Biophys Acta* **559**, 1–37.
- Parry, G. & Estelle, M. (2004).** Regulation of cullin-based ubiquitin ligases by the Nedd8/RUB ubiquitin-like proteins. *Semin Cell Dev Biol* **15**, 221–229.
- Pearson, M., Carbone, R., Sebastiani, C., Cioce, M., Fagioli, M., Saito, S., Higashimoto, Y., Appella, E., Minucci, S., Pandolfi, P. P. & Pelicci, P. G. (2000).** PML regulates p53 acetylation and premature senescence induced by oncogenic Ras. *Nature* **406**, 207–210.
- Pederson, T. & Tsai, R. Y. L. (2009).** In search of nonribosomal nucleolar protein function and regulation. *J Cell Biol* **184**, 771–776.
- Pelka, P., Ablack, J. N. G., Torchia, J., Turnell, A. S., Grand, R. J. A. & Mymryk, J. S. (2008).** Transcriptional control by adenovirus E1A conserved region 3 via p300/CBP. *Nucleic Acids Res* **37**, 1095–1106.
- Pellicer, A., Wigler, M., Axel, R. & Silverstein, S. (1978).** The transfer and stable integration of the HSV thymidine kinase gene into mouse cells. *Cell* **14**, 133–141.
- Pennella, M. A., Liu, Y., Woo, J. L., Kim, C. A. & Berk, A. J. (2010).** Adenovirus E1B 55-Kilodalton Protein Is a p53-SUMO1 E3 Ligase That Represses p53 and Stimulates Its Nuclear Export through Interactions with Promyelocytic Leukemia Nuclear Bodies. *J Virol* **84**, 12210–12225.
- Pérez-berná, A. J., Marabini, R., Scheres, S. H. W., Menéndez-Conejero, R., Dmitriev, I. P., Curiel, D. T., Mangel, W. F., Flint, S. J. & San Martín, C. (2009).** Structure and uncoating of immature adenovirus. *J Mol Biol* **392**, 547–557.
- Pérez-Berná, A. J., Marion, S., Chichón, F. J., Fernández, J. J., Winkler, D. C., Carrascosa, J. L., Steven, A. C., Šiber, A. & San Martín, C. (2015).** Distribution of DNA-condensing protein complexes in the adenovirus core. *Nucleic Acids Res* **43**, 4274–4283.
- Perez-Romero, P., Tyler, R. E., Abend, J. R., Dus, M. & Imperiale, M. J. (2005).** Analysis of the interaction of the adenovirus L1 52/55-kilodalton and IVa2 proteins with the packaging sequence in vivo and in vitro. *J Virol* **79**, 2366–2374.
- Pérez-Vargas, J., Vaughan, R. C., Houser, C., Hastie, K. M., Kao, C. C. & Nemerow, G. R. (2014).** Isolation and characterization of the DNA and protein binding activities of adenovirus core protein V. *J Virol* **88**, 9287–9296.
- Perricaudet, M., Akusjärvi, G., Virtanen, A. & Pettersson, U. (1979).** Structure of two spliced mRNAs from the transforming region of human subgroup C adenoviruses. *Nature* **281**, 694–696.
- Perry, T. L., Diamond, S. & Hansen, S. (1969).** Epsilon-N-methyl lysine: An additional amino-acid in human plasma. *Nature* **222**, 668.
- Perucho, M., Hanahan, D. & Wigler, M. (1980).** Genetic and physical linkage of exogenous sequences in transformed cells. *Cell* **22**, 309–317.
- Pestov, D. G., Strezoska, Z. & Lau, L. F. (2001).** Evidence of p53-Dependent Cross-Talk between Ribosome Biogenesis and the Cell Cycle: Effects of Nucleolar Protein Bop1 on G1/S Transition. *Mol Cell Biol* **21**, 4246–4255.
- Peter, M., Nakagawa, J., Dorée, M., Labbé, J. C. & Nigg, E. A. (1990).** Identification of major nucleolar proteins as candidate mitotic substrates of cdc2 kinase. *Cell* **60**, 791–801.
- Pett, M. & Coleman, N. (2007).** Integration of high-risk human papillomavirus: A key event in cervical carcinogenesis? *J Pathol* **212**, 356–367.
- Pettersson, U. & Roberts, R. J. (1986).** Adenovirus gene expression and replication: A historical

- review. *Cancer Cells* **4**, 37–57.
- Phelps, W. C., Yee, C. L., Munger, K. & Howley, P. M. (1988).** The human papillomavirus type 16 E7 gene encodes transactivation and transformation functions similar to those of adenovirus E1A. *Cell* **53**, 539–547.
- Pihan, G. A., Purohit, A., Wallace, J., Knecht, H., Woda, B., Quesenberry, P. & Doxsey, S. J. (1998).** Centrosome defects and genetic instability in malignant tumors. *Cancer Res* **58**, 3974–3985.
- Plehn-Dujowich, D., Bell, P., Ishov, A. M., Baumann, C. & Maul, G. G. (2000).** Non-apoptotic chromosomal condensation induced by stress: Delineation of interchromosomal spaces. *Chromosoma* **109**, 266–279.
- Poletto, M., Lirussi, L., Wilson, D. M., 3rd & Tell, G. (2014).** Nucleophosmin modulates stability, activity and nucleolar accumulation of base excision repair proteins. *Mol Biol Cell* **25**, 1641.
- Polgar, L. (1964).** Specific Acetylation of a Lysine Residue during the Hydrolytic Action of Glyceraldehyde-3-phosphate Dehydrogenase. *Acta Physiol Acad Sci Hung* **25**, 1–4.
- Prage, L., Pettersson, U., Hoglund, S., Lonberg-Holm, K. & Philipson, L. (1970).** Structural proteins of adenoviruses. IV. Sequential degradation of the adenovirus type 2 virion. *Virology* **42**, 341–358.
- Puntener, D., Engelke, M. F., Ruzsics, Z., Strunze, S., Wilhelm, C. & Greber, U. F. (2011).** Stepwise Loss of Fluorescent Core Protein V from Human Adenovirus during Entry into Cells. *J Virol* **85**, 481–496.
- Puvion-Dutilleul, F. & Christensen, M. E. (1993).** Alterations of fibrillar distribution and nucleolar ultrastructure induced by adenovirus infection. *Eur J Cell Biol* **61**, 168–176.
- Puvion-Dutilleul, F., Pedron, J. & Cajean-Feroldi, C. (1984).** Identification of intranuclear structures containing the 72K DNA-binding protein of human adenovirus type 5. *Eur J Cell Biol* **34**, 313–322.
- Puvion-Dutilleul, F., Chelbi-Alix, M. K., Koken, M., Quignon, F., Puvion, E. & de The, H. (1995).** Adenovirus infection induces rearrangements in the intranuclear distribution of the nuclear body-associated PML protein. *Exp Cell Res* **218**, 9–16.
- Qiu, W.-R., Xiao, X., Lin, W.-Z. & Chou, K.-C. (2015).** iUbiq-Lys: Prediction of lysine ubiquitination sites in proteins by extracting sequence evolution information via a gray system model. *J Biomol Struct Dyn* **33**, 1731–1742.
- Querido, E., Teodoro, J. G. & Branton, P. E. (1997a).** Accumulation of p53 induced by the adenovirus E1A protein requires regions involved in the stimulation of DNA synthesis. *J Virol* **71**, 3526–3533.
- Querido, E., Marcellus, R. C., Lai, A., Charbonneau, R., Teodoro, J. G., Ketner, G. & Branton, P. E. (1997b).** Regulation of p53 levels by the E1B 55-kilodalton protein and E4orf6 in adenovirus-infected cells. *J Virol* **71**, 3788–3798.
- Querido, E., Morrison, M. R., Chu-Pham-Dang, H., Thirlwell, S. W., Boivin, D. & Branton, P. E. (2001a).** Identification of three functions of the adenovirus e4orf6 protein that mediate p53 degradation by the E4orf6-E1B55K complex. *J Virol* **75**, 699–709.
- Querido, E., Blanchette, P., Yan, Q., Kamura, T., Morrison, M., Boivin, D., Kaelin, W. G., Conaway, R. C., Conaway, J. W. & Branton, P. E. (2001b).** Degradation of p53 by adenovirus E4orf6 and E1B55K proteins occurs via a novel mechanism involving a Cullin-containing complex. *Genes Dev* **15**, 3104–3117.
- Radivojac, P., Iakoucheva, L. M., Oldfield, C. J., Obradovic, Z., Uversky, V. N. & Dunker, A. K. (2007).** Intrinsic disorder and functional proteomics. *Biophys J* **92**, 1439–1456.
- Radko, S., Jung, R., Olanubi, O. & Pelka, P. (2015).** Effects of Adenovirus Type 5 E1A Isoforms on Viral Replication in Arrested Human Cells. *PLoS One* **10**, e0140124.
- Raghava, G. P. S. (2002).** A combination method for protein secondary structure prediction based on neural network and example based learning. *CASP5 A*-132.
- Rao, L., Debbas, M., Sabbatini, P., Hockenbery, D., Korsmeyer, S. & White, E. (1992).** The adenovirus E1A proteins induce apoptosis, which is inhibited by the E1B 19-kDa and Bcl-2 proteins. *Proc Natl Acad Sci U S A* **89**, 7742–7746.
- Raška, I., Shaw, P. J. & Cmarko, D. (2006).** New Insights into Nucleolar Architecture and Activity. In *Int Rev Cytol*, pp. 177–235.
- Razin, S. V., Iarovaia, O. V. & Vassetzky, Y. S. (2014).** A requiem to the nuclear matrix: From a controversial concept to 3D organization of the nucleus. *Chromosoma* **123**, 217–224.
- Reddy, V. S. & Nemerow, G. R. (2014a).** Structures and organization of adenovirus cement proteins

- provide insights into the role of capsid maturation in virus entry and infection. *Proc Natl Acad Sci U S A* **111**, 11715–11720.
- Reddy, V. S. & Nemerow, G. R. (2014b)**. Reply to Campos: Revised structures of adenovirus cement proteins represent a consensus model for understanding virus assembly and disassembly. *Proc Natl Acad Sci U S A* **111**, E4544-4545.
- Reddy, V. S., Natchiar, S. K., Stewart, P. L. & Nemerow, G. R. (2010)**. Crystal structure of human adenovirus at 3.5 Å resolution. *Science (80- )* **329**, 1071–1075.
- Reich, N. C., Sarnow, P., Duprey, E. & Levine, A. J. (1983)**. Monoclonal antibodies which recognize native and denatured forms of the adenovirus DNA-binding protein. *Virology* **128**, 480–484.
- Rekosh, D. M. K., Russell, W. C., Bellett, A. J. D. & Robinson, A. J. (1977)**. Identification of a protein linked to the ends of adenovirus DNA. *Cell* **11**, 283–295.
- Ren, J., Gao, X., Jin, C., Zhu, M., Wang, X., Shaw, A., Wen, L., Yao, X. & Xue, Y. (2009)**. Systematic study of protein sumoylation: Development of a site-specific predictor of SUMOsp 2.0. *Proteomics* **9**, 3409–3412.
- Reymond, A., Meroni, G., Fantozzi, A., Merla, G., Cairo, S., Luzi, L., Riganelli, D., Zanaria, E., Messali, S., Cainarca, S., Guffanti, A., Minucci, S., Pelicci, P. G. & Ballabio, A. (2001)**. The tripartite motif family identifies cell compartments. *EMBO J* **20**, 2140–2151.
- Robins, D. M., Ripley, S., Henderson, A. S. & Axel, R. (1981)**. Transforming DNA integrates into the host chromosome. *Cell* **23**, 29–39.
- Robinson, C. M., Singh, G., Lee, J. Y., Dehghan, S., Rajaiya, J., Liu, E. B., Yousuf, M. a, Betensky, R. a, Jones, M. S., Dyer, D. W., Seto, D. & Chodosh, J. (2013)**. Molecular evolution of human adenoviruses. *Sci Rep* **3**, 1812.
- Robinson, C. M., Singh, G., Henquell, C., Walsh, M. P., Peigue-Lafeuille, H., Seto, D., Jones, M. S., Dyer, D. W. & Chodosh, J. (2011)**. Computational analysis and identification of an emergent human adenovirus pathogen implicated in a respiratory fatality. *Virology* **409**, 141–147.
- Rodríguez, E., Ip, W. H., Kolbe, V., Hartmann, K., Pilnitz-Stolze, G., Tekin, N., Gómez-Medina, S., Muñoz-Fontela, C., Krasemann, S. & Dobner, T. (2017)**. Humanized Mice Reproduce Acute and Persistent Human Adenovirus Infection. *J Infect Dis* **215**, 70–79.
- Rodríguez, M. S., Dargemont, C. & Hay, R. T. (2001)**. SUMO-1 Conjugation in Vivo Requires Both a Consensus Modification Motif and Nuclear Targeting. *J Biol Chem* **276**, 12654–12659.
- Roelvink, P. W., Lizonova, A., Lee, J. G., Li, Y., Bergelson, J. M., Finberg, R. W., Brough, D. E., Kovesdi, I. & Wickham, T. J. (1998)**. The coxsackievirus-adenovirus receptor protein can function as a cellular attachment protein for adenovirus serotypes from subgroups A, C, D, E and F. *J Virol* **72**, 7909–7915.
- Van Roey, K., Uyar, B., Weatheritt, R. J., Dinkel, H., Seiler, M., Budd, A., Gibson, T. J. & Davey, N. E. (2014)**. Short linear motifs: Ubiquitous and functionally diverse protein interaction modules directing cell regulation. *Chem Rev* **114**, 6733–6778.
- Rosa-Calatrava, M., Puvion-Dutilleul, F., Lutz, P., Dreyer, D., De Thé, H., Chatton, B. & Kedinger, C. (2003)**. Adenovirus protein IX sequesters host-cell promyelocytic leukaemia protein and contributes to efficient viral proliferation. *EMBO Rep* **4**, 969–975.
- Rosenfeld, M. A., Siegfried, W., Yoshimura, K., Yoneyama, K., Fukayama, M., Stier, L. E., Pääkkö, P. K., Gilardi, P., Stratford-Perricaudet, L. D. & Perricaudet, M. (1991)**. Adenovirus-mediated transfer of a recombinant alpha 1-antitrypsin gene to the lung epithelium in vivo. *Science* **252**, 431–434.
- Rowe, W. P., Huebner, R. J., Gilmore, L. K., Parrott, R. H. & Ward, T. G. (1953)**. Isolation of a cytopathogenic agent from human adenoids undergoing spontaneous degeneration in tissue culture. *Proc Soc Exp Biol Med* **84**, 570–573.
- Roy, A., Kucukural, A. & Zhang, Y. (2010)**. I-TASSER: A unified platform for automated protein structure and function prediction. *Nat Protoc* **5**, 725–738.
- Roy, S., Calcedo, R., Medina-Jaszek, A., Keough, M., Peng, H. & Wilson, J. M. (2011)**. Adenoviruses in Lymphocytes of the Human Gastro-Intestinal Tract. *PLoS One* **6**, e24859.
- Russell, Jackie, Zomerdijk, J. (2006)**. The RNA polymerase I transcription machinery. *Biochem Soc Symp* **73**, 203–216.
- Russo, A. & Russo, G. (2017)**. Ribosomal Proteins Control or Bypass p53 during Nucleolar Stress. *Int J Mol Sci* **18**, 140.
- Russo, G., Ricciardelli, G. & Pietropaolo, C. (1997)**. Different domains cooperate to target the human

- ribosomal L7a protein to the nucleus and to the nucleoli. *J Biol Chem* **272**, 5229–5235.
- Ruzindana-umunyana, A., Imbeault, L. & Weber, J. M. (2002).** Substrate specificity of adenovirus protease. *Virus Res* **89**, 41–52.
- Ryan, K. M., Phillips, A. C. & Vousden, K. H. (2001).** Regulation and function of the p53 tumor suppressor protein. *Curr Opin Cell Biol* **13**, 332–337.
- Saban, S. D., Silvestry, M., Nemerow, G. R. & Stewart, P. L. (2006).** Visualization of alpha-helices in a 6-angstrom resolution cryoelectron microscopy structure of adenovirus allows refinement of capsid protein assignments. *J Virol* **80**, 12049–12059.
- Sahin, U., Lallemand-Breitenbach, V. & de Thé, H. (2014a).** PML nuclear bodies: Regulation, function and therapeutic perspectives. *J Pathol* **234**, 289–291.
- Sahin, U., Ferhi, O., Carnec, X., Zamborlini, A., Peres, L., Jollivet, F., Vitaliano-Prunier, A., de Thé, H. & Lallemand-Breitenbach, V. (2014b).** Interferon controls SUMO availability via the Lin28 and let-7 axis to impede virus replication. *Nat Commun* **5**, 4187.
- Sahin, U., de Thé, H. & Lallemand-Breitenbach, V. (2015).** PML nuclear bodies: Assembly and oxidative stress-sensitive sumoylation. *Nucleus* **5**, 499–507.
- Saiki, R. K., Gelfand, D. H., Stoffel, S., Scharf, S. J., Higuchi, R., Horn, G. T., Mullis, K. B. & Erlich, H. A. (1988).** Primer-directed enzymatic amplification of DNA with a thermostable DNA polymerase. *Science* **239**, 487–491.
- Saitoh, H. & Hinchey, J. (2000).** Functional heterogeneity of small ubiquitin-related protein modifiers SUMO-1 versus SUMO-2/3. *J Biol Chem* **275**, 6252–6258.
- Salomoni, P. & Pandolfi, P. P. (2002).** The Role of PML in Tumor Suppression. *Cell* **108**, 165–170.
- Samad, M. A., Okuwaki, M., Haruki, H. & Nagata, K. (2007).** Physical and functional interaction between a nucleolar protein nucleophosmin/B23 and adenovirus basic core proteins. *FEBS Lett* **581**, 3283–3288.
- Samad, M. A., Komatsu, T., Okuwaki, M. & Nagata, K. (2012).** B23/nucleophosmin is involved in regulation of adenovirus chromatin structure at late infection stages, but not in virus replication and transcription. *J Gen Virol* **93**, 1328–1338.
- Sambrook, J., Fritsch, E. F. & Maniatis, T. (1989).** *Molecular cloning: A laboratory manual*, 2nd edn. (T. Maniatis, E. F. Fritsch & J. Sambrook, Eds.). New York: Cold Spring Harbor Laboratory Press.
- Sampson, D. A., Wang, M. & Matunis, M. J. (2001).** The Small Ubiquitin-like Modifier-1 (SUMO-1) Consensus Sequence Mediates Ubc9 Binding and Is Essential for SUMO-1 Modification. *J Biol Chem* **276**, 21664–21669.
- San Martín, C. (2012).** Latest Insights on Adenovirus Structure and Assembly. *Viruses* **4**, 847–877.
- San Martín, C., Glasgow, J. N., Borovjagin, A., Beatty, M. S., Kashentseva, E. A., Curiel, D. T., Marabini, R. & Dmitriev, I. P. (2008).** Localization of the N-terminus of minor coat protein IIIa in the adenovirus capsid. *J Mol Biol* **383**, 923–934.
- Sarnow, P., Sullivan, C. A. & Levine, A. J. (1982).** A monoclonal antibody detecting the adenovirus type 5-E1b-58Kd tumor antigen: Characterization of the E1b-58kD tumor antigen in adenovirus-infected and -transformed cells. *Virology* **120**, 510–517.
- Sato, H., Furuno, A. & Yoshiike, K. (1989).** Expression of human papillomavirus type 16 E7 gene induces DNA synthesis of rat 3Y1 cells. *Virology* **168**, 195–199.
- Sato, K. & Hosokawa, K. (1984).** Analysis of the interaction between DNA and major core protein in adenovirus chromatin by circular dichroism and ultraviolet light induced cross-linking. *J Biochem* **95**, 1031–1039.
- Savkur, R. S. & Olson, M. O. (1998).** Preferential cleavage in pre-ribosomal RNA by protein B23 endoribonuclease. *Nucleic Acids Res* **26**, 4508–4515.
- Savón, C., Acosta, B., Valdés, O., Goyenechea, A., Gonzalez, G., Piñón, A., Más, P., Rosario, D., Capó, V., Kourí, V., Martínez, P. A., Marchena, J. J., González, G., Rodríguez, H. & Guzmán, M. G. (2008).** A myocarditis outbreak with fatal cases associated with adenovirus subgenera C among children from Havana City in 2005. *J Clin Virol* **43**, 152–157.
- Sawada, Y., Föhring, B., Shenk, T. E. & Raska, K. (1985).** Tumorigenicity of adenovirus-transformed cells: Region E1A of adenovirus 12 confers resistance to natural killer cells. *Virology* **147**, 413–421.
- Schachter, H. (1974).** The subcellular sites of glycosylation. *Biochem Soc Symp* 57–71.
- Scheer, U. & Hock, R. (1999).** Structure and function of the nucleolus. *Curr Opin Cell Biol* **11**, 385–

- 390.
- Scheffner, M., Romanczuk, H., Munger, K., Huibregtse, J. M., Mietz, J. A. & Howley, P. M. (1994).** Functions of human papillomavirus proteins. *Curr Top Microbiol Immunol* **186**, 83–99.
- Scherer, M. & Stamminger, T. (2016).** Emerging role of PML nuclear bodies in innate immune signaling. *J Virol* **90**, 5850–5854.
- Schmidt, M. F. (1983).** Fatty acid binding: A new kind of posttranslational modification of membrane proteins. *Curr Top Microbiol Immunol* **102**, 101–129.
- Schmitz, M. L. & Grishina, I. (2012).** Regulation of the tumor suppressor PML by sequential post-translational modifications. *Front Oncol* **2**, 204.
- Schreiner, S. (2010).** *Analysen zur Funktion des zellulären Transkriptionsfaktors Daxx im produktiven Replikationszyklus von Adenovirus Typ 5.* Hamburg.
- Schreiner, S., Wimmer, P., Sirma, H., Everett, R. D., Blanchette, P., Groitl, P. & Dobner, T. (2010).** Proteasome-dependent degradation of Daxx by the viral E1B-55K protein in human adenovirus-infected cells. *J Virol* **84**, 7029–7038.
- Schreiner, S., Wimmer, P., Groitl, P., Chen, S.-Y., Blanchette, P., Branton, P. E. & Dobner, T. (2011).** Adenovirus Type 5 Early Region 1B 55K Oncoprotein-Dependent Degradation of Cellular Factor Daxx Is Required for Efficient Transformation of Primary Rodent Cells. *J Virol* **85**, 8752–8765.
- Schreiner, S., Martinez, R., Groitl, P., Rayne, F., Vaillant, R., Wimmer, P., Bossis, G., Sternsdorf, T., Marcinowski, L., Ruzsics, Z., Dobner, T. & Wodrich, H. (2012).** Transcriptional Activation of the Adenoviral Genome Is Mediated by Capsid Protein VI. *PLoS Pathog* **8**, e1002549.
- Schrier, P. I., Bernardis, R., Vaessen, R. T., Houweling, A. & van der Eb, A. J. (1983).** Expression of class I major histocompatibility antigens switched off by highly oncogenic adenovirus 12 in transformed rat cells. *Nature* **305**, 771–775.
- Schwartz, R. A., Lakdawala, S. S., Eshleman, H. D., Russell, M. R., Carson, C. T. & Weitzman, M. D. (2008).** Distinct requirements of adenovirus E1b55K protein for degradation of cellular substrates. *J Virol* **82**, 9043–9055.
- Seeler, J.-S. & Dejean, A. (2003).** Nuclear and unclear functions of SUMO. *Nat Rev Mol Cell Biol* **4**, 690–699.
- Seto, D., Chodosh, J., Brister, J. R., Jones, M. S. & Members of the Adenovirus Research Community, M. of the A. R. (2011).** Using the whole-genome sequence to characterize and name human adenoviruses. *J Virol* **85**, 5701–5702.
- Shah, G. A. & O’Shea, C. C. (2015).** Viral and Cellular Genomes Activate Distinct DNA Damage Responses. *Cell* **162**, 987–1002.
- Shang, Q., Wang, H., Song, Y., Wei, L., Lavebratt, C., Zhang, F. & Gu, H. (2014).** Serological data analyses show that adenovirus 36 infection is associated with obesity: A meta-analysis involving 5739 subjects. *Obesity* **22**, 895–900.
- Shao, J., Xu, D., Tsai, S.-N. & Yifei Wang, S.-M. N. (2009).** Computational Identification of Protein Methylation Sites through Bi-profile Bayes Feature Extraction. *PLoS One* **4**, 4920.
- Shao, J., Xu, D., Hu, L., Kwan, Y.-W., Wang, Y., Kong, X. & Ngai, S.-M. (2012).** Systematic analysis of human lysine acetylation proteins and accurate prediction of human lysine acetylation through bi-relative adapted binomial score Bayes feature representation. *Mol Biosyst* **8**, 2964–2973.
- Sharp, P. A. (1994).** Split genes and RNA splicing. *Cell* **77**, 805–815.
- Shauer, A., Gotsman, I., Keren, A., Zwas, D. R., Hellman, Y., Durst, R. & Admon, D. (2013).** Acute viral myocarditis: Current concepts in diagnosis and treatment. *Isr Med Assoc J IMAJ* **15**, 180–185.
- Shaw, A. R. & Ziff, E. B. (1980).** Transcripts from the adenovirus-2 major late promoter yield a single early family of 3' coterminal mRNAs and five late families. *Cell* **22**, 905–916.
- Shen, T. H., Lin, H.-K., Scaglioni, P. P., Yung, T. M. & Pandolfi, P. P. (2006a).** The Mechanisms of PML-Nuclear Body Formation. *Mol Cell* **24**, 331–339.
- Shen, T. H., Lin, H.-K., Scaglioni, P. P., Yung, T. M. & Pandolfi, P. P. (2006b).** The Mechanism of PML-Nuclear Body Formation. *Mol Cell* **24**, 331–339.
- Shenk, T. (2001).** Adenoviridae: The viruses and their replication. In *Virology*, Fourth., pp. 2265–2300. Edited by P. M. Howley & D. M. Knipe. New York: Lippincott-Raven.
- Shiio, Y. & Eisenman, R. N. (2003).** Histone sumoylation is associated with transcriptional repression. *Proc Natl Acad Sci* **100**, 13225–13230.

- Smith, J. G., Silvestry, M., Lindert, S., Lu, W., Nemerow, G. R. & Stewart, P. L. (2010). Insight into the mechanisms of adenovirus capsid disassembly from studies of defensin neutralization. *PLoS Pathog* **6**, e1000959.
- Song, J., Durrin, L. K., Wilkinson, T. A., Krontiris, T. G. & Chen, Y. (2004). Identification of a SUMO-binding motif that recognizes SUMO-modified proteins. *Proc Natl Acad Sci* **101**, 14373–14378.
- Sonntag, F., Schmidt, K. & Kleinschmidt, J. A. (2010). A viral assembly factor promotes AAV2 capsid formation in the nucleolus. *Proc Natl Acad Sci U S A* **107**, 10220–10225.
- Spector, D. J., McGrogan, M. & Raskas, H. J. (1978). Regulation of the appearance of cytoplasmic RNAs from region 1 of the adenovirus 2 genome. *J Mol Biol* **126**, 395–414.
- Spector, D. L., Ochs, R. L. & Busch, H. (1984). Silver staining, immunofluorescence and immunoelectron microscopic localization of nucleolar phosphoproteins B23 and C23. *Chromosoma* **90**, 139–148.
- Speiseder, T., Hofmann-Sieber, H., Rodríguez, E., Schellenberg, A., Akyüz, N., Dierlamm, J., Spruss, T., Lange, C. & Dobner, T. (2017). Efficient transformation of primary human mesenchymal stromal cells by adenovirus early region 1 oncogenes. *J Virol* **91**, e01782-16.
- Stadler, M., Chelbi-Alix, M. K., Koken, M. H., Venturini, L., Lee, C., Saïb, A., Quignon, F., Pelicano, L., Guillemain, M. C. & Schindler, C. (1995). Transcriptional induction of the PML growth suppressor gene by interferons is mediated through an ISRE and a GAS element. *Oncogene* **11**, 2565–2573.
- Staub, O. (2004). Ubiquitylation and isgylation: Overlapping enzymatic cascades do the job. *Sci STKE signal Transduct Knowl Environ* **2004**, pe43.
- Steegenga, W. T., Shvarts, A., Riteco, N., Bos, J. L. & Jochemsen, A. G. (1999). Distinct regulation of p53 and p73 activity by adenovirus E1A, E1B and E4orf6 proteins. *Mol Cell Biol* **19**, 3885–3894.
- Steegenga, W. T., Riteco, N., Jochemsen, A. G., Fallaux, F. J. & Bos, J. L. (1998). The large E1B protein together with the E4orf6 protein target p53 for active degradation in adenovirus infected cells. *Oncogene* **16**, 349–357.
- Stefl, R., Skrisovska, L. & Allain, F. H.-T. (2005). RNA sequence- and shape-dependent recognition by proteins in the ribonucleoprotein particle. *EMBO Rep* **6**, 33–38.
- Steinwaerder, D. S., Carlson, C. A. & Lieber, A. (2001). Human papilloma virus E6 and E7 proteins support DNA replication of adenoviruses deleted for the E1A and E1B genes. *Mol Ther* **4**, 211–216.
- Stephens, C. & Harlow, E. (1987). Differential splicing yields novel adenovirus 5 E1A mRNAs that encode 30 kd and 35 kd proteins. *EMBO J* **6**, 2027–2035.
- Sternsdorf, T., Jensen, K. & Will, H. (1997). Evidence for covalent modification of the nuclear dot-associated proteins PML and Sp100 by PIC1/SUMO-1. *J Cell Biol* **139**, 1621–1634.
- Sternsdorf, T., Jensen, K., Reich, B. & Will, H. (1999). The nuclear dot protein sp100, characterization of domains necessary for dimerization, subcellular localization and modification by small ubiquitin-like modifiers. *J Biol Chem* **274**, 12555–12566.
- Stewart, P. L., Chiu, C. Y., Huang, S., Muir, T., Zhao, Y., Chait, B., Mathias, P. & Nemerow, G. R. (1997). Cryo-EM visualization of an exposed RGD epitope on adenovirus that escapes antibody neutralization. *EMBO J* **16**, 1189–1198.
- Stewart, P. L., Burnett, R. M., Cyrklaff, M. & Fuller, S. D. (1991). Image reconstruction reveals the complex molecular organization of adenovirus. *Cell* **67**, 145–154.
- Stillman, B., Tamanoi, F. & Matthews, M. B. (1982). Purification of an adenovirus-coded DNA polymerase that is required for initiation of DNA replication. *Cell* **31**, 613–623.
- Stillman, B. W., Lewis, J. B., Chow, L. T., Mathews, M. B. & Smart, J. E. (1981). Identification of the gene and mRNA for the adenovirus terminal protein precursor. *Cell* **23**, 497–508.
- Stracker, T. H., Carson, C. T. & Weitzman, M. D. (2002). Adenovirus oncoproteins inactivate the Mre11-Rad50-NBS1 DNA repair complex. *Nature* **418**, 348–352.
- Strunze, S., Trotman, L. C., Boucke, K. & Greber, U. F. (2005). Nuclear targeting of adenovirus type 2 requires CRM1-mediated nuclear export. *Mol Biol Cell* **16**, 2999–3009.
- Stuurman, N., Meijne, A. M., van der Pol, A. J., de Jong, L., van Driel, R. & van Renswoude, J. (1990). The nuclear matrix from cells of different origin. Evidence for a common set of matrix proteins. *J Biol Chem* **265**, 5460–5465.

- Subong, E. N., Shue, M. J., Epstein, J. I., Briggman, J. V., Chan, P. K. & Partin, A. W. (1999). Monoclonal antibody to prostate cancer nuclear matrix protein (PRO:4-216) recognizes nucleophosmin/B23. *Prostate* **39**, 298–304.
- Subramanian, T., Malstrom, S. E. & Chinnadurai, G. (1991). Requirement of the C-terminal region of adenovirus E1a for cell transformation in cooperation with E1b. *Oncogene* **6**, 1171–1173.
- Sung, K. S., Lee, Y.-A., Kim, E. T., Lee, S.-R., Ahn, J.-H. & Choi, C. Y. (2011). Role of the SUMO-interacting motif in HIPK2 targeting to the PML nuclear bodies and regulation of p53. *Exp Cell Res* **317**, 1060–1070.
- Sung, M. T., Cao, T. M., Coleman, R. T. & Budelier, K. A. (1983). Gene and protein sequences of adenovirus protein VII, a hybrid basic chromosomal protein. *Proc Natl Acad Sci U S A* **80**, 2902–2906.
- Suomalainen, M., Nakano, M. Y., Keller, S., Boucke, K., Stidwill, R. P. & Greber, U. F. (1999). Microtubule-dependent plus- and minus end-directed motilities are competing processes for nuclear targeting of adenovirus. *J Cell Biol* **144**, 657–672.
- Suomalainen, M., Luisoni, S., Boucke, K., Bianchi, S., Engel, D. A. & Greber, U. F. (2013). A direct and versatile assay measuring membrane penetration of adenovirus in single cells. *J Virol* **87**, 12367–12379.
- Suresh, B., Lee, J., Kim, K. S. & Ramakrishna, S. (2016). The Importance of Ubiquitination and Deubiquitination in Cellular Reprogramming. *Stem Cells Int* **2016**.
- Swaney, D. L., Beltrao, P., Starita, L., Guo, A., Rush, J., Fields, S., Krogan, N. J. & Villen, J. (2013). Global analysis of phosphorylation and ubiquitylation cross-talk in protein degradation. *Nat Meth* **10**, 676–682.
- Szebeni, A., Hingorani, K., Negi, S. & Olson, M. O. J. (2003). Role of Protein Kinase CK2 Phosphorylation in the Molecular Chaperone Activity of Nucleolar Protein B23. *J Biol Chem* **278**, 9107–9115.
- Tago, K., Chiocca, S. & Sherr, C. J. (2005). Sumoylation induced by the Arf tumor suppressor: A p53-independent function. *Proc Natl Acad Sci U S A* **102**, 7689–7694.
- Tanaka, K., Isselbacher, K. J., Khoury, G. & Jay, G. (1985). Reversal of oncogenesis by the expression of a major histocompatibility complex class I gene. *Science* **228**, 26–30.
- Tatham, M. H., Jaffray, E., Vaughan, O. A., Desterro, J. M., Botting, C. H., Naismith, J. H. & Hay, R. T. (2001). Polymeric chains of SUMO-2 and SUMO-3 are conjugated to protein substrates by SAE1/SAE2 and Ubc9. *J Biol Chem* **276**, 35368–35374.
- Tatham, M. H., Rodriguez, M. S., Xirodimas, D. P. & Hay, R. T. (2009). Detection of protein SUMOylation in vivo. *Nat Protoc* **4**, 1363–1371.
- Tavalai, N. & Stamminger, T. (2008). New insights into the role of the subnuclear structure ND10 for viral infection. *Biochim Biophys Acta - Mol Cell Res* **1783**, 2207–2221.
- Tavalai, N., Papior, P., Rechter, S. & Stamminger, T. (2008). Nuclear domain 10 components promyelocytic leukemia protein and hDaxx independently contribute to an intrinsic antiviral defense against human cytomegalovirus infection. *J Virol* **82**, 126–137.
- Tavalai, N., Adler, M., Scherer, M., Riedl, Y. & Stamminger, T. (2011). Evidence for a Dual Antiviral Role of the Major Nuclear Domain 10 Component Sp100 during the Immediate-Early and Late Phases of the Human Cytomegalovirus Replication Cycle. *J Virol* **85**, 9447–9458.
- Temperley, S. M. & Hay, R. T. (1992). Recognition of the adenovirus type 2 origin of DNA replication by the virally encoded DNA polymerase and preterminal proteins. *EMBO J* **11**, 761–768.
- Teodoro, J. G. & Branton, P. E. (1997). Regulation of p53-dependent apoptosis, transcriptional repression and cell transformation by phosphorylation of the 55-kilodalton E1B protein of human adenovirus type 5. *J Virol* **71**, 3620–3627.
- Terzic, M. (2014). *Role of E2A/DBP SUMOylation during productive infection with Human Adenovirus Type 5*.
- Texari, L. & Stutz, F. (2015). Sumoylation and transcription regulation at nuclear pores. *Chromosoma* **124**, 45–56.
- de Thé, H., Lavau, C., Marchio, A., Chomienne, C., Degos, L. & Dejean, A. (1991). The PML-RAR alpha fusion mRNA generated by the t(15;17) translocation in acute promyelocytic leukemia encodes a functionally altered RAR. *Cell* **66**, 675–684.
- Thomas, G. P. & Mathews, M. B. (1980). DNA replication and the early to late transition in adenovirus infection. *Cell* **22**, 523–533.

- Thomas, J. J., Abed, M., Heuberger, J., Rostislav, N., Zohar, Y., Beltran Lopez, A. P., Trausch-Azar, J. S., Ilagan, M. X. G., Benhamou, D., Dittmar, G., Kopan, R., Birchmeier, W., Schwartz, A. L. & Orian, A. (2016). RNF4-Dependent Oncogene Activation by Protein Stabilization. *Cell Rep* **16**, 3388–3400.
- Tokuyama, Y., Horn, H. F., Kawamura, K., Tarapore, P. & Fukasawa, K. (2001). Specific Phosphorylation of Nucleophosmin on Thr199 by Cyclin-dependent Kinase 2-Cyclin E and Its Role in Centrosome Duplication. *J Biol Chem* **276**, 21529–21537.
- Tollefson, A. E., Ying, B., Doronin, K., Sidor, P. D. & Wold, W. S. M. (2007). Identification of a New Human Adenovirus Protein Encoded by a Novel Late I-Strand Transcription Unit. *J Virol* **81**, 12918–12926.
- Torok, D., Ching, R. W. & Bazett-Jones, D. P. (2009). PML nuclear bodies as sites of epigenetic regulation. *Front Biosci* **14**, 1325–1336.
- Treacy, A., Carr, M. J., Dunford, L., Palacios, G., Cannon, G. A., O’Grady, A., Moran, J., Hassan, J., Loy, A., Connell, J., Devaney, D., Kelehan, P. & Hall, W. W. (2010). First report of sudden death due to myocarditis caused by adenovirus serotype 3. *J Clin Microbiol* **48**, 642–645.
- Trentin, J. J., Yabe, Y. & Taylor, G. (1962). The quest for human cancer viruses. *Science* **137**, 835–841.
- Tribouley, C., Lutz, P., Staub, A. & Kedinger, C. (1994). The product of the adenovirus intermediate gene IVa2 is a transcriptional activator of the major late promoter. *J Virol* **68**, 4450–4457.
- Trotman, L. C., Mosberger, N., Fornerod, M., Stidwill, R. P. & Greber, U. F. (2001). Import of adenovirus DNA involves the nuclear pore complex receptor CAN/Nup214 and histone H1. *Nat Cell Biol* **3**, 1092–1100.
- Tsai, R. Y. L. & Pederson, T. (2014). Connecting the nucleolus to the cell cycle and human disease. *FASEB J* **28**, 3290–3296.
- Turcu, F. E. R., Ventii, K. H. & Wilkinson, K. D. (2009). Regulation and Cellular Roles of Ubiquitin-specific Deubiquitinating Enzymes. *Annu Rev Biochem* **78**, 363–397.
- Ugai, H., Borovjagin, A. V., Le, L. P., Wang, M. & Curiel, D. T. (2007). Thermostability/infectivity defect caused by deletion of the core protein V gene in human adenovirus type 5 is rescued by thermo-selectable mutations in the core protein X precursor. *J Mol Biol* **366**, 1142–1160.
- Ugai, H., Wang, M., Le, L. P., Matthews, D. A., Yamamoto, M. & Curiel, D. T. (2010). In Vitro dynamic visualization analysis of fluorescently labeled minor capsid protein IX and core protein V by simultaneous detection. *J Mol Biol* **395**, 55–78.
- Ugai, H., Dobbins, G. C., Wang, M., Le, L. P., Matthews, D. a & Curiel, D. T. (2012). Adenoviral protein V promotes a process of viral assembly through nucleophosmin 1. *Virology* **432**, 283–295.
- Ugrinova, I., Monier, K., Ivaldi, C., Thiry, M., Storck, S., Mongelard, F. & Bouvet, P. (2007). Inactivation of nucleolin leads to nucleolar disruption, cell cycle arrest and defects in centrosome duplication. *BMC Mol Biol* **8**, 66.
- Umut, S., Ferhi, O., Jeanne, M., Benhenda, S., Berthier, C., Jollivet, F., Niwa-Kawakita, M., Faklaris, O., Setterblad, N., de Thé, H. & Lallemand-Breitenbach, V. (2014). Oxidative stress-induced assembly of PML nuclear bodies controls sumoylation of partner proteins. *J Cell Biol* **204**, 931–945.
- Valverde, R., Edwards, L. & Regan, L. (2008). Structure and function of KH domains. *FEBS J* **275**, 2712–2726.
- Vascotto, C., Lirussi, L., Poletto, M., Tiribelli, M., Damiani, D., Fabbro, D., Damante, G., Demple, B., Colombo, E. & Tell, G. (2014). Functional regulation of the apurinic/aprimidinic endonuclease 1 by nucleophosmin: Impact on tumor biology. *Oncogene* **33**, 2876–2887.
- Vascotto, C., Fantini, D., Romanello, M., Cesaratto, L., Deganuto, M., Leonardi, A., Radicella, J. P., Kelley, M. R., D’Ambrosio, C., Scaloni, A., Quadrifoglio, F. & Tell, G. (2009). APE1/Ref-1 Interacts with NPM1 within Nucleoli and Plays a Role in the rRNA Quality Control Process. *Mol Cell Biol* **29**, 1834–1854.
- Vayda, M. E. & Flint, S. J. (1987). Isolation and characterization of adenovirus core nucleoprotein subunits. *J Virol* **61**, 3335–3339.
- Vayda, M. E., Rogers, A. E. & Flint, S. J. (1983). The structure of nucleoprotein cores released from adenovirions. *Nucleic Acids Res* **11**, 441–460.
- Vertegaal, A. C. O., Ogg, S. C., Jaffray, E., Rodriguez, M. S., Hay, R. T., Andersen, J. S., Mann, M. & Lamond, A. I. (2004). A proteomic study of SUMO-2 target proteins. *J Biol Chem* **279**,

- 33791–33798.
- Vink, E., Zheng, Y., Yeasmin, R., Stamminger, T., Krug, L. & Hearing, P. (2015). Impact of Adenovirus E4-ORF3 Oligomerization and Protein Localization on Cellular Gene Expression. *Viruses* **7**, 2428–2449.
- Virtanen, A., Gilardi, P., Näslund, A., LeMoullec, J. M., Pettersson, U. & Perricaudet, M. (1984). mRNAs from human adenovirus 2 early region 4. *J Virol* **51**, 822–831.
- Vliet, P. C. & Sussenbach, J. S. (1975). An adenovirus type 5 gene function required for initiation of viral DNA replication. *Virology* **67**, 415–426.
- Voelkerding, K. & Klessig, D. F. (1986). Identification of two nuclear subclasses of the adenovirus type 5-encoded DNA-binding protein. *J Virol* **60**, 353–362.
- Voet, P. D., Voet, J. G. & W., C. (2006). *Fundamentals of biochemistry: Life at the molecular level*, 2nd edn. Hoboken, NJ: Wiley.
- Vojtesek, B., Bartek, J., Midgley, C. A. & Lane, D. P. (1992). An immunochemical analysis of the human nuclear phosphoprotein p53. New monoclonal antibodies and epitope mapping using recombinant p53. *J Immunol Methods* **151**, 237–244.
- de Vrij, J., van den Hengel, S. K., Uil, T. G., Koppers-Lalic, D., Dautzenberg, I. J. C., Stassen, O. M. J. A., Bárcena, M., Yamamoto, M., de Ridder, C. M. A., Kraaij, R., Kwappenberg, K. M., Schilham, M. W. & Hoeben, R. C. (2011). Enhanced transduction of CAR-negative cells by protein IX-gene deleted adenovirus 5 vectors. *Virology* **410**, 192–200.
- Wadell, G. (1984). Molecular epidemiology of human adenoviruses. *Curr Top Microbiol Immunol* **110**, 191–220.
- Walsh, C. (2006). *Posttranslational modification of proteins: Expanding nature's inventory*. Englewood, Colo.: Roberts and Company Publishers, c2006.
- Walters, R. W., Freimuth, P., Moninger, T. O., Ganske, I., Zabner, J. & Welsh, M. J. (2002). Adenovirus fiber disrupts CAR-mediated intercellular adhesion allowing virus escape. *Cell* **110**, 789–799.
- Walton, T. H., Moen, P. T., Fox, E. & Bodnar, J. W. (1989). Interactions of minute virus of mice and adenovirus with host nucleoli. *J Virol* **63**, 3651–3560.
- Wang, D., Umekawa, H. & Olson, M. O. (1993). Expression and subcellular locations of two forms of nucleolar protein B23 in rat tissues and cells. *Cell Mol Biol Res* **39**, 33–42.
- Wang, D., Baumann, A., Szebeni, A. & Olson, M. (1994). The Nucleic Acid Binding Activity of Nucleolar Protein B23.1 Resides in Its Carboxyl-terminal End. *J Biol Chem* **269**, 30994–30998.
- Wang, G. & Berk, A. J. (2002). In vivo association of adenovirus large E1A protein with the human mediator complex in adenovirus-infected and -transformed cells. *J Virol* **76**, 9186–9193.
- Wang, H., Zhao, L.-N., Li, K.-Z., Ling, R., Li, X.-J. & Wang, L. (2006). Overexpression of ribosomal protein L15 is associated with cell proliferation in gastric cancer. *BMC Cancer* **6**, 91.
- Wang, I.-H., Suomalainen, M., Andriasyan, V., Kilcher, S., Mercer, J., Neef, A., Luedtke, N. W. & Greber, U. F. (2013). Tracking Viral Genomes in Host Cells at Single-Molecule Resolution. *Cell Host Microbe* **14**, 468–480.
- Wang, K., Huang, S., Kapoor-Munshi, A. & Nemerow, G. (1998a). Adenovirus internalization and infection require dynamin. *J Virol* **72**, 3455–3458.
- Wang, L., Du, Y., Lu, M. & Li, T. (2012). ASEB: A web server for KAT-specific acetylation site prediction. *Nucleic Acids Res* **40**, W376–W379.
- Wang, P., Xiao, X. & Chou, K.-C. (2011). NR-2L: A Two-Level Predictor for Identifying Nuclear Receptor Subfamilies Based on Sequence-Derived Features. *PLoS One* **6**, e23505.
- Wang, W., Budhu, A., Forgues, M. & Wang, X. W. (2005). Temporal and spatial control of nucleophosmin by the Ran-Crm1 complex in centrosome duplication. *Nat Cell Biol* **7**, 823–830.
- Wang, Y. & Dasso, M. (2009). SUMOylation and deSUMOylation at a glance. *J Cell Sci* **122**, 4249–4252.
- Wang, Z.-G., Ruggero, D., Ronchetti, S., Zhong, S., Gaboli, M., Rivi, R. & Pandolfi, P. P. (1998b). Pml is essential for multiple apoptotic pathways. *Nat Genet* **20**, 266–272.
- Warner, J. R. & McIntosh, K. B. (2009). How Common Are Extraribosomal Functions of Ribosomal Proteins? *Mol Cell* **34**, 3–11.
- Weber, J. M. & Khittoo, G. (1983). The role of phosphorylation and core protein V in adenovirus assembly. *J Gen Virol* **64** (Pt 9), 2063–2068.
- Weber, R. G., Bridger, J. M., Benner, A., Weisenberger, D., Ehemann, V., Reifenberger, G. &

- Lichter, P. (1998).** Centrosome amplification as a possible mechanism for numerical chromosome aberrations in cerebral primitive neuroectodermal tumors with TP53 mutations. *Cytogenet Genome Res* **83**, 266–269.
- Weidtkamp-Peters, S., Lenser, T., Negorev, D., Gerstner, N., Hofmann, T. G., Schwanitz, G., Hoischen, C., Maul, G., Dittrich, P. & Hemmerich, P. (2008).** Dynamics of component exchange at PML nuclear bodies. *J Cell Sci* **121**, 2731–2743.
- Weinberg, R. A., Hahn, W. C., Stewart, S. A., Brooks, M. W., York, S. G., Eaton, E., Kurachi, A., Beijersbergen, R. L., Knoll, J. H. M. & Meyerson, M. (1999a).** Inhibition of telomerase limits the growth of human cancer cells. *Nat Med* **5**, 1164–1170.
- Weinberg, R. A., Hahn, W. C., Counter, C. M., Lundberg, A. S., Beijersbergen, R. L. & Brooks, M. W. (1999b).** Creation of human tumour cells with defined genetic elements. *Nature* **400**, 464–468.
- Weis, K., Rambaud, S., Lavau, C., Jansen, J., Carvalho, T., Carmo-Fonseca, M., Lamond, A. & Dejean, A. (1994).** Retinoic acid regulates aberrant nuclear localization of PML-RAR alpha in acute promyelocytic leukemia cells. *Cell* **76**, 345–356.
- Wentzensen, N., Vinokurova, S. & von Knebel Doeberitz, M. (2004).** Systematic Review of Genomic Integration Sites of Human Papillomavirus Genomes in Epithelial Dysplasia and Invasive Cancer of the Female Lower Genital Tract. *Cancer Res* **64**, 3878–3884.
- White, E., Spector, D. & Welch, W. (1988).** Differential distribution of the adenovirus E1A proteins and colocalization of E1A with the 70-kilodalton cellular heat shock protein in infected cells. *J Virol* **62**, 4153–4166.
- White, E., Sabbatini, P., Debbas, M., Wold, W. S., Kusher, D. I. & Gooding, L. R. (1992).** The 19-kilodalton adenovirus E1B transforming protein inhibits programmed cell death and prevents cytolysis by tumor necrosis factor alpha. *Mol Cell Biol* **12**, 2570–2580.
- Wickham, T. J., Mathias, P., Cheresch, D. A. & Nemerow, G. R. (1993).** Integrins alpha v beta 3 and alpha v beta 5 promote adenovirus internalization but not virus attachment. *Cell* **73**, 309–319.
- Wiethoff, C. M., Wodrich, H., Gerace, L. & Nemerow, G. R. (2005).** Adenovirus Protein VI Mediates Membrane Disruption following Capsid Disassembly. *J Virol* **79**, 1992–2000.
- Wiethoff, C. M. & Nemerow, G. R. (2015).** Adenovirus membrane penetration: Tickling the tail of a sleeping dragon. *Virology* **479–480**, 591–599.
- Williams, J. F., Zhang, Y., Williams, M. A., Hou, S., Kushner, D. & Ricciardi, R. P. (2004).** E1A-based determinants of oncogenicity in human adenovirus groups A and C. *Curr Top Microbiol Immunol* **273**, 245–288.
- Wimmer, P., Schreiner, S., Everett, R. D., Sirma, H., Groitl, P. & Dobner, T. (2010).** SUMO modification of E1B-55K oncoprotein regulates isoform-specific binding to the tumour suppressor protein PML. *Oncogene* **29**, 5511–5522.
- Wimmer, P., Blanchette, P., Schreiner, S., Ching, W., Groitl, P., Berscheminski, J., Branton, P. E., Will, H. & Dobner, T. (2013).** Cross-talk between phosphorylation and SUMOylation regulates transforming activities of an adenoviral oncoprotein. *Oncogene* **32**, 1626–1637.
- Wimmer, P., Berscheminski, J., Blanchette, P., Groitl, P., Branton, P. E., Hay, R. T., Dobner, T. & Schreiner, S. (2015).** PML isoforms IV and V contribute to adenovirus-mediated oncogenic transformation by functionally inhibiting the tumor-suppressor p53. *Oncogene* **35**, 69–82.
- Winberg, G. & Shenk, T. (1984).** Dissection of overlapping functions within the adenovirus type 5 E1A gene. *EMBO J* **3**, 1907–1912.
- Windheim, M., Hilgendorf, A. & Burgert, H. G. (2004).** Immune evasion by adenovirus E3 proteins: Exploitation of intracellular trafficking pathways. *Curr Top Microbiol Immunol* **273**, 29–85.
- Wodrich, H., Cassany, A., D'Angelo, M. A., Guan, T., Nemerow, G. & Gerace, L. (2006).** Adenovirus Core Protein pVII Is Translocated into the Nucleus by Multiple Import Receptor Pathways. *J Virol* **80**, 9608–9618.
- Wodrich, H., Henaff, D., Jammart, B., Segura-Morales, C., Seelmeir, S., Coux, O., Ruzsics, Z., Wiethoff, C. M. & Kremer, E. J. (2010).** A capsid-encoded PPxY-motif facilitates adenovirus entry. *PLoS Pathog* **6**, e1000808.
- Wold, W. S., Tollefson, A. E. & Hermiston, T. W. (1995).** E3 transcription unit of adenovirus. *Curr Top Microbiol Immunol* **199 (Pt 1)**, 237–274.
- Wold, W. S. M. & Horwitz, M. S. (2007).** Adenoviruses. In *Fields Virol*, 5th edn., pp. 2395–2436. Edited by D. M. Knipe & P. M. Howley. Lippincott Williams & Wilkins.

- Woods, S. J., Hannan, K. M., Pearson, R. B. & Hannan, R. D. (2015).** The nucleolus as a fundamental regulator of the p53 response and a new target for cancer therapy. *Biochim Biophys Acta - Gene Regul Mech* **1849**, 821–829.
- Wright, P. E. & Dyson, H. J. (2015).** Intrinsically disordered proteins in cellular signalling and regulation. *Nat Rev Mol Cell Biol* **16**, 18–29.
- Wu, K., Orozco, D. & Hearing, P. (2012).** The adenovirus L4-22K protein is multifunctional and is an integral component of crucial aspects of infection. *J Virol* **86**, 10474–10483.
- Wu, K., Guimet, D. & Hearing, P. (2013).** The adenovirus L4-33K protein regulates both late gene expression patterns and viral DNA packaging. *J Virol* **87**, 6739–6747.
- Wu, M. H. & Yung, B. Y. M. (2002).** UV stimulation of nucleophosmin/B23 expression is an immediate-early gene response induced by damaged DNA. *J Biol Chem* **277**, 48234–48240.
- Würtele, H., Little, K. & Chartrand, P. (2003).** Illegitimate DNA integration in mammalian cells. *Gene Ther* **10**, 1791–1799.
- Xiang Chen, Qiu, J., Shi, S., Suo, S., Huang, S. & Liang, R. (2013).** Incorporating key positions and amino acids features to identify general and species-specific ubiquitin conjugation sites. *Bioinformatics* **29**, 1614–1622.
- Xu, Z. X., Zou, W. X., Lin, P. & Chang, K. S. (2005).** A role for PML3 in centrosome duplication and genome stability. *Mol Cell* **17**, 721–732.
- Yang, J. & Zhang, Y. (2015).** I-TASSER server: New development for protein structure and function predictions. *Nucleic Acids Res* **43**, W174–W181.
- Yang, J., Yan, R., Roy, A., Xu, D., Poisson, J. & Zhang, Y. (2015).** The I-TASSER Suite: Protein structure and function prediction. *Nat Methods* **12**, 7–8.
- Yang, K., Wang, M., Zhao, Y., Sun, X., Yang, Y., Li, X., Zhou, A., Chu, H., Zhou, H., Xu, J., Wu, M., Yang, J. & Yi, J. (2016).** A redox mechanism underlying nucleolar stress sensing by nucleophosmin. *Nat Commun* **7**, 13599.
- Yang, Y., Nunes, F. A., Berencsi, K., Furth, E. E., Gönczöl, E. & Wilson, J. M. (1994).** Cellular immunity to viral antigens limits E1-deleted adenoviruses for gene therapy. *Proc Natl Acad Sci U S A* **91**, 4407–4411.
- Yang, Y., Jooss, K. U., Su, Q., Ertl, H. C. & Wilson, J. M. (1996).** Immune responses to viral antigens versus transgene product in the elimination of recombinant adenovirus-infected hepatocytes in vivo. *Gene Ther* **3**, 137–144.
- Yao, Q., Li, H., Liu, B. Q., Huang, X. Y. & Guo, L. (2011).** SUMOylation-regulated protein phosphorylation, evidence from quantitative phosphoproteomics analyses. *J Biol Chem* **286**, 27342–27349.
- Yao, Z., Duan, S., Hou, D., Wang, W., Wang, G., Liu, Y., Wen, L. & Wu, M. (2010).** B23 acts as a nucleolar stress sensor and promotes cell survival through its dynamic interaction with hnRNPU and hnRNPA1. *Oncogene* **29**, 1821–1834.
- Yew, P. R. & Berk, A. J. (1992).** Inhibition of p53 transactivation required for transformation by adenovirus early 1B protein. *Nature* **357**, 82–85.
- Ying, B., Tollefson, A. E. & Wold, W. S. M. (2010).** Identification of a Previously Unrecognized Promoter That Drives Expression of the UXP Transcription Unit in the Human Adenovirus Type 5 Genome. *J Virol* **84**, 11470–11478.
- Yoshitomi, H., Sera, N., Gonzalez, G., Hanaoka, N. & Fujimoto, T. (2016).** First isolation of a potentially new type of human adenovirus (genotype 72), species Human mastadenovirus B (B2) from sewage water in Japan. *J Med Virol*.
- Yu, Y., Maggi, L. B., Brady, S. N., Apicelli, A. J., Dai, M.-S., Lu, H. & Weber, J. D. (2006).** Nucleophosmin Is Essential for Ribosomal Protein L5 Nuclear Export. *Mol Cell Biol* **26**, 3798–3809.
- Yueh, A. & Schneider, R. J. (1996).** Selective translation initiation by ribosome jumping in adenovirus-infected and heat-shocked cells. *Genes Dev* **10**, 1557–1567.
- Yueh, A. & Schneider, R. J. (2000).** Translation by ribosome shunting on adenovirus and hsp70 mRNAs facilitated by complementarity to 18S rRNA. *Genes Dev* **14**, 414–421.
- Yun, C., Wang, Y., Mukhopadhyay, D., Backlund, P., Kolli, N., Yergey, A., Wilkinson, K. D. & Dasso, M. (2008).** Nucleolar protein B23/nucleophosmin regulates the vertebrate SUMO pathway through SENP3 and SENP5 proteases. *J Cell Biol* **183**, 589–595.
- Zamanian, M. & La Thangue, N. B. (1992).** Adenovirus E1a prevents the retinoblastoma gene product

- from repressing the activity of a cellular transcription factor. *EMBO J* **11**, 2603–2610.
- Zantema, A., Fransen, J. A., Davis-Olivier, A., Ramaekers, F. C., Vooijs, G. P., DeLeys, B. & Van der Eb, A. J. (1985). Localization of the E1B proteins of adenovirus 5 in transformed cells, as revealed by interaction with monoclonal antibodies. *Virology* **142**, 44–58.
- Zatsepina, O. V., Rousselet, A., Chan, P. K., Olson, M. O., Jordan, E. G. & Bornens, M. (1999). The nucleolar phosphoprotein B23 redistributes in part to the spindle poles during mitosis. *J Cell Sci* **112**, 455–466.
- Zerler, B., Roberts, R. J., Mathews, M. B. & Moran, E. (1987). Different functional domains of the adenovirus E1A gene are involved in regulation of host cell cycle products. *Mol Cell Biol* **7**, 821–829.
- Zhang, D.-E. D. & Zhang, D.-E. D. (2011). Interferon-stimulated gene 15 and the protein ISGylation system. *J Interf cytokine Res Off J Int Soc Interf Cytokine Res* **31**, 119–130.
- Zhang, W. & Imperiale, M. J. (2000). Interaction of the adenovirus IVa2 protein with viral packaging sequences. *J Virol* **74**, 2687–2693.
- Zhang, W., Low, J. A., Christensen, J. B. & Imperiale, M. J. (2001). Role for the adenovirus IVa2 protein in packaging of viral DNA. *J Virol* **75**, 10446–10454.
- Zhang, W. & Arcos, R. (2005). Interaction of the adenovirus major core protein precursor, pVII, with the viral DNA packaging machinery. *Virology* **334**, 194–202.
- Zhang, W. & Imperiale, M. J. (2003). Requirement of the Adenovirus IVa2 Protein for Virus Assembly. *J Virol* **77**, 3586–3594.
- Zhang, Y., Xiong, Y. & Yarbrough, W. G. (1998). ARF promotes MDM2 degradation and stabilizes p53: ARF-INK4a locus deletion impairs both the Rb and p53 tumor suppression pathways. *Cell* **92**, 725–734.
- Zhang, Y. (2008). I-TASSER server for protein 3D structure prediction. *BMC Bioinformatics* **9**, 40.
- Zhang, Y. & Lu, H. (2009). Signaling to p53: Ribosomal Proteins Find Their Way. *Cancer Cell* **16**, 369–377.
- Zhao, L.-J., Subramanian, T., Vijayalingam, S. & Chinnadurai, G. (2007). PLDLS-dependent interaction of E1A with CtBP: Regulation of CtBP nuclear localization and transcriptional functions. *Oncogene* **26**, 7544–7551.
- Zhao, L.-J., Subramanian, T. & Chinnadurai, G. (2006). Changes in C-terminal Binding Protein 2 (CtBP2) Corepressor Complex Induced by E1A and Modulation of E1A Transcriptional Activity by CtBP2. *J Biol Chem* **281**, 36613–36623.
- Zhao, Q., Xie, Y., Zheng, Y., Jiang, S., Liu, W., Mu, W., Liu, Z., Zhao, Y., Xue, Y. & Ren, J. (2014). GPS-SUMO: A tool for the prediction of sumoylation sites and SUMO-interaction motifs. *Nucleic Acids Res* **42**, W325–W330.
- Zhong, S., Muller, S., Ronchetti, S., Freemont, P. S., Dejean, A. & Pandolfi, P. P. (2000a). Role of SUMO-1-modified PML in nuclear body formation. *Blood* **95**, 2748–2752.
- Zhong, S., Salomoni, P. & Pandolfi, P. P. (2000b). The transcriptional role of PML and the nuclear body. *Nat Cell Biol* **2**, E85–E90.
- Zhu, J., The, H. De, Takahashi, Y. & Lallemand-Breitenbach, V. (2004). PML nuclear bodies and apoptosis. *Oncogene* **23**, 2819–2824.
- Ziv, O., Zeisel, A., Mirlas-Neisberg, N., Swain, U., Nevo, R., Ben-Chetrit, N., Martelli, M. P., Rossi, R., Schiesser, S., Canman, C. E., Carell, T., Geacintov, N. E., Falini, B., Domany, E. & Livneh, Z. (2014). Identification of novel DNA-damage tolerance genes reveals regulation of translesion DNA synthesis by nucleophosmin. *Nat Commun* **5**, 5437.

## 7 Publications

---

### 7.1. Publications in scientific journals

**Freudenberger N., Dobner T., Schreiner S., (2017).** The lack of consensus sites for SUMOylation within HAdV-C5 pV accelerates the productive viral infection. (manuscript in preparation)

**Freudenberger N., Speiseder T., Dobner T., Schreiner S., (2017).** HAdV-C5 pV represses the oncogenic transformation of primary baby rat kidney cells mediated by HAdV-C5 E1 oncogenes. (manuscript in preparation)

### 7.2. Presentations at scientific meetings

#### 7.2.1. Oral presentations

- 12<sup>th</sup> International Adenovirus Meeting (IAM) in Barsinghausen, Germany (2016)
- ICGEB DNA Tumor Virus Meeting in Trieste, Italy (2015)
- Retreat of the Institute of Virology of the technical University of Munich (TUM) in Tutzing, Germany (2015)

#### 7.2.2. Poster presentations

- HPI Retreat in Hamburg, Germany (2016)
- HPI Retreat in Hamburg, Germany (2015)
- 25<sup>nd</sup> Annual Meeting of the GfV (Gesellschaft für Virologie) in Bochum, Germany (2015)

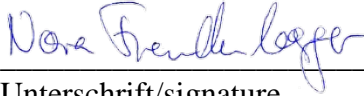
## **8 Declaration on oath/Eidesstattliche Versicherung**

---

Hiermit erkläre ich, Nora Freudenberger, an Eides statt, dass ich die vorliegende Dissertationsschrift selbst verfasst und keine anderen als die angegebenen Quellen und Hilfsmittel benutzt habe.

I hereby declare, on oath, that I have written the present dissertation by my own and have not used other than the acknowledged resources and aids.

Hamburg, den 24.05.2017

  
\_\_\_\_\_  
Unterschrift/signature

## 9 Acknowledgements/Danksagung

---

I want to thank my supervisor Prof. Dr. Thomas Dobner for giving me the opportunity to work on this interesting project. During this work, I got the chance to develop a reflected scientific thinking. I was encouraged to face challenges on my own and to work independently. Moreover, I was enabled to participate in international scientific meetings. All of which will help me during my future career.

I also want to thank the members of my examining board; Prof. Dr. Nicole Fischer for her support as my second supervisor and for evaluating my dissertation and Prof. Dr. Julia Kehr for chairing the disputation.

My special thanks go to Dr. Sabrina Schreiner of the TU München, who supported me during the whole project. She helped me to stay focused, to develop ideas. She empowered me, if necessary and financed my last 1.5 years in Hamburg. Without her, this project would not have been realized.

I am exceptionally grateful for my lab members. We have been a real team through all this time and I will miss especially my girl's lab. It was quite a journey full of fruitful discussions with Wingi and Maggie and lots of laughing with Sarah, Tina, Jana, Caro and Julia.

Particularly, I want to thank Hendrik. Thank you for knowing what it means to be a doctoral student in science. Thank you for being at my side, no matter what.